Experimental and Analytical

Analysis of Perimeter

Radiant Heating Panels

By

Martin Kegel

A thesis

presented to the University of Waterloo

in fulfillment of the

thesis requirement for the degree of

Master of Applied Science

in

Mechanical Engineering

Waterloo, Ontario, Canada, 2006

I hereby declare that I am the sole author of this thesis. This is a true copy of the thesis, including any required final revisions, as accepted by my examiners.

I understand that my thesis may be made electronically available to the public.

Abstract

In recent years the U.S. and Canada have seen a steady increase in energy consumption. The U.S. in particular uses 25% more energy than it did 20 years ago. With declining natural resources and an increase in fuel costs, it has become important to find methods of reducing energy consumption, in which energy conservation in space heating and cooling has become a widely researched area. One method that has been identified to reduce the energy required for space heating is the use of radiant panels. Radiant panels are beneficial because the temperature set points in a room can be lowered without sacrificing occupant comfort. They have therefore become very popular in the market. Further research, however, is required to optimize the performance of these panels so energy savings can be realized.

An analytical model has been developed to predict the panel temperature and heat output for perimeter radiant panel systems with a known inlet temperature and flow rate, based on a flat plate solar collector (RSC) model. As radiative and convective heat transfer coefficients were required to run the model, an analytical analysis of the radiative heat transfer was performed, and a numerical model was developed to predict the convective heat transfer coefficient. Using the conventional radiative heat exchange method assuming a three-surface enclosure, the radiative heat transfer could be determined. Numerically, a correlation was developed to predict the natural convective heat transfer.

To validate the analytical model, an experimental analysis was performed on radiant panels. A 4m by 4m by 3m test chamber was constructed in which the surrounding walls and floor were maintained at a constant temperature and the heat

output from an installed radiant panel was measured. Two radiant panels were tested; a 0.61m wide panel with 4 passes and a 0.61m wide panel with 8 passes. The panels were tested at 5 different inlet water temperatures ranging from 50°C to 100°C.

The RSC model panel temperature and heat output predictions were in good agreement with the experimental results. The RSC model followed the same trends as that in the experimental results, and the panel temperature and panel heat output were within experimental uncertainty, concluding that the RSC model is a viable, simple algorithm which could be used to predict panel performance.

Acknowledgements

Dedication

I would like to dedicate this thesis towards the development of installing efficient radiant

panel heating applications for the commercial sector.

Table of Contents

List of Tables

List of Figures

Nomenclature

Symbol

A	Surface Area, m^2
AUST	Area-weighted surface temperature, K
AR	Radiant panel aspect ratio ($L_{panel}/L_{ceiling}$), dimensionless
b	Bond width, m
b	Sutherland equation constant ($1.458 \times 10\text{-}6 \ kg/(msK^{1/2})$)
C_b	Bond conductance, W/mK
C_p	Specific heat, J/kgK
C_μ, f_μ, l	Coefficients for the k-l turbulence model
D	Diameter, m
D_H	Hydraulic Diameter (4xPerimeter/Area)
E_{bi}	Emissive Power from surface i, W/m^2
f	friction factor, dimensionless
F	View factor
F	Fin efficiency factor
F'	Fin efficiency factor, dimensionless
F_R	Heat removal factor, dimensionless
g	Gravitational constant ($9.81 \ m/s^2$)
G	Irradiation, W/m^2
Gr	Grashof number, dimensionless
h	Convective heat transfer coefficient, W/m^2K
h_L	Head loss, m of H_2O
J	Radiosity, W/m^2
k	Thermal conductivity, W/mK
k-l	Turbulence model coefficient
K_L	Loss coefficient, dimensionless
ℓ	Pipe length, m
L	Panel length, m
$\dot{m}$	Mass flow rate, kg/s
n	Number of surfaces
n	Number of passes
Nu	Nusselt number, dimensionless
p	Pressure, Pa
Pr	Prandtl number, dimensionless
q	Heat transfer, W
q'	Heat Tranfer per unit length, W/m
q"	Heat flux, W/m^2
R	Radial distance, m
R	Gas constant (287 J/kgK for air)
Ra	Rayleigh number, dimensionless
Re	Reynolds number, dimensionless
S	Molecular viscosity constant for the Sutherland Equation (110.4, K)
t	Thickness, m

T	Temperature, K
u	x-direction velocity, m/s
U_L	Overall heat transfer coefficient, W/m²K
v	y-direction velocity, m/s
V	Velocity, m/s
W	Tube or Pipe Spacing, m
W	Radiant panel width, m

Greek Letters

α	Thermal diffusivity, m²/s
β	Volumetric thermal expansion coefficient, K⁻¹
δ	Plate thickness, m
Δ	Increment
ε	Emissivity
μ	Dynamic viscosity, Ns/m²
μ_t	Turbulence viscosity, Ns/m²
ν	Kinematic viscosity, m²/s
θ	Polar angle, radians
ρ	Reflectivity, density, kg/m³
σ	Stefan-Boltzman constant (5.67x10⁻⁸ W/m²K⁴)

Subscripts

a	Air
avg	Average
b	Bond
back	Back
backloss	Backloss
c	Convective
cell	Cell
cond	Conductive
conv	Convective
f	Fluid average
f,in	Fluid inlet
f,out	Fluid Outlet
fin	Section of the radiant panel
flux,in	Incoming flux
i	Inner, surface
i-j	From surface i to surface j
ins	Insulation
j	Surface
o	Outer
out	Out
p	Pipe
panel	Panel

panel-j	Panel to surrounding surface, j
PEX	PEX
rad	Radiative
sur	Surrounding
w	Water
wall	Wall

Abbreviations

MRT	Mean Radiant Temperature
MWT	Mean Water Temperature
RSC	Reverse Solar Collector

Chapter 1

Introduction

1.1   Background

In recent years, the U.S. and Canada have seen a steady increase in energy consumption. The U.S. in particular currently uses 25% more energy than it did 20 years ago, and it is forecasted that this trend will continue for the next 20 years (DOE, 2005). With a decline in natural resources, and an increase in fuel costs, it has become important to find methods of reducing energy consumption and finding alternative energy sources. When looking at the statistics for energy consumption, a significant portion is spent on heating and cooling of buildings. In the U.S commercial sector, 25% of the total energy consumption is used for space heating and cooling alone (DOE, 2005) (Figure 1.1). For the U.S residential sector, 32% of the energy goes towards space heating and 11% towards space cooling (DOE, 2005).
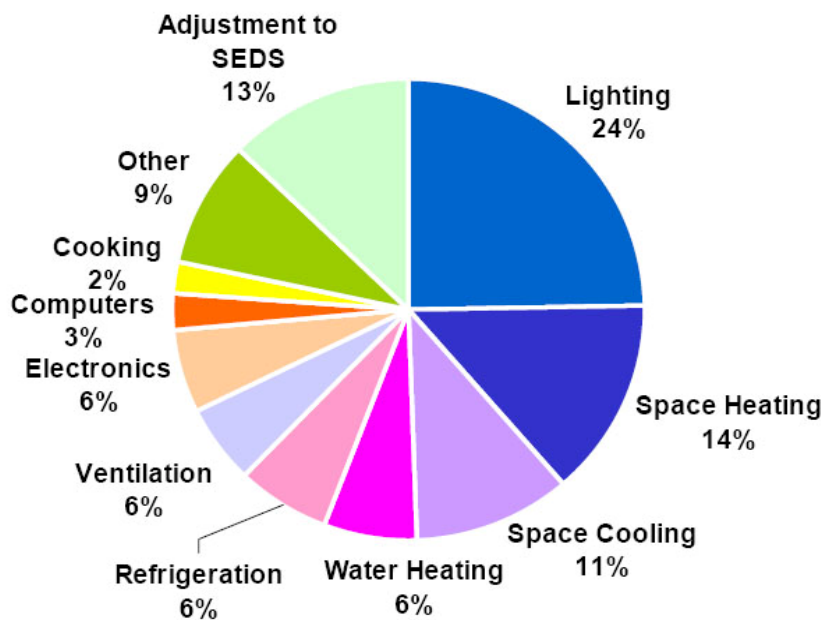
Figure 1.1: Commercial Energy use break down for the U.S. (DOE, 2005)

Over the last few years energy conservation in space heating and cooling has become a widely researched area. Energy can be saved by improving the insulating values in walls and windows, controlling the solar heat gain to a room by using shading devices, or by reducing the heating and cooling load in a building by adjusting temperature set points. The temperature set points impact occupant comfort and are established through convective heating systems, such as baseboard radiators and ducted HVAC systems. To adjust the temperature set points without sacrificing occupant comfort, radiant panels can be used.

A radiant panel is a temperature controlled surface in a conditioned space, in which 50% or more of the heat transfer is through radiation (ASHRAE, 2003). A constant temperature can be maintained through electric resistance elements or by circulating water or air through tubes mounted on the backside of the surface. The benefits of such systems are that through the radiant heat transfer, surfaces in the conditioned space can be warmed or cooled, while maintaining a lower than normal ambient air temperature.

Radiant panel systems have been in existence for centuries. Radiant heating dates back to the Romans in 50 BC, when they constructed their buildings with hollow floors to allow hot gases from the central fire to travel under the floor (Adlam, 1949). The tiles above the floor would warm up, giving way to a radiant heating system. The heating source did not change until 1790 when hot water was introduced as the working fluid. Sir John Stone set up a system in London, U.K. by placing several large pipes, behind or under grilles, carrying hot water from a boiler. In 1908 radiant heating was introduced on a commercial basis (Adlam, 1949). Professor Arthur H. Barker discovered that small hot

water pipes embedded in plaster or concrete made an efficient heating system. The principles behind radiant heating have since then remained the same.

Thus far, Europe has been the leader in utilizing these systems for a wide variety of commercial and residential applications (Simmonds, 1996). In Germany, more than 50% of newly constructed buildings and residences incorporate radiant panel systems (Kilkis et al., 1994). In North America however, designers have rarely used radiant panel systems, believing the North American climate was not suitable for such systems (Buckley, 1989), believing cooling and heating loads could not be met.

Today, radiant ceiling panels are constructed from copper tubing bonded, pressed or clipped onto an aluminum extruded sheet or a heat conducting rail glued onto the back-side of the panel (ASHRAE, 2004). Depending on the design constraints and desired energy output, the copper tubing can be run in a serpentine circuit, Figure 1.2a, or as a parallel circuit, Figure 1.2b.

T_{in}

T_{in}

T_{out}

T_{in}

T_{out}

a) Serpentine Circuit   b) Parallel Circuit
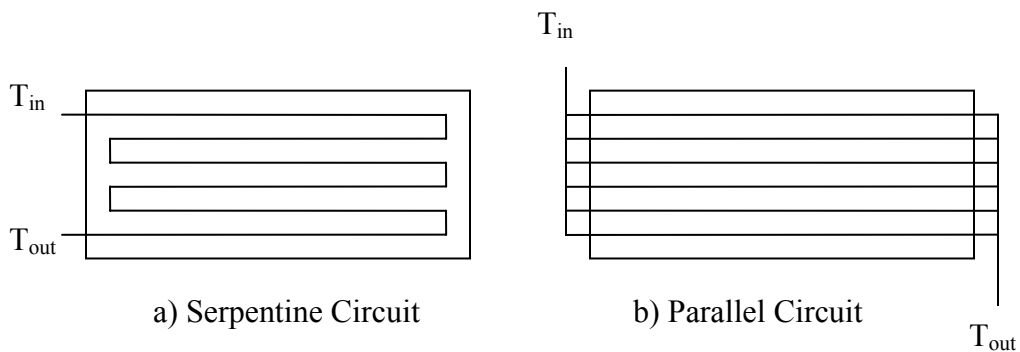
Figure 1.2: Serpentine and Parallel Radiant Panel Circuits

The panels are specified based on their width and number of passes. Imperial units are always used in North America to specify radiant panel sizing, so for a typical 36 inch, 6 pass radiant panel, a 36-6 panel would be specified. A 36-6 serpentine radiant panel manufactured by Sigma Convectors is shown in Figure 1.3.

Figure 1.3: 36-6, Perimeter Radiant Heating Panel, Back-side shown

Recent studies have shown that human comfort can be obtained by radiant transfer in any type of climate (Buckley, 1989), leading to a recent emergence of radiant heating/cooling applications in North America. Typical residential radiant panel systems are grid coils in the floor or copper tubing systems in the ceiling. In office buildings and schools, copper tubing ceiling panels are used as perimeter heaters to balance out the heating load and minimize mechanical equipment noise. In hospitals, perimeter radiant panel heating and cooling systems are ideal, providing a draft free, thermally stable environment.   Other applications include swimming pools, residential buildings and general space heating or cooling in industrial buildings (Shoemaker, 1954).

When designing radiant heating or cooling systems, the size, temperature and location of the panel are important factors affecting the performance of the system and the thermal comfort of the occupants. Properly designed systems can produce long term energy savings of up to 30% (Conroy, 2001). Thermal discomfort, however, can occur if the panels are not properly sized. In order to achieve the desired comfort level, it is important that the heat output of a radiant panel be estimated accurately within the context of the room and building. If the correct panel size is not chosen, energy savings may not be realized and comfort levels not satisfied.

1.2   Industrial Motivation

The number of manufacturers producing radiant panels is growing every year. In the early 1990's, Europe saw a 20% increase of radiant panel manufacturers in one year, leading to various products promising performance capabilities unattainable in actual scenarios (Kochendörfer, 1996). With no standardized test in place, a European rating standard was developed (DIN 4715, 1994).

Currently, the use of radiant panels in North America is increasing. One manufacturing company, Sigma Convectors, has predicted an increase of 300% in sales over the next year in radiant heating panels alone (Kramer, 2005). With an increase in market demand for radiant panels, many companies strive towards selling low-cost and high performance panels. Similar to Europe, manufacturers have rated their products with insufficient descriptions of testing conditions, leading to the need for North America to develop a standardized test and rating method as well.

Sigma Convectors currently manufacturers various air and hydronic heating and cooling systems. With the increasing need to verify heating and cooling outputs from heating and cooling panels, they contacted the University of Waterloo to help develop a radiant panel test booth. Their ultimate objective with this test booth was to be able to showcase their products to potential customers, and to show them in progress testing of their radiant panels.

1.3   Analytical Motivation

Various theoretical/experimental results show that radiant systems have the potential to achieve energy savings up to 30% (Laouadi, 2004). Currently, manufacturers of these systems simply approximate the required panel sizing for panel heating/cooling

5

applications from experimental data. Often times, the panels specified are not optimized for the required application. It is therefore ideal to develop an accurate prediction model capable of helping building and system designers to specify and size radiant systems.

1.4   Objectives

Although space heating and space cooling energy savings are equally important to the North American climate, the focus of this thesis was on radiant heating. This is because the sponsoring company manufactures and distributes radiant heating panels, and limited research has been done in heating applications. The specific objectives of this thesis are:

1.   To construct a radiant panel testing facility based on existing and potential standards.

2.   To develop an analytical model for predicting the mean radiant ceiling panel temperature and heat output based on size, tube spacing, water flow rate and inlet water temperature.

3.   To numerically model the test chamber to predict the natural convective heat transfer from a ceiling mounted radiant panel over various panel temperatures and sizes.

4.   To validate the analytical model with experimental results obtained from the radiant panel test chamber.

1.5   Thesis Outline

Chapter 2 presents a literature review on the radiant ceiling panel topic. Theoretical models, radiant panel test chambers and potential or existing standards will be discussed.   In particular any models used to predict the mean radiant panel temperature will be examined as well as any correlations developed to predict the convective heat transfer from a heated ceiling panel.

Chapter 3 discusses the construction of the radiant panel test facility and the results obtained.

Chapter 4 presents the development of the analytical model used to predict the panel temperature and heat output. In addition to the analytical model, Chapter 4 will present a CFD model used to predict the natural convective heat transfer inside the test chamber and show derivations to calculate the radiative and conductive heat transfer coefficients. The obtained values will be compared to current accepted models.

Chapter 5 presents the validation of the analytical model. Discrepancies between the analytical model and experimental results will be discussed.

Chapter 6 presents the summary, conclusions and recommendations resulting from this research.

Chapter 2

Literature Review

As a significant portion of this thesis is dedicated to the development of an analytical model used to predict the panel heat output and mean radiant panel temperature. This Chapter will begin with a literature review of existing radiant panel prediction models. Following this, particular emphasis will be placed on research done to determine the radiative and convective heat transfer coefficients for the system. Finally, a review of any existing radiant panel test chambers will be discussed as well as any standards currently used to rate radiant panels.

2.1   Existing Mean Radiant Panel Temperature Models

The earliest model used to predict the radiant panel temperature was developed in 1943 (Heid and Kollmar, 1943), using the assumption that the radiant panel operated like a plate fin with heat losses from the upper surface (Figure 2.1). With the knowledge of the radiative, convective and conductive heat transfer coefficients, a fin efficiency was calculated. This enabled the authors to predict the mean radiant panel temperature based on the mean water temperature (MWT).
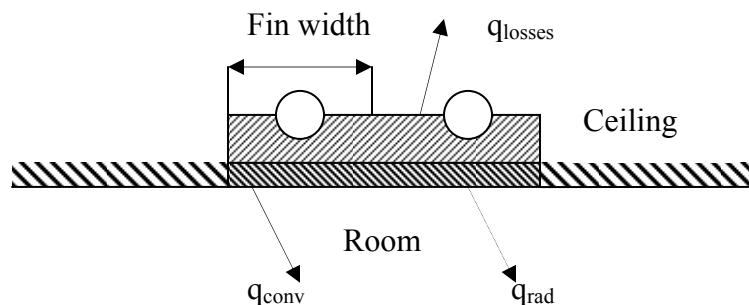
Figure 2.1: Cross section of a Radiant Panel

Approximately 40 years later, as computational power improved significantly, a finite difference algorithm was developed to study the heat transfer characteristics of a radiant ceiling panel (Zhang and Pate, 1986). Using a 2D numerical model, the authors modelled the transient and steady state temperature distribution across the panel. This enabled them to investigate the effects of tube spacing and the convective heat transfer coefficient on the panel performance. Their numerical results were in good agreement with some of their experimental results. They found, however, that it was difficult to evaluate their numerical model because no exact analytical solution existed.

Kilkis et al., (1994) developed an analytical model to estimate the heating capacity based on pipe spacing and mean water temperature. Using the practical fin ceiling model from Heid and Kollmar (1943), the authors showed that the heat output from the panel, q_{panel}, could be calculated as follows:

$$q_{panel} = \frac{\pi}{\frac{1}{h_w D_i} + \frac{1}{2k_p}\ln(\frac{D_o}{D_i})}(T_o - T_f)\frac{1000}{W}$$

(2.1)

where: h_w is the convective heat transfer coefficient of the water
k_p is the conductivity of the pipe
T_o is the outer surface temperature of the pipe
T_f is the average water temperature
W is the pipe spacing
D_o and D_i are the outer and inner pipe diameters respectively

The authors then used the fin efficiency model from Heid and Kollmar (1943) to predict the panel temperature based on heating load. Although they presented a case study to show the effectiveness of radiant floor heating, the model was never validated with experimental results.

Conroy et al. (2001) presented a novel approach to predicting the mean radiant panel temperature. Recognizing that radiant cooling panels were constructed very

similarly to flat plate solar collectors, the authors showed that using the solar collector model of Hottel, Whillier and Bliss (1958) the mean panel temperature could be calculated as follows:

$$T_{p,mean} = T_{f,in} + \frac{\dot{m}C_p(T_{f,out} - T_{f,in})}{A_{panel}F_R U_L}(1 - F_R)$$
(2.2)

where: $\dot{m}$ is the mass flow rate of the panel
C_p is the specific heat of water
$T_{f,in}$ and $T_{f,out}$ are the inlet and outlet fluid temperatures respectively
A_{panel} is the surface area of the panel
F_r is the heat removal factor
U_L is the overall heat transfer coefficient

The authors went on to use this model to show how effective radiant cooling ceiling panels could be in the North American climate. They never verified this model, however, with the previously presented solutions or any experimental data.

Hadlock (2004) studied the possibility that the flat plate solar collector model could be used for radiant heating applications. In comparison to the classical fin-tube model developed by Heid and Kollmar (1943), Hadlock showed that the flat plate collector model was within 13% of the predicted heat output. As the analytical models were compared to heating performance curves provided by Sigma Convectors (Sigma, 2004), the results were only within 40% of actual values, leading to the desire to develop a test chamber to determine actual radiant panel heat outputs under known conditions.

In 2005 the solar absorber model was further improved by modeling radiant cooling panels with heat conducting rails (HCR) (Figure 2.2) (Xia et al., 2005). The analysis is very similar to the existing solar collector model. It accounts, however, for the heat transfer through the heat conducting rail in Equation 2.2. Similar to the previously developed models, an equation was developed that was used to predict the radiant panel

temperature based on a mean water temperature (MWT). Again, this method was not validated.
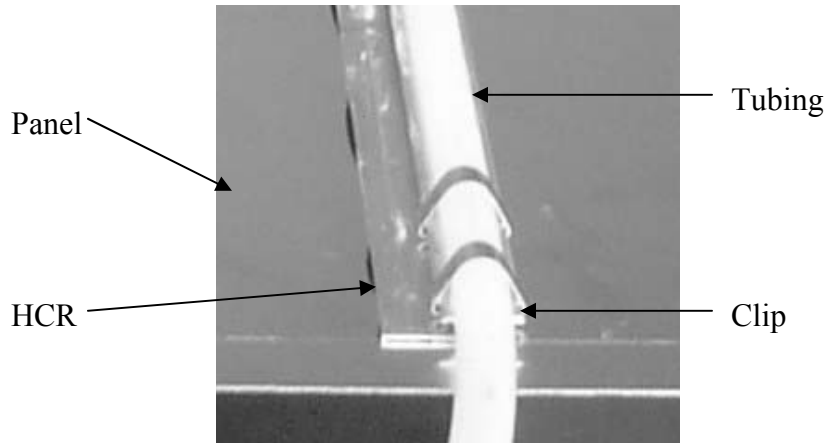
Figure 2.2: Cross-section of a Radiant Panel with Heat Conducting Rails

Each of the preceding models require an overall heat transfer coefficient that includes radiative and convective heat transfer. Sections 2.2 and 2.3 will review existing methods and correlations used to calculate an overall heat transfer coefficient.

2.2   Existing Radiant Interchange Models

To determine the net radiative heat transfer in an enclosure, the fundamental radiative heat transfer equation can be used.

$$q_{rad}^{"} = \sum_{j=1}^{n} \sigma F_{panel-j}(T_{panel}^{4} - T_{j}^{4}) \tag{2.3}$$

where: σ is the Stefan – Boltzman constant
   n is the number of surfaces
   $F_{panel-j}$ is view factor between panel surface and surrounding surface j
   T_{panel} is the radiant panel temperature
   T_{j} is the surrounding surface temperature

Several models have been developed to simplify the net radiative heat transfer calculation, minimizing the need for complex view factor calculations.

Walton (1980) presented an algorithm, known as the mean radiant temperature (MRT) method, which predicted the radiant interchange between surfaces in a room. This method assumes a fictitious surface represented the surrounding enclosure with a similar temperature and emissivity as the enclosure it replaced. This method simplifies a system greatly because only two surfaces need to be analysed. It has been shown, however, that this method is only applicable for cases where the temperature difference between the radiant panel and surrounding enclosure surfaces is not great.

To improve the accuracy of the MRT method, an MRT correction method was presented by Steinman et al. (1989). Using the MRT equation developed by Walton (1980), and adding a correction component accounting for exact view factors, the panel heat flux was shown to be:

$$q_{rad}^{"} = \sigma \left[\left(\frac{\sum_{j \neq i}^{n} A_j T_j}{\sum_{j \neq i}^{n} A_j} \right)^4 - \sum_{j \neq i}^{n} F_{panel-j} T_j^{\,4} \right] \tag{2.4}$$

This method required more computational time because of view factor calculations, but is more accurate than the previous uncorrected MRT method.

2.3   Existing Convective Heat Transfer Models

Limited research has been done to determine the convective heat transfer coefficient from radiant ceiling panels because it is typically deemed to be negligible. The earliest study on convective heat transfer was done in 1956 in the American Society of Heating and Ventilating Engineers (ASHVE) environment laboratory by Min et al. (1956). To determine the convective heat transfer from a radiant ceiling panel, temperature gradients below the panel were measured for three different sized rooms,

12

without any air infiltration and ceiling panel temperatures ranging from 32°C to 65°C. The walls and floor were maintained at a constant temperature and the entire ceiling was used as a radiant panel. The results obtained from the experiment are plotted in Figure 2.3.
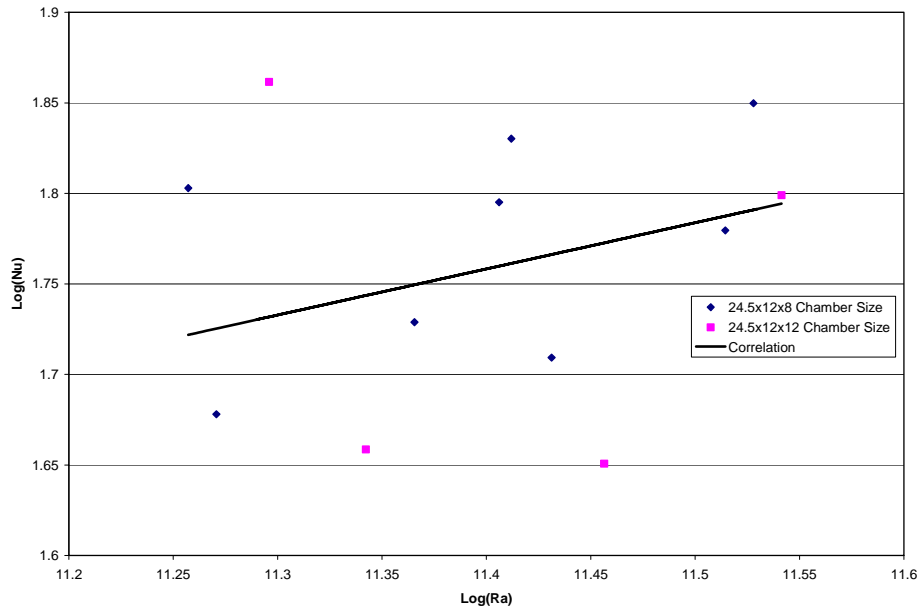
Figure 2.3: Convective Heat Transfer from a Radiant Ceiling Panel (Min et al., 1956)

A convective heat transfer correlation was developed.

$$q_c^{"} = 0.2(T_{panel} - T_a)^{1.25} / D_H^{\,0.24} \qquad (2.5)$$

where: T_a is the air temperature (1.5m above the floor)
D_H is hydraulic diameter of the radiant panel (4xPerimeter/Area)

The R^2-value (correlation coefficient) from Figure 2.3 was found to equal 0.04, reflecting the wide range of scatter in the plot and significant error associated with the correlation.

Schutrum and Vouris (1954) concluded that the effects of room size on panel performance of heated ceiling panels was relatively small and Equation 2.5 could be simplified to:

$$q_c^{"} = 0.138(T_{panel} - T_a)^{1.25}$$ (2.6)

The authors conclusions, however, were based only on completely heated ceilings.

Awbi and Hatton (1999) questioned the accuracy of the measurements of the previous experiments and constructed their own test chamber. They used the most accurate temperature measurements techniques available to determine the natural heat transfer coefficient and their tests covered a wide range of heated ceiling conditions and chamber sizes. They gave no mention, however, of the exact radiant panel setup. The air temperature in the chamber was maintained at 20°C by adjusting the wall and floor temperatures. It was also known that one wall was maintained at a much colder temperature than the other surfaces. The test results for the various heated panel sizes showed great variation (Figure 2.4) and a heat transfer coefficient was correlated shown in Equation 2.7.
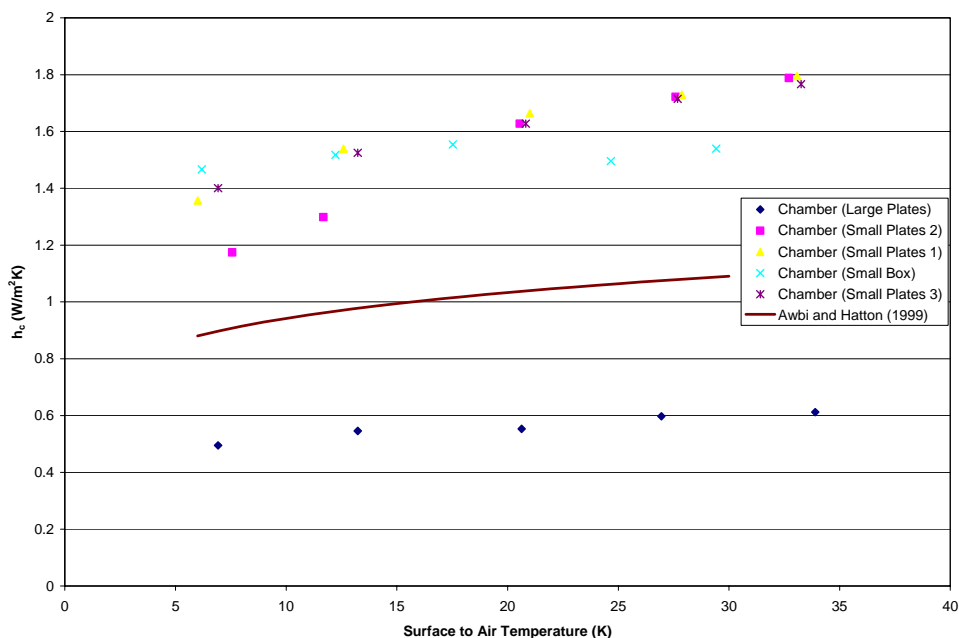
Figure 2.4:   *Experimental Results for the Convective Heat Transfer Coefficient for a Radiant Ceiling Panel (Awbi et al., 1999)*

14

$$q_c^" = \frac{0.704(T_{panel} - T_a)^{1.133}}{D_H^{0.601}}$$ (2.7)

The correlation coefficient for Equation 2.7 was shown to be equal to 0.87. Although Figure 2.4 shows a wide range of scatter, it can be concluded that the room size and panel size affect the natural convection coefficient for perimeter radiant ceiling panels, contrary to the conclusions from Schutrum and Vouris (1954).

Comparing the correlated convective heat transfer correlations from Min et al. (1956), Schutrum and Vouris (1954) and Awbi and Hatton (1999) in Figure 2.5 for a panel hydraulic diameter of 1.025m, the total heat transfer can be off by as much as 60% if the incorrect correlation is used. It is therefore necessary to accurately determine the convective heat transfer from a radiant ceiling panel.
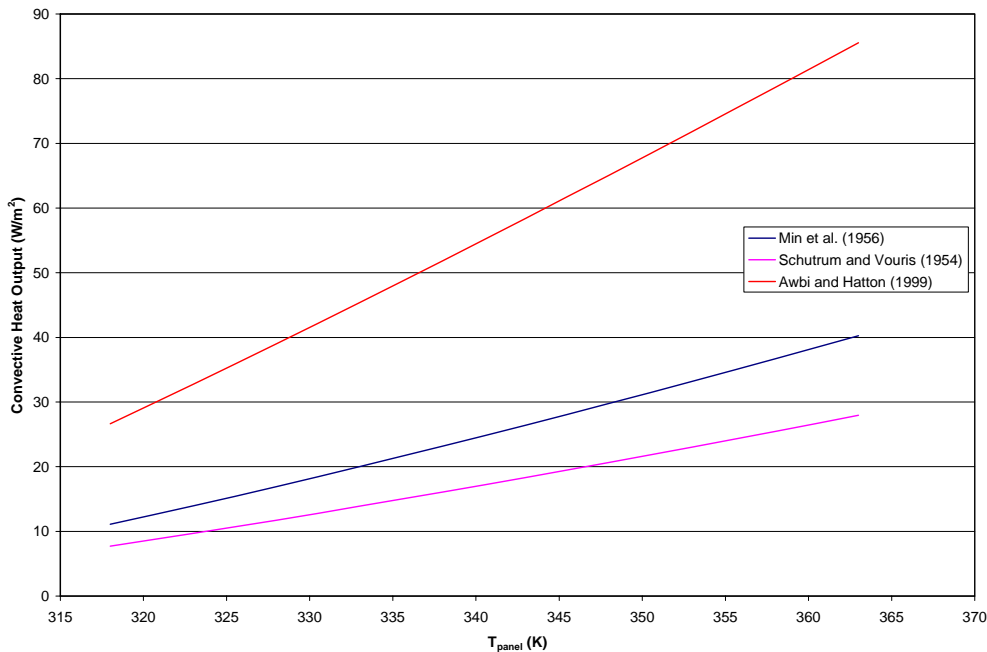
Figure 2.5:   *Comparative plot of the Convective Heat Flux Correlations developed by Min et al. (1956), Schutrum and Vouris (1954) and Awbi and Hatton (1999)*

2.4 Currently Accepted Radiant Panel Model

The 2004 American Society of Heating, ventilating and Air-Conditioning Engineers (ASHRAE) HVAC Systems and Equipment Handbook (ASHRAE, 2004) summarizes the standard radiant panel model. Walton's MRT method (1980) is considered to be an acceptable method to determine the radiant heat exchange in a simple enclosure. For a two surface radiation heat exchange, the thermal radiation for a panel is shown to be:

$$q_{rad}^{"} = 5*10^{-8}[(T_{panel} + 273.15)^4 - (AUST + 273.15)^4] \qquad (2.8)$$

where: AUST is the area-weighted temperature of the non heated indoor surfaces

The natural convective heat transfer was calculated based on the studies from Min et. al. in the ASHVE test facility (1956). For a heated ceiling surface the convective heat transfer is shown to be:

$$q_c^{"} = 0.20\frac{(T_{panel} - T_a)^{1.25}}{D_H^{0.24}} \qquad (2.9)$$

2.5 Existing Test Facilities for Radiant Heating

Tasker, Humphreys, Parmelee and Schutrum (1952), describe an ASHVE Environment Laboratory capable of testing radiant ceiling and floor panels in a cooling or heating mode. Measuring 7.3m long by 3.66m wide by 3.66m high, the chamber was capable of testing the panels under a wide variety of surrounding temperature conditions and chamber infiltration rates. Serpentine and parallel copper tubing circuits were mounted on the exterior of the walls, ceiling and floor to establish constant temperature and ethylene glycol was used as the working fluid. Copper tubing was arranged such that each surface could be individually controlled to simulate a hot or cold wall, floor and

ceiling. Any combination of wall temperatures was attainable. In addition, an air guard barrier was constructed around the walls to ensure the surface temperatures would remain constant. The temperatures of the walls, ceiling and floor were measured using approximately 400 thermocouples and heat flow meters were used to measure the heat exchange between the surfaces of each wall. The heat flow meters accurately measured the temperature difference between opposite sides of a thermal resistance layer and were set up to measure low rates of heat flow (Huebscher et al., 1952). In order to give a detailed account on variables which affect the performance of radiant panels, air temperature, air temperature gradients and air motion were also measured. It should be noted that this facility was constructed to ultimately become a psychometric laboratory, so it contained additional instrumentation and capabilities that are not required for just a radiant panel test facility.

2.6   Radiant Panel Standards

The German Standardization Institute (DIN) developed a radiant cooling panel standard (DIN 4715, 1994), which has become widely accepted in Europe. The standard states that a cooling panel is to be tested in a 4m long by 4m wide by 3m high room, with temperature controllable walls (Kochendörfer, 1996). No additional ventilation is to be added to the room and the cooling panel must cover at least 70% of the ceiling. To simulate actual conditions, 12 electric heaters are used to simulate people who require cooling. The radiant panel cooling load is determined by measuring the inlet and outlet fluid temperature difference.

An ASHRAE standard for testing hydronic radiant ceiling panels has been developed, and is currently in a public review process (Chapman, 2005). The radiant

panel is to be tested in a 3.66m wide by 3.66m long by 3m high chamber, in which three walls and the floor are maintained at a constant temperature of 20°C and the back (cold) wall at 10°C. The radiant panel is to be installed above the cold wall to offset the heat los caused by a cold window. Figure 2.6 is a sketch of the proposed radiant panel test facility and location of the radiant panel relative to the chamber surfaces. Each surface of the enclosure is to be divided into quadrants and the temperature measured at the geometric center of each quadrant. The inlet and outlet water temperature difference across the heating panel is measured and the output is calculated knowing the water flow rate. The details of the proposed standard can be found in Appendix A.
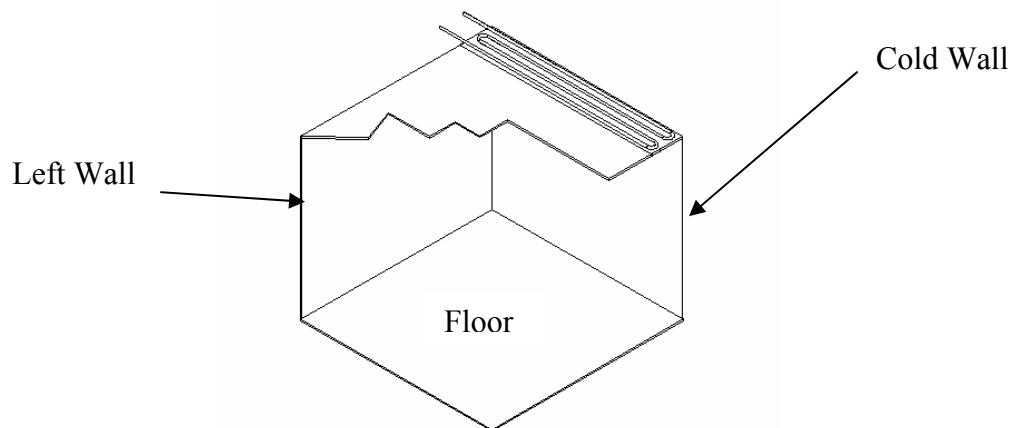
Figure 2.6: ASHRAE Proposed Radiant Panel Test Chamber

Chapter 3

Radiant Panel Test Chamber

This chapter describes the construction of an experimental facility that can be used to rate and test the radiant panels. Details of the test method are also summarized. The chamber can simulate a wide range of test conditions, while giving an accurate estimate of the panel heat output. The test chamber was built to test a line of Sigma Convector radiant panels and to demonstrate the effectiveness of radiant perimeter heating to potential customers.

3.1 Purpose of Test Facility

Radiant heating panels are directly influenced by particular environmental conditions. Therefore, the primary purpose of the test facility is to create a testing environment with known surrounding conditions. As stated in Chapter 2, radiant panels are dominated by two modes of heat transfer – convection and radiation. The convective heat transfer is dependant on the surrounding air temperature, air motion and enclosure size, while the radiative heat transfer is dependant on surrounding surface temperatures, surface emissivities and chamber size.

The radiant panel heat output (q_{out}) can be calculated theoretically by adding the conductive (q_{cond}), convective (q_{conv}) and radiative (q_{rad}) heat transfer.

$$q_{out} = q_{cond} + q_{conv} + q_{rad} \tag{3.1}$$

Measuring each mode of heat transfer can become difficult and tedious, and might lead to a significant error. Alternatively the total heat output (q_{out}), including losses, can be determined using:

$$q_{out} = \dot{m}C_p(T_{f,in} - T_{f,out}) \tag{3.2}$$

By accurately measuring the flow rate and temperature change across the panel an accurate heat output can be determined for a known air temperature and specific heat, C_p.

3.2   Radiant Panel Test Chamber Construction

It was decided to construct a radiant panel test facility according to the ASHRAE Draft Standard 138P (Appendix A). The test chamber, however, was sized according to the DIN cooling standard test chamber (Kochendörfer, 1996).   The details and specifications of the test chamber (Figure 3.1) are listed below:

- The chamber is to be 4m by 4m by 3m high
- The back wall (exterior wall) is to be maintained at $10^{o}C$ +/- $0.5^{o}C$
- The other surrounding walls and floor are to be maintained at $20^{o}C$ +/-$0.5^{o}C$
- The radiant panel should be mounted within 2.54 cm from the back wall
- The emissivity of the walls should be 0.9
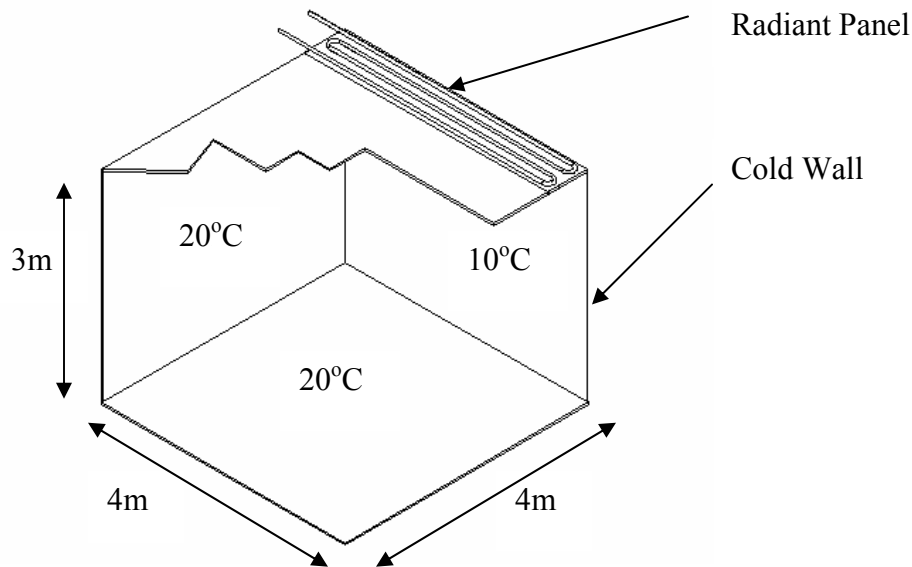
Figure 3.1: Cut Away Sketch of Radiant Panel Test Facility

The construction of the test booth is shown in Figures 3.2 and 3.3.

Figure 3.2: Test Booth Construction – Indoor View of Walls
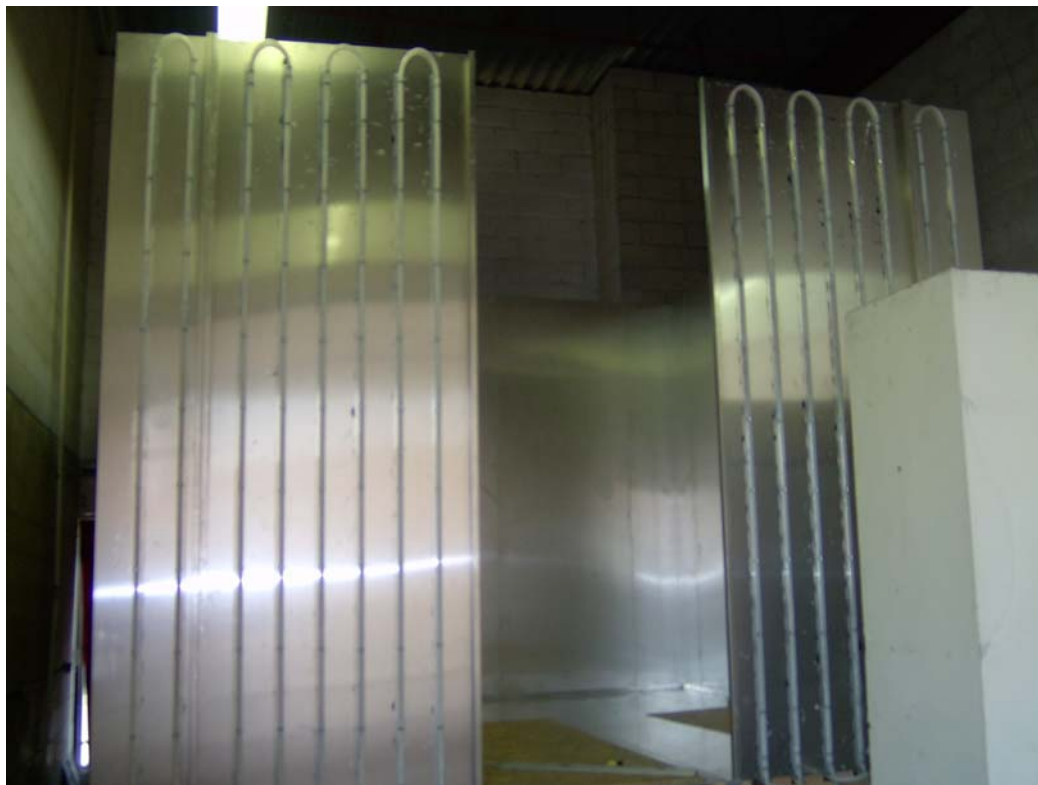
Figure 3.3: Test Booth Construction – Outdoor View of Walls

3.2.1   Temperature Controllable Walls

To maintain a constant surrounding temperature the four walls and floor must be temperature controllable and made from highly conductive material. It was decided to mount cross-linked polyethylene (PEX) tubing on the exterior of each wall and the floor, while controlling the temperature by circulating water from a constant temperature source.   The wall material was made out of aluminum because of its excellent conductivity and reasonable cost. The PEX tubing was clipped onto heat conducting rails (HCR), which were glued onto the exterior of the aluminum panels (Figure 3.4). Also shown is an insert of the cross section of the tubing mounted on the wall
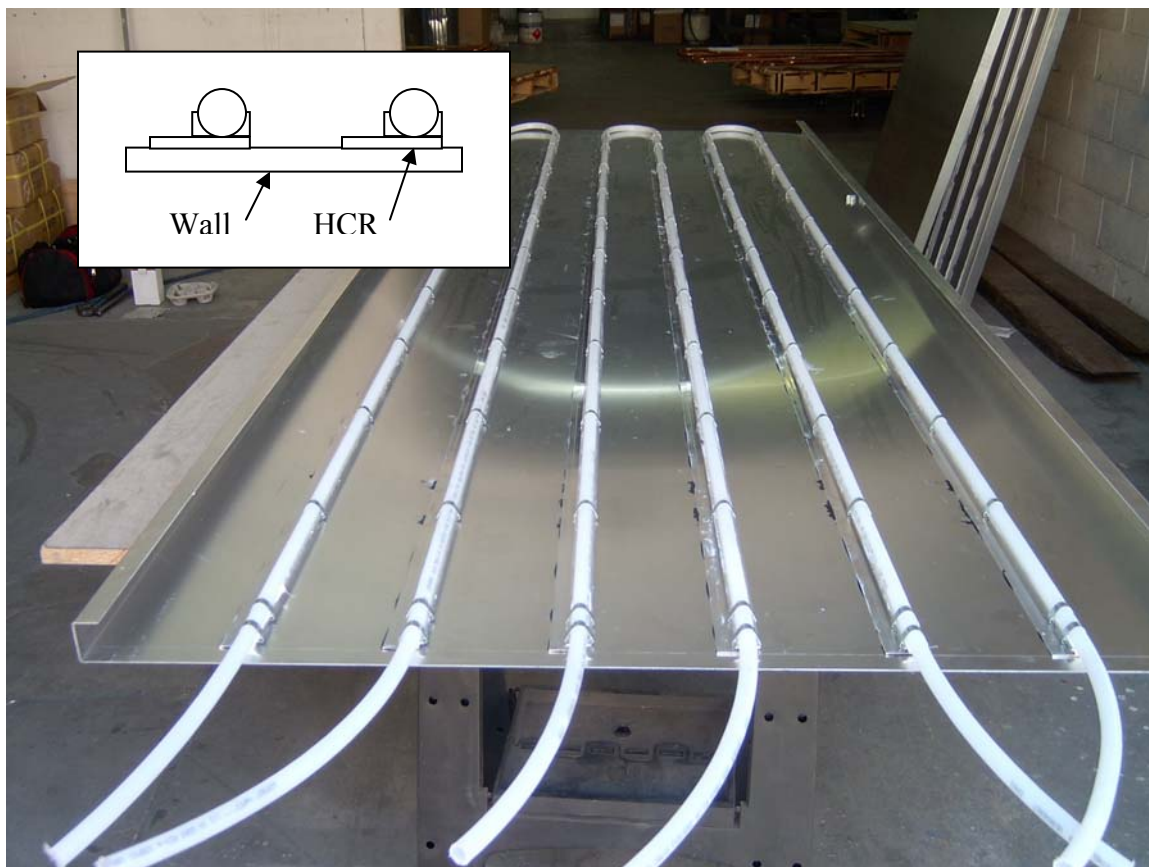
Figure 3.4: Mounting PEX Tubing to Exterior Surface of Chamber Wall

To optimize the heat transfer and temperature controllability of the walls and floor, several improvements were suggested. For example, clipping copper tubes onto the back of each surface and building an enclosure around the chamber to maintain a constant surrounding air temperature would have been useful. With a limited budget, however, these suggestions were deemed unfeasible and PEX tubing was used instead of copper and the exterior walls were heavily insulated, minimizing heat loss or gain from the back of the wall.

The walls and floor were painted with a high gloss white paint to reduce reflectivity for long wave radiation. Infiltration into the room was prevented by taping over the seams of wall and floor using Turf® tape (Figure 3.5).

To determine the necessary pipe spacing, an energy balance at each wall had to be performed. Neglecting the temperature difference between the exterior and interior of the wall and assuming the back losses to be negligible, the energy balance gives:

$$q_w = q_{rad} + q_c \tag{3.3}$$

where: q_w is the heat removed by circulating water
q_c is the convective heat transfer

To determine the amount of tubing required on the wall, the following assumptions were made:

- Wall emissivity was equal to 0.9 because it would be painted white
- Interior convective heat transfer coefficient was equal to 6 W/m²K (Awbi, 1999)
- Interior air temperature was equal to 22°C
- PEX tube thickness of 5mm with a conductivity of 20 W/mK
- Mean back wall water temperature was 9°C
- Mean surrounding wall and floor water temperatures were 18°C
- Negligible convective and conductive back losses from the exterior surfaces

Figure 3.5: Chamber Interior, Back, Left and Front Wall with Door

If the heat removed by the water is assumed to be equal to the net incoming radiative and convective heat transfer, then the radiant heat flux can be estimated as:

$$q_{rad}'' = F\varepsilon\sigma(T_{panel}^4 - T_{sur}^4) \tag{3.4}$$

where: T_{sur} is the surrounding surface temperature
ε is the emissivity of the surface

The tube spacing was designed for a 1.2 m wide panel at a temperature of 100°C. The view factors, F_{ij}, were calculated from first principles given by:

$$F_{ij} = \frac{1}{A_i}\int_{A_i}\int_{A_j}\frac{\cos\theta_i\cos\theta_j}{\pi R^2}dA_i dA_j \tag{3.5}$$

where: θ_i and θ_j are the polar angles between the surface normal
R is the radial distance from the point of interest to the surface of interest

The view factors were calculated using Mathcad 11, as documented in Appendix B, and the results are summarized in Table 3.1 below. To verify that the equation was correct, the view factor from the panel to the back wall was compared to a published view factor equation (Siegel and Howell, 1981) and all view factors were checked to add to unity.

Table 3.1: View Factors of Radiant Panel Test Chamber Surfaces

Surfaces (i – j)	View Factor
Panel – Back Wall	0.337
Panel - Floor	0.257
Panel – Front Wall	0.067
Panel – Left Wall	0.169
Panel – Right Wall	0.169

The convective heat transfer can be calculated knowing the heat transfer coefficient, h, and the temperature of the surface (T_{sur}) and air (T_a).

$$q_c = h(T_a - T_{sur}) \tag{3.6}$$

The difficulty was to determine an accurate convective heat transfer coefficient. Awbi and Hatton (1999) reported that the convective heat transfer coefficients for walls, floors and windows can vary between 1 and 6 W/m²K. Assuming the worst case, a heat transfer coefficient of 6 W/m²K was used to calculate the energy transferred through convection. With knowledge of the radiant and convective heat transfer, the amount of energy to be removed by the water can be calculated using Equations 3.4 and 3.6. The incoming heat flux for each wall and floor is summarized in Table 3.2 below and shown in Appendix B.

Table 3.2: Incoming Heat Flux for each surface

Surface	Temperature (K)	Incoming Heat Flux (W/m²)
Back Wall	283	260
Floor	293	143
Front Wall	293	46
Left/Right Wall	293	98

Using Fourier's law (Equation 3.7), the contact surface area of tubing required to balance out the incoming energy could be calculated

$$q_{out} = k_p A_p \frac{dT}{dx} \qquad (3.7)$$

where: dT is the temperature difference between the water and wall
dx is the distance between the surface of the wall to the inner portion of the pipe
A_p is the pipe contact surface area

Approximately 1/3 of the PEX tubing surface area is in contact with the heat conducting rail mounted to the wall. We can therefore approximate the surface area of the pipe to equal:

$$A_p = \frac{\pi D_o \ell}{3} \qquad (3.8)$$

where: ℓ is the total length in contact

Having calculated the heat flux on each wall (Table 3.2), the tube spacing, W, was determined by equating the heat flux to Equation 3.7 to obtain.

$$W = \frac{16k_{PEX}\pi D_o(T_{wall} - T_w)}{0.015q_{fluxin}A_{.wall}}$$

(3.9)

where: q_{fluxin} is the incoming radiative and convective heat flux

The tube spacing and pipe runs for each surface were calculated (Appendix B) and summarized in Table 3.3.

Table 3.3: Pipe Spacing and Pipe Runs

Wall/Floor	Pipe Spacing (m)	Number of Pipe Runs
Back Wall	0.27	15
Floor	0.75	6
Front Wall	3.07	2
Left Wall	1.44	3
Right Wall	1.44	3

It was ultimately decided to use the same number of pipe runs for each surface because it was desired to be able to mount the radiant ceiling panel anywhere in the chamber and have the capability of maintaining a cold wall temperature on any surface of the enclosure.

To ensure the wall temperature remained steady, the water was circulated through the pipes at a high flow rate, thus minimizing the water temperature change. The circulating water flow rate was calculated using:

$$q = \dot{m}C_p(T_{f,out} - T_{f,in})$$

(3.10)

For a 0.5°C water temperature increase, a flow rate of 0.125 L/s was calculated for the cold wall (Appendix B).

To select a pump, it was important to estimate the pressure loss across the serpentine piping circuit mounted on the walls. In total, 5 circuits were used for 5 walls,

each circuit having a separate pump. To account for any additional heat transfer, a total of 22 pipe runs were installed per wall. Seventy meters of PEX tubing was mounted to each wall and ninety meters was installed for the floor. The pressure drop across each circuit was approximated using the head loss equation (Munson et al., 2002):

$$h_L = f \frac{\ell}{D_i} \frac{V^2}{2g}$$
(3.11)

where: f is the friction factor
      V is the velocity
      g is the gravitational constant = 9.81m/s^2

The friction factor, f, was determined using a Moody Chart (Appendix B) with the knowledge of the Reynolds number given by:

$$\mathrm{Re} = \frac{\rho V D}{\mu}$$
(3.12)

where: ρ is the fluid density
      μ is the dynamic viscosity

Using PEX tubing, a smooth surface roughness condition could be assumed. Calculating a Reynolds number of approximately 15000 (Appendix B) a friction factor value of 0.027 was determined. To connect the pipe runs a total of 21 U-bends were used. The head loss caused by each U-bend was calculated using the following equation (Munson et al., 2002):

$$h_L = K_L \frac{V^2}{2g}$$
(3.13)

where: K_L is the loss coefficient

Using a K_L value of 0.2 for each U-bend (Munson, 2002), the pressure drop for each circuit was calculated (Appendix B) and summarized in Table 3.4.

Table 3.4: Pressure Drops for each circuit

Wall/Floor	Pressure Drop (kPa)
Back Wall	138
Floor	193
Front Wall	138
Left/Right Wall	138

The wall temperatures were maintained at a constant temperature using a motorized three way control valve. Using a data acquisition and control system, an average wall temperature was measured using 4 thermocouples located at the center of each surface quadrant. The motorized three way ball valve opens and closes to control the amount of cold water being mixed with the return water, thus ensuring a steady wall temperature. A diagram of the system is shown in Figure 3.6.

The chamber temperature conditions were maintained using two water storage tanks. The back wall had a separate storage tank, because it would require a cold water source no matter what the surrounding test conditions were. The other surfaces would require heating or cooling depending on the season (summer requires cooling, winter requires heating). The wall temperatures were controlled using a proportional-integral (PI) control loop, which compared the measured wall temperature to the set point temperature. If the wall temperature was above the set point, the analog output module from the data logging system would send out a voltage signal between 2 to 10V to energize the ball valve, thereby adjusting the amount of hot or cold water entering the system.
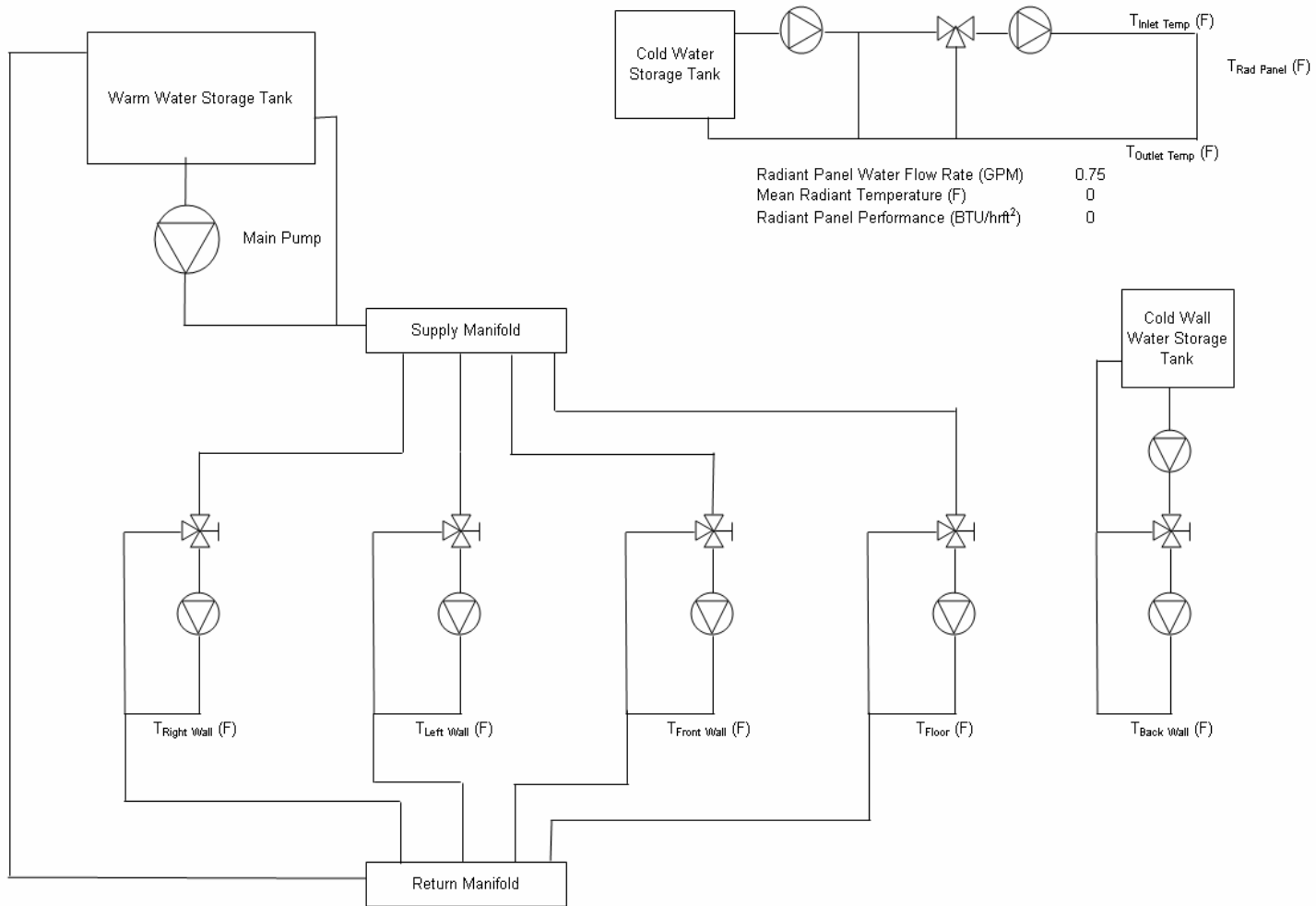
Figure 3.6: Radiant Panel Test Chamber Enclosure Temperature Control System

3.2.2 The Ceiling

The ceiling design was split into two parts. One part was made up of regular ceiling tiles heavily insulated to simulate an adiabatic surface. The second portion was the radiant ceiling panel insulated with ½" thick Batt insulation.

The radiant panel control loop was designed to behave in much the same way as for the walls. The panel was divided into six equal segments and panel temperature readings were taken at the center of each segment. The inlet and outlet temperature difference was measured using two thermocouples.

The temperature of the radiant panel was controlled based on the desired inlet water temperature and using a PI loop controlling the 3-way ball valve, adjusting the amount of hot water allowed into the system. The water flow rate was set and measured using a circuit balancing valve. A system schematic is shown in Figure 3.7.

Similar to the surrounding walls, the pump for the radiant panel was specified based on the desired flow rate knowing the overall pressure drop. Copper tubing was used to circulate the water because of the high water temperature (100°C). For the main line 1" copper tubing was used to minimize the pipe friction and ½" copper tubing was used for the radiant panel. The pumps were specified before construction of the radiant panel circuit, so the pressure was estimated by approximating pipe lengths. The maximum desired flow rate was 0.2 L/s, so a friction factor of 0.027 was estimated from the Moody Chart (Appendix B). With the known flow rate, the pressure drop was calculated to be 48.3 kPa (Appendix B) for the pipe circuit up to the radiant panel and the maximum radiant panel pressure drop was known to be 41.4 kPa, so a pump was selected which could supply 0.2 L/s at a pressure drop of 89.7 kPa.
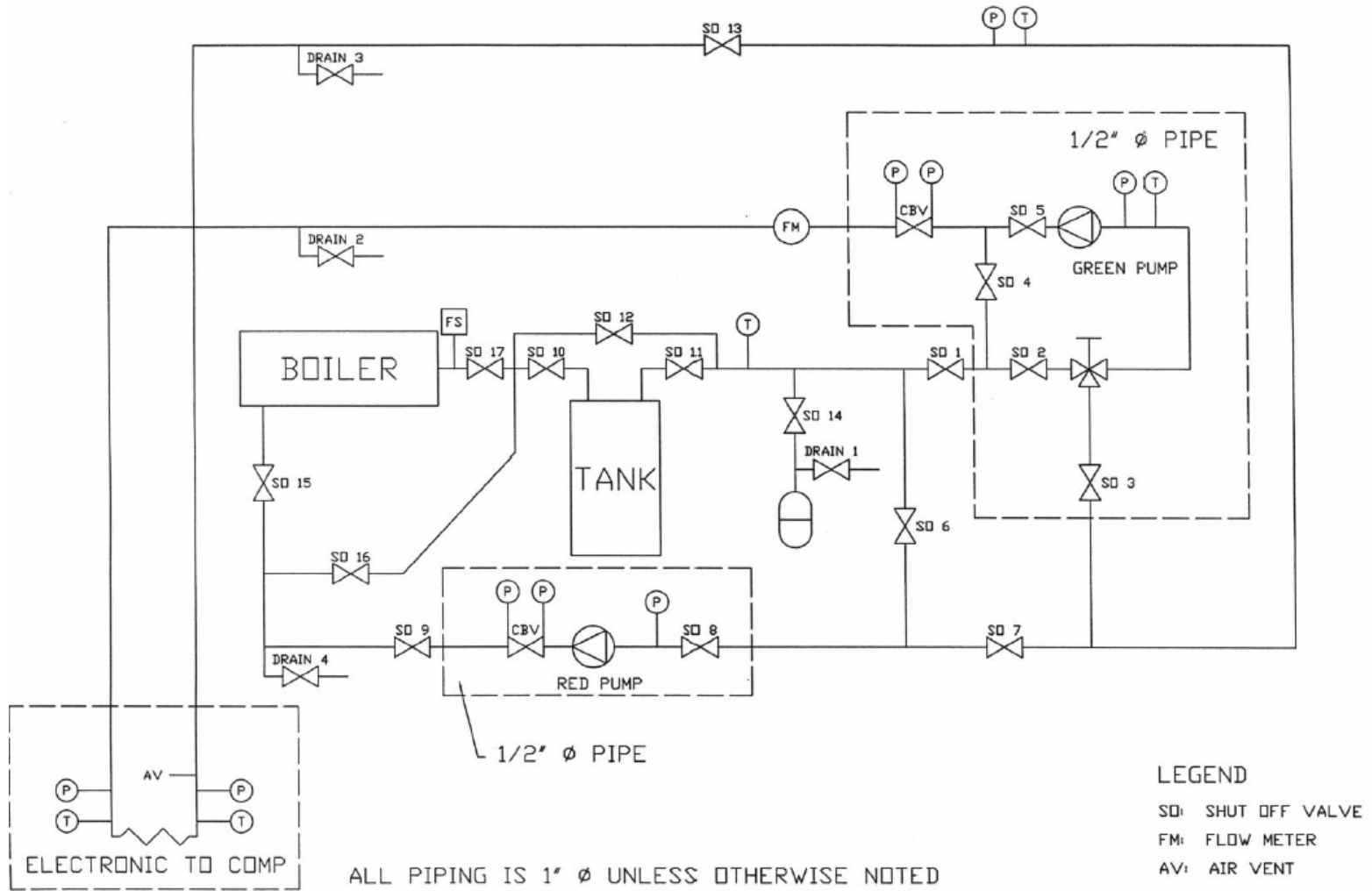
Figure 3.7: Radiant Panel Control Circuit

To minimize infiltration through the ceiling, all tiles were taped to prevent air flow into the room (Figure 3.8). The exterior of the completed test chamber is shown in Figure 3.9.

Tape

Radiant Panel
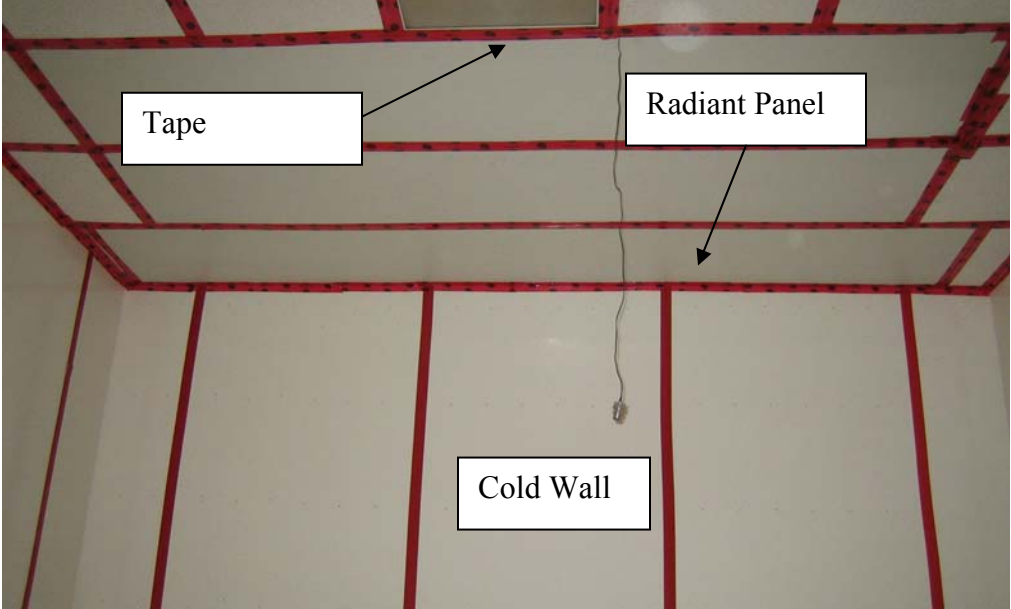
Cold Wall

Figure 3.8: Chamber Interior, Radiant Panel and Cold Wall

Insulation

Data Acquisition System

Figure 3.9: Overall View of Completed Radiant Panel Test Facility

3.3   Procedures and Data Processing

The temperature of each wall and floor was measured using four T-Type thermocouples (Omega). Each surface was divided into four quadrants and the temperature was measured and recorded at each quadrant center. The radiant panel surface temperature was measured using six T-Type thermocouples equally spaced over the radiant panel. To determine the radiant panel heat output the temperature difference between the inlet and outlet port of the radiant panel had to be measured. To minimize experimental error, a thermopile was assembled capable of measuring the temperature difference. The voltage measured from the thermopile was converted to a temperature reading. It was later discovered that the data acquisition system was not sensitive enough to measure the EMF voltage from the thermopile. As a solution, two regular T-Type thermocouples were installed at the inlet and outlet ports of the radiant panel. It was planned that these thermocouples would eventually be replaced with thermistors. Finally, the air temperature was measured using a shielded regular T-Type thermocouple suspended 1.8m above the center of floor. The variables measured during the experiment are listed in Table 3.5.

Table 3.5: List of Data Recorded from Experiment

Measured Quantity	Description
T_{in} and T_{out}	Radiant Panel Inlet and Outlet Temp (^{o}C)
$T_{backwall}$	Avg. Exterior Wall Temperature (^{o}C)
T_{floor}	Avg. Floor Temperature (^{o}C)
$T_{frontwall}$	Avg. Front Wall Temperature (^{o}C)
$T_{leftwall}$	Avg. Left Wall Temperature (^{o}C)
$T_{rightwall}$	Avg. Right Wall Temperature (^{o}C)
T_{air}	Center Room Air Temperature (^{o}C)

Using a Superlogics data acquisition system communicating with Dasylab (Dasylab, 2005), the average wall, floor, radiant panel and air temperatures were recorded

into excel along with the inlet and outlet radiant panel water temperatures. The Superlogics data acquisition system had 32 thermocouple input channels, 8 analog input channels and 8 analog output channels.

The wall temperatures and radiant panel inlet water temperature were controlled using the motorized three way ball valves. The valves were installed such that the hot or cold return water from the circuits would mix with the source temperature water. Using a PI controller in DasyLab (Dasylab, 2005), a voltage signal through the output modules was sent to the valve based on the average wall or inlet water temperature.

The radiant panel flow rate was determined by measuring the pressure difference across the circuit balancing valve. Two Omega analog pressure gauges were used to measure the pressure and then converted into a flow rate using the conversion chart supplied with the valve (Armstrong Pumps, 2006) (Appendix B). Ideally, a pressure differential should be read across the circuit balancing valve and then converted to a flow rate, however, due to budget limitations, no differential pressure gauge was installed.

3.3.1 Test Procedure

To determine the radiant panel temperature and heat output under known surrounding conditions, the walls, floor and radiant panel had to be maintained at their desired temperatures. To begin the experiment, the surrounding surfaces and radiant panel were brought to their corresponding set point temperatures and held at constant temperatures for as long as possible. Running a steady state temperature test as shown in Figure 3.10, the stabilization time took approximately 1 hour (Appendix C).
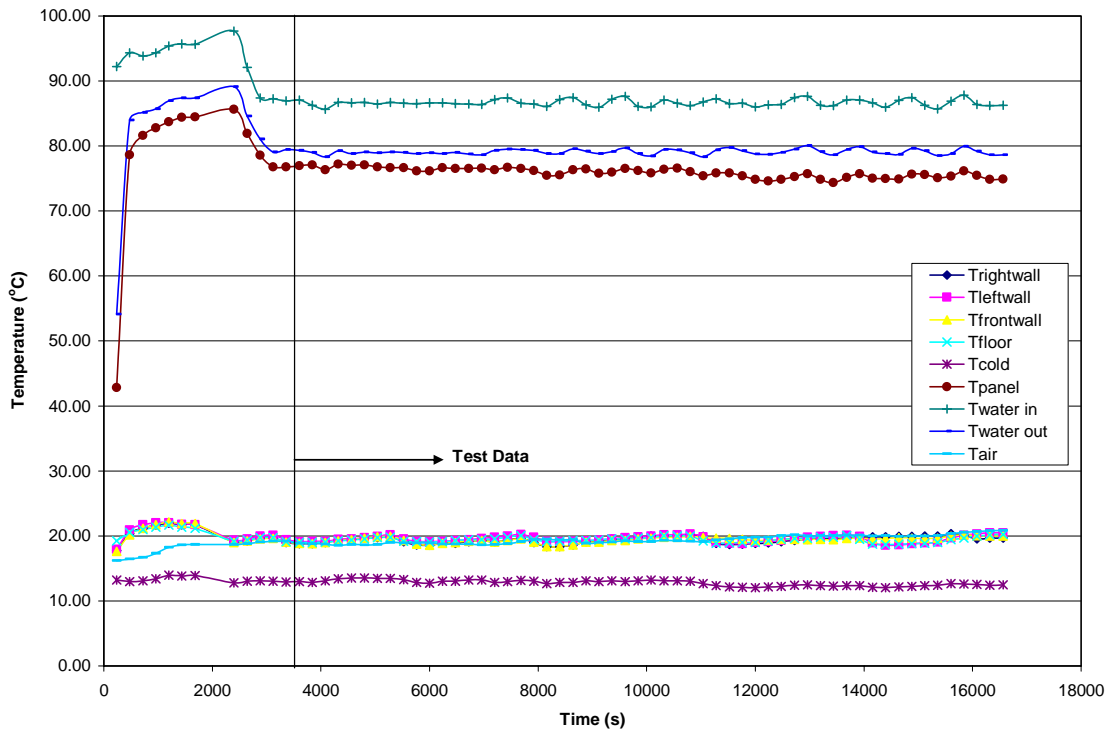
Figure 3.10: Surface and Water Temperature versus time

Once the walls were maintained at a steady state, temperature measurements were taken every 4 minutes for at least 30 minutes.

3.3.2   Test Samples

Two sample radiant panels were tested. A 24 inch, 4 pass (24-4) and a 24 inch, 8 pass (24-8) radiant panel were tested. Each panel was insulated, and the seams between the panel and ceiling tiles were taped to eliminate any infiltration. Tests were done at 5 different inlet water temperatures ranging from 50°C to 100°C.

3.4   Test Results

The test results for the 24-4 and 24-8 panels tested are summarized in Tables 3.6 and 3.7 below. The experimental data can be found in Appendix C.

36

Table 3.6: Experimental results, 24-4

$T_{f,in}$ (^{o}C)	T_{panel} (^{o}C)	T_{air} (^{o}C)	Heat Output (W/m)
51.78	46.98	20.94	207.89
61.35	55.18	18.94	298.47
73.91	64.56	20.27	374.18
86.66	75.92	19.30	490.74
100.4	86.89	19.57	613.29

Table 3.7: Experimental Results, 24-8

$T_{f,in}$ (^{o}C)	T_{panel} (^{o}C)	T_{air} (^{o}C)	Heat Output (W/m)
51.96	48.10	20.13	261.67
62.77	56.45	19.99	332.03
73.71	66.75	20.52	407.68
86.11	77.75	21.01	553.51
99.66	87.46	21.68	700.08

For each panel, the heat output, panel temperature and air temperature were recorded for five inlet water temperatures. The surrounding conditions were maintained at a relative steady temperature, although it slightly deviated from the desired set temperature. The back wall was maintained at 12°C by running city water through the back wall circuit. The other surrounding surface temperatures were maintained between 19 and 21°C. The panel temperature versus the inlet water temperature for both panels is plotted in Figure 3.11 and the panel heat output versus mean water temperature is plotted in Figure 3.12. The error bars shown in Figure 3.11 and 3.12 based on the uncertainty analysis in the test results, which can be found in Appendix D.
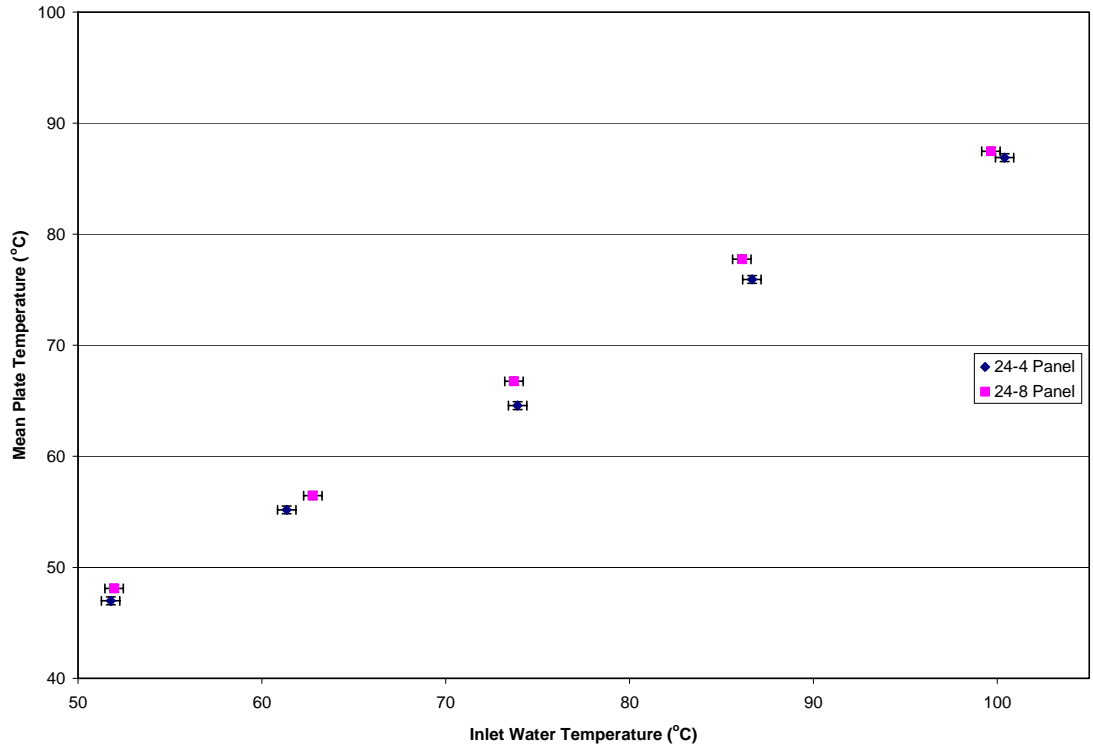
Figure 3.11: Mean Panel Temperature versus Panel Inlet Water Temperature
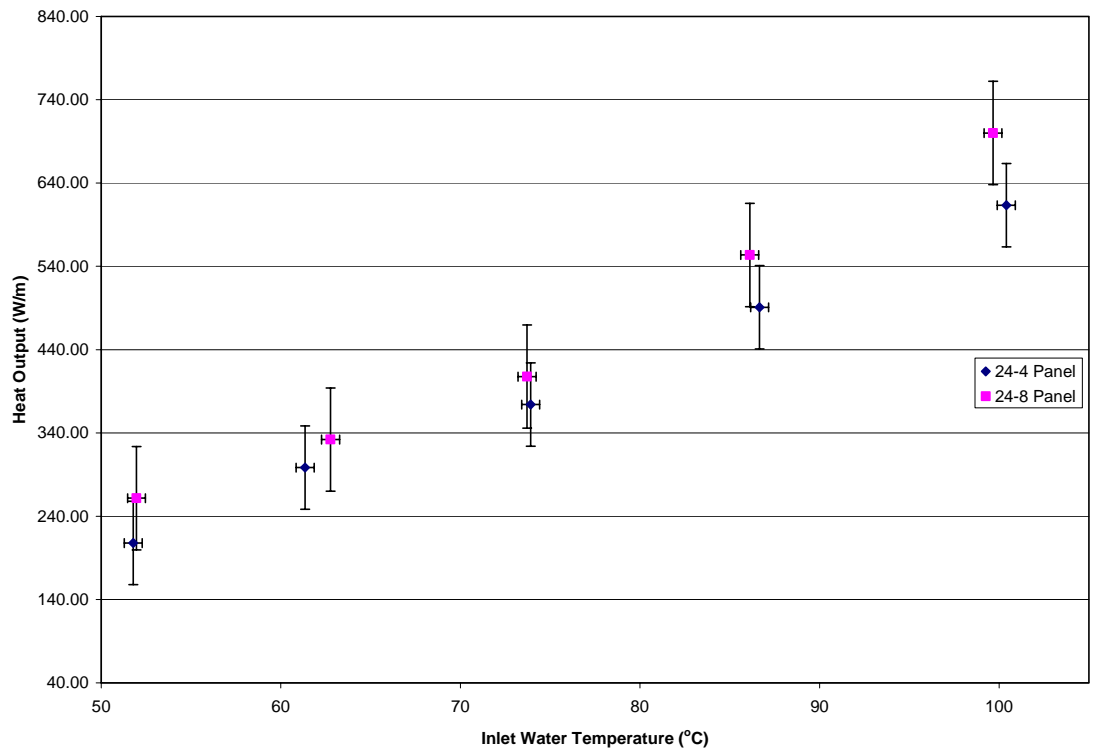
Figure 3.12: 24-4 and 24-8 Heat Output versus Panel Inlet Water Temperature

Chapter 4

Heat Transfer Model

The current Chapter presents the development of an analytical model for a perimeter radiant heating panel. The model was developed as an extension of the model by Hadlock (2004). With knowledge of the inlet flow conditions, the overall heat transfer coefficient, back losses and bond conductance between the tube and panel, the model can be used to predict the mean panel temperature and heat output. To determine the overall heat transfer coefficient, an analytical analysis on the radiative heat transfer was performed, and a numerical analysis on the convective portion. The back losses were approximated by measuring the insulation thickness on the back of the panel and the effects of the bond conductance on panel performance are discussed.

4.1   Reverse Solar Collector Model

Most radiant panel models predict the heat output based on an estimated panel temperature. The panel temperature, however, is rarely known in actual applications. In reality, manufacturers install radiant panels based on their estimated heat output, calculated using a known water flow rate and an estimated inlet fluid temperature. Therefore, a radiant panel model should be related to these known variables.

The current Reverse Solar Collector (RSC) model is based on the classical fin tube solar collector model presented by Hottel, Whillier, Bliss (1958). It relates the heat output and panel temperature to panel size, mean water temperature and surrounding air temperature. Figure 4.1 shows the geometry used to derive this model.
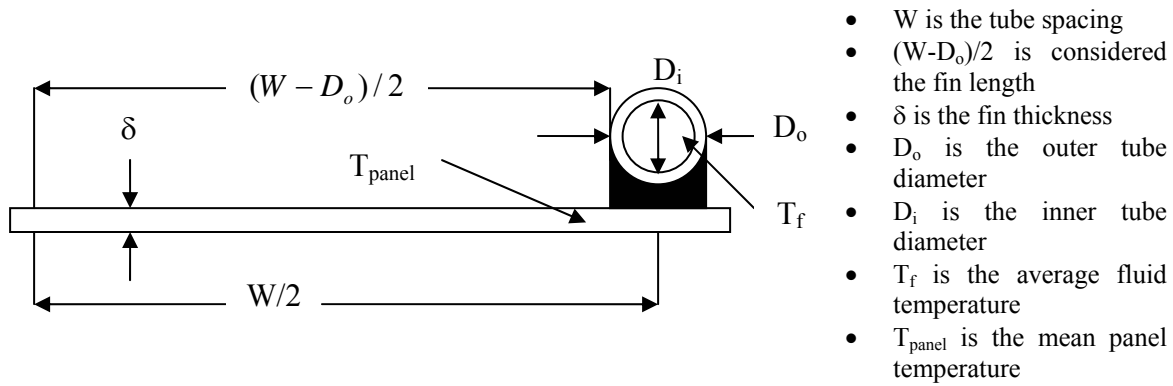
Figure 4.1: Radiant Panel Sheet and Tube Dimensions

- W is the tube spacing
- $(W-D_o)/2$ is considered the fin length
- δ is the fin thickness
- D_o is the outer tube diameter
- D_i is the inner tube diameter
- T_f is the average fluid temperature
- T_{panel} is the mean panel temperature

A radiant panel version of the model is derived in the following manner. An energy balance on a small elemental region on the fin surface (Figure 4.2), yields:

$$q_x = q_{x+dx} + dq_c + dq_{rad} + dq_{back} \tag{4.1}$$
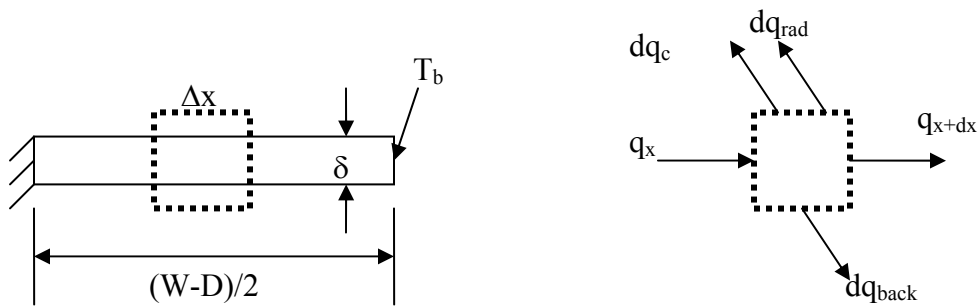
Figure 4.2: Energy Balance on Fin Element

From Fourier's law we know that:

$$q_x = -k\delta L \frac{dT}{dx}\Big|_x \tag{4.2}$$

where: L is the panel length

40

and

$$q_{x+dx} = -k\delta L \frac{dT}{dx}\Big|_x - k\delta L \frac{d^2T}{dx^2}\Big|_x dx - ...$$

(4.3)

The convective heat transfer rate can be expressed as:

$$dq_c = h_c \Delta x L (T - T_a)$$

(4.4)

Similarly, the radiative heat transfer rate can be expressed as:

$$dq_{rad} = h'_{rad} \Delta x L (T - T_a)$$

(4.5)

where the radiative heat transfer coefficient is given by:

$$h'_r = \frac{q''_{rad}}{T_{panel} - T_a}$$

(4.6)

The back losses can be estimated, knowing that the radiant panels are heavily insulated in the back, as:

$$dq_{back} = \frac{k_{ins} \Delta x L (T - T_a)}{t_{ins}}$$

(4.7)

where: t_{ins} is the thickness of the insulation

Equation 4.7 is based on the assumption that the surrounding air temperature is close to the bulk air temperature in the enclosure.

The convective, radiative and back loss coefficients can be added together to give an overall heat transfer coefficient:

$$U_L = h_c + h'_r + \frac{k_{ins}}{t_{ins}}$$

(4.8)

Details on how the heat transfer coefficients were obtained are discussed in the later sections of this Chapter.

By substituting Equations 4.2 to 4.8 into Equation 4.1 a new equation can be developed:

$$-U_L \Delta x L(T-T_a) - k\delta L \frac{dT}{dx} - (-k\delta L \frac{dT}{dx} - k\delta L \frac{d^2T}{dx^2} \Delta x - ...) = 0 \qquad (4.9)$$

By dividing Equation 4.9 by Δx and L and as Δx approaches 0, Equation 4.10 can be written as:

$$\frac{d^2T}{dx^2} = \frac{U_L}{k\delta}(T-T_a) \qquad (4.10)$$

To solve the 2nd order differential equation two boundary conditions have to be specified. At the centerline of the fin (the ends where the fins connect) symmetry is assumed, so at x = 0:

$$\frac{dT}{dx}\bigg|_{x=0} = 0 \qquad (4.11)$$

The portion of the fin which connects to the plate just above the tubing is assumed to take the same base plate temperature, thus:

$$T\big|_{x=(W-D)/2} = T_{panel} \qquad (4.12)$$

Solving the 2nd order differential equation (Hottel, Whillier and Bliss, 1958), with the corresponding boundary conditions, the temperature of the fin can be expressed as:

$$T = \frac{\cosh(mx)(T_{panel}-T_a)}{\cosh(m(W-D)/2)} + T_a \qquad (4.13)$$

where,

$$m = \sqrt{\frac{U_L}{k\delta}} \qquad (4.14)$$

and T is the temperature of the plate at some location x.

By applying Fourier's law at the base of the fin to both sides of the tube, the energy collected can be shown to be:

$$q'_{fin} = (W - D)F[-U_L(T_{panel} - T_a)] \tag{4.15}$$

where: F is the fin efficiency factor, equal to:

$$F = \frac{\tanh(m(W - D)/2)}{m(W - D)/2} \tag{4.16}$$

To complete the heat transfer for a section of the radiant panel, the portion of the plate over the tube must be accounted for as well. By doing a similar analysis, it can be shown that the heat output for a radiant panel is:

$$q'_u = ((W - D_o)F + D_o)[U_L(T_{panel} - T_a)] \tag{4.17}$$

Equation 4.17 predicts the heat transfer rate of a radiant panel based on known air and panel temperatures. Ideally, however, the net heat output of the panel should be calculated based on the inlet fluid temperature, which is generally known.

A resistance network can be used to estimate the panel temperature based on the fluid temperature, as seen in Figure 4.3.
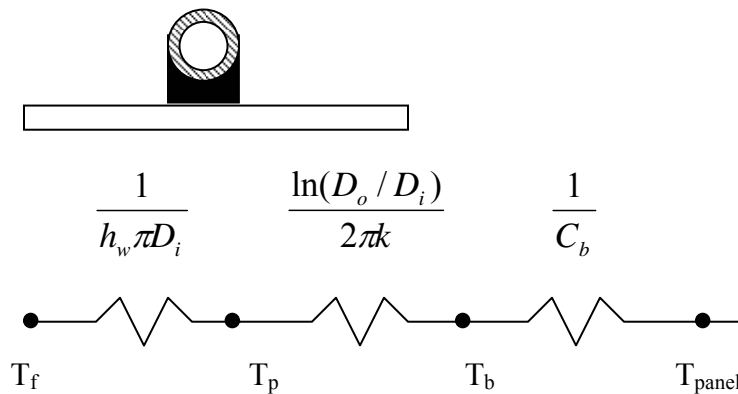
Figure 4.3: Radiant Panel Resistance Network

To maximize heat transfer, radiant panels are typically made from copper tubing. Having a high thermal conductivity, the temperature change across the pipe is minimal, and the conductive heat transfer through the pipe can be assumed to be negligible. The heat transfer from the fluid to the plate can therefore be written as:

$$q'_{panel} = \frac{T_f - T_{panel}}{\frac{1}{h_w \pi D_i} + \frac{1}{C_b}}$$

(4.18)

where: C_b is the bond conductance, and is equal to:

$$C_b = \frac{k_b b}{t_b}$$

(4.19)

where: b is the bond width

Adding the fluid, bond and panel thermal resistances, the panel heat output can be shown to equal:

$$q'_{panel} = WF'[U_L(T_f - T_a)]$$

(4.20)

where: F' is:

$$F' = \frac{1/U_L}{W\left[\frac{1}{U_L[D_o + (W - D_o)F]} + \frac{1}{C_b} + \frac{1}{\pi D_i h_w}\right]}$$

(4.21)

Equation 4.21 can be used to estimate the heat transfer of the panel based on the fluid temperature and air temperature for a section of the radiant panel. The total heat transfer rate for multiple pass systems depend on the radiant panel tube configuration (serpentine or parallel header). From Equation 4.20, for a serpentine system, the heat transfer for the first pipe run can be expressed as:

$$q'_{panel_1} = \dot{m}C_p(T_{f,in} - T_{f,out1})$$

(4.22)

For a 4 pass system the other three passes can be written as:

$$q'_{panel_2} = \dot{m}C_p(T_{f,out1} - T_{f,out2})$$ (4.23)

$$q'_{panel_3} = \dot{m}C_p(T_{f,out2} - T_{f,out3})$$ (4.24)

$$q'_{panel_4} = \dot{m}C_p(T_{f,out3} - T_{f,out4})$$ (4.25)

By summating Equations 4.22 to 4.25, the total heat transfer rate can be written as:

$$q'_{paneltotal} = \dot{m}C_p(T_{f,in} - T_{f,out4})$$ (4.26)

For the parallel circuit system, since each pass will have the same inlet and outlet fluid temperature, the heat transfer rate can be determined by multiplying Equation 4.20 by the number of passes, giving:

$$q'_{paneltotal} = \dot{m}C_p n(T_{f,in} - T_{f,out,n})$$ (4.27)

where: n is the number of passes

Equation 4.26 was used for the analysis, since serpentine radiant panels were used in the experiment. The tradeoffs between a header system and a serpentine system can be seen based on the outlet temperature.

For the serpentine circuit, the fluid outlet temperature can be predicted at the end of each circuit by setting Equations 4.22 to 4.25 equal to Equation 4.20. For example:

$$\dot{m}C_p \frac{dT_f}{dy} = WF'[U_L(T_f - T_a)]$$ (4.28)

where: y is the position along the tube.

Solving the first order differential equation (Equation 4.28) it can be shown that:

$$\frac{T_{f,outfinal} - T_a}{T_{f,in} - T_a} = \exp\left[-\frac{A_{panel}U_L F'}{\dot{m}C_p}\right] \tag{4.29}$$

When trying to predict the heat output from the panel, the outlet water temperature is usually not known. The inlet fluid temperature and flow rate are generally known. It would, therefore, be convenient to determine an equation which can predict the heat output from the panel, based on known parameters. This can be achieved by using a heat removal factor, F_R, defined as the ratio of the actual heat output of the panel to the heat output if the entire panel were at the fluid inlet temperature. Following a similar derivation as in Duffie and Beckman (1991), the heat removal factor for a radiant heating panel can be shown to be:

$$F_R = \frac{\dot{m}C_p}{A_{panel}U_L}\left[1 - \exp\left(-\frac{A_{panel}F'U_L}{\dot{m}C_p}\right)\right] \tag{4.30}$$

Finally, the heat output from the panel can be shown to be:

$$q_{panel} = A_{panel}F_R U_L (T_{f,in} - T_a) \tag{4.31}$$

and the mean plate temperature (Duffie and Beckman, 1991):

$$T_{p,mean} = T_{f,in} - \frac{\dot{m}C_p (T_{f,in} - T_{f,out})}{A_{panel}F_R U_L}(1 - F_R) \tag{4.32}$$

4.2   Radiant Exchange Model

Several methods of determining the radiant heat exchange for a panel have been presented (Walton, 1980 and Steinman et al., 1989). As discussed in Chapter 2, most of these models, however, assume a 2D radiant heat exchange, and do not account for temperature differences between the surfaces. They also assume low temperature differences between the panel and surrounding surface temperatures. In radiant perimeter

heating applications, the panel temperature is often at a much higher temperature than the surrounding conditions, and surrounding surface temperatures also vary significantly. It is therefore necessary to determine which method can be used to approximate the radiative heat transfer from a radiant perimeter heating panel. The exact solution will be discussed first, and then a three-surface radiation model. Finally, both methods will be compared to Walton's MRT method accepted by ASHRAE (ASHRAE, 2004).

Exact Radiation Heat Exchange Model

For an enclosure similar to the radiant panel test chamber, discussed in Chapter 3, there are a total of seven surfaces (Figure 4.4).
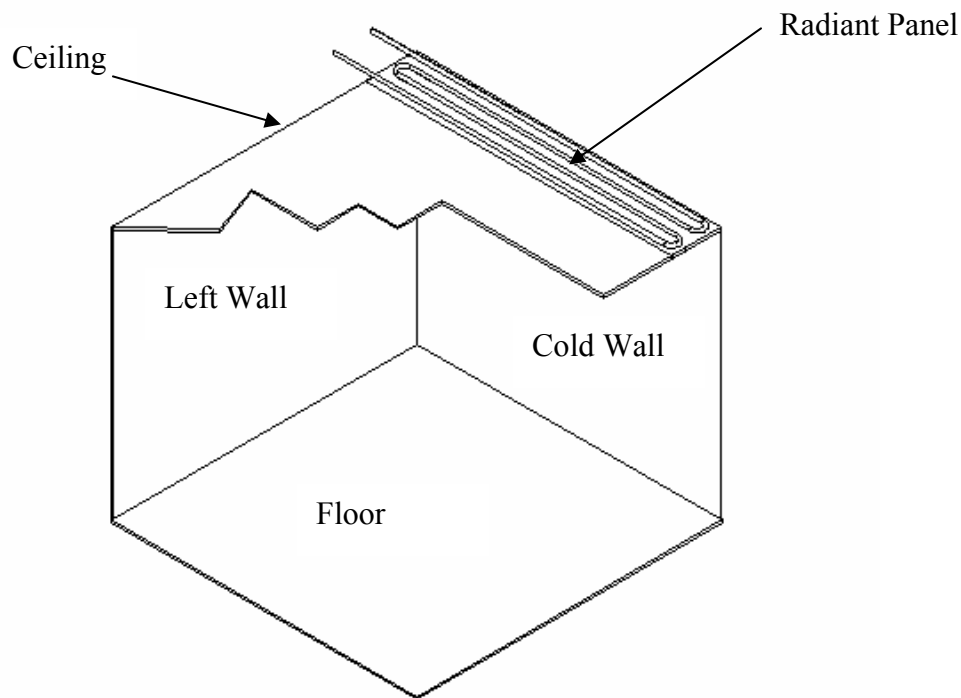
Figure 4.4: Cut Away Sketch of a Seven Surface Radiant Panel Test Chamber

Each surface in the enclosure has some portion of radiant energy leaving the surface and another portion incident on it. The net radiant energy leaving the surface is known as the

radiosity, J, which includes the emitted and reflected radiative components as shown in Equation 4.33. For a given opaque surface, it can be shown that $\rho_i = 1 - \varepsilon_i$ and hence:

$$J_i = \varepsilon_i E_{bi} + (1 - \varepsilon_i)G_i \qquad (4.33)$$

where: E_{bi} is the emissive power of a surface i
$\quad\quad$ G_i is the incident radiation on a surface i
$\quad\quad$ ρ is the reflectivity of the surface

The incident radiation on a surface is known as the irradiance, G and is given by Equation 4.34. As shown in Equation 4.35, the net radiation transferred to the panel can be solved from the radiosity at each surface.

$$G_i = \sum_{j=1}^{n} F_{i-j} J_j \qquad (4.34)$$

$$q_{flux} = \sum_{j=1}^{n} F_{i-j} (J_i - J_j) \qquad (4.35)$$

For a seven surface enclosure the net radiation heat transfer from the panel can be determined by solving Equation 4.35. This requires the knowledge of view factors that can be computed explicitly in this case. For each surface, the radiosity can be found substituting Equation 4.34 into Equation 4.33 giving the following equation (ASHRAE, 2005).

$$J_i = \varepsilon_i \sigma T_i^4 + (1 - \varepsilon_i) \sum_{j=1}^{N} F_{ij} J_j \qquad (4.36)$$

Equation 4.36 can be expressed in matrix form by performing a net radiation balance at each surface and bearing in mind that the surfaces cannot view themselves. This equation can be shown to be:

$$(1-\varepsilon)\begin{bmatrix} (1-\varepsilon)^{-1} & F_{12} & F_{13} & F_{14} & F_{15} & F_{16} & 0 \\ F_{21} & (1-\varepsilon)^{-1} & F_{23} & F_{24} & F_{25} & F_{26} & F_{27} \\ F_{31} & F_{32} & (1-\varepsilon)^{-1} & F_{34} & F_{35} & F_{36} & F_{37} \\ F_{41} & F_{42} & F_{43} & (1-\varepsilon)^{-1} & F_{45} & F_{46} & F_{47} \\ F_{51} & F_{52} & F_{53} & F_{54} & (1-\varepsilon)^{-1} & F_{56} & F_{57} \\ F_{61} & F_{62} & F_{63} & F_{64} & F_{65} & (1-\varepsilon)^{-1} & F_{67} \\ 0 & F_{72} & F_{73} & F_{74} & F_{75} & F_{76} & (1-\varepsilon)^{-1} \end{bmatrix} \begin{bmatrix} J_1 \\ J_2 \\ J_3 \\ J_4 \\ J_5 \\ J_6 \\ J_7 \end{bmatrix} = \varepsilon\sigma \begin{bmatrix} T_1^4 \\ T_2^4 \\ T_3^4 \\ T_4^4 \\ T_5^4 \\ T_6^4 \\ T_7^4 \end{bmatrix} \quad (4.37)$$

Equation 4.37 can be solved by matrix inversion to obtain the radiosities at each surfaces. With knowledge of the surface temperatures and emissivities, the radiosities can be calculated and hence the net radiative transfer from the panel can be determined as follows:

$$q''_{rad} = J_{panel} - \sum_{j=1}^{n} F_{panel-j} J_j \quad (4.38)$$

where: J_{panel} = total radiosity leaving the panel surface
J_j = Radiosity from other surfaces in the room

Simplification to the Exact Radiant Heat Exchange Model

The exact radiant heat transfer can be calculated using a seven surface enclosure. For reasons of simplicity, a three surface enclosure was assumed (Figure 4.5) because five of the seven surrounding surfaces have equal surface temperatures and emissivities.
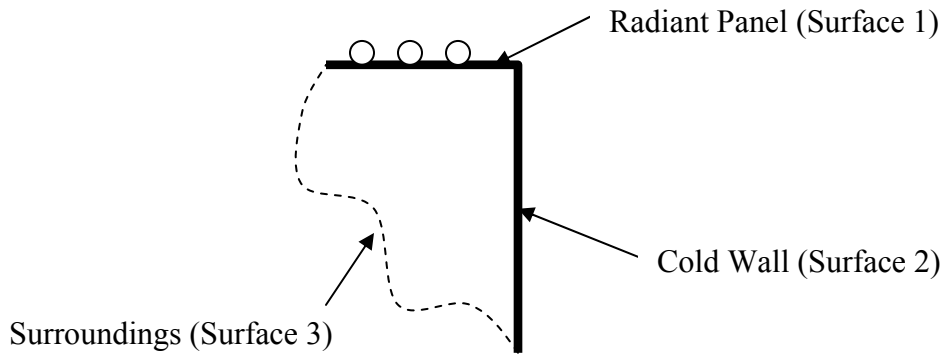
Figure 4.5: Three Surface Enclosure Approximation

Considering only three surfaces, the set of radiosity equations derived from Equation 4.36 can be written matrix form as:

$$(1-\varepsilon)\begin{bmatrix} (1-\varepsilon)^{-1} & -F_{12} & -F_{13} \\ -F_{21} & (1-\varepsilon)^{-1} & -F_{23} \\ -F_{31} & -F_{32} & (1-\varepsilon)^{-1} - F_{33} \end{bmatrix}\begin{bmatrix} J_1 \\ J_2 \\ J_3 \end{bmatrix} = \varepsilon\sigma\begin{bmatrix} T_1^4 \\ T_2^4 \\ T_3^4 \end{bmatrix}$$ (4.39)

The view factor from the panel to the cold wall, F_{12}, can be calculated using the published view factor equation for perpendicular rectangles with a common edge. The view factor from the panel to the third surface, F_{13}, is simply 1 - F_{12}, since the sum of all view factors in an enclosure is equal to unity. The remaining view factors can be calculated using the reciprocity equation. The radiant heat transfer from the panel can be calculated using Equation 4.39 by solving for the radiosities by matrix inversion.

MRT Method

The ASHRAE HVAC and Systems Handbook (ASHRAE, 2004) suggests that the radiant heat transfer from a panel can be calculated using Walton's (1980) MRT method. Walton assumes the radiant panel would exchange energy with a fictitious surface. The fictitious surface would have the same overall characteristics of the actual enclosure thus minimizing the error associated with the assumption. Doing a net energy balance on each surface, Walton showed that the net heat flux from radiation could be expressed as:

$$q''_{rad} = \sum_{j=1}^{n} 4\sigma\varepsilon_j F_{panel-j} T_{avg}^{*3} (T_j - T_{panel})$$ (4.40)

where: T_{avg}^* is the area weighted average enclosure temperature

To use Equation 4.40, Walton assumed that the temperature difference between surfaces was not great and that surface *panel* was much smaller than surface *j*. In most radiant

heating perimeter ceiling cases this is not true. Radiant perimeter ceiling panels are typically significantly warmer than the surrounding temperatures, so some degree of error would be associated with using Equation 4.40.

Method Comparison

The radiant heat output in an enclosure with the same properties as the Sigma radiant panel test chamber for the three models discussed are compared in Figure 4.6 below. The solutions for each case can be found in Appendix E. It can be seen that the MRT method is within 8% of the actual solution and the three-surface enclosure is within 0.3%. It was therefore decided to use the three-surface enclosure approximation to determine the radiant heat transfer from the panel, because accuracy was not compromised over computation time.
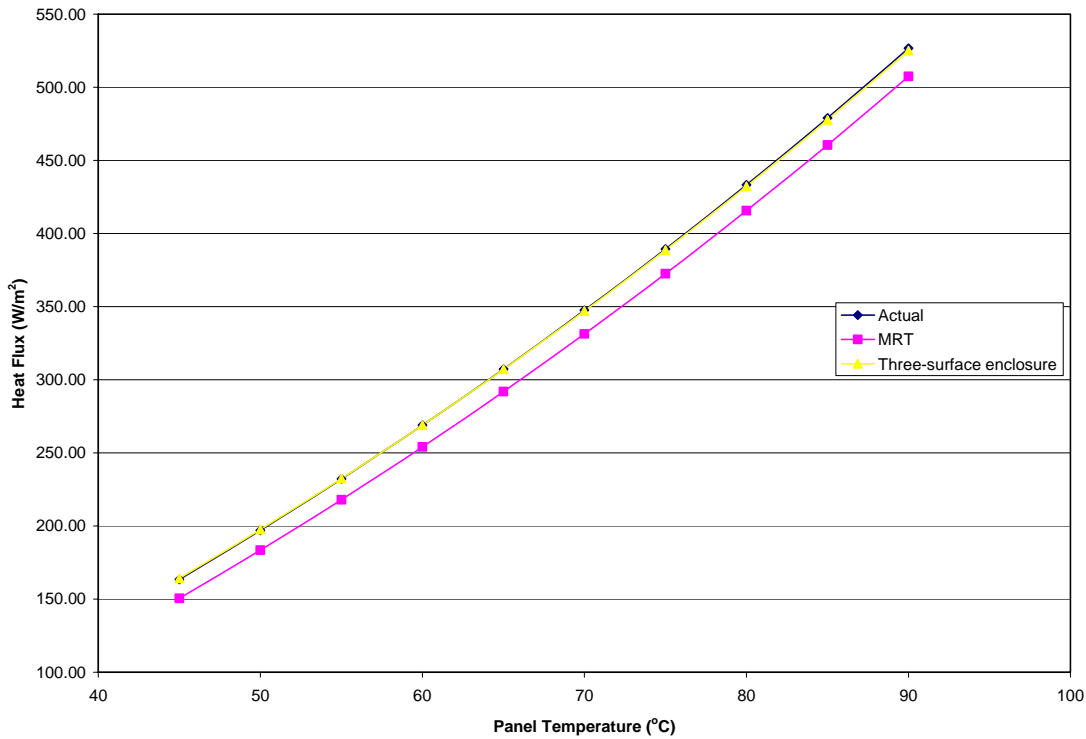
Figure 4.6: Predicted Radiative Heat Flux versus Panel Temperature for Three Analytical Models

To use the reverse solar collector (RSC) model derived in Section 4.1, the radiative heat transfer must be expressed as a heat transfer coefficient. Using the heat flux calculated for the three-surface enclosure assumption, the heat transfer coefficient can be calculated by dividing it by the panel to air temperature difference.

$$h_r^{'} = \frac{q_{rad}^{''}}{T_{panel} - T_a}$$

(4.41)

4.3 Convective Heat Transfer Coefficient

In current analytical radiant panel models, the convective heat transfer is based on a correlation from Min et al.'s (1956) ASHVE test facility data. Those experiments were based on full sized ceiling panels with a uniform surrounding enclosure temperature. The ASHRAE HVAC and Systems Handbook (2004) has accepted this correlation, since it is believed that the convective heat transfer has a minimal effect on panel performance. Lomas (1995), however, has found that the radiant panel heat output can vary as much as 27% if the incorrect convective heat transfer coefficient is used. Awbi and Hatton (1999) conducted various experiments to determine the natural convective heat transfer, however, they gave limited details concerning the surrounding conditions and limitations to the developed correlations.

It was therefore decided to determine the convective heat transfer coefficient using a CFD model simulating the test chamber conditions. The heat transfer coefficients were then obtained for various panel sizes and temperatures and the correlation used in the RSC model.

4.3.1 Numerical Model

The system studied is shown in Figure 4.7. It consists of five surfaces; four of which are considered isothermal, and one surface which is considered adiabatic. The end walls (AB and CD) are set a distance, L, apart. The ceiling (DA) is made of two parts, the radiant panel (EA) of length, W, and assumed to be isothermal, and the acoustic tiles (DE) considered to be adiabatic. The ceiling is a distance, H, above the isothermal floor (BC) assumed to be at T_{warm}. No infiltration was added to the model, since the radiant panel test chamber was sealed during tested.
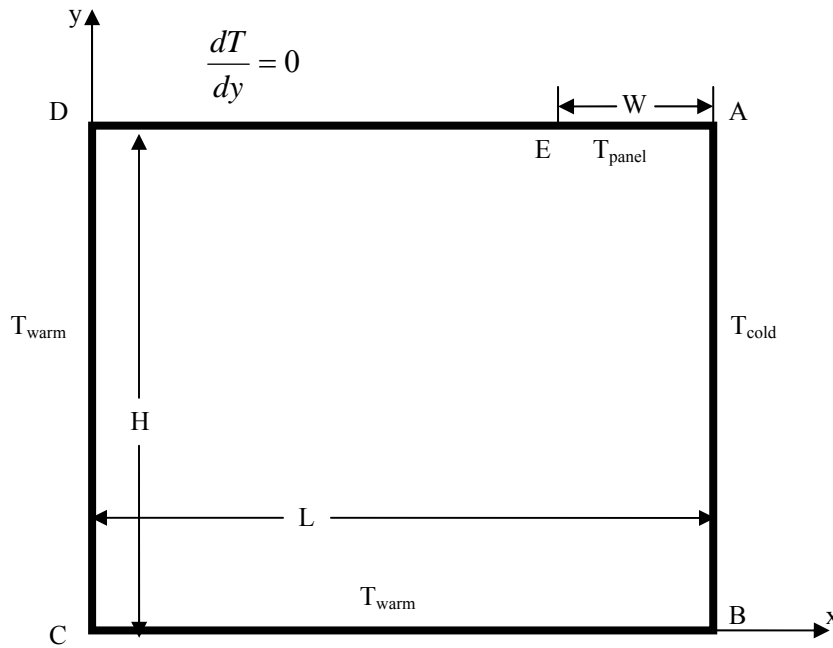
Figure 4.7: Schematic of CFD Model

4.3.2 Governing Numerical Equations

In natural convective heat transfer, the fundamental laws of mass, momentum and energy conservation apply. Using the Boussinesq approximation, which relates the density change to temperature change, and assuming that the fluid is incompressible, and

has negligible viscous dissipation, the governing equations can be written. The mass conservation or continuity equation is given by:

$$\frac{du}{dx} + \frac{dv}{dy} = 0 \qquad (4.42)$$

where: u and v are velocities in the x and y-direction respectively.

The momentum x and y-equations are:

$$\rho\left(u\frac{\partial u}{\partial x} + v\frac{\partial v}{\partial y}\right) = -\frac{\partial p}{\partial x} + \mu\left(\frac{\partial^2 u}{\partial x^2} + \frac{\partial^2 u}{\partial y^2}\right) \qquad (4.43)$$

$$\rho\left(u\frac{\partial u}{\partial x} + v\frac{\partial v}{\partial y}\right) = -\frac{\partial p}{\partial y} + (\mu_l + \mu_t)\left(\frac{\partial^2 v}{\partial x^2} + \frac{\partial^2 v}{\partial y^2}\right) + g\rho\beta(T - T_\infty) \qquad (4.44)$$

where: p is the pressure
β is the volumetric thermal expansion coefficient

The energy equation is given by:

$$\left(u\frac{\partial T}{\partial x} + v\frac{\partial T}{\partial y}\right) = \alpha\left(\frac{\partial^2 T}{\partial x^2} + \frac{\partial^2 T}{\partial y^2}\right) \qquad (4.45)$$

where: α is thermal diffusivity

The viscous dissipation has been neglected in Equation 4.45, which is a valid assumption when the air velocities caused by buoyancy effects are very small in natural convective heat transfer.

Due to some thermal instability caused by the cold wall, the air velocities could not be assumed to be negligible. To take this effect into account, a turbulence model was assumed adding a component to the governing laminar convective equation. The added component accounted for the turbulent eddy transport of momentum. The turbulence viscosity, μ_t, can be expressed by various models. For example, the k-l model is:

$$\mu_t = f_u C_\mu^{1/4} \rho k^{1/2} l \qquad\qquad (4.46)$$

where: C_μ is an empirical coefficient and f_μ is another coefficient
      k and l are the model parameters

In this work the STAR CD constant turbulence model was used with a turbulence viscosity of 0.005 Ns/m^2.

4.3.3 Model Parameters

A total of 10 different panel temperatures were simulated over 9 different panel sizes. The temperatures ranged from 318 K to 363K, with an incremental value of 5 K. The panel sizes simulated ranged from 0.25m to 2m, typically incremented by 0.25m. To simulate the test chamber constructed at Sigma, the model dimensions were 3.9624m in length (BC) and 3.048m in height (AB). The cold wall (AB) was set to a temperature of 283 K, while the floor (BC) and front wall (CD) were set to 293K. A total of 90 simulations were run, each simulation gave a temperature profile within the room. No radiative effects were included since the model was simply used to predict the natural convective heat transfer coefficient. The specific heat and thermal conductivity of the air were evaluated at a reference air temperature of 293 K, varying minimally over the expected air temperature range and because the convective heat transfer was evaluated at the bulk mean air temperature. The density was evaluated from the ideal gas law, $\rho = p/RT$. The percentage change of this variable for the expected temperature range was 15%, and therefore they were set as functions of temperature. For the same reasons, the molecular viscosity was calculated from the Sutherland equation (LMNO, 2003), shown below:

$$\mu = \frac{bT_a^{3/2}}{T_a + S}$$ (4.47)

where: b = 1.458*10-6 kg/(msK$^{1/2}$) for air
    S = 110.4 K for air

It was later decided to add a turbulence model making the laminar viscosity negligible, however it was still evaluated using the Sutherland equation.

4.3.4   Numerical Simulation Method

Using the STAR-CD's Create Geometry option, the 2D model of the radiant panel test chamber was created. The following steps were performed to create the model:

- 26 vertex locations described the main structure of the test chamber
- The vertices were connected with splines, creating a 2D block structure.
- Using the mesh command, the grid was generated for the 2D block structure. A coarse grid size of 0.032m was used for the interior, while at the boundary locations a very fine grid was used (6.25x10^{-5}m) which expanded (x2) to the coarse grid size. Section 4.3.6 will discuss the grid refinement.
- The generated blocks were merged and the boundary locations identified and fluid properties specified.

The governing equations (mass, momentum and energy) are specified in STAR CD's Properties option. To solve these equations, they must be integrated over the control volumes generated by the mesh. These integral equations were solved using the CD differencing scheme and the SIMPLE solution algorithm.

Between 1000 to 4000 iteration were required to solve the governing equations at a specified tolerance of 10^{-5}. The u and v velocity components were calculated with a relaxation factor of 0.7 and the temperature was calculated with a relaxation factor of 0.95. The density and laminar viscosity relaxation factors were set to 1, while the pressure relaxation factor was set to 0.3.

4.3.5 Data Analysis

To determine the natural convective heat transfer coefficient it was necessary to calculate the heat flux from the panel at every cell location immediately below the panel. The temperature gradient divided by the cell size gave the heat flux which was ultimately converted into the total heat output of the panel, through convection. The convection coefficient, h_c, was calculated with knowledge of the heat output and the temperature of the air at the center of the chamber.

$$h_c = \frac{q''_{panel}}{(T_{panel} - T_{air})} \tag{4.48}$$

The corresponding Nu, Gr and Ra numbers (Equations 4.49, 4.50 and 4.51) were calculated using the properties of air at the measured value.

$$Nu = \frac{h_c D_H}{k_a} = + \frac{dT*}{dy*} \bigg|_{y*=0} \tag{4.49}$$

$$Gr = \frac{g\beta(T_{panel} - T_a)D_H^3}{\nu^2}, \beta = \frac{1}{T_a} \tag{4.50}$$

$$Ra = Gr\Pr = \frac{g\beta(T_{panel} - T_a)D_H^3}{\nu\alpha} \tag{4.51}$$

where: ν is the kinematic viscosity

The temperature gradients within 1 cm from the corner of the cold wall and radiant panel were ignored. This was done because at this point the temperature gradient approached infinity because of the singularity in the model. The heat output from this unaccounted section is varies for each panel size and temperature, however on average 15W are not accounted for – 1% of the total panel heat output.

4.3.6 Grid Refinement

To determine the grid size required to simulate the natural convection in a perimeter ceiling heated room, it was necessary to compare the heat output from the panel over various coarse grid refinements and boundary grid refinements. To determine the effects immediately below the panel it was necessary to have a very small grid size. To simulate the entire enclosure, however, such a fine mesh size was not necessary and would be very time consuming. The finest grid refinement was done at the panel and cold wall surfaces because these surfaces had the greatest influence on the air temperature distribution. The grid refinement procedure was two-fold. The steps taken were:

- Refine the boundary grid size start at the panel and cold wall and compare to the previous grid
- Refine the coarse grid and compare to previous grid

The temperature gradient for the ceiling was taken within 1 cm of the exterior wall and the non-heated ceiling was assumed to be adiabatic. The grid size along the front wall and floor started at 0.05cm and had a grid expansion of two until it matched the coarse grid size. The following results tabulated in Table 4.1 below summarize the grid refinement procedure (Appendix F).

Table 4.1: Grid Refinement Results

Coarse Grid Size (cm)	Grid Size Start at Panel and Cold Wall (cm)	Heat Flux (W/m^2)
0.064	0.025	19.26
0.064	0.0125	19.47
0.064	0.00625	19.82
0.064	0.003125	19.59
0.032	0.025	19.12
0.032	0.0125	19.32
0.032	0.00625	19.4
0.032	0.003125	19.42

From the grid refinement results, a coarse grid size of 0.032cm was chosen with a starting grid size of 0.00625cm for the cold wall and panel. The other boundaries had a starting mesh size of 0.05cm. For each surface, the grid expansion factor was 2 until it reached the coarse mesh size.

4.3.7 Model validation

The model was validated by simulating the ASHVE test chamber (Min et al., 1956) and comparing the predicted CFD results to the experimental values based on measurements done almost 50 years ago. This model was selected because the test chamber was described in detail (Tasker et al., 1952) and the experimental results are accepted by ASHRAE and used to predict the natural convective heat transfer for radiant panels. The natural convective heat transfer coefficient was calculated by measuring the air temperature below the panel at specific locations and determining the temperature gradient. These results were collected manually, by positioning the thermocouple in the exact location and holding it steady.

Using the same method that was used to model Sigma Convectors radiant panel test chamber, the ASHVE test chamber was created in STAR-CD. The differences between the ASHVE test chamber and Sigma Convectors test chamber was the size and the boundary conditions. The ASHVE test chamber had a uniform surrounding temperature of 293 K at each wall and floor and the entire ceiling was a radiant heating panel. The same solution algorithms were used as those in the above model. The Nu, Gr and Ra numbers were calculated and compared to the obtained experimental data. Figure 4.8 is similar to the model developed for the ASHVE test chamber, however, the panel width is the entire ceiling at a constant temperature and the chamber length is 7.47 m and

2.44 m high. Only one panel size had to be modelled and the panel temperature was varied from 308K to 348K in 10K increments. A total of 5 simulations were performed. The ASHVE test data showed a wide range of scatter as shown in Figure 4.8 below. On the other hand, the predicted results from STAR-CD were within the experimental results (Appendix F), thus supporting the 2D model used to determine the natural convective heat transfer coefficient.
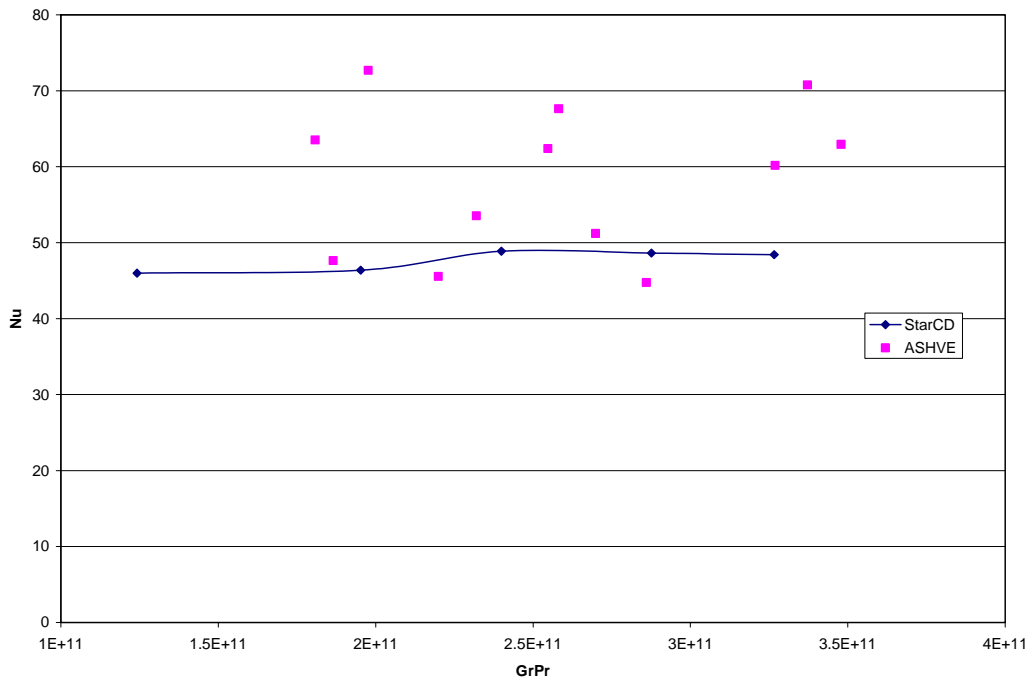
Figure 4.8:   Nusselt versus Rayleigh number for numerical model results and experimental results from the ASHVE laboratory

The temperature profile for a 348 K heated ceiling in the room is shown in Figure 4.9.

The experimental chamber was, in reality, not infinitely wide, so an attempt was made to predict 3D effects on the natural convective heat transfer coefficient. The ASHVE test facility consisted of 4 walls and a floor at 293K. The convective heat transfer effects from the left and right walls, not included in the 2D simulation, could be

taken into account by assuming a temperature distribution similar to that of the front wall is generated.
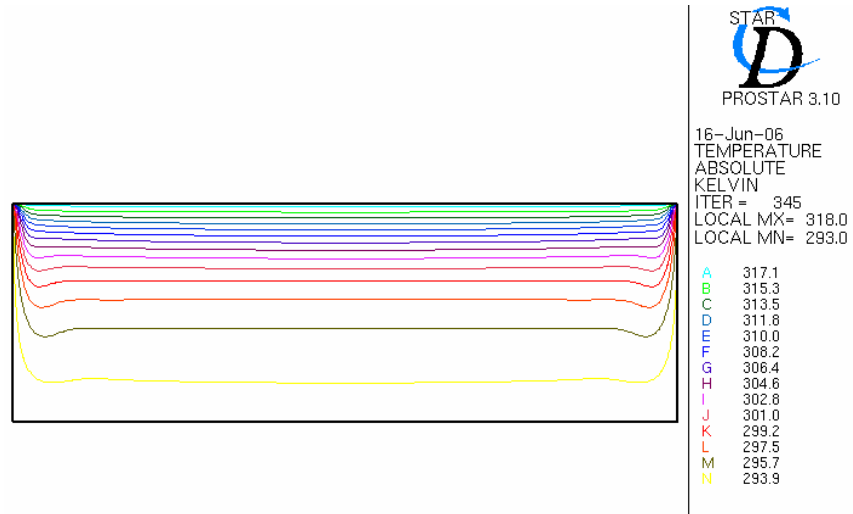
Figure 4.9:   Temperature Profile for the Numerically Simulated ASHVE Test Facility

From Figure 4.10 it can be seen that the front and rear wall x-temperature gradient eventually becomes zero at a certain distance from the wall. The temperature gradient can then be applied to the left and right wall and a natural convective heat transfer coefficient can be calculated (Appendix F). The distance it took for the temperature gradient to become constant was determined from the numerical model results of the ASHVE test facility. A Nusselt number was calculated for each cell below the heated ceiling. The percentage change of the Nusselt number from cell to cell was calculated and when the difference was below 1%, the distance from the wall was recorded. This temperature gradient was then applied to the left and right wall, and the Nusselt number was calculated. Figure 4.11 compares the 2D results from STAR-CD with the 3D approximation and the ASHVE test results.
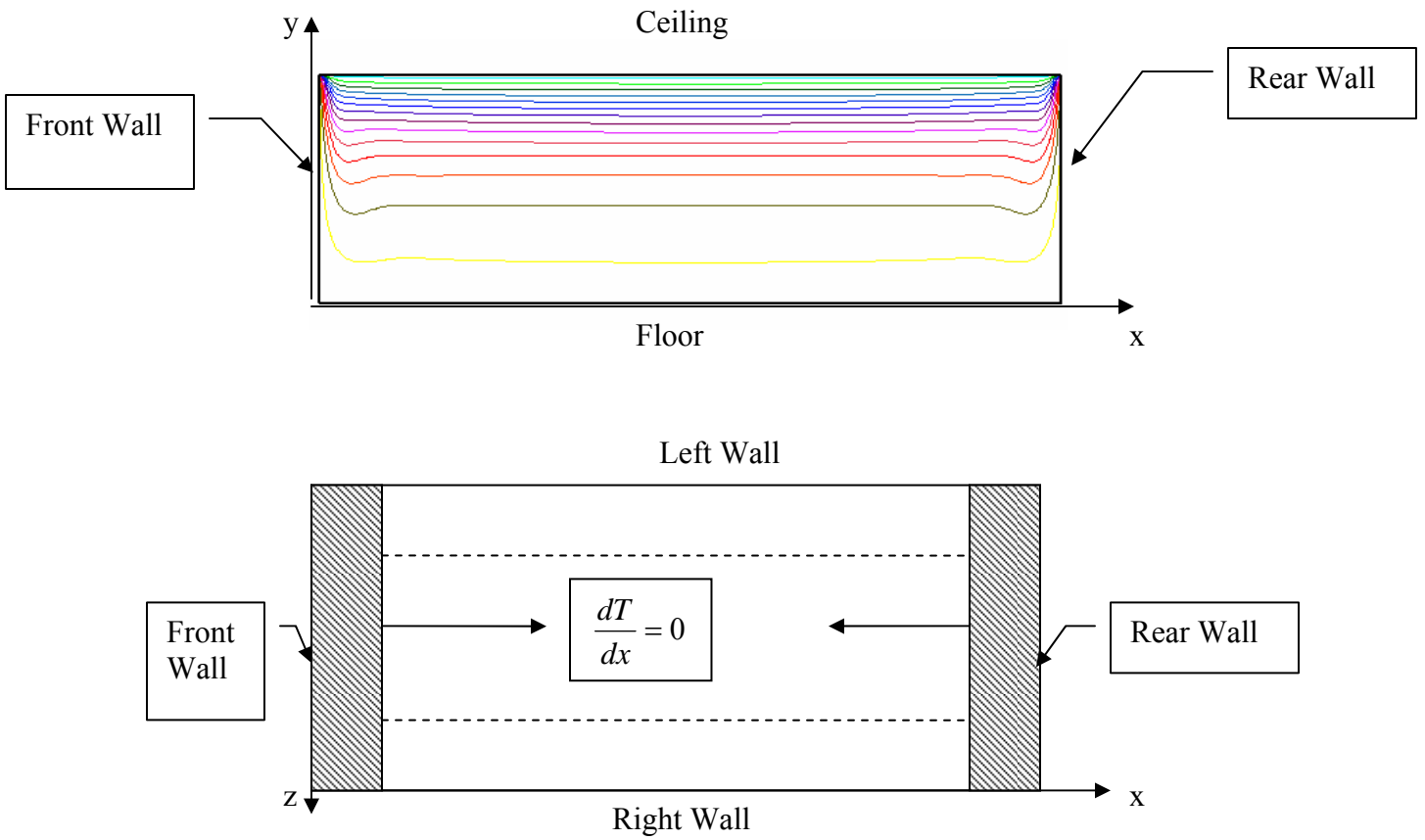
Figure 4.10: *Side profile and Top View of ASHVE Test Chamber and y Direction Temperature Gradient Profile*
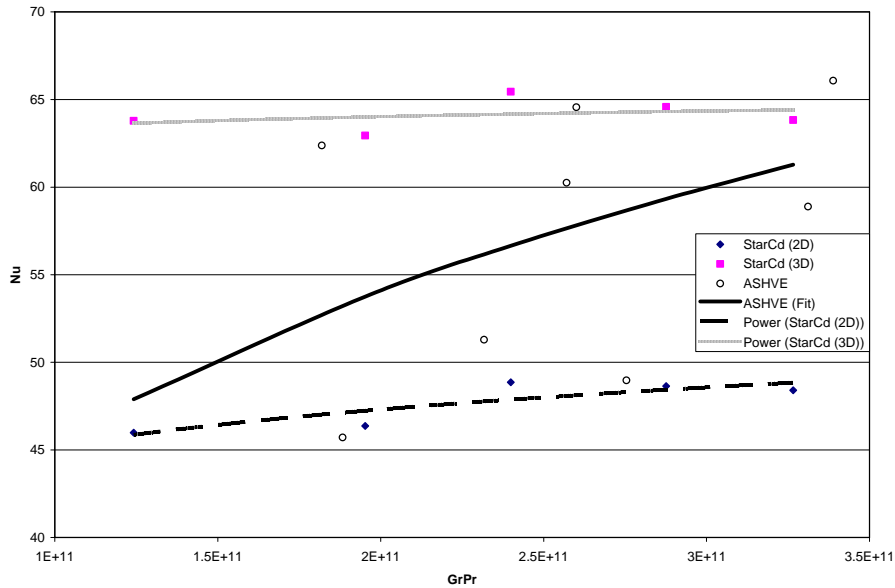
Figure 4.11: *2D and 3D numerical model simulation results versus ASHVE experimental data*

As a conclusion, since the ASHVE experimental results are almost 50 years old and measurement techniques have greatly improved, the 2D predicted results from STAR-CD are deemed acceptable.

4.3.8   Numerical results

The effects of panel size and temperature on the natural convective heat transfer coefficient was determined simulating 9 panel sizes over 10 panel temperatures (Appendix F). For each case, the temperature gradient under the panel was measured and a heat flux for each cell was calculated using Fourier's law:

$$q''_{cell} = k \frac{dT}{dy} \tag{4.52}$$

The total heat flux from the panel was calculated by adding up the heat output from each cell and dividing by the panel area.

$$q_{panel} = \frac{\sum_{i=1}^{n} q_{cell_i} A_{cell_i}}{A_{panel}} \tag{4.53}$$

The heat transfer coefficient was then calculated using Equation 4.48, having recorded the air temperature at the center of the chamber. Taking the properties of the air at the center of the room, the Nusselt, Grashof and Rayleigh numbers were calculated for each panel size and temperature.

An example of the simulation results of the natural convective heat transfer are shown in Figure 4.12. As expected, some stratification under the radiant panel occurs, however, the cold wall gave rise to air circulation within the center of the room.

The Nusselt number was compared to the aspect ratio of the panel width to the chamber size (Figure 4.13). This would indicate the effect of the convection heat transfer coefficient with panel size.
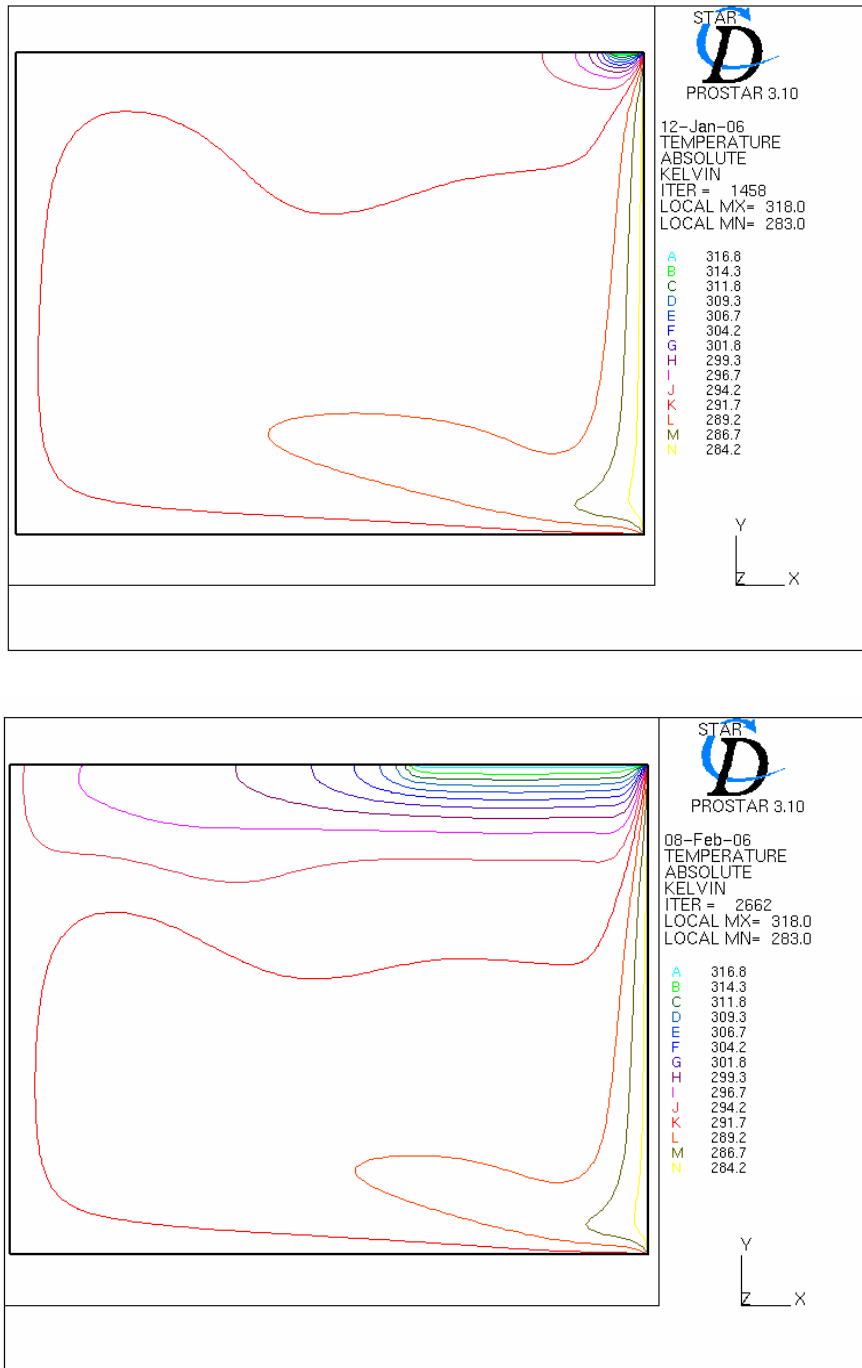
Figure 4.12: Temperature profile for a 0.25m and a 1.5m panel at 318K
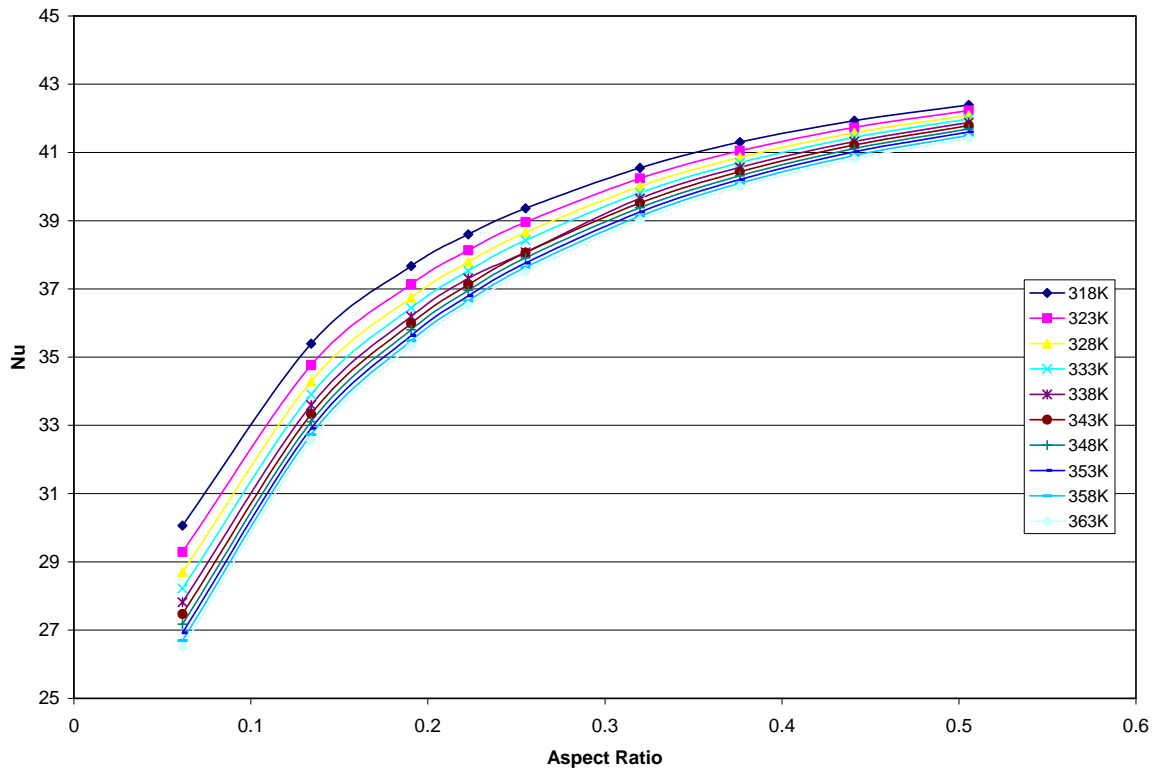
Figure 4.13: Nusselt Number versus Aspect Ratio

As expected the Nusselt number increased as the aspect ratio increased. This was because the smaller panel sizes had a smaller characteristic length, which is proportional to the Nusselt number. At larger panel sizes, as the aspect ratio increased, the air temperature distribution beneath the panel was not affected by the cold wall as greatly as with the smaller panel sizes. Therefore, the characteristic length played a much smaller role. Temperature plots of the small panel size and larger panel size can be seen in Figure 4.12.

The Rayleigh number was compared to the aspect ratio (Figure 4.14). As expected with higher panel temperatures, the Rayleigh number increases. This is because there is a greater effect of the cold wall on the air motion. Correspondingly, the Rayleigh

number remains fairly constant over the various aspect ratios indicating that the air motion is primarily due to the temperature difference between the panel and the exterior wall.
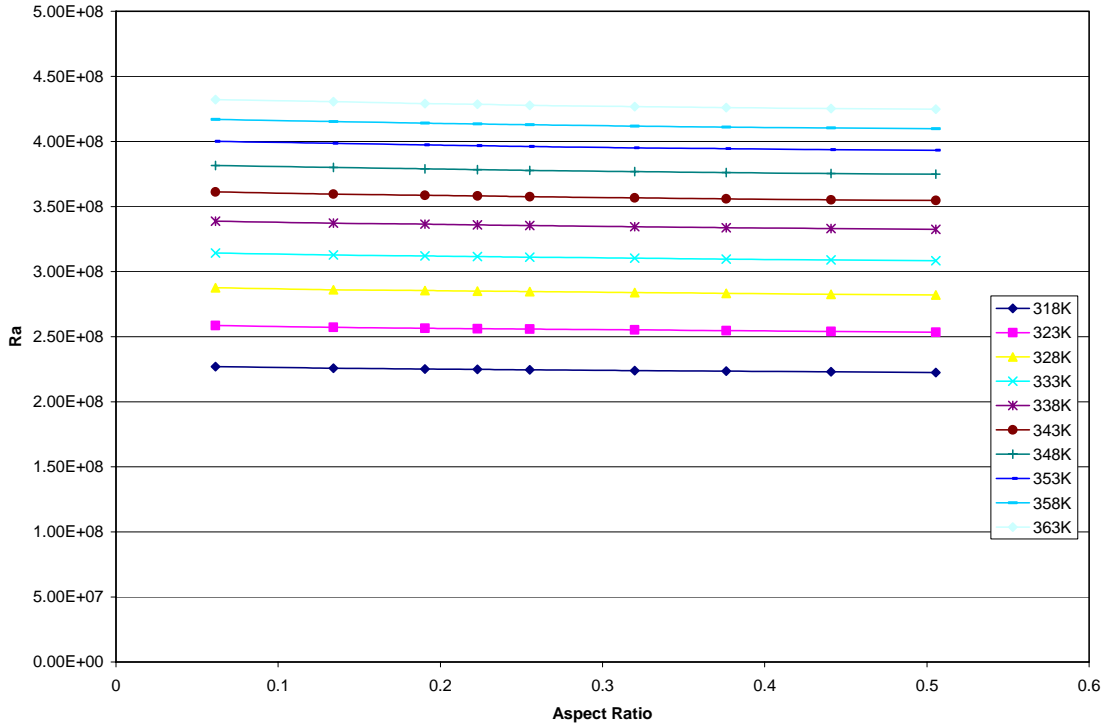
Figure 4.14: Rayleigh number versus Aspect Ratio

Finally, the Nusselt number versus the Rayleigh number (Figure 4.15) was plotted. From previous experiments, it was expected that as the Rayleigh number increased, the Nusselt number would increase as well because the convective heat transfer coefficient should increase as more air motion occured. From Figure 4.15, it can be seen that the expected results did not occur. As the Rayleigh number increased, the Nusselt number decreased. This can be explained in the following manner; as the radiant panels became warmer, the surrounding air warmed up and became stratified. This was seen in the minimal air temperature change at the 1.5m level when a hotter panel

66

temperature was simulated. When stratification occurs, the convective heat transfer decreases, lowering the Nusselt number, while the Rayleigh number increases because of the less dense air.
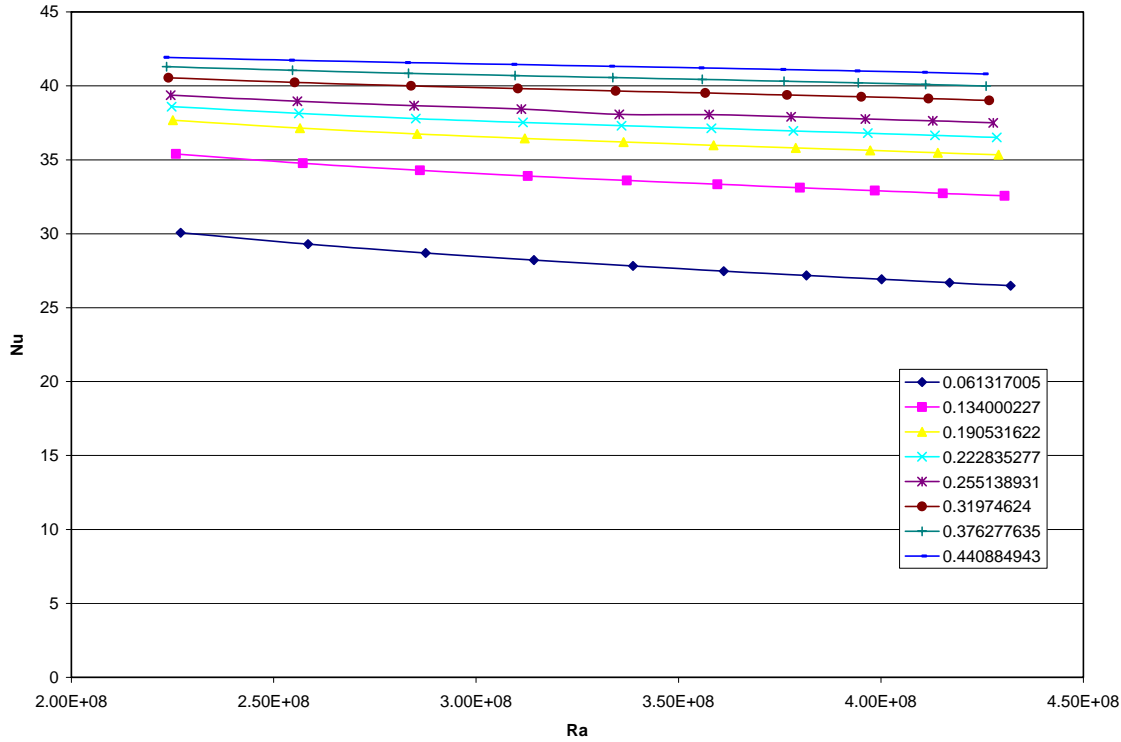
Figure 4.15: Nusselt versus Rayleigh number

From these results, it can be concluded that the Nusselt and Rayleigh number are dependant on panel temperature and panel sizing. Schutrum and Vouris (1954) stated that the convective heat transfer coefficient was not dependant on panel size, which is the case for full size panels occupying the entire area of the ceiling. From Figure 4.12, however, it can be seen that the convective heat transfer is dependant on the ratio of the panel length to the ceiling length. As this ratio increases, the Nusselt number flattens out showing that the panel size will have minimal effect on the convective heat transfer coefficient.

The combined effect of panel temperature and panel size on the convective heat transfer is plotted in Figure 4.16 below.
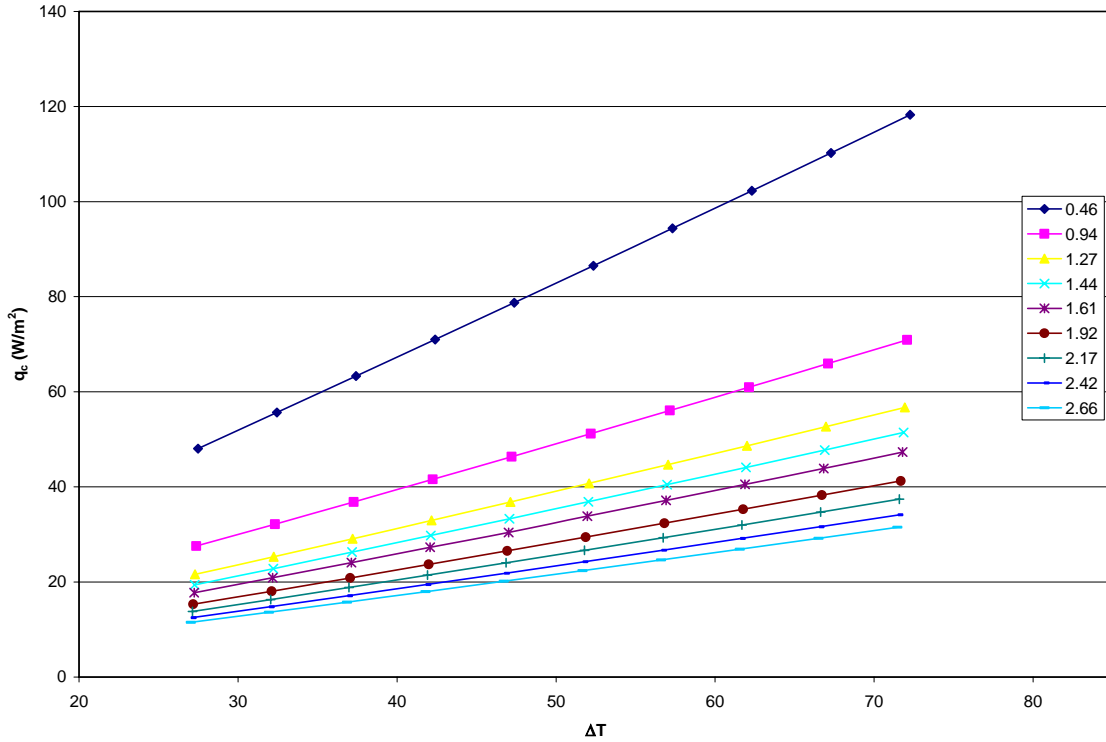
Figure 4.16: Convective Heat flux versus panel temperature and panel size

From the plot it can be concluded that the convective heat transfer is fairly significant in smaller panel sizes, and is minimal at larger panel sizes. This is expected because previous case studies have shown that the convective heat transfer is small for large panel sizes compared to the radiative heat transfer (Schutrum and Vouris, 1954). In perimeter heating cases, however, this is not the case, because the convective heat transfer is an important component in determining the heat output from a panel.

From the results of STAR-CD, a correlation was developed to determine the heat flux from the air temperature, panel size and panel temperature (Appendix G). For comparative purposes, the results from STAR-CD were correlated to the same variables

as the published equations from Min et al. (1956) and Awbi and Hatton (1999). The heat flux equation is shown in Equation 4.54 below and has a correlation coefficient of $R^2 = 0.9997$ (Appendix G).

$$q_c^{"} = \frac{0.9937}{D_H^{1.0046}} (T_p - T_a)^{0.0615 \ln(D_H) + 0.9832}$$

(4.54)

where: D_H is the hydraulic diameter of the panel

Figure 4.17 below compares the correlated STAR-CD convective heat flux with the published equations from Min et al. (1956), Schutrum and Vouris (1954) and Awbi and Hatton (1999). In this comparison, the characteristic length was 1.44m, while the air temperature was assumed to be 291K.
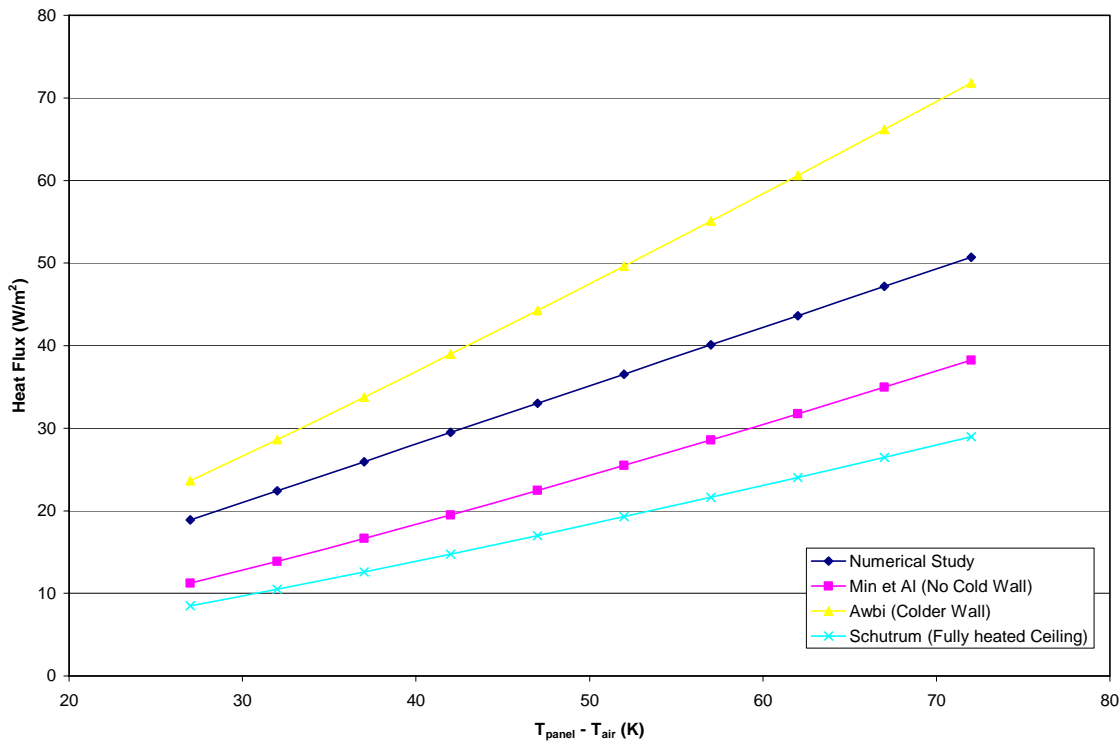
Figure 4.17: Comparison of various Heat Flux Correlations

As can be seen the STAR-CD correlation lies between Min et al.'s (1956) correlation and Awbi and Hatton's (1999) correlation, indicating that the convective heat flux equation is within the acceptable range. It should be noted that Equation 4.54 is valid for a hydraulic diameter range from 0.45m to 2.65m and a panel temperature range from 318K to 363K.

Equation 4.54 predicts the convective heat transfer from a radiant panel with knowledge of the hydraulic diameter and panel temperature. From Figures 4.13 and 4.16, it can be seen that the convective heat transfer is dependant on the size of the radiant panel relative to the size of the ceiling. For radiant panel perimeter heating applications, it would be more useful to determine the convective heat transfer with respect to the aspect ratio. Using a similar derivation to Equation 4.54, Equation 4.55 predicts the convective heat flux with knowledge of the aspect ratio, panel temperature and air temperature (Appendix G).

$$q_c^" = \frac{0.201}{AR^{0.8375}}(T_{panel} - T_{air})^{0.0511\ln(AR)+1.0808} \tag{4.55}$$

where: AR is the aspect ratio ($L_{panel}/L_{ceiling}$)

This equation is valid for a panel temperature ranging from 318 K to 363 K and an aspect ratio of 0.06 to 0.5 and has a correlation coefficient of $R^2 = 0.99$ (Appendix G).

For the purposes of the thesis, comparing the RSC model to the experimental data, Equation 4.55 will be used to predict the natural convective heat transfer coefficient.

4.4   Back Losses

Typically radiant panels are either installed embedded in the ceiling, or mounted hanging beneath the ceiling. For the radiant panels which are mounted under the ceiling,

the back losses can be determining by calculating radiative and convective heat transfer coefficients above the panel. In cases where the panel is embedded in the ceiling (as in the radiant panel test chamber) it is necessary to insulate the back portion in order to minimize the heat transfer to the outside surfaces. In this case, the back losses are determined using a conductive heat transfer model.

The back losses can be estimated from Equation 4.7, knowing the thickness and conductivity of the material. The back loss heat transfer coefficient can be shown to be:

$$h_{backloss} = \frac{k_{ins}}{t_{ins}} \tag{4.56}$$

Plotting the effects of insulation thickness on panel performance (Figure 4.18) using the RSC model (Appendix H), as much as 50% of the heat transfer can be lost if the panel is not properly insulated. Therefore, to validate the reverse solar collector model, the back losses must be taken into account.
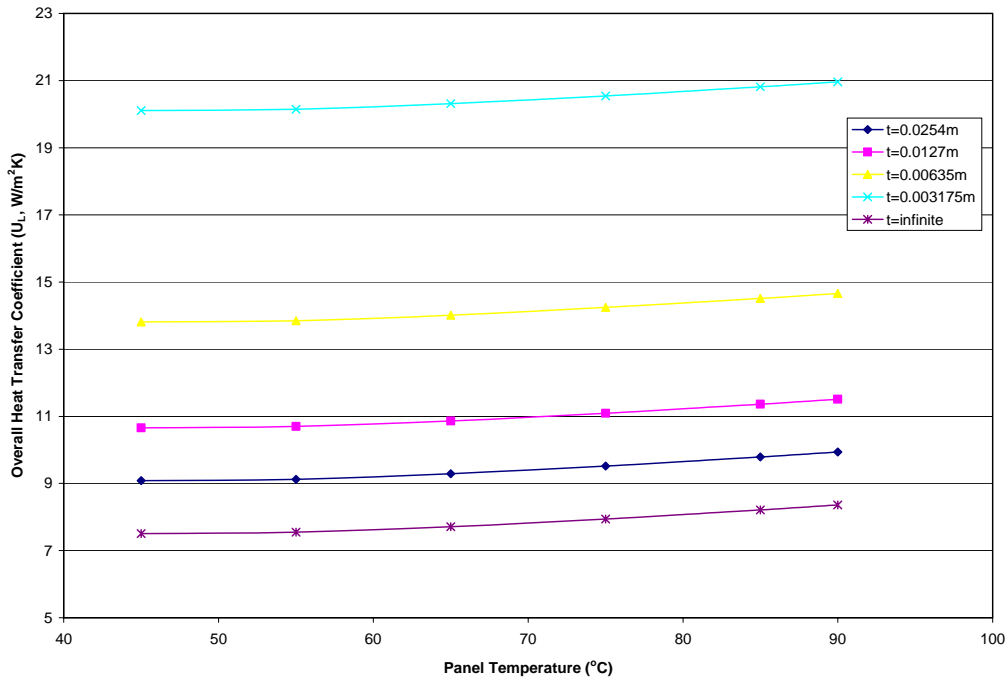
Figure 4.18: Effect of Panel Insulation on the Overall Heat Transfer Coefficient

The proposed ASHRAE standard 138P (Chapman, 2005) suggests that the panel should be insulated with 2.54 cm thick insulation with a minimum conductivity, k, of 0.04 W/mK. Measuring the insulation used during testing, it was found that it was 1.2 cm thick and had a conductivity value of 0.08 W/mK. Thicker insulation was not added, because Sigma Convectors wanted to simulate their actual installation conditions using the insulation they provide. Although, this resulted in a significantly higher panel output than actual proposed test conditions, the effective panel performance could be estimated knowing the radiative and convective heat transfer.

4.5   Bond Conductance

To optimize panel performance, the panel thermal resistance should be minimized. There are several methods used to minimize the thermal resistance, each manufacturer using an alternative method. Sigma Convectors, for example, improves the bond conductance by adding a conductive heat paste between the tube and panel.

Equation 4.20 can be used to estimate the bond conductance, if the conductivity, thickness and width of the heat paste are known. The conductivity of the heat paste is known to be 1.5W/mK. It was however difficult to estimate the thickness and width. During manufacturing, a 0.5 cm wide and 0.3 cm thick strip of heat paste is applied to the extruded aluminum panel used for the 24-4. The tube is then clipped into place, thus spreading the heat conducting paste over the entire contact area. Assuming the paste distributes evenly and over the entire contact area, the width of the paste is estimated to be 1.67 cm. From conservation of volume, the thickness can be calculated to be 0.09 cm.

Following a similar analysis for the 24-8 panel the heat paste had a width of 1.67cm with a thickness of 0.013cm.

Plotting the effects of bond conductance on the panel temperature (Figure 4.19) using the RSC model developed (Appendix I), the results show that the panel temperature can vary by as much as 5°C with a variation in thickness of 1mm. By increasing the heat paste thickness by 0.5mm, a panel temperature difference over 2°C can be seen.
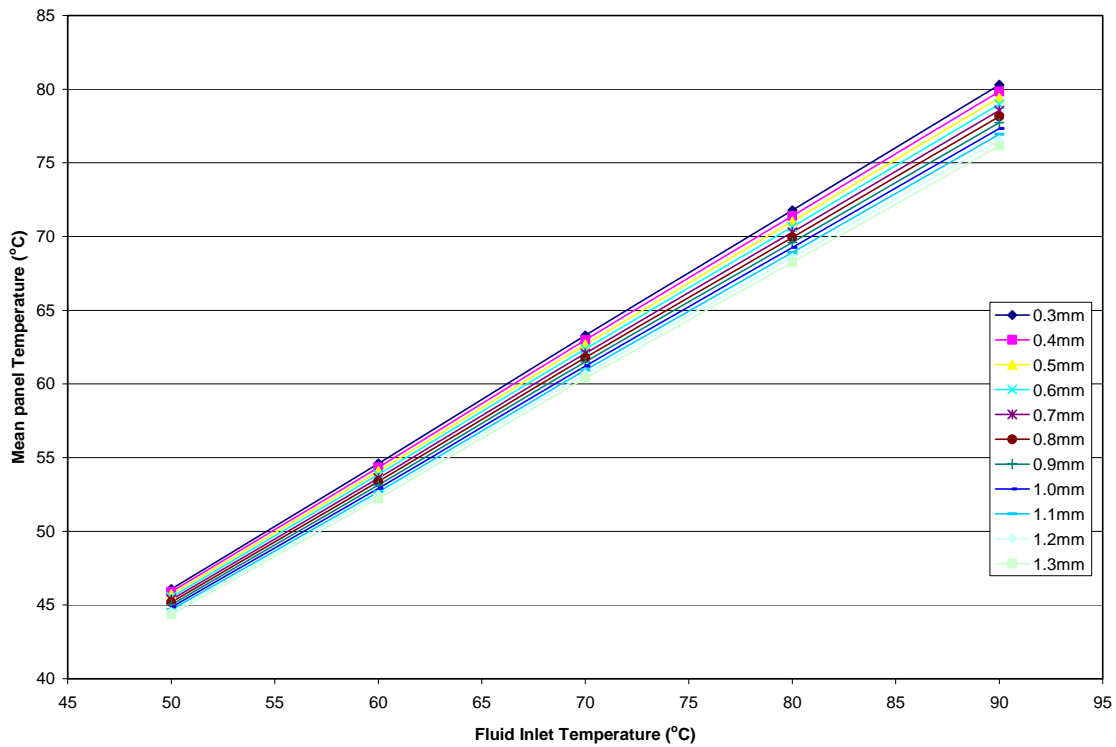
Figure 4.19: Effect of Heat Paste Thickness on Panel Performance

With a 2°C temperature difference the heat output from the panel can vary as much as 20W/m as documented in Appendix I. To minimize the uncertainty in the calculation of heat output from a panel, it is important to precisely know the dimensions of the heat paste.

4.6   Solution Method

Having calculated the necessary variables to predict the panel heat output and panel temperature, the solution methodology is summarized below. The convective and radiative heat transfer coefficients are dependant on panel temperature, and therefore an iterative procedure is required to determine the unknowns.

The steps for solving are as follows:

1. Input the fluid inlet temperature

2. Estimate the panel temperature

3. Calculate the radiative, convective and conductive heat transfer coefficients

4. Calculate the outlet fluid temperature using Equation 4.30

5. Calculate the heat output using Equation 4.31

6. Solve for the panel temperature using Equation 4.32

The solution is considered to be converged once the predicted panel temperature is within $0.001^{\circ}C$ of the previous calculated temperature.

Chapter 5

Results and Discussion

This chapter compares the experimental and RSC model results for the two radiant panels tested and discusses the assumptions and errors associated with both cases.

5.1   Results

The analytical model was used to simulate the conditions of the radiant panel test chamber as closely as possible. The following parameters were therefore used to run the model:

- The surrounding temperatures during the experiment were maintained at 20°C and the cold wall was at 12°C.
- The insulation on the back of the panel was measured to be 12.7mm thick with an estimated conductivity of 0.08W/mK.
- The heat conducting paste between the tube and the panel was 1.67cm wide with a thickness of 0.09cm and a conductivity of 1.5W/mK for the 24-4 panel. The heat paste was calculated to be 0.13cm thick for the 24-8 panel.
- The panel sizes were 0.61m wide and had 4 and 8 tube passes connected in serpentine fashion.
- The water flow rate was 0.057L/s.

Running the model at the experimentally obtained inlet water temperatures, the results are summarized in Table 5.1 for the 24-4 panel and Table 5.2 for the 24-8 panel. The experimental results can be found in Appendix C and RSC model results in Appendix I.

Table 5.1: RSC Model Results and Experimental Results for the 24-4 Panel

	RSC Model		Experiment	
$T_{f,in}$ (^{o}C)	T_{panel} (^{o}C)	Heat Output (W/m)	T_{panel} (^{o}C)	Heat Output (W/m)
51.78	46.51	216.65	46.98	207.89
61.35	54.26	291.39	55.18	298.47
73.91	64.71	378.25	64.56	374.18
86.66	75.02	478.46	75.92	490.74
100.4	86.13	586.56	86.89	613.29

Table 5.2: RSC Model Results and Experimental Results for the 24-8 Panel

	RSC Model		Experiment	
$T_{f,in}$ (^oC)	T_{panel} (^oC)	Heat Output (W/m)	T_{panel} (^oC)	Heat Output (W/m)
51.96	48.05	233.10	48.1	261.68
62.77	57.49	314.95	56.46	332.03
73.71	67.03	398.35	66.75	407.68
86.11	77.76	497.32	77.75	553.61
99.66	89.42	610.02	87.46	700.08

5.1.1   Mean Radiant Panel Temperature

The mean radiant panel temperature is plotted against the inlet fluid temperature

for RSC model and experiment in Figure 5.1 below for the 24-4 panel.
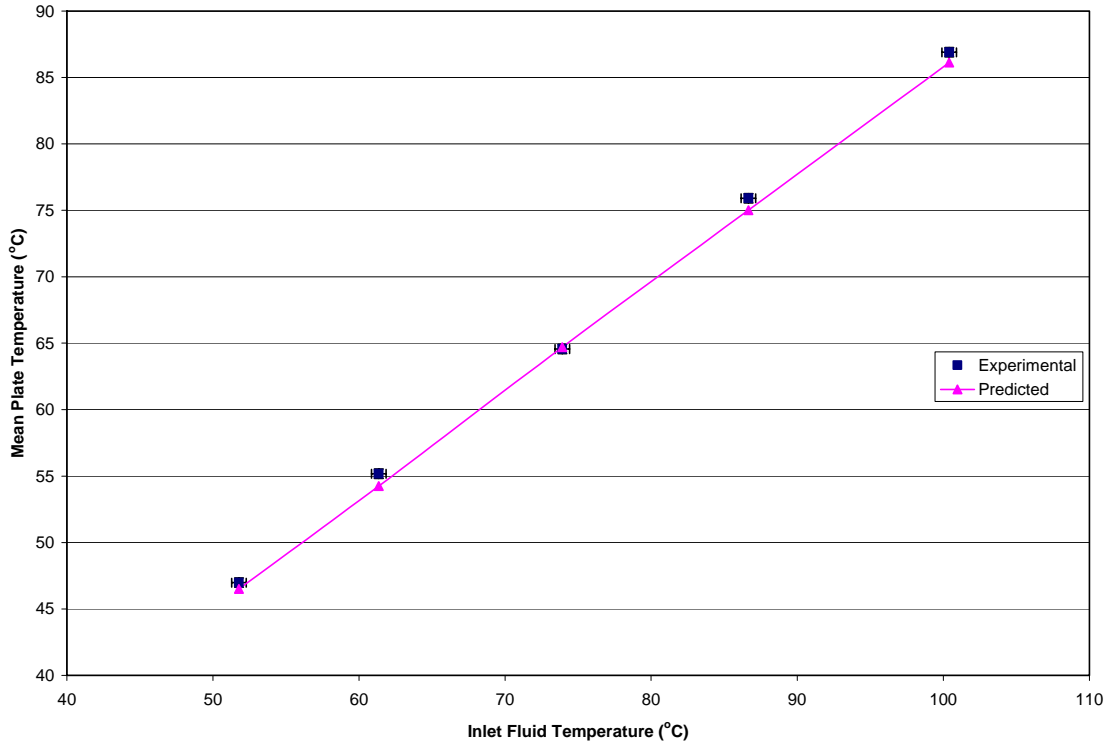
*Figure 5.1:   Experimental and Analytical Model Panel Temperature versus the Inlet
Water Temperature for a 24-4 Panel*

As can be seen the model predicts the actual mean radiant panel temperature very closely.

The model is within 2% for each of the five measured panel temperatures (Appendix I).

The accuracy of the model is further shown in Figure 5.2, a plot comparing the predicted panel temperatures to the experimental measured values. The predicted values are very close to the ideal case, where experimental and predicted panel temperatures are equal, concluding that the mean plate temperature predicted by the RSC model is a valid analytical method for radiant heating panels.
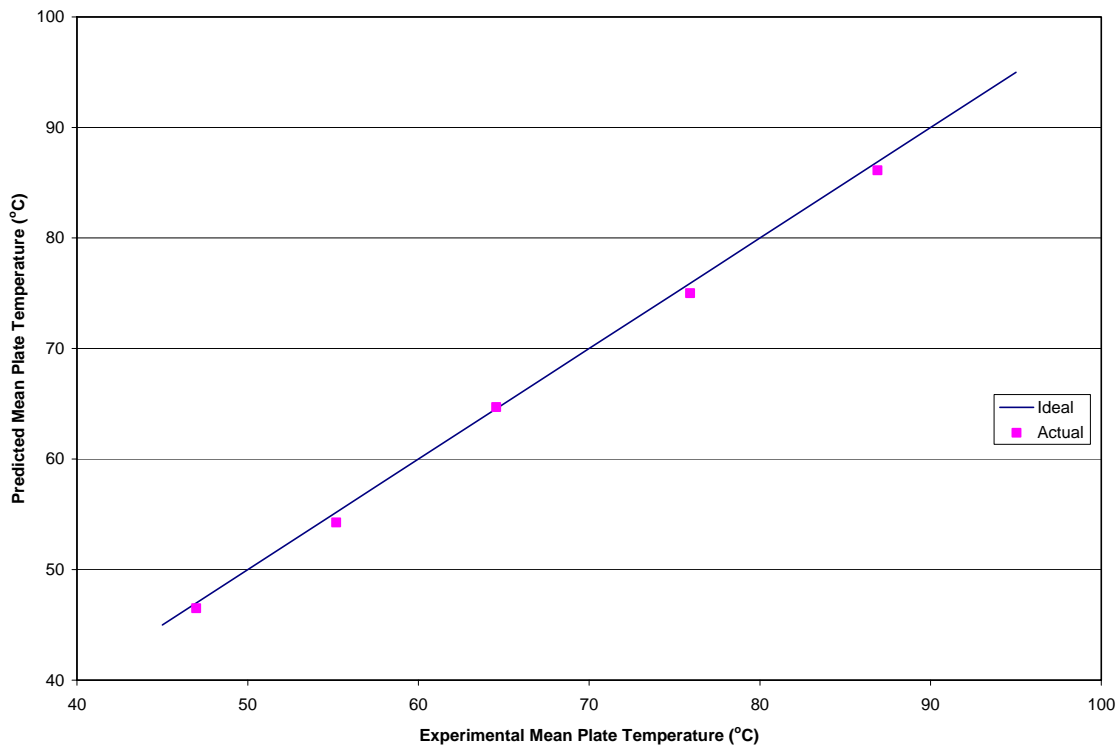
Figure 5.2: *Predicted Panel Temperature versus Actual Panel Temperature for a 24-4 Panel*

The experimental results for the 24-8 radiant panel tested are compared to the RSC model in Figure 5.3 and Figure 5.4 below.
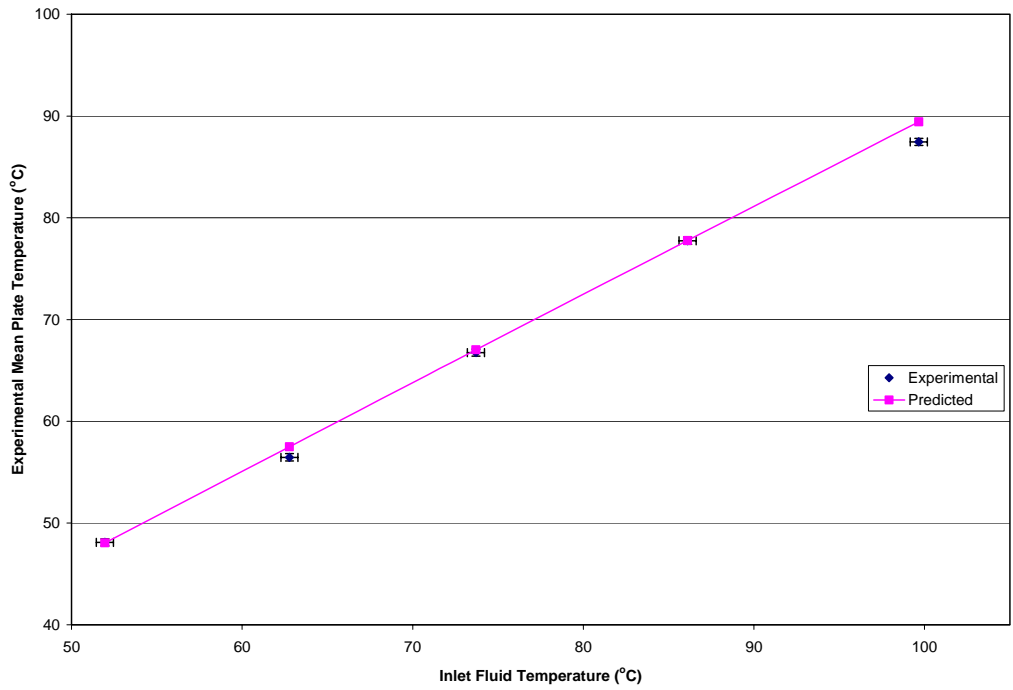
Figure 5.3:   Experimental and Analytical Model Panel Temperature versus the Inlet Water Temperature for a 24-8 Panel
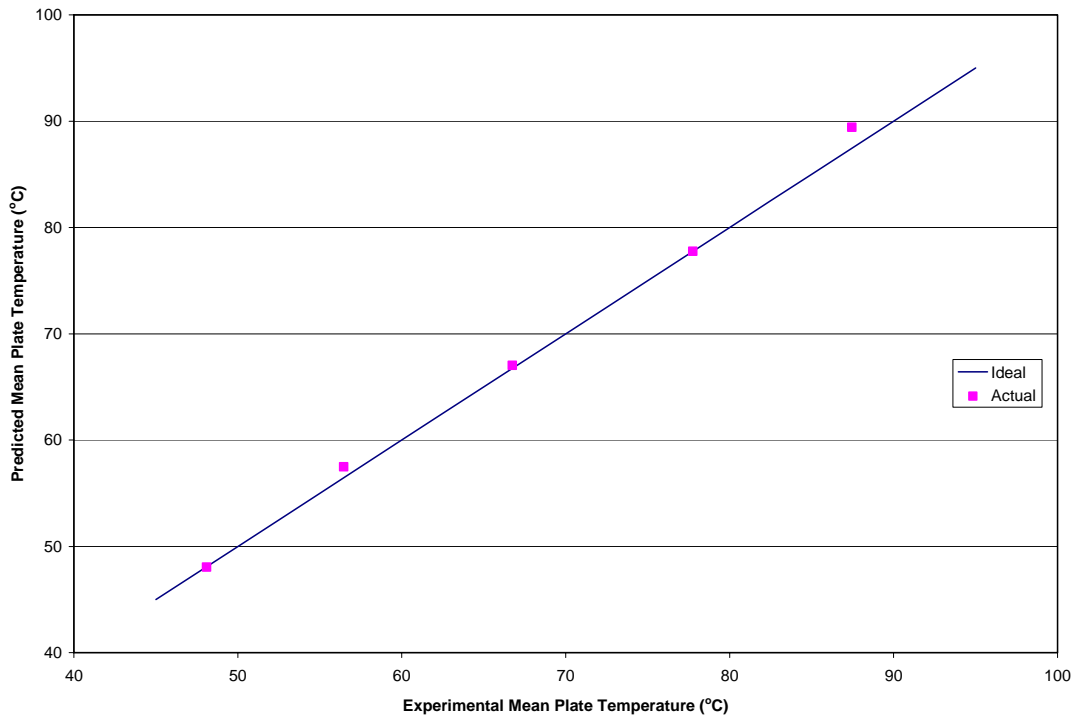
Figure 5.4:   Predicted Panel Temperature versus Actual Panel Temperature for a 24-8 Panel

Similar to the 24-4 panel temperature results, the predicted model is within 2% of the measured data – the greatest deviation occurring at the higher panel temperature (Appendix I). The predicted panel temperatures are still in good agreement with the experimental data, concluding that the RSC is a valid mean panel temperature prediction method.

5.1.2   Radiant Panel Heat Output

Figure 5.5 and Figure 5.6 compare the RSC model panel heat output with the experimental results for both test cases.
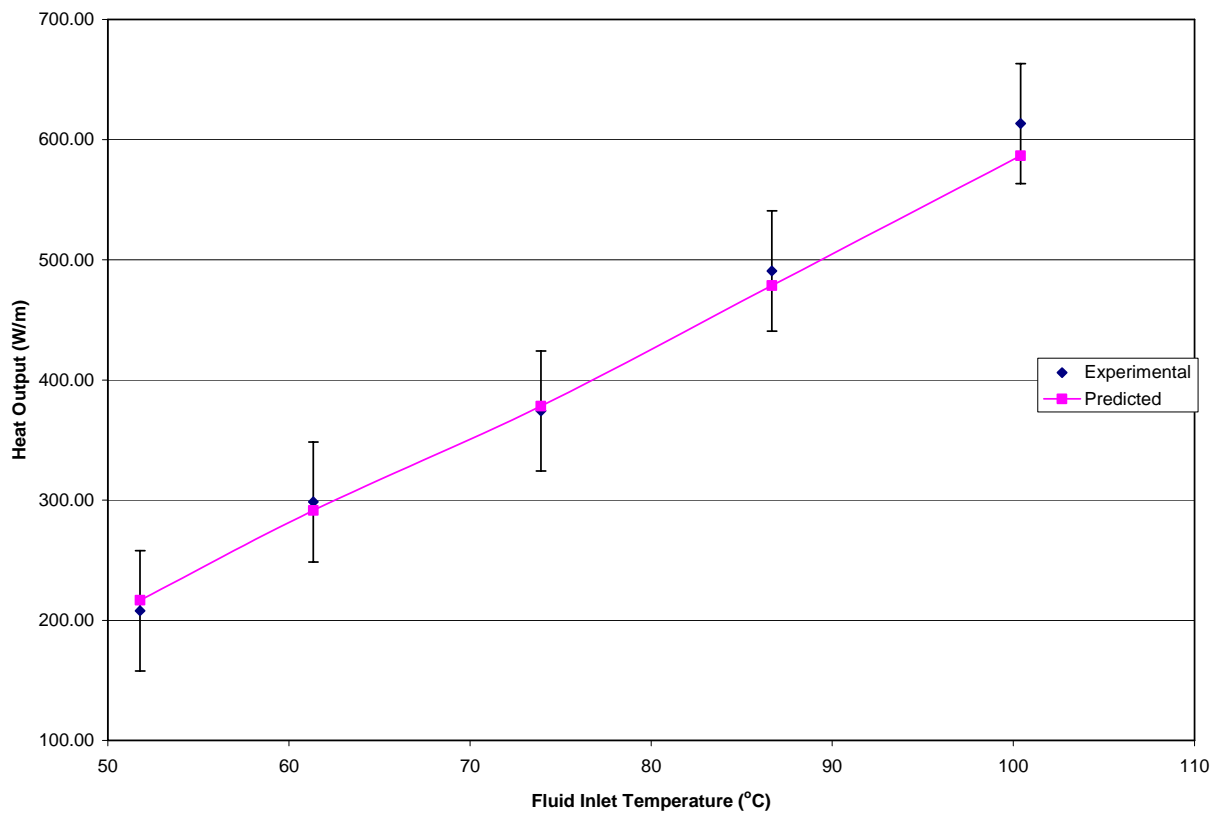
Figure 5.5:   Experimental and Analytical Heat Output versus Inlet Water Temperature for a 24-4 Panel
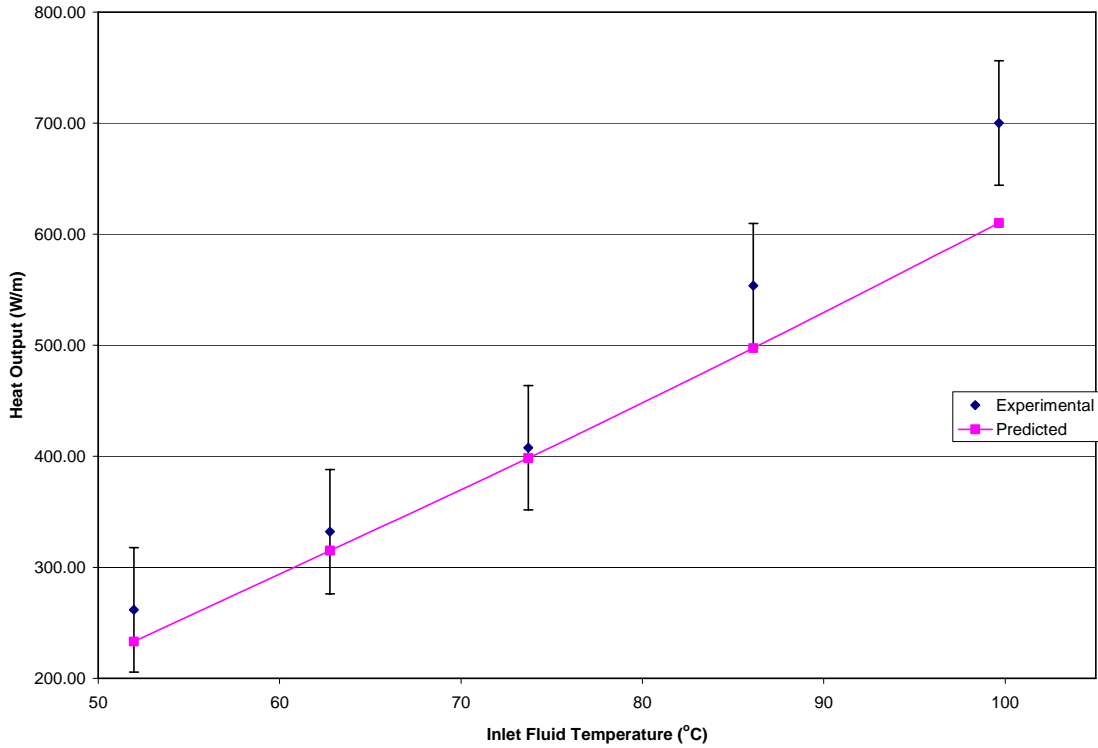
Figure 5.6: Experimental and Analytical Heat Output versus Inlet Water Temperature for a 24-8 Panel

Overall, the model is accurate within 5% of the 24-4 experimental results and 10% for the 24-8 results the greatest error occurring at the higher panel temperatures. At the higher mean water temperatures, the RSC under-predicts the actual heat output. This under-prediction is expected because of the radiant panel installation and temperature measurement setup. Uninsulated, quick-disconnect hoses, 0.3 meters in length, were installed between the radiant panel and the radiant panel water source. At the higher mean water temperatures, more heat was lost to the surroundings, which was unaccounted for by the analytical model.

In most of the test runs, a significant air flow was felt around the chamber, caused by the opening of a garage door located close to the radiant panel test chamber. This additional air flow contributed to the heat output measured from the experimental test

chamber. Identifying that this was a source of error, the air flow around the chamber was minimized during the 24-8, 70°C mean water temperature test. Running the RSC model for this scenario the results are close to the obtained experimental results as can be seen in Figure 5.6.

5.1.3   Predicted Air Temperature Results

To determine the convective heat transfer, the air temperature at the geometric center of the room must be determined. The air temperature inside the room was experimentally measured using a shielded thermocouple located 1.83m above the floor at the center of the room. Figure 5.7 below compares the experimentally measured air temperature for the 0.61m wide panel to the results predicted by the STAR-CD simulation for a 0.53m wide panel and a 0.75m wide panel.
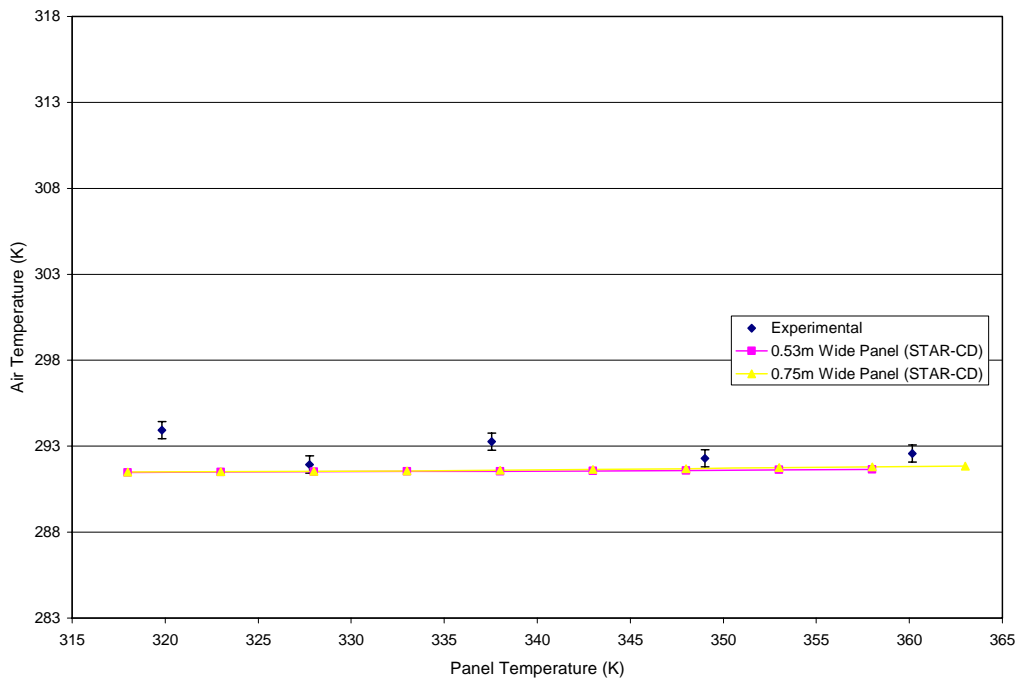
Figure 5.7:   *Experimental Air Temperature Measurements for a 0.61m Panel and the Predicted Air Temperature from the Numerical Model at the Center of the Radiant Panel Test Chamber versus The Panel Temperature*

The measured air temperature was as much as 2.5^{o}C higher in some cases than the predicted numerical results. Looking at the numerical results, the air temperature increases in a linear fashion versus the panel temperature. This would be expected because only the panel temperature is varied, and the walls remain at the same temperature. During the experiment, the wall temperatures were difficult to maintain at a constant value without a chilling system. Cold water had to be constantly added to the system in order to maintain a 20°C temperature on the wall. Due to this temperature control method, the wall temperatures fluctuated, which ultimately caused the variation in air temperature. The air temperature results therefore deviated slightly from the expected results. In addition, STAR-CD modelled the chamber in 2D, so the effects of the side walls were not accounted for.

5.2   Uncertainties and simplifications in the RSC Model

As in any heat transfer model, several assumptions and simplifications have been made to use the RSC model. Three cases in particular will be discussed. First an attempt will be made to quantify the uncertainty associated with the measurement of the heat paste thickness, and secondly, the effects of the cold wall temperature not being at 10°C on the correlated convective heat transfer coefficient will be analysed. Finally, the air temperature measurement location and increase caused by the increased back wall temperature will be considered.

5.2.1 Thickness of the Heat Paste

As discussed in Section 4.5, the bond conductance has a significant impact on the predicted panel temperature. For instance, varying the thickness of the heat paste by

0.5mm could result in a panel temperature increase/decrease of 2°C. When the radiant panels for testing were built, the heat paste was applied though a caulking gun. By applying the heat paste manually, the amount used varied from panel to panel. During the construction of the 24-4 and 24-8 radiant panels used for testing the initial thickness and width of the heat paste was measured, which was accurate to within 0.5mm. For example, the width of the heat paste measured was 0.5cm +/-0.05cm and the thickness measured 0.3cm +/-0.05cm for the 24-4 panel. To relate bond conductance to the temperature of the panel, Equation 4.18 was considered:

$$T_{panel} = T_f - q'_{panel}\left(\frac{1}{h_w \pi D_i} + \frac{1}{C_b}\right) \tag{5.1}$$

and the bond conductance, C_b, is calculated from Equation 4.19:

$$C_b = \frac{k_b b}{t_b} \tag{5.2}$$

To determine the error associated with the bond conductance, it was assumed that no uncertainty was associated with the heat transfer from the panel, the fluid temperature or the heat transfer coefficient of the circulated water. The uncertainty in the bond conductance was then determined using the RSS method (Appendix D) and shown to equal 5.4 W/mK. At this level of uncertainty, the predicted panel temperature is within 4°C of the calculated value (Appendix D). Table 5.3 below summarizes the uncertainty of each predicted panel temperature at various different inlet fluid temperatures.

From these results it can be concluded that at greater inlet fluid temperatures, the uncertainty in the panel temperature increases. This was expected because as the heat flux from the panel increases, the heat paste temperature drop becomes a greater, ultimately affecting the panel temperature.

Table 5.3: Uncertainty associated with bond conductance

$T_{f,in}$ (^{o}C)	Heat Output (W/m)	T_{panel} (^{o}C)	Uncertainty (^{o}C)
51.78	216.65	46.51	1.51
61.35	291.39	54.26	2.03
73.91	378.25	64.71	2.64
86.66	478.46	75.02	3.34
100.4	586.56	86.13	4.09

5.2.2   Convective heat transfer coefficient

To determine the convective heat transfer coefficient, the test chamber was simulated in STAR-CD using the same boundary conditions as initially proposed. One difference, however, was the temperature of the cold wall. To determine how the convective heat transfer was affected by this temperature difference, the STAR-CD model for a 0.61 m wide panel was run at various panel temperatures and two back wall temperatures (10°C and 12°C) (Appendix F). Comparing the results for the 12°C and 10°C back wall temperature, Figure 5.8 shows a minimal change in the predicted convective heat output.
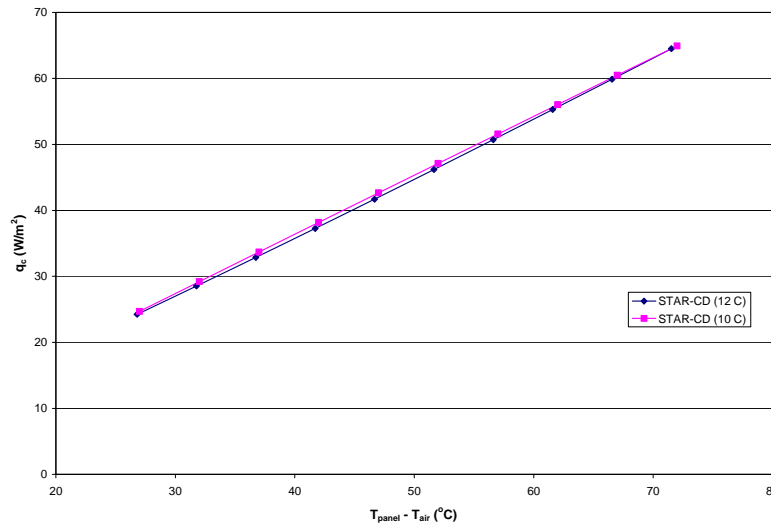
Figure 5.8:   Convective Heat Transfer versus Panel minus Air Temperature at different back wall temperatures

With such a small change, the cold wall temperature difference had a minimal effect on the convective heat transfer.

5.2.3 Air Temperature

As mentioned earlier the air temperature is dependant on the surrounding wall temperatures. When comparing the STAR-CD results to the experimental results, the predicted results were below the actual measured temperature values (Figure 5.7). This can be explained by various causes, one being that the numerical model was in 2D and the left and right wall temperature effects were not taken into account and another cause being that the back wall during the experiment was not at the desired temperature.

To take into account the left and right wall effects in a numerical model, a 3D enclosure would need to be set up, which would become a very tedious task in STAR-CD. It was therefore decided to consider only the effects caused by a difference in the back wall temperature on the predicted air temperature.

The air temperature, caused by the difference in expected surrounding temperatures, can be approximated considering the numerical model for the 0.61m panel used in Section 5.2.2. Comparing the results, a temperature increase of 0.5°C at the center of the room is expected (Appendix F). In addition, since the air temperature was measured 1.83m above the floor instead of 1.5m during the experiment, the numerical model temperatures were taken at the experimental height. Comparing these predicted air temperatures to the experimental results for the 24-4 panel (Figure 5.9), some measured values are within experimental error.
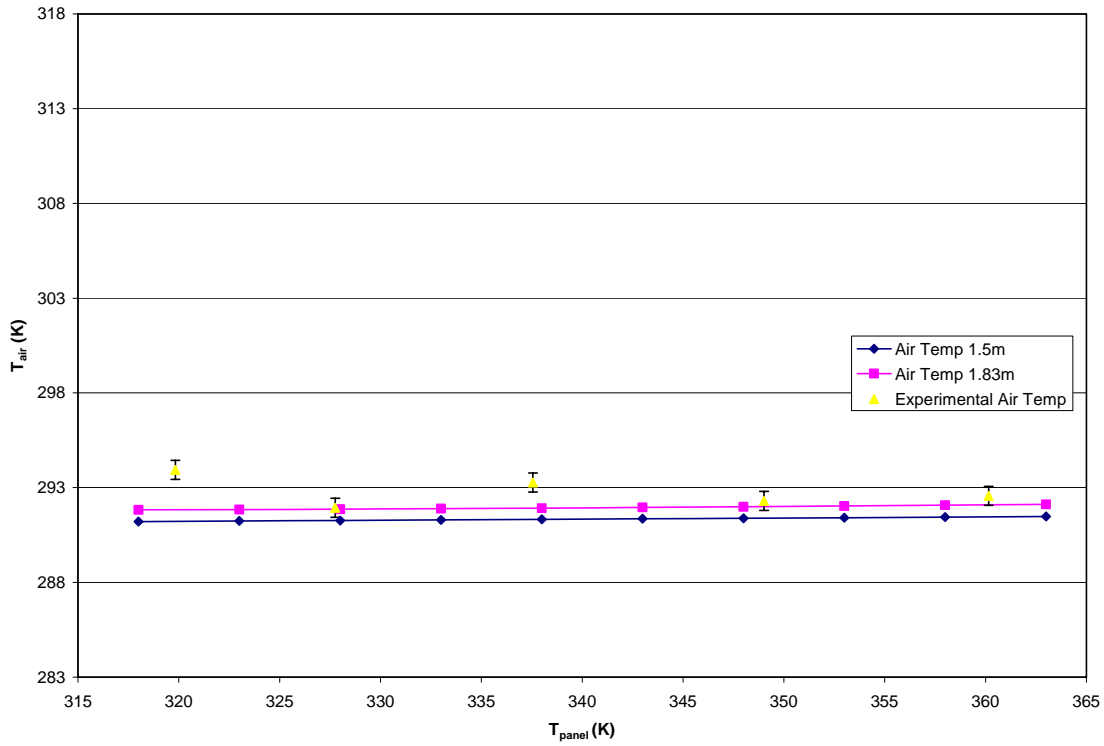
Figure 5.9: Air Temperature versus Panel Temperature for the 24-4 Panel

The air velocity profiles predicted by STAR-CD for the 10°C and 12°C cold wall temperature, the results were very close to each other. A slightly higher air velocity was predicted for the lower cold wall temperature, which was expected, because of the buoyancy effects of the air. The air velocity profile plots are shown in Figure 5.10.
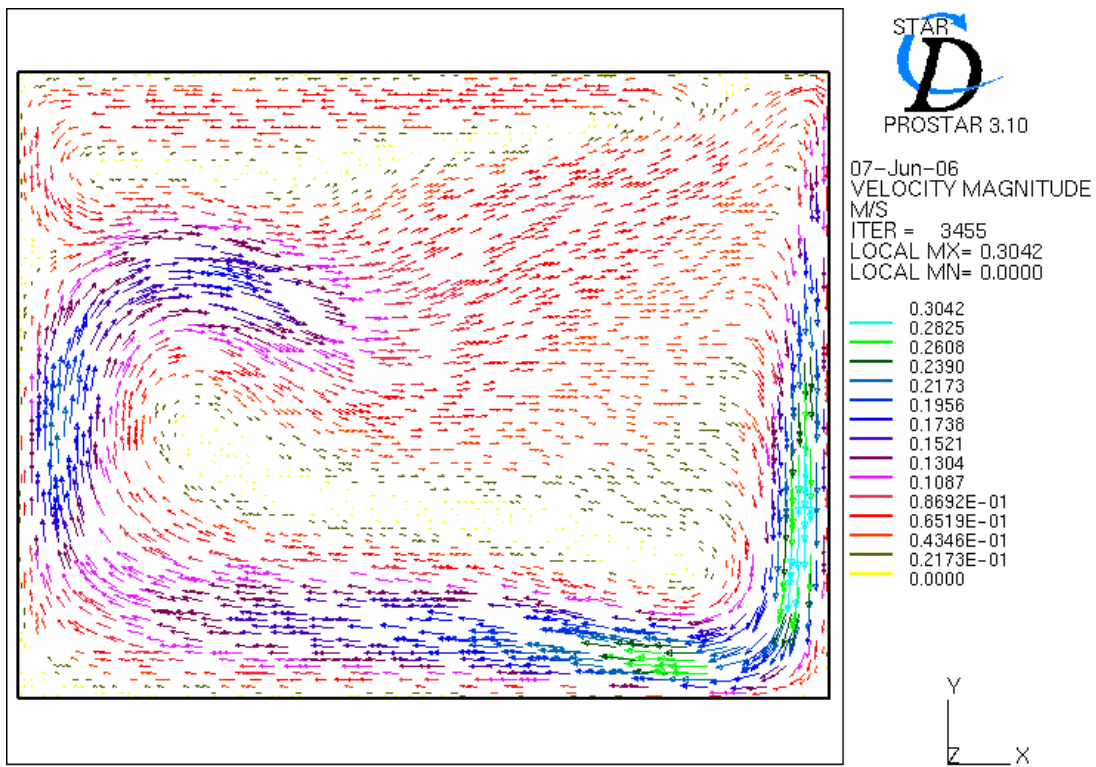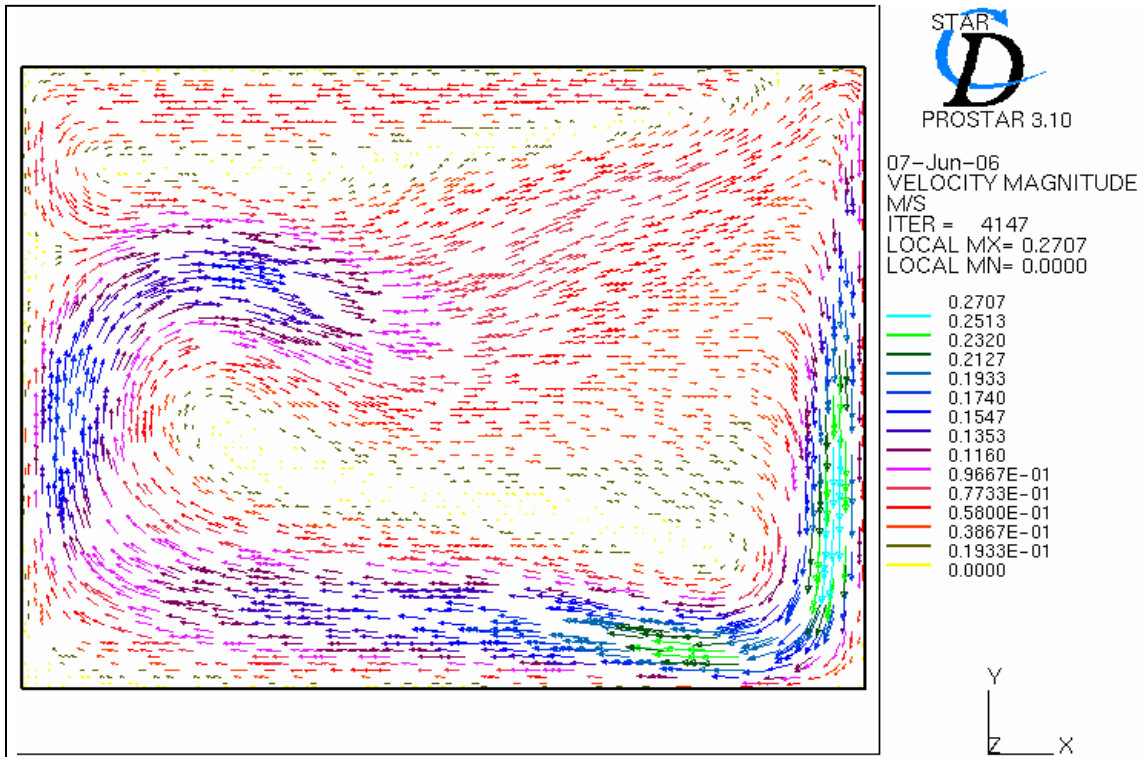
Figure 5.10: Predicted Air Velocity Profile with 12°C and 10°C back wall Temperature

Chapter 6

Summary and Conclusions

6.1 Summary

An analytical model has been developed to predict the panel temperature and heat output for perimeter radiant panel systems with a known inlet temperature and flow rate, based on a flat plate solar collector model. As radiative and convective heat transfer coefficients were required to run the model, an analytical analysis of the radiative heat transfer was performed, and a numerical model was developed to predict the convective heat transfer coefficient. Using the conventional radiative heat exchange method assuming a three-surface enclosure, the radiative heat transfer could be determined. Numerically, a correlation was developed to predict the natural convective heat transfer.

To validate the analytical model, an experimental analysis was performed on radiant panels. A 4m by 4m by 3m test chamber was constructed in which the surrounding walls and floor were maintained at a constant temperature and the heat output from an installed radiant panel was measured. Two radiant panels were tested; a 0.61m wide panel with 4 passes and a 0.61m wide panel with 8 passes. The panels were tested at 5 different inlet water temperatures ranging from 50°C to 100°C.

The RSC model panel temperature and heat output predictions were in good agreement with the experimental results. The RSC model followed the same trends as that in the experimental results, and the panel temperature and panel heat output were within experimental uncertainty, concluding that the RSC model is a viable, simple algorithm which could be used to predict panel performance.

6.2   Conclusions

From the analytical and numerical model results several conclusions can be drawn, which are validated by the experimental results and observations. The numerical model was used to determine the convective heat transfer coefficient and the air temperature in the chamber. The analytical model was used to predict the panel heat output and panel temperature.

The conclusions drawn from the model are:

- Higher convective heat transfer coefficients are observed when physically smaller sized radiant panels are installed adjacent to a colder wall. The smaller the aspect ratio, the greater the heat transfer coefficient. This is an important observation because radiant panels are typically installed as perimeter heaters adjacent to cold walls. The convective heat transfer will have a greater effect on the overall heat output.

- The panel temperature had a small effect on the convective heat transfer coefficient. The variation was not as significant as the characteristic length, D_H, of the panel.

- The air temperature predicted by the numerical model was close to the measured air temperature, however in some cases it was not within the measured air temperature uncertainty. The numerical model assumed an infinite wide chamber, so the left and right wall effects were not accounted for, explaining the temperature difference.

- A correlation has been developed relating the characteristic length and temperature of the radiant panel to the convective heat transfer coefficient.

Conclusions that can be drawn from the analytical model validated with the experimental results are:

- The analytical model used to predict the panel temperature is within experimental uncertainty.

- The heat output from the panel was predicted within the experimental error. With knowledge of the inlet water temperature, surrounding temperatures, air temperature and water flow rate, the reverse flat plate solar collector model was within 10% of the measured experimental results for both panels tested. More accurate results were obtained when the air flow around the exposed radiant panel pipe was minimized. As expected, as the panel temperature increased, the overall heat output also increased.

- The back losses have a significant effect on the panel performance. Almost half of the total heat output is due to the losses through the back using the regular supplied 12.7mm thick Batt insulation.

- Approximately 85% of the effective panel heat output is through radiation. It is therefore important to accurately determine and specify the surrounding conditions.

6.3   Recommendations

Currently, the experimental test chamber predicts the heat output with an uncertainty of up to 25%. This is mainly due to the inaccuracy in the measured water temperature. This problem was identified in the early stages of the experiment, so a thermopile was installed. The purchased data logger, however, was incapable of measuring the millivolt signal generated by the thermopile. An alternative would be to

install a thermistor to measure the water temperature, which can be accurate up to 0.1^{o}C. Due to budget constraints, this could not be done immediately.

From the observations made, almost 50% of the measured heat output was due to the back losses. Typically, radiant panels are insulated within the ceiling panels, as installed in the booth, or installed below the ceiling. Installing the radiant panel below the ceiling would give a better estimate of the effective heat transfer to the room, and should be considered in order to get more realistic results.

During the experiment, the cold wall temperature was maintained around 12°C. The back wall temperature was maintained by running city water through the mounted copper and PEX tubing. The city water was incapable of maintaining a back wall temperature of 10°C. A small chiller should be installed in the system to cool the water down and save on water. In addition, although the other surrounding wall temperatures were maintained at 20°C, a small chiller should be installed in this system as well, to ensure that a steady temperature can be maintained.

The analytical model assumes constant surrounding temperatures when predicting the radiant heat transfer. Observations during the experiment, however, indicated that the surrounding temperatures fluctuated approximately 1.5^{o}C and were maintained within 1°C between quadrants. A model should therefore be developed that takes into account the variability of the surrounding surface temperatures.

Other studies that could be looked into are the effects of the convective heat transfer on various back wall temperatures. It was noted that a 2°C increase had minimal effects, however it would be interesting to determine at which temperature the back wall will have a significant effect on the air flow.

References

Adlam, T.N., 1949, "Radiant Heating," 2nd edition, The Industrial Press, New York, USA.

Armstrong Pumps – Circuit Balancing Valves, 2006, "ArmFlo Venturi Style," http://www.armstrongpumps.com/Data/performancecurves/Links/01_02_005/CBV-V_composite_curves.pdf.

ASHRAE, 2003, "Handbook of HVAC Applications – SI Edition," American Society of Heating, Refrigeration and Air Conditioning Engineers, Inc., Atlanta.

ASHRAE, 2004, "Handbook of HVAC Systems and Equipment – SI Edition," American Society of Heating, Refrigeration and Air Conditioning Engineers, Inc., Atlanta.

ASHRAE, 2005, "Handbook of Fundamentals – SI Edition," American Society of Heating, Refrigeration and Air Conditioning Engineers, Inc., Atlanta.

Awbi, H.B., Hatton, A., 1999, "Natural Convection from Heated Room Surfaces," Energy and Buildings, vol. 32.

Buckley, N.A., 1989, "Application of Radiant Heating Saves Energy," ASHRAE Journal 31(9), Atlanta.

Chapman, K., 2005, Personal Communication on the status of the ASHRAE Standard – Method of Testing for Rating Hydronic Radiant Ceiling Panels.

Conroy, C., and Mumma, S.A., 2001, "Ceiling Radiant Cooling Panels as a Viable Distributed Parallel Sensible Cooling Technology Integrated with Dedicated Outdoor Air Systems," ASHRAE Transactions, vol. 107, part 1.

Dasylab, 2005, "Instruction Manual for Dasylab Data Acquisition System Laboratory, Version 8."

Din 4715, 1994, "Method of testing and rating cooling panels," Halle, Germany.

DOE (U.S. Department of Energy), 2005, "2005 Buildings and Energy Data Book," Office of the Energy Efficiency and Renewable Energy.

Duffie, J.A., Beckman, W.A., 1991, "Solar Engineering of Thermal Processes," John Wiley & Sons, Inc. Toronto, Canada.

Hadlock, C.J., 2004, "Heat Transfer Model for Radiant Heating," University of Waterloo, Waterloo, Canada

Heid, H., Kollmar, A., 1943, "Die Strahlungsheizung," Carl Marhold Verlagsbuchhand-lung, Halle, Germnay.

Hottel, H.C., Whillier, A., 1958, "Evaluation of Flat-Plate Collector Performance," Trans. Of the Conference on the Use of Solar Energy, vol. 2.

Huang, N.Y, 2005, "Thermal Performance of Double Glazed Windows with Inner-Pane Venetian Blinds," University of Waterloo, Waterloo, Canada.

Huebscher, R.G., Schutrum, L.F., Parmalee, G.V., 1952, "A Low-Inertia Low-Resistance Heat Flow Meter," ASHVE Transactions, vol. 58.

Kilkis, I.B., Sager, S.S., Uludag, M., 1994, "A simplified model for radiant heating and cooling panels," Simulation Practice and Theory 2.

Kochendörfer, C., 1996, "Standardized Testing of Cooling Panels and Their Use in System Planning," ASHRAE Transactions, vol. 102, part 1.

Kramer, J., 2005, Personal communication on the manufacturing of radiant heating panels.

Laouadi, A., 2004, "Development of a radiant heating and cooling model for building energy simulation software," Building and Environment, vol. 39, Issue 4.

LMNO Engineering, Research and Software Limited, 2003, "Gas Viscosity Calculator," http://www.lmnoeng.com/Flow/GasViscosity.htm.

Lomas, K.J., 1995, "The UK applicability study: an evaluation of thermal simulation programs for passive solar house design," Building and Environment, vol. 31.

Min, T.C., Schutrum, L.F., Parmalee, G.V., Vouris, J.D., 1956, "Natural Convection and Radiation in a Panel-Heated Room," ASHAE Research Report No. 1576.

Munson, B.R., Young, D.F., Okiishi, T.H., 2002, "Fundamentals of Fluid Mechanics, 4th edition," John Wiley & Sons, Inc., Toronto.

OMEGA, 2004, "The Temperature Handbook and Encyclopedia," 5th edition, Omega Engineering, Inc.

Schutrum, L.F., Vouris, J.D., 1954, "Effects of Room Size and Non-Uniformity of Panel Temperature on Panel Performance," ASHVE Transactions, vol. 60.

Shoemaker, R.W., 1954, "Radiant Heating," 2nd edition, McGraw-Hill, New York

Siegel, R., Howell, J.R., 1981, "Thermal Radiation Heat Transfer," McGraw-Hill, New York.

Sigma Convectors, 2004, "Radiant heating Panel Product Information Catalogue," Brampton.

Simmonds, P., 1996, "Practical Applications of Radiant Heating and Cooling to Maintain Comfort Conditions," ASHRAE Transactions, vol. 1996, part 2.

STAR-CD, 2001, "STAR-CD Version 3.15 Methodology," Computational Dynamics Limited.

Steinman, M., Kalisperis, L.N., Summers, L.H., 1989, "The MRT-Correction Method: A New Method of Radiant Heat Exchange," ASHRAE Transactions, vol. 95, Part 1.

Tasker, C., Humphreys, C.M., Parmalee, G.V., Schutrum, L.F., 1952, "The A.S.H.V.E Environment Laboratory," ASHVE Transactions, vol. 58.

Walton, G.N., 1980, "A New Algorithm for Radiant Interchange in Room Loads Calculations," ASHRAE Transactions, vol. 86, Part 2.

Xia, Y., Mumma, S.A., 2005, "Ceiling Radiant Cooling Panels Employing Heat-Conducting Rails: Deriving the Governing Heat Transfer Equations," ASHRAE Transactions, vol. 112, Part 1.

Zhang, Z., Pate, M.B., 1986, "A numerical study of heat transfer in a hydronic radiant ceiling panel," Numerical Methods in Heat Transfer, ASME HTD 62.

Appendix A

ASHRAE Draft Standard 138P

ASHRAE STANDARD

BSR/ASHRAE Standard 138P

Method of Testing for Rating Hydronic Radiant Ceiling Panels

PUBLIC REVIEW DRAFT
August 1999

AMERICAN SOCIETY OF HEATING, REFRIGERATING AND AIR-CONDITIONING ENGINEERS, INC.
1791 Tullie Circle, NE · Atlanta GA 30329

96

N O T I C E

COMMENTS ON DRAFT STANDARDS
(Revised December 4, 1998)

1. INSTRUCTIONS FOR FILING COMMENTS:

a) Comments on this standard:
1) must comply with these and other instructions provided in the Form for Commenting;
2) must be received by **October 4, 1999**;
3) must be substantiated;
4) must be signed and dated;
5) may be submitted electronically on the Form for Commenting attached to the standard (submittal in paper form is acceptable, but electronic submittal is preferred);
6) must be sent to ASHRAE Manager of Standards.

b) Comment forms may be submitted electronically either as files (MS Word 7 preferred) attached to e-mail (UUENCODE preferred), files uploaded to an ftp site, or on 3.5" floppy disk. **Commenters' signatures are required on all electronic files sent on disk, uploaded to the ftp site, or sent via e-mail to convey non-exclusive copyright.** For signature submittal, choose one of the following methods:

(1)   sign the comment forms electronically, or

(2)   send a copy of the comment form via mail or fax with the commenter's signature and indicate whether the original comments are on disk, uploaded to the ftp site, or sent via e-mail.

NOTE: If method (2) is used, then the box beneath the signature line on the Form for Commenting must be checked.

Submit public review comments to:
Manager of Standards
ASHRAE
1791 Tullie Circle, NE
Atlanta, GA 30329-2305
E-mail: *public.review.comment@ashrae.org*
Ftp server address: *ftp.ashrae.org*, logon to anonymous ftp in directory: *public.review.comment.*
(Alternatively, mail paper versions to ASHRAE address or fax: 404-321-5478.)

c) In your comments, please specify whether you approve or disapprove of the proposed document. If you provide technical comments with your approval, indicate whether approval is contingent upon considering them for inclusion (1) in the current proposal or (2) in future revisions of the current proposal. If you disapprove, give your reasons.

d) Supplemental background documents to support your comments may be included. Highlighting pens should not be used since highlights will not reproduce. Please do not return marked-up copies of the draft.

2. INFORMATION ON REVIEW AND DISPOSITION OF COMMENTS:

All comments received by ASHRAE will be acknowledged. Comments submitted on the Form for Commenting provided and complying with the instructions provided on the Form and in 1(a)-(b) above will be forwarded to the Project Committee for consideration. The Project Committee will inform commenters

of the proposed disposition of their comments unless the Manager of Standards informs commenters that there will be another public review.

3. SUPPLEMENTAL INSTRUCTIONS TO COMMENTERS

Commenters must submit comments to ASHRAE Headquarters on the form provided. Submittal in electronic form is preferred. Submittal in paper form is acceptable. A paper version of the comment form is included in the public review draft standard.

Following are supplementary instructions for some of the numbered sections in the Form for Commenting:

a) Provide all of commenter's contact information, including E-mail or Internet address if available.
b) Sign and date the non-exclusive copyright release. (See 1b.)
c) Identify the specific section that is the subject of the comment. Use a separate form for each comment.
d) Provide specific wording changes or action that would resolve commenter's concerns.
e) Provide a brief substantiation statement that presents the rationale, and supporting documentation as well as any technical data and back up. Provide an abstract of lengthy substantiations. If supplementary documents are provided, electronic files in wordprocessed (MS Word 7 preferred) or scanned form are preferred. Indicate whether attachments have been provided.

1. Purpose

This standard establishes uniform methods of laboratory testing for rating the thermal performance of hydronic radiant ceiling panels used for heating and/or cooling of indoor spaces. The goal is to allow rating of panels for heat transferred to or from the space to be conditioned.

2. Scope

2.1 This standard specifies procedures, apparatus, and instrumentation for determination of heating and cooling capacities for hydronic ceiling panels in a specific indoor configuration and thermal environment.

2.2 Panel performance is measured as a function of hydronic working fluid (water) temperature, panel surface characteristics, and the temperature of the surrounding space.

2.3 This standard covers testing of hydronic ceiling panels in the following surface temperature ranges:

Heating panels: room air temperature to $150^{\circ}C$ ($300^{\circ}F$)
Cooling panels: below room air temperature

2.4 This standard does not cover:

      a) electric heating panels,
      b) heating panels that are part of the ceiling or floor structure, or
      c) test methods for design, production, or field testing.

3. Units of Measurement

3.1 System of Units

The International System of Units (SI) has been employed in the text with inch-pound (I-P) units shown parenthetically. Values shall be based on the National Institute of Standards (NIST) values, which, in turn, are based on the fundamental values of the International Bureau of Weights and Measures.

3.2 Basic Units. The unit of length is either the millimetre, designated mm (inch, in) or the metre, designated m (foot, ft). The unit of mass is the kilogram, designated kg (pound, lb) and the unit of time is the second, designated s. The unit of temperature is the degree Celsius, designated ^{o}C (degree Fahrenheit, ^{o}F) or the kelvin, designated K.

3.3 Flow Rate. The unit of mass flow rate is kilograms per second, kg/s (2.2 lb_m/s) and the unit of volumetric flow rate is cubic metres per second, m^3/s (35.314 ft^3/s).

3.4 Area. The unit of area is square meters, m^2 (10.768 ft^2).

3.5 Force. The unit of force is the newton, N (0.2248 lb_f).

3.6 Pressure. The unit of pressure is the pascal, Pa, or the kilopascal, kPa (psig).

3.7 Energy and Work. The unit of energy or work is the joule, J (9.48×10^{-4} Btu). The unit of power is the watt, W (3.412 Btu/hr).

3.8 Fluid Density. The unit of density is kilogram per cubic meter designated as kg/m^3 (lb_m/ft^3). The density of water at standard conditions, 101.325 kPa (29.92 in Hg) and $20^{o}C$ ($68^{o}F$) is 998.2 kg/m^3 (62.3 lb_m/ft^3).

3.9 Viscosity. The units of dynamic viscosity are N s/m^2 (lb_m/ft hr) and the units of kinematic viscosity are m^2/s (ft^2/hr). The two are related through the density of the fluid. The viscosity of water decreases with increasing temperature as shown below.

Temperature	Dynamic Viscosity N s/m^2 (lb_m/ft hr)	Kinematic Viscosity m^2/s (ft^2/hr)
20°C (68°F)	1.02 x 10^{-3} (2.47)	1.02 x 10^{-6} (0.0395)
40°C (104°F)	6.51 x 10^{-4} (1.57)	6.56 x 10^{-7} (0.0254)
60°C (140°F)	4.60 x 10^{-4} (1.11)	4.67 x 10^{-7} (0.0181)
80°C (176°F)	3.50 x 10^{-4} (0.85)	3.60 x 10^{-7} (0.0140)
100°C(212°F)	2.82 x 10^{-4} (0.68)	2.94 x 10^{-7} (0.0114)

3.10 Specific Heat. For water the specific heat, C_p, is 4.179 kJ/kg·K at 60°C (0.998 Btu/lb°F at 140°F).

3.11 Reynolds Number R_e. Reynolds Number is a dimensionless quantity used to indicate whether a flowing fluid is laminar or turbulent.

3.12 Barometric Pressure. Barometric pressure is the atmospheric pressure measured at the location of the test room and used to correct panel ratings to standard conditions of 101.325 kPa (29.92 in Hg)(1 standard atmosphere).

4 Symbols Used

SYMBOL	DESCRIPTION	UNIT
A_p	effective panel surface area	m^2 (ft^2)
C	panel performance coefficient	$W/m^2 \cdot t^n$ ($Btu/ft^2 \cdot t^n$)
C_p	specific heat	$kJ/kg \cdot K$ ($Btu/lb_m \,^oF$)
$\underline{m}$	mass flow rate	kg/s (lb_m/s)
n	panel performance exponent (from $q=C\Delta t^n$)	dimensionless
p_b	barometric pressure	kPa (in Hg)
Δh	energy loss in the hydronic circuit	$m\ H_2O$ (psig)
q	heat transfer rate per unit area	W/m^2 ($Btu/hr\ ft^2$)
R_e	Reynolds Number	dimensionless
t_a	air temperature	^oC (^oF)
t_e	enclosure exterior wall temperature	^oC (^oF)
t_i	panel inlet water temperature	^oC (^oF)
t_g	globe temperature	^oC (^oF)
t_m	panel mean water temperature	^oC (^oF)
t_o	panel outlet water temperature	^oC (^oF)
t_p	panel effective surface temperature	^oC (^oF)
AUST	area weighted average enclosure surface temperature	^oC (^oF)
Δt	temperature difference	^oC (^oF)
v	air velocity	m/s (ft/s)
μ	dynamic viscosity	$N \cdot s/m^2$ ($lb_m/ft\ hr$)
v	kinematic viscosity	m^2/s (ft^2/hr)

5 Definitions

air temperature: Temperature of the air in the test enclosure obtained using a sensor shielded to

minimize radiation effects between the sensor and the enclosure (see section 7.1.2).

cooling panel: A panel specifically designed for conditioning of a space through energy transfer

to the panel from the occupants or space.

effective panel surface temperature: The area weighted average surface temperature of the

panel under test.

enclosure surface temperature (AUST): The area weighted average surface temperature of the enclosure or test chamber in which the panel to be tested has been installed.

globe temperature: The equilibrium temperature obtained inside a uniformly painted 150 mm (6 in) diameter black globe. The temperature obtained is a result of thermal equilibrium between energy gained or lost by radiation and convection (see section 7.1.3).

head loss: The measured energy loss in the flowing fluid across a panel under test at the specified mass flow rate.

heating panel: A panel specifically designed for conditioning of a space through energy transfer from the panel to the occupants or space.

hemispherical emittance: A property of a material that governs the emission of energy by radiation relative to that emitted by a perfect emitter, or black body at the same temperature.

inlet water temperature: The temperature of the water at the inlet to the panel under test.

outlet water temperature: The temperature of the water at the outlet of the panel under test.

mean water temperature: The arithmetic average between the inlet and outlet water temperature.

6. Instruments and Methods of Measurement

6.1 Accuracy and Precision. The specifications for instruments and methods of measurement that follow include accuracy and precision requirements. The specified requirements correspond to two standard deviations about the mean and are based on an assumed normal distribution of the errors involved. Random errors can be determined only from an adequate statistical sample.

Instrument errors shall be such that two standard deviations of the accumulated data from the mean (precision) do not exceed the specified values.

6.2 Resolution. The resolution of an instrument is the smallest change in input that will result in a measurable change in output. In no case shall the resolution of the measurement device be greater than the accuracy specified for the instrument.

6.3 Temperature Measurements

6.3.1 Standard Practice. Temperature measurements shall be made in accordance with ASHRAE Standard 41.1-1986(RA 91)[1].

6.3.2 Accuracy and Precision. The accuracy and precision of the instruments, including their associated readout devices, shall be within the following limits. Two sets of values have been shown for water temperature as it is possible to make the measurements using individual sensors or sensors connected to read differentially.

	Accuracy	Precision
Water Temperature (individual sensors)	0.05°C (0.1°F)	0.05°C (0.1°F)
Water Temperature (differential sensors)	0.1°C (0.2°F)	0.1°C (0.2°F)
Air Temperature	0.2°C (0.4°F)	0.2°C (0.4°F)
Surface Temperature	0.2°C (0.4°F)	0.2°C (0.4°F)
Air Velocity	0.1 m/s (0.3 ft/s)	0.1 m/s (0.3 ft/s)

6.4 Flow Rate Measurements

6.4.1 Standard Practice. Flow rate measurements shall be made in accordance with ASHRAE Standard 41.8-1989[2].

6.4.2 Accuracy. The accuracy of the liquid flow rate measurement shall be 0.1% of the measured quantity in mass units per unit time.

6.4.3 Mass Flow Meter Calibration. For calibration of the mass flow measurement devices, time and mass measurements shall be made with an accuracy of 0.05%.

6.4.4 Thermal Energy Measurements. Energy transferred to or from a panel under test may be directly measured by thermal energy measurement techniques if conducted using a meter calibrated in accordance with ANSI/ASHRAE Standard 125-1992[3].

7. Equipment and Setup

7.1 Test Chamber. Tests shall be performed in a chamber with inner dimensions of not less than 3.66m (12ft.) by 3.66m (12 ft.) by 3.05 m (10 ft.) high. All interior surfaces shall have a smooth, flat-painted finish with a surface emittance of 0.9 or higher and shall be temperature-controlled. The control of interior surface temperature shall be such that one wall of the enclosure, designated the exterior wall, can be maintained at a temperature different from the remaining walls.

The chamber shall be constructed so as to minimize infiltration or exfiltration. Prior to being used to test panels, the chamber shall be tested for air tightness in accordance with ANSI/ASHRAE 119-1988 (RA 94)[4] and shall have a leakage class of A or B. For cooling tests the humidity shall be controlled so as to prevent condensation on a test panel or any of the enclosure surfaces. This condition shall be deemed to have been met if the dew point of the air in the chamber is more than 2°C (3.6°F) below the panel inlet water temperature.

7.1.1 AUST Temperature Uniformity. The uniformity of the interior surface temperature will be determined by the heating or cooling method used to maintain the temperatures as well as the control system. As a minimum, the temperature of each surface of the enclosure shall be measured at four locations using a temperature sensor specifically designed for surface measurements. The surface shall be divided into quadrants and a temperature sensor located at the geometric center of each quadrant. The temperature of each surface of the enclosure shall be

controlled so that the variation in average surface temperature between surfaces (other than the exterior wall) is less than 1°C (1.8°F).

7.1.2 Panel Effective Surface Temperature. The test panel effective surface temperature shall be determined as the arithmetic average of surface temperature measurements from at least six locations on the panel.

7.1.3 Air Temperature. Air temperature in the chamber shall be measured using a shielded temperature sensor located at a height of 0.75 m (2.5 ft) above the floor of the enclosure. The sensor shall be placed at the geometric center of the floor.

7.1.4 Globe Temperature. Globe temperature in the test chamber shall be measured using a 150 mm (6 in.) diameter black globe thermometer. Globe temperature shall be measured at a location as near as practical to the air temperature measurement location.

7.1.5 Air Velocity. Air velocity in the vicinity of the panel(s) under test shall be measured using a temperature compensated hot wire or hot film anemometer. The measurement shall be made within 300 mm (12 in.) of the face of the panel under test.

7.1.6 Head Loss. The head loss across the panel(s) under test shall be measured as the pressure difference between the panel inlet and panel outlet. The measurements should be made as close as practical to the inlet and outlet water temperature measurement locations.

7.2 Test Panel Installation. A specific installation is detailed below and referred to as Installation Method A. Installation Method A shall be used if it does not conflict with the manufacturer's design application for the panel under test. An alternate method, designated Installation Method B, has been included in this standard for cases where a standard installation is inappropriate.

In all installations the test panel supply and return water lines shall be insulated when within the chamber. The insulation shall be a minimum of 6 mm (0.25 in) thick and have a thermal conductivity of 0.030 W/mK (0.017 Btu/h·ft·°F) or lower. Inlet and outlet water temperatures shall be measured within 300 mm (12 in) of the connection to the test panel(s).

In the event that the test panel consists of more than one individual panel, the individual panels shall be plumbed in series. In no case shall the total tubing length of the test panel(s) exceed 61 m (200 ft).

7.2.1 Installation Method A. A standard T-grid acoustical ceiling system shall be installed such that the lower surface of the ceiling is 2.44 m (8.0 ft) above the floor surface of the enclosure. The panel(s) to be tested shall be installed such that the long axis is parallel to the exterior wall of the enclosure. The edge of the panel(s) under test shall be placed within 25 mm (1 in.) of the exterior wall of the chamber. All other spaces in the T-grid shall be filled with acoustical tiles. The test panel(s) shall be horizontal and shall be placed such that the lower surface is flush with the bottom surface of the acoustical tiles (2.44 m, 8.0 ft.). The back of the test panel(s) shall be insulated using 25 mm (1 in) glass fibre insulation without a foil backing. The insulation shall have a density of 13 kg/m^3 (0.75 lb$_m$/ft^3) and a thermal conductivity of 0.04 W/mK (0.023 Btu/h·ft·°F).

7.2.2 Installation Method B. Method B allows the test panel to be installed in configurations different from that specified in Method A. An example might be a cooling panel intended to hang from a ceiling so that air is free to circulate around the panel or a panel (heating or cooling) that is intended to be installed in a vertical position. If Method B is used, complete details of the installation must be included with the test results. Complete details shall include both a written

and a graphical description of the installation. In all cases the panel location relative to the enclosure surfaces shall be described as is required for Method A.

8. Method of Conducting a Test

8.1 General Test Requirements.

8.1.1 Test Points. The number of determinations required to establish the performance of a panel depends on the purpose of the panel, heating or cooling. For heating panels the test shall include a minimum of five panel mean water temperatures equally spaced over the operating range specified by the manufacturer. For cooling panels the test shall include four panel mean water temperatures, 10^oC (50^oF), 12.5^oC (55^oF), 15^oC (60^oF) and 18^oC (65^oF).

8.1.2 Equilibrium. Equilibrium conditions shall be established before each determination. To test for equilibrium, trial observations shall be made until steady readings are obtained. As a minimum, five sequential readings of all required measurements, each spaced in time by five minutes, shall be at the required value and remain within test tolerances. (See Section 8.3)

8.2 Data to be Recorded.

8.2.1 Test Panel. The description of the test panel shall be recorded. The description shall include panel manufacturer, model, physical dimensions, tube sizing and placement as well as surface finish. In the case of a heating panel the area of a panel to be tested shall not be less than $4.65 \ m^2$ ($50 \ ft^2$). For cooling panels the area of test panels combined shall be not less than $9.3 \ m^2$ ($100 \ ft^2$).

8.2.2 Test Setup. The description of the test setup including panel placement shall be recorded. This is particularly important in the event that Method B has been used in the rating of a panel.

8.2.3 Instruments. The instruments and apparatus used in the rating of a panel shall be recorded. Names, model numbers, serial numbers and calibration information shall be recorded. It is not necessary to include this information in the test report but it must be kept on file in the event of a question with respect to the overall accuracy of the test results.

8.2.4 Test Data. Test data for each determination shall be recorded. Readings of all relevant data shall be made simultaneously wherever possible. Flow rate through the panel(s) under test shall be adjusted to achieve a Reynolds Number greater than 10000 to ensure turbulent flow within the tubes carrying water. Reynolds number can be calculated using equation 1, below.

$$R_e = \frac{4\dot{m}}{\pi d \mu}$$

where
      $\underline{m}$ = mass flow rate of water, kg/s (lb_m/s)
      $\underline{d}$ = inside diameter of the panel tubes, m (ft)
      μ = dynamic viscosity of water, N·s/m^2 (lb_m/ft hr)

Regardless of whether Method A or Method B is used, the following readings will be made at each mean water temperature: Inlet water temperature, t_i, outlet water temperature, t_o, fluid mass flow rate, $\underline{m}$, enclosure air temperature, t_a, globe temperature, t_g, enclosure surface temperature, AUST, exterior wall temperature, t_e, head loss across the panel, Δh, and air velocity in the vicinity of the panel. Data shall be recorded at a minimum of 5 minute intervals until equilibrium, as defined in section 8.1.2, is reached. Local barometric pressure shall be measured at the test location or obtained from a local weather station.

8.3 Test Conditions

8.3.1   Heating Panels. The surface temperature of the exterior wall of the chamber shall be 10°C ±0.5^{o}C (50°F ±0.9^{o}F). All other test chamber surfaces shall be maintained at 20°C ±0.5^{o}C (68°F ±0.9^{o}F). Air temperature in the chamber shall remain between 18°C and 21°C (65°F to 70°F) during steady state operation.

Tests shall be conducted at a minimum of five mean panel water temperatures equally spaced over the manufacturer's specified operating range. The mean water temperatures shall include the highest and lowest operating temperatures specified by the manufacturer.

8.3.2 Cooling Panels. The surface temperature of the exterior wall of the chamber shall be 30°C ±0.5^{o}C (85°F ±0.9^{o}F). All other test chamber surfaces shall be maintained at 23°C ±0.5^{o}C (75°F ±0.9^{o}F). Air temperature in the chamber shall remain between 21°C and 24°C (70°F to 75°F) during steady state operation and humidity in the chamber shall be maintained so that the dew point of the air in the chamber is at least 2°C (3.6^{o}F) below the panel inlet water temperature.

For cooling panels the test shall include four panel mean water temperatures, 10°C (50°F), 12.5^{o}C (55°F), 15°C (60°F) and 18°C (65°F).

9. Calculation of Results

9.1 Panel Output. The output of the panel shall be calculated for all test conditions listed. The output shall be calculated using the measured data and either equation 2 (heating panels) or equation 3 (cooling panels) and shall be normalized with the area of the panel tested.

Heating Panels

$$q = \frac{\dot{m}\, C_p (t_i - t_o)}{A_p}$$

$$q = \frac{\dot{m}\, C_p (t_o - t_i)}{A_p}$$

Cooling Panels

9.2 Average Chamber Surface Temperature, AUST. The average chamber surface temperature shall be calculated as the area weighted average temperature of the six surfaces, excluding the panel under testing, which make up the chamber as indicated in equation 4.

$$AUST = \frac{t_1 A_1 + t_2 A_2 + t_2 A_3 + t_4 A_4 + t_5 A_5 + t_6 A_6}{A_1 + A_2 + A_3 + A_4 + A_5 + A_6}$$

9.3 Mean Water Temperature. The mean panel water temperature shall be calculated at each test condition as the arithmetic average of the panel inlet and panel outlet temperature as indicated in equation 5.

$$t_m = \frac{t_i + t_o}{2}$$

9.4 Characteristic Performance. A characteristic performance equation for the panel tested shall be determined using the method of least squares, Appendix A, to determine the coefficients C and n shown in equation 6 below. The characteristic performance relates the panel output to

the temperature difference between the panel surface and the average surface temperature of the enclosure.

$$q = C\Delta t^n$$

where $\Delta t = t_m$ - AUST (for heating panels)

   Δt = AUST - t_m (for cooling panels)

10. Report and Results of a Test

10.1 Report. The report of a laboratory test of a radiant heating or cooling panel shall include the object, results, uncertainty in results, test data, descriptions of the panel tested and any deviations from the standard. The report shall also identify the name of the person who conducted the test and the laboratory at which the test was performed.

10.2 Characteristic Performance. The characteristic performance of a panel shall be identified on a plot with the test temperature difference, ΔT, shown as the abscissa and panel output, q, shown on the ordinate axis.

Test points shall be identified on the graph using a series of circled points.

The list that follows will serve as a check list for the preparation of performance reports.

Testing Facility
        Name of Testing Organization
        Location of Facility
        Person Conducting Test

Panel Information
        Manufacturer
        Model Information (trade name, make, model number, etc.)

Panel Description
        Dimensions (external, tube size)
        panel material
        panel surface finish (paint, gloss, matte, surface properties)

Test Conditions
        Exact panel installation
        Detailed description and figures if Method B used
        Raw test results (temperatures, flow rates, pressure, drop etc.)

Test Results
        Panel output at each test condition
        Uncertainty in panel output at each condition
        Characteristic performance (coefficients of fitted equation)
        Plot of derived characteristic performance and actual test points

11. References

1. ASHRAE Standard 41.1-1986(RA 91), "Standard Method for Temperature Measurement, American Society of Heating, Refrigerating and Air-Conditioning Engineers, Inc. 1791 Tullie Circle NE, Atlanta, Georgia.

2. ASHRAE Standard 41.8-1989, "Standard Methods of Measurement of Flow of Liquids in Pipes Using Orifice Flowmeters", American Society of Heating, Refrigerating and Air-Conditioning Engineers, Inc. 1791 Tullie Circle NE, Atlanta, Georgia.

3. ANSI/ASHRAE Standard 125-1992, "Method of Testing Thermal Energy Meters for Liquid Streams in HVAC Systems", American Society of Heating, Refrigerating and Air-Conditioning Engineers, Inc. 1791 Tullie Circle NE, Atlanta, Georgia.

4. ANSI/ASHRAE 119-1988 (RA 94), "Air Leakage Performance for Detached Single-Family Residential Buildings", American Society of Heating, Refrigerating and Air-Conditioning Engineers, Inc. 1791 Tullie Circle NE, Atlanta, Georgia.

(This appendix is part of this standard and is included as a normative appendix.)

Appendix A
Curve Fitting by Least Squares

The following method of least squares shall be used to determine the relationship between panel temperature difference and energy output as defined in Section 9.4. Since the characteristic equation is a power function it must be linearized by taking the log of each term in the equation. Thus the equation

$$q = C\Delta t^n \tag{A-1}$$

is linearized as

$$\log(q) = \log(C) + n \log(\Delta t) \tag{A-2}$$

and the standard method of minimizing the residual

$$\varepsilon_r^2 \equiv \sum_{i=1}^{n}(y_i - y_{fitted,i})^2 \tag{A-3}$$

In this case the residual to be minimized is

$$\varepsilon_r^2 = \sum_{i=1}^{p}(y_i - (A + Bx_i))^2 \tag{A-4}$$

where $y_i = \log(q)$
   $x_i = \log(\Delta t)$
   $A = \log(C)$
   $B = n$
   p = number of data points

to do this we must generate the appropriate sums

$$\Sigma y = \Sigma log(q)$$
$$\Sigma x = \Sigma log(\Delta t)$$
$$\Sigma x^2 = \Sigma(log(q))^2$$

and

$$\Sigma xy = \Sigma log(q)log(\Delta t)$$

which are then used to solve for the coefficients A and B in the linear fit.

$$A = \frac{\Sigma y_i - B\Sigma x_i}{p} \tag{A-5}$$

$$B = \frac{p\Sigma x_{iy_i} - \Sigma x_i \Sigma y_i}{p\Sigma x^2 - (\Sigma x_i)^2} \tag{A-6}$$

In this case p is the number of data points used in the fit. Since the original power function was linearized by taking the log of each term the coefficient C must be determined by taking the exponential of A as indicated in (A-7).

$$C = exp(A). \tag{A-7}$$

(This appendix is not part of this standard but is included for information purposes only.)

Appendix B

Uncertainty Analysis of Panel Output

  The rating of a heating or cooling panel depends on a number of measurements that each contain systematic and random errors. Without careful calibrations these errors can result in very large uncertainties associated with calculated panel output. This appendix gives an example of how an uncertainty analysis on panel output could be carried out.

  Starting with equation A1, the calculation of panel output on the basis of the measured quantities m and Δt,

$$q = \dot{m} C_p \Delta t \tag{B-1}$$

it can be seen that the individual uncertainties in mass flow rate and temperature difference will influence the result. Since the equation is purely multiplicative, the following method can be used to estimate the uncertainty in the derived result.

$$\varepsilon_q^2 = [\,\frac{\partial q}{\partial \dot{m}}\,\varepsilon_{\dot{m}}\,]^2 + [\,\frac{\partial q}{\partial C_p}\,\varepsilon_{C_p}\,]^2 + [\,\frac{\partial q}{\partial \Delta t}\,\varepsilon_{\Delta t}\,]^2 \tag{B-2}$$

Taking the derivative of equation B-1 and squaring

$$\varepsilon_q^2 = C_p^2 \Delta t^2 \varepsilon_{\dot{m}}^2 + \dot{m}^2 \Delta t^2 \varepsilon_{C_p}^2 + \dot{m}^2 C_p^2 \varepsilon_{\Delta t}^2 \tag{B-3}$$

Dividing the equation by

$$q^2 = \dot{m}^2 C_p{}^2 \Delta t^2 \tag{B-4}$$

gives the fractional error in panel output as a function of the fractional error in the remaining quantities as shown in equation B-5.

$$\left(\frac{\varepsilon_q}{q}\right)^2 = \left(\frac{\varepsilon_{\dot{m}}}{\dot{m}}\right)^2 + \left(\frac{\varepsilon_{C_p}}{C_p}\right)^2 + \left(\frac{\varepsilon_{\Delta t}}{\Delta t}\right)^2 \tag{B-5}$$

Given that it can be assumed that there is no uncertainty in the specific heat, equation B-5 reduces to

$$\frac{\varepsilon_q}{q} = \sqrt{\left(\frac{\varepsilon_{\dot{m}}}{\dot{m}}\right)^2 + \left(\frac{\varepsilon_{\Delta t}}{\Delta t}\right)^2} \tag{B-6}$$

(This appendix is not part of this standard but is included for information purposes only.)

Appendix C

Using Test Results to Estimate Panel Capacities at Other Than Test Conditions

When design conditions are different than the standard test conditions, the actual performance of the panel changes. Under these circumstances, radiative and convective components of the total output need to be separately adjusted. The standard test result may be adjusted to design conditions using the following relationships.

$$C_s = C[(\frac{q_r \alpha F_c}{q_p 0.87}) + abc(1 - \frac{\alpha q_r}{q_p})] \qquad \text{(C-1)}$$

In this equation, C_s is the performance constant at design conditions and C is the performance constant derived from the test results at standard conditions using equation 6. The ratio q_r/q_p is the average ratio of radiant energy transfer to total energy transfer determined in the performance test and are defined in Chapter 6 of *ASHRAE Handbook,* HVAC Systems and Equipment, 1996[1].

1. Radiative Output Adjustment. The first term in equation C-1 represents the adjustment for the radiative heat transfer component of the panel output. The first adjustment, α, corrects for mean temperature difference between the panel and surroundings at conditions other than standard.

$$\alpha = \frac{1 \pm k[t_a - AUST]_s}{1 \pm k[t_a - AUST]} \qquad \text{(C-2)}$$

For ceiling cooling k is 0.1 and the negative(-) sign is used and for ceiling heating k is 0.02 and the positive sign (+) is used. $[t_a-AUST]$ is the difference between the air temperature and the

AUST, maintained and recorded during the standard test. $[t_a\text{-}AUST]_s$ is the anticipated

temperature difference at a 50% design load condition at the location where the panels are to be

installed.

The second adjustment is made to account for differences in radiation angle factor, F_c,

$$F_c = \frac{1}{1/F_{p\text{-}r} + [(1/\varepsilon_p) - 1] + A_p/A_r[(1/\varepsilon_r) - 1]} \qquad \text{(C-3)}$$

(*ASHRAE Handbook*, HVAC Systems and Equipment, 1996, Chapter 6[1]).

When F_c differs from the value of 0.87 derived for the test chamber, a correction involving three

factors is required.

i)   If the panels are to be installed in a different geometry with respect to the walls and floor.

      $F_{p\text{-}r}$ is the radiation angle factor. $F_{p\text{-}r}$ approaches unity if the panels are flat, horizontal

      and flush with the finished ceiling. For other selected configurations, $F_{p\text{-}r}$ may be

      calculated from related figures and tables in the *ASHRAE Handbook* of Fundamentals,

      Chapter 3. 1997[2].

ii)   If the thermal emittance of various surfaces deviate from 0.9. ε_p and ε_r are the thermal

      emittance of the panel and inside room surfaces respectively. They may be obtained from

      Table 3, [2]*ASHRAE Handbook*, Fundamentals, 1997, Chapter 36.

iii) If the term $A_p/A_r \cdot [(1/\varepsilon_r)-1]$ is not close to zero. A_p and A_r are the surface area of the

      panel agglomerate, and the total surface of the unconditioned surfaces within the

      conditioned space respectively. Using actual design data for A_p, A_r and ε_r, this term may

      be adjusted in equation C-3 through F_c.

2. Convective Output Adjustment. The second term in equation C-1 represents an adjustment for the convective heat transfer component from the panel surface. It consists of three separate effects:

i)   Size effect - the equivalent diameter, D_{es}, of the panel agglomerate at the intended installation. D_e is the equivalent diameter of the panel under test. The equivalent diameter is four times the panel (or panel agglomerate) area divided by the length of the perimeter.

ii)   Pressure (altitude) effect - barometric pressure at the intended installation location, p_s. p_b is the barometric pressure at test conditions.

iii) Air Velocity effect - the anticipated air velocity, v_s, in the vicinity of the panel surfaces.

Table C-1 shows the adjustment coefficients for each term in the correction equation.

Table C-1 Convective Panel Output Adjustments for Conditions Differing From Standard

Coefficient	System of Units	
	SI	IP
a	$(D_e/D_{es})^{0.08}$	$(D_e/D_{es})^{0.08}$
b^1	$(p_s/p_b)^n$	$(p_s/p_b)^n$
c	$(v_s/0.15)^{0.8}$	$(v_s/0.5)^{0.8}$

Notes with respect to Table C-1:

D_{es} = [4 area/perimeter] of panel agglomerate, m (ft)
p_s = barometric pressure at actual location, kPa (in Hg)
p_b = barometric pressure at test conditions, kPa (in Hg)
v_s = anticipated air velocity at design conditions, m/s (ft/s)
n = 0.62 for ceiling panel cooling and 0.50 for ceiling panel heating

1) Correction for altitude above sea level may also be made using the following relationships.

$$b = \{(1 - 2.22 \times 10^{-5} h_s)/(1 - 2.22 \times 10^{-5} h)\}^n \quad h, h_s \text{ in meters,}$$
$$b = \{(1 - 0.67 \times 10^{-5} h_s)/(1 - 0.67 \times 10^{-5} h)\}^n \quad h, h_s \text{ in feet.}$$

where h_s is the altitude of the actual location and h is the altitude of the test location.

References

1. ASHRAE Handbook, HVAC Systems and Equipment, 1996,American Society of Heating, Refrigerating and Air Conditioning Engineers, 1791 Tullie Circle NE, Atlanta, Georgia.

2. ASHRAE Handbook, Fundamentals, 1997, American Society of Heating, Refrigerating and Air Conditioning Engineers, 1791 Tullie Circle NE, Atlanta, Georgia.

Appendix B

Radiant Panel Test Booth Calculations

B.1   View Factor Calculations

This section summarizes the view factor calculations for the largest sized panel that would be tested at the Sigma Radiant Panel Test booth.   This was done to determine the approximate the radiant incoming heat flux to each surface and determine how much energy must be removed by the circulating water on the exterior of the wall.   The calculations were done in MathCad 11 and are shown below.   The first principle view factor equation is given below (Equation B.1)

$$F_{ij} = \frac{1}{A_i} \int_{A_i} \int_{A_j} \frac{\cos\theta_i \cos\theta_j}{\pi R^2} dA_i dA_j \tag{B.1}$$

A diagram of the radiant panel test booth is shown below. The co-ordinate system used to calculate the view factors is shown on the diagram.
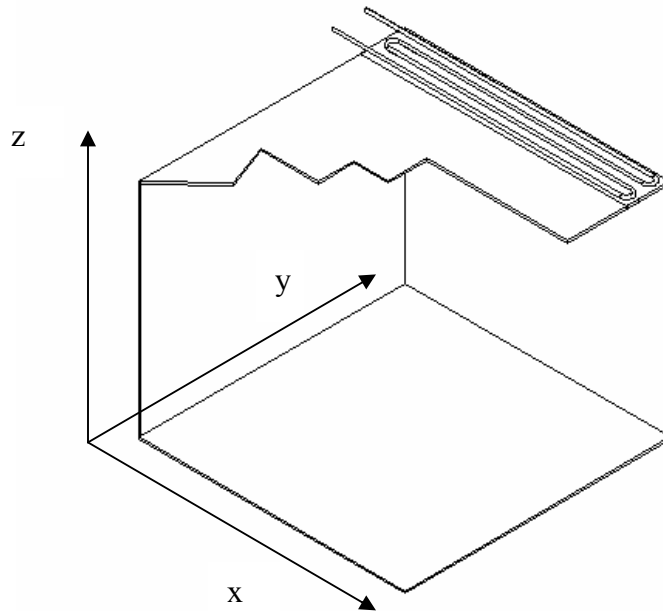
Figure B.1: Co-ordinate system to determine the radiant panel to surface view factors

Surface i is the radiant panel and surface j is other surface. For example consider surface j to be the floor.

To describe the location of the radiant panel

x-co-ordinates: $x_{i1} = 0$, $x_{i2} = 3.9624$

y-co-ordinates: $y_{i1} = 3.9624 - panellength$, $y_{i2} = 3.9624$

z-co-ordinates: $z_{i1} = 3.048$, $z_{i2} = 3.048$

To describe the location of the floor

x-co-ordinates: $x_{j1} = 0$, $x_{j2} = 3.9624$

y-co-ordinates: $y_{j1} = 0$, $y_{j2} = 3.9624$

z-co-ordinates: $z_{j1} = 0$, $z_{j2} = 0$

The radial distance, R, is the distance between any two points from surface i to j. The radial distance can be calculated with the following equation:

$$R^2 = (x_i - x_j)^2 + (y_i - y_j)^2 + (z_i - z_j)^2 \qquad (B.2)$$

The polar angles can be expressed in terms of the x,y and z co-ordinates. A polar angle is defined as the angle it makes with surface normal (Siegel and Howell, 1981). The surface normals are the same for the floor and radiant panel, so $\theta_i = \theta_j$. Expressing the polar angles in terms of the x,y and z coordinates:

$$\cos \theta = \frac{z_i}{R} \qquad (B.3)$$

Substituting Equations B.2 and B.3 into Equation B.1, the view factor can be solved. Figures B.2, B.3 and B.4 show the view factor calculations

View Factors Calculations for Radiant Heating Panel

Radiant Panel Width

$length := 48$ length is in Inches

Radiant Panel Location (Coordinates)

x is the width of the radiant panel

y is the length of the radiant panel

z is the height of the radiant panel

$x_{i1} := 0$ $y_{i1} := 3.9624 - length \cdot 0.0254$ $z_i := 3.048$

$x_{i2} := 3.9624$ $y_{i2} := 3.9624$

View Factor from radiant panel to the floor

Front Wall Coordinates

$x_{j1} := 0$ $y_{j1} := 0$ $z_{j1} := 0$

$x_{j2} := 3.9624$ $y_{j2} := 3.9624$

$$F_{topbottom} := \frac{1}{[(x_{i2} - x_{i1}) \cdot (y_{i2} - y_{i1})]} \cdot \int_{x_{i1}}^{x_{i2}} \int_{y_{i1}}^{y_{i2}} \int_{x_{j1}}^{x_{j2}} \int_{y_{j1}}^{y_{j2}} \frac{z_i^2}{\pi \cdot \left[(x_i - x_j)^2 + (y_i - y_j)^2 + z_i^2 \right]^2} \, dy_j \, dx_j \, dy_i \, dx_i$$

$F_{topbottom} = 0.257$

Figure B.2: MathCad Worksheet to Calculate the View Factors

View Factor from the radiant panel to the left/right wall

Left Wall Coordinates

$$x_j := 0 \qquad\qquad y_{j1} := 0 \qquad\qquad z_{j1} := 0$$

$$y_{j2} := 3.9624 \qquad\qquad z_{j2} := 3.048$$

$$F_{topside} := \frac{1}{\left[(x_{i2} - x_{i1}) \cdot (y_{i2} - y_{i1})\right]} \cdot \int_{z_{j1}}^{z_{j2}} \int_{y_{j1}}^{y_{j2}} \int_{x_{i1}}^{x_{i2}} \int_{y_{i1}}^{y_{i2}} \frac{(3.048 - z_j) \cdot (x_i - 0)}{\pi \cdot \left[(x_j - x_i)^2 + (y_j - y_i)^2 + (z_j - z_i)^2\right]^2} \, dy_i \, dx_i \, dy_j \, dz_j$$

$$F_{topside} = 0.169$$

View Factor from the radiant panel to the exterior (cold wall)

Exterior Wall Coordinates

$$x_{j1} := 0 \qquad\qquad y_j := 3.9624 \qquad\qquad z_{j1} := 0$$

$$x_{j2} := 3.9624 \qquad\qquad z_{j2} := 3.048$$

$$F_{topback} := \frac{1}{(x_{i2} - x_{i1}) \cdot (y_{i2} - y_{i1})} \cdot \int_{y_{i1}}^{y_{i2}} \int_{x_{i1}}^{x_{i2}} \int_{x_{j1}}^{x_{j2}} \int_{z_{j1}}^{z_{j2}} \frac{(3.048 - z_j) \cdot (3.9624 - y_i)}{\pi \cdot \left[(x_j - x_i)^2 + (y_j - y_i)^2 + (z_j - z_i)^2\right]^2} \, dz_j \, dx_j \, dx_i \, dy_i$$

$$F_{topback} = 0.337$$

Figure B.3: MathCad Worksheet to Calculate the View Factors

View Factor from the radiant panel to the front wall

Front Wall Coordinates

$$x_{j1} := 0 \qquad\qquad y_j := 0 \qquad\qquad z_{j1} := 0$$

$$x_{j2} := 3.9624 \qquad\qquad\qquad z_{j2} := 3.048$$

$$+$$

$$F_{topfront} := \frac{1}{\left[\left(x_{i2} - x_{i1}\right) \cdot \left(y_{i2} - y_{i1}\right)\right]} \cdot \int_{z_{j1}}^{z_{j2}} \int_{x_{i1}}^{x_{j2}} \int_{y_{i1}}^{y_{i2}} \int_{x_{i1}}^{x_{i2}} \frac{\left(3.048 - z_j\right) \cdot \left(y_i - 0\right)}{\pi \cdot \left[\left(x_j - x_i\right)^2 + \left(y_j - y_i\right)^2 + \left(z_j - z_i\right)^2\right]^2} \, dx_i \, dy_i \, dx_j \, dz_j$$

$$F_{topfront} = 0.067$$

Figure B.4: MathCad Worksheet to Calculate the View Factors

The view factors calculated can be summarized in Table B.1.

Table B.1: Summary of View Factors

Surfaces (i – j)	View Factor
Panel – Back Wall	0.337
Panel - Floor	0.257
Panel – Front Wall	0.067
Panel – Left Wall	0.169
Panel – Right Wall	0.169

The published view factor equation by Siegel and Howell (1981) is shown in Figure B.5 on

the next page and verifies the view factor equation.

From Siegel and Howell, 1981 for Perpendicular Rectangles with a Common Edge the View Factor can be calculated with the following Equation:

$$H := \frac{3.048}{3.9624}$$

H is the ratio of the panel length to the wall height

$$W := \frac{1.2192}{3.9624}$$

W is the ratio of the panel width to th epanel length

$$F_{ij} := \frac{1}{\pi \cdot W} \cdot \left[W \cdot \operatorname{atan}\left(\frac{1}{W}\right) + H \cdot \operatorname{atan}\left(\frac{1}{H}\right) - \sqrt{H^2 + W^2} \cdot \operatorname{atan}\left(\frac{1}{\sqrt{H^2 + W^2}}\right) + \frac{1}{4} \cdot \ln\left[\frac{\left[(1 + W^2) \cdot (1 + H^2)\right]}{(1 + W^2 + H^2)} \cdot \left[\left[\frac{\left[W^2 \cdot (1 + W^2 + H^2)\right]^{W^2}}{\left[(1 + W^2) \cdot (W^2 + H^2)\right]^{W^2}} \right] \cdot \left[\frac{\left[H^2 \cdot (1 + H^2 + W^2)\right]^{H^2}}{\left[(1 + H^2) \cdot (H^2 + W^2)\right]^{H^2}} \right] \right] \right] \right]$$

$$F_{ij} = 0.337$$

Figure B.5: MathCad Worksheet using a Published View Factor Equation to Validate View Factor Calculations

127

B.2   Energy Balance on Each Surface

With knowledge of the view factors, the radiant heat flux incoming to each wall can be calculated. The total incoming heat flux can be estimated by assuming the convective heat transfer coefficient is 6 W/m²K and the air temperature inside the chamber is 22°C.

The radiative heat transfer was calculated with the following equation (B.4)

$$q_{rad}^{"} = F\varepsilon\sigma(T_{panel}^4 - T_{sur}^4)$$
(B.4)

where: F is the calculated view factor from above.

The convective heat transfer can be calculated knowing a heat transfer coefficient. Assuming the worst case from published values (Awbi and Hatton, 1999), a coefficient of 6 W/m²K was used with the following equation (B.5).

$$q_c^{"} = h(T_a - T_{sur})$$
(B.5)

The panel temperature was assumed to be 363K, while the surrounding surfaces were at 293 K, except for the cold wall which was at 283 K.

The calculations are summarized in Figure B.6 on the following page:

Calculating the Incoming Heat Flux for Each Surrounding Surface

Calculated View Factors - For a 4ft Panel

$F_{backwall} := 0.337$ $T_{backwall} := 283$ $T_{air} := 295$

$F_{floor} := 0.257$ $T_{floor} := 293$ $h_{air} := 6$

$F_{FrontWall} := 0.067$ $T_{FrontWall} := 293$ $T_{panel} := 363$

$F_{LeftWall} := 0.169$ $T_{LeftWall} := 293$ $\varepsilon := 0.9$

$F_{RightWall} := 0.169$ $T_{RightWall} := 293$ $\sigma := 5.67 \cdot 10^{-8}$

Back Wall Incoming Heat Flux (W/m^2)

$$q_{backwall} := F_{backwall} \cdot \varepsilon \cdot \sigma \cdot \left(T_{panel}^4 - T_{backwall}^4 \right) + h_{air} \cdot \left(T_{air} - T_{backwall} \right)$$

$q_{backwall} = 260.288$

Floor Incoming Heat Flux (W/m^2)

$$q_{floor} := F_{floor} \cdot \varepsilon \cdot \sigma \cdot \left(T_{panel}^4 - T_{floor}^4 \right) + h_{air} \cdot \left(T_{air} - T_{floor} \right)$$

$q_{floor} = 143.056$

Front Wall Incoming Heat Flux (W/m^2)

$$q_{FrontWall} := F_{FrontWall} \cdot \varepsilon \cdot \sigma \cdot \left(T_{panel}^4 - T_{FrontWall}^4 \right) + h_{air} \cdot \left(T_{air} - T_{FrontWall} \right)$$

$q_{FrontWall} = 46.166$

Left/Right Wall Incoming Heat Flux (W/m^2)

$$q_{RightWall} := F_{RightWall} \cdot \varepsilon \cdot \sigma \cdot \left(T_{panel}^4 - T_{RightWall}^4 \right) + h_{air} \cdot \left(T_{air} - T_{RightWall} \right)$$

$q_{RightWall} = 98.18$

Figure B.6: MathCad Worksheet to Calculate the Incoming Heat Flux to Each Wall

B.3 Pipe Spacing

The derivation for the pipe spacing is shown below. It is derived from the Fourier's law and assuming a 1/3 of the pipe is in contact with the wall. Heat conduction rail effects have been ignored as well as any bond conductance. Solving for the pipe length required the number of pipe-runs can be calculated, since each pipe-run will be 4m long. From the number of pipe-runs the tube spacing can be calculated dividing the length of the chamber of the total number of pipe-runs. Figure B.7 and Figure B.8 show the calculation.

Calculating the Required Pipe Spacing for Each Surface

$D := 0.0127$ $thickness := 0.005$

$k_{PEX} := 20$

$T_{backwallwater} := 282$ $A_{backwall} := 4.3$

$T_{otherwallwater} := 291$ $A_{floor} := 4.4$

                       $A_{surface} := 4.3$

Deriving Pipe Spacing Equation

$$q_{out} := k A \cdot \left(\frac{d}{dx} T \right)$$

$$q_{out} := k_{PEX} \cdot \frac{\pi \cdot D \cdot L}{3} \cdot \frac{\left(T_{surface} - T_{water} \right)}{thickness}$$

$$L := \frac{3 \cdot q_{out} \cdot thickness}{k_{PEX} \cdot \pi \cdot D \cdot \left(T_{surface} - T_{water} \right)}$$

$$q_{out} := q_{surfaceflux} \cdot A_{surface}$$

$$Piperuns := \frac{L}{4}$$

$$Spacing := \frac{4}{Piperuns}$$

Therefore,

$$Spacing := 16 k_{PEX} \cdot \pi \cdot D \cdot \frac{\left(T_{surface} - T_{water} \right)}{0.015 \cdot q_{surface} \cdot A_{surface}}$$

Figure B.7: MathCad Worksheet to Calculate the Tube Spacing

Pipe Spacing for Back Wall

$$\text{Spacing} := 16 \cdot k_{pEX} \cdot \pi \cdot D \cdot \frac{\left(T_{backwall} - T_{backwallwater} \right)}{0.015 \cdot q_{backwall} \cdot A_{backwall}}$$

$$\text{Spacing} = 0.273$$

$$\text{Piperuns} := \frac{4}{\text{Spacing}}$$

$$\text{Piperuns} = 14.679$$

Pipe Spacing for Floor

$$\text{Spacing} := 16 \cdot k_{pEX} \cdot \pi \cdot D \cdot \frac{\left(T_{floor} - T_{otherwallwater} \right)}{0.015 \cdot q_{floor} \cdot A_{floor}}$$

$$\text{Spacing} = 0.744$$

$$\text{Piperuns} := \frac{4}{\text{Spacing}}$$

$$\text{Piperuns} = 5.378$$

Pipe Spacing for Front Wall

$$\text{Spacing} := 16 \cdot k_{pEX} \cdot \pi \cdot D \cdot \frac{\left(T_{FrontWall} - T_{otherwallwater} \right)}{0.015 \cdot q_{FrontWall} \cdot A_{surface}}$$

$$\text{Spacing} = 3.073$$

$$\text{Piperuns} := \frac{4}{\text{Spacing}}$$

$$\text{Piperuns} = 1.302$$

Pipe Spacing for Right/Left Wall

$$\text{Spacing} := 16 \cdot k_{pEX} \cdot \pi \cdot D \cdot \frac{\left(T_{RightWall} - T_{otherwallwater} \right)}{0.015 \cdot q_{RightWall} \cdot A_{surface}}$$

$$\text{Spacing} = 1.445$$

$$\text{Piperuns} := \frac{4}{\text{Spacing}}$$

$$\text{Piperuns} = 2.768$$

Figure B.8: MathCad Worksheet to Calculate the Tube Spacing

B.4 Pressure Drop Calculations

The pressure drop from each circuit can be estimated from the head loss equation for pipe friction and the loss coefficient for tube u-bends given by Munson et al. (2002). Equations B.6 and B.7 are the head loss equations used to determine the pipe circuit pressure drop.

$$h_L = f \frac{\ell}{D_i} \frac{V^2}{2g} \tag{B.6}$$

$$h_L = K_L \frac{V^2}{2g} \tag{B.7}$$

The friction factor for the tubing can be determined from the Moody chart (Figure B.9), knowing the Reynolds number and assuming a smooth surface roughness condition for the PEX tubing. The Reynolds is given by:

$$\text{Re} = \frac{\rho V D}{\mu} \tag{B.8}$$
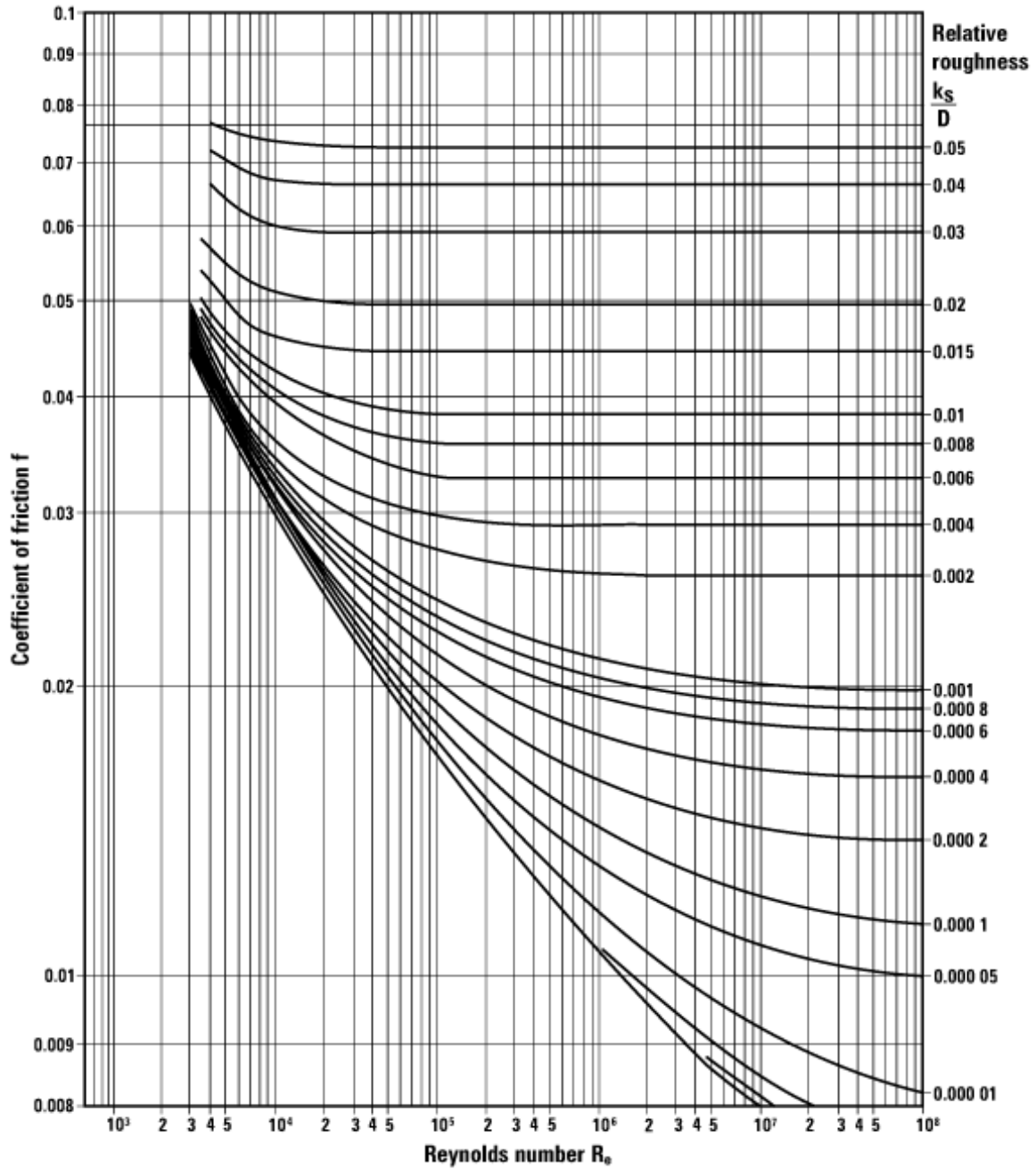
Figure B.9: Moody Chart

133

Specifying the desired flow rate to obtain a minimal pressure drop, the pressure drop for each

circuit is summarized in the work sheets below (Figure B.10, Figure B.11)

Pump Specification

Determining the Pump Flow Rate

For the back wall

$\Delta T := 0.5$

$C_p := 4179$

$$Flowrate_{mass} := \frac{q_{backwall}}{C_p \cdot \Delta T}$$

$Flowrate_{mass} = 0.125$

Converting mass flowrate to volumatric flowrate

$$Flowrate_{volumetric} := Flowrate_{mass} \cdot \frac{1000}{1000}$$

Determining the head loss

$f := 0.027$ $\rho_{water} := 1000$ $l_{floor} := 90$

$l_{wall} := 70$ $\mu := 1.307 \cdot 10^{-3}$

$D := 0.009525$ $K_L := 0.2$

$g := 9.81$

$$V := \frac{Flowrate_{mass} \cdot 4}{\pi \cdot D^2 \cdot \rho_{water}}$$

$V = 1.748$

$$Re := \frac{\rho_{water} \cdot V \cdot D}{\mu}$$

$Re = 1.274 \times 10^4$

Figure B.10: MathCad Worksheet to Calculate the Pressure Drop for Each Cicuit

$$h_{Lwall} := f \cdot \frac{l_{wall}}{D} \cdot \frac{V^2}{2g} + K_L \cdot 21 \cdot \frac{V^2}{2g}$$

$$h_{Lwall} = 31.563$$

$$h_{Lwallpsi} := h_{Lwall} \cdot 1.422$$

$$h_{Lwallpsi} = 44.883$$

$$h_{Lfloor} := f \cdot \frac{l_{floor}}{D} \cdot \frac{V^2}{2g} + K_L \cdot 21 \cdot \frac{V^2}{2g}$$

$$h_{Lfloor} = 40.394$$

$$h_{Lfloorpsi} := h_{Lfloor} \cdot 1.422$$

$$h_{Lfloorpsi} = 57.44$$

There are two circuits per surface, so the total pressure drop is half

Radiant Panel Pressure Drop

$$l_{panel} := 20 \qquad\qquad D := 0.0127$$

$$f := 0.027$$

$$V := \frac{0.2 \cdot 4}{\rho_{water} \cdot \pi \cdot D^2} \qquad\qquad V = 1.579$$

$$h_{Lpanelpsi} := 1.422 \cdot \left(f \cdot \frac{l_{panel}}{D} \cdot \frac{V^2}{2g} \right)$$

$$h_{Lpanelpsi} = 7.682$$

Figure B.11: MathCad Worksheet to Calculate the Pressure Drop for Each Circuit

B.5   Circuit Balancing Valve

The Circuit Balacing Valve Conversion chart to determine the flow rate from a pressure
differential reading is shown in Figure B.12.
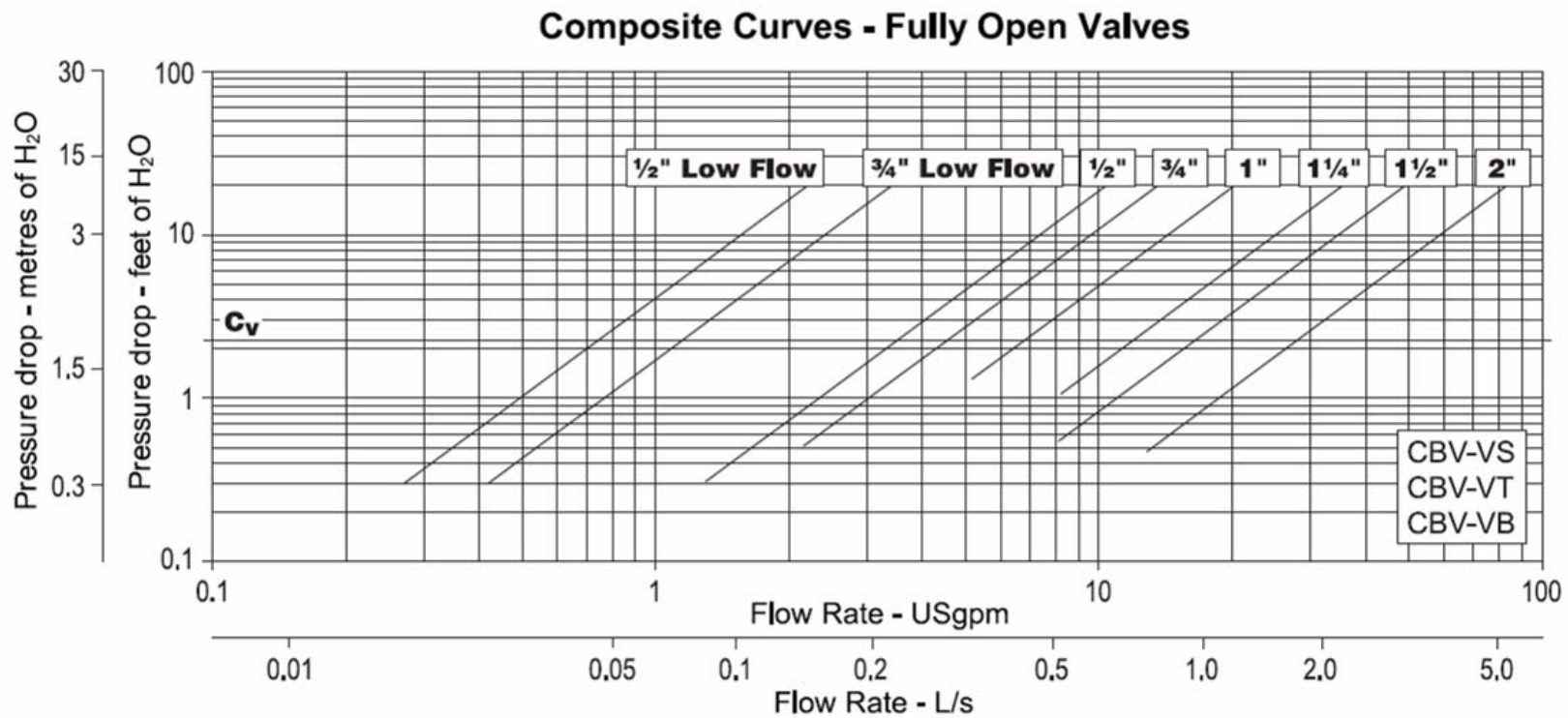
Figure B.12: Circuit Balancing Valve Conversion Chart

Appendix C

Experimental Test Data

C.1 Experimental Data

The following tables are the experimental results for the 24-4 and 24-8 panels tested. Each panel was tested at five different mean water temperatures. The surface temperatures, inlet and outlet panel water temperatures, panel temperature, air temperature and flow rate were recorded. Using Equation C.1 the heat output for each panel was calculated.

$$q_{out} = \dot{m}C_p(T_{panel} - T_a) \tag{C.1}$$

The results are in imperial units because Sigma Convectors requested that all the experimental data should be this way.

Experimental Data for 24-4 Panel, MWT = 49°C

A_{panel} (ft^2)   24.00

$T_{rightwall}$ (F)	$T_{leftwall}$ (F)	$T_{frontwall}$ (F)	T_{floor} (F)	T_{cold} (F)	T_{panel} (F)	$T_{water\ in}$ (F)	$T_{water\ out}$ (F)	T_{air} (F)	Flow Rate (GPM)	Heat Flux (BTU/hrft^2)	MWT (F)	Heat Flux (BTU/hrft)
61.87	61.87	61.99	64.70	61.22	60.42	61.59	61.41	60.49	0.90	3.38	61.50	6.75
64.63	64.56	66.66	72.69	62.56	61.78	62.53	62.33	61.65	0.90	3.75	62.43	7.50
71.66	72.58	73.97	73.00	63.49	62.94	62.87	62.80	62.62	0.90	1.31	62.84	2.63
73.67	74.83	74.88	72.05	63.49	64.14	63.10	62.96	63.73	0.90	2.63	63.03	5.25
72.71	73.95	74.06	71.10	58.49	64.82	65.89	65.03	64.62	0.90	16.13	65.46	32.25
72.07	73.23	73.32	70.52	57.52	78.43	92.53	78.44	65.10	0.90	264.19	85.49	528.38
71.61	72.54	72.74	70.12	57.23	91.04	98.26	92.03	65.30	0.90	116.81	95.15	233.63
71.38	72.02	72.46	69.83	56.94	88.88	91.09	85.78	65.73	0.90	99.56	88.44	199.13
71.20	71.55	71.96	69.55	56.36	84.10	87.30	79.23	66.16	0.90	151.31	83.27	302.63
70.70	70.95	71.32	69.15	56.01	80.59	90.32	74.48	66.45	0.90	297.00	82.40	594.00
70.56	70.77	71.02	69.06	56.06	78.07	87.31	71.85	66.69	0.90	289.88	79.58	579.75
70.21	70.50	70.58	68.99	56.08	75.98	80.40	70.23	67.08	0.90	190.69	75.32	381.38
69.89	70.21	70.28	68.92	56.15	74.71	75.27	75.02	66.96	0.90	4.69	75.15	9.38
69.44	69.99	69.87	68.91	55.87	72.50	72.12	71.67	67.08	0.90	8.44	71.90	16.88
69.22	70.00	69.48	68.86	55.47	70.51	70.99	84.67	66.96	0.90	-256.50	77.83	-513.00
68.92	69.70	69.24	68.70	55.29	92.33	118.47	99.64	66.83	0.90	353.06	109.06	706.13
68.60	69.53	68.91	68.72	54.94	100.79	118.04	104.40	66.65	0.90	255.75	111.22	511.50
68.45	69.60	68.65	68.85	54.83	113.43	124.81	117.48	66.85	0.90	137.44	121.15	274.88
68.41	69.51	68.74	68.93	55.02	116.28	126.63	119.64	67.19	0.90	131.06	123.14	262.13
68.61	69.66	68.87	69.05	55.30	118.29	128.01	121.35	67.33	0.90	124.88	124.68	249.75
68.38	69.61	68.64	69.04	55.07	118.84	128.86	122.14	67.39	0.90	126.00	125.50	252.00
68.18	69.57	68.49	69.13	54.76	119.56	130.96	123.46	67.32	0.90	140.63	127.21	281.25
68.19	69.63	68.35	69.21	54.61	121.72	134.42	126.36	67.17	0.90	151.13	130.39	302.25
68.05	69.61	68.17	69.22	54.39	124.64	137.19	129.13	67.46	0.90	151.13	133.16	302.25
67.97	69.60	68.05	69.18	54.32	126.81	138.63	131.11	67.42	0.90	141.00	134.87	282.00
68.05	69.74	67.97	69.24	54.23	127.75	139.28	131.90	67.82	0.90	138.38	135.59	276.75

T_rightwall (F)	T_leftwall (F)	T_frontwall (F)	T_floor (F)	T_cold (F)	T_panel (F)	T_water in (F)	T_water out (F)	T_air (F)	Flow Rate (GPM)	Heat Flux (BTU/hrft^2)	MWT (F)	Heat Flux (BTU/hrft)
67.95	69.73	67.91	69.30	54.30	128.32	140.31	132.64	68.00	0.90	143.81	136.48	287.63
68.04	69.79	67.91	69.31	54.35	129.93	143.17	134.73	67.93	0.90	158.25	138.95	316.50
68.17	69.78	67.87	69.33	54.23	132.70	146.23	137.14	68.02	0.90	170.44	141.69	340.88
68.40	69.93	68.63	69.39	54.39	131.46	141.44	135.32	68.38	0.90	114.75	138.38	229.50
68.37	70.02	69.22	69.55	54.36	126.80	135.37	130.21	68.47	0.90	96.75	132.79	193.50
68.39	70.11	69.24	69.66	54.39	122.18	130.12	125.42	68.68	0.90	88.13	127.77	176.25
68.43	70.18	68.96	69.57	54.31	118.15	125.73	121.26	68.56	0.90	83.81	123.50	167.63
68.50	70.35	68.97	69.78	54.36	114.91	122.49	117.99	68.67	0.90	84.38	120.24	168.75
68.40	70.31	68.85	69.76	54.30	113.08	121.84	116.47	68.83	0.90	100.69	119.16	201.38
68.44	70.37	68.58	69.67	54.21	113.05	122.76	116.71	68.81	0.90	113.44	119.74	226.88
68.39	70.39	68.43	69.63	54.05	113.93	124.14	117.75	68.70	0.90	119.81	120.95	239.63
68.30	70.33	68.27	69.60	54.07	114.99	125.46	118.94	68.83	0.90	122.25	122.20	244.50
68.35	70.36	68.38	69.66	54.23	116.15	126.77	120.16	68.85	0.90	123.94	123.47	247.88
68.33	70.29	68.35	69.72	54.28	116.80	126.90	120.78	68.81	0.90	114.75	123.84	229.50
68.48	70.47	68.22	69.65	54.15	116.38	126.37	120.34	68.76	0.90	113.06	123.36	226.13
68.40	70.42	68.30	69.77	54.23	116.04	125.89	119.97	68.83	0.90	111.00	122.93	222.00
68.44	70.49	68.27	69.81	54.21	115.29	125.02	119.34	68.88	0.90	106.50	122.18	213.00
68.45	70.48	68.20	69.75	54.25	114.91	124.61	118.92	69.01	0.90	106.69	121.77	213.38
68.36	70.40	68.12	69.66	54.08	114.58	124.25	118.53	68.92	0.90	107.25	121.39	214.50
68.42	70.49	68.31	69.81	54.41	114.62	124.54	118.72	69.12	0.90	109.13	121.63	218.25
68.42	70.50	68.32	69.89	54.32	114.55	124.65	118.72	68.94	0.90	111.19	121.69	222.38
68.50	70.65	68.23	69.94	54.04	114.40	124.95	118.99	68.95	0.90	111.75	121.97	223.50
68.48	70.66	68.22	69.97	54.36	114.90	125.65	119.62	69.35	0.90	113.06	122.64	226.13
68.50	70.69	68.31	70.11	54.26	115.17	126.18	120.11	69.30	0.90	113.81	123.15	227.63
68.58	70.74	68.16	69.93	54.11	115.72	149.58	118.96	69.19	0.90	574.13	134.27	1148.25
68.63	70.67	68.17	69.84	54.06	115.59	131.56	119.14	69.08	0.90	232.88	125.35	465.75
68.75	70.72	68.27	69.90	54.17	114.05	125.76	117.97	69.22	0.90	146.06	121.87	292.13
68.69	70.59	68.72	70.17	54.85	113.18	123.53	117.32	68.97	0.90	116.44	120.43	232.88
68.80	70.69	68.71	70.11	54.84	112.76	123.22	117.18	68.79	0.90	113.25	120.20	226.50
68.85	70.74	68.70	70.14	54.84	113.81	124.97	118.02	69.28	0.90	130.31	121.50	260.63
68.95	70.85	68.81	70.23	54.96	118.79	125.22	129.09	69.13	0.90	-72.56	127.16	-145.13

$T_{rightwall}$ (F)	$T_{leftwall}$ (F)	$T_{frontwall}$ (F)	T_{floor} (F)	T_{cold} (F)	T_{panel} (F)	$T_{water\ in}$ (F)	$T_{water\ out}$ (F)	T_{air} (F)	Flow Rate (GPM)	Heat Flux (BTU/hrft^2)	MWT (F)	Heat Flux (BTU/hrft)
68.97	70.85	68.71	70.18	55.04	116.58	126.21	122.29	68.63	0.90	73.50	124.25	147.00
68.86	70.66	68.93	70.26	55.38	115.58	125.33	119.79	69.15	0.90	103.88	122.56	207.75
68.80	70.60	68.72	70.03	54.95	114.14	124.05	118.38	68.67	0.90	106.31	121.22	212.63
68.97	70.71	69.11	70.39	55.17	115.09	124.12	118.40	69.91	0.90	107.25	121.26	214.50
69.06	70.71	69.21	70.32	55.13	115.06	124.36	118.53	69.03	0.90	109.31	121.45	218.63
68.99	70.62	69.33	70.42	55.28	115.68	124.79	119.03	69.39	0.90	108.00	121.91	216.00
69.09	70.62	69.15	70.21	55.34	116.10	124.86	119.01	69.31	0.90	109.69	121.94	219.38
69.14	70.63	69.32	70.31	55.44	116.47	125.20	119.37	69.51	0.90	109.31	122.29	218.63
69.11	70.57	69.31	70.34	55.49	116.37	125.40	119.39	69.33	0.90	112.69	122.40	225.38
69.24	70.60	69.42	70.30	55.46	116.85	125.19	119.35	69.35	0.90	109.50	122.27	219.00
69.31	70.64	69.37	70.26	55.49	116.86	125.35	119.52	69.35	0.90	109.31	122.44	218.63
69.25	70.65	69.27	70.19	55.44	116.83	125.44	119.43	69.26	0.90	112.69	122.44	225.38
69.09	70.54	69.29	70.29	55.43	117.02	125.74	119.82	69.51	0.90	111.00	122.78	222.00
69.13	70.69	69.29	70.43	55.36	117.28	126.01	119.97	69.76	0.90	113.25	122.99	226.50
69.13	70.81	69.21	70.45	54.98	117.04	125.83	119.95	69.76	0.90	110.25	122.89	220.50
69.07	70.89	69.31	70.67	54.91	117.28	125.76	120.18	70.66	0.90	104.63	122.97	209.25
69.05	70.91	69.35	70.77	55.08	117.15	125.28	119.79	71.08	0.90	102.94	122.54	205.88
69.23	71.04	69.49	70.81	55.27	116.53	124.70	119.25	70.81	0.90	102.19	121.98	204.38
69.29	71.07	69.44	70.74	55.36	115.99	124.20	118.67	70.56	0.90	103.69	121.44	207.38
69.36	70.97	69.49	70.61	55.49	112.91	120.70	115.56	70.23	0.90	96.38	118.13	192.75
68.68	70.53	68.90	70.15	57.90	100.25	108.30	103.14	70.47	0.90	96.75	105.72	193.50
68.61	70.46	68.87	70.13	58.17	98.89	107.10	101.97	70.29	0.90	96.19	104.54	192.38

Note: Shaded Test Data was the experimental data used

Experimental Data for 24-4 Panel, MWT = 57°C

A_{panel} (ft^2)   24.00

$T_{rightwall}$ (F)	$T_{leftwall}$ (F)	$T_{frontwall}$ (F)	T_{floor} (F)	T_{cold} (F)	T_{panel} (F)	$T_{water\ in}$ (F)	$T_{water\ out}$ (F)	T_{air} (F)	Flow Rate (GPM)	Heat Flux (BTU/hrft^2)	MWT (F)	Heat Flux (BTU/hrft)
66.64	68.01	66.71	67.48	54.00	138.64	188.31	130.12	66.54	0.90	1091.06	159.22	2182.13
67.50	68.68	67.17	67.81	54.48	141.39	145.87	142.90	66.36	0.90	55.69	144.39	111.38
67.98	68.89	67.86	68.07	55.06	139.32	141.71	141.87	66.70	0.90	-3.00	141.79	-6.00
67.85	68.92	67.90	67.77	54.88	133.71	140.20	136.78	66.67	0.90	64.12	138.49	128.25
66.57	67.66	67.92	66.60	54.79	128.95	136.35	130.89	67.03	0.90	102.38	133.62	204.75
65.32	66.37	67.82	66.01	54.29	125.11	133.79	127.11	66.83	0.90	125.25	130.45	250.50
65.11	66.10	67.87	66.06	54.44	124.99	135.16	126.73	66.90	0.90	158.06	130.95	316.13
65.51	66.20	67.87	66.06	54.68	127.08	137.66	128.75	66.72	0.90	167.06	133.21	334.13
66.29	66.46	68.09	66.34	54.87	129.54	140.86	131.49	66.45	0.90	175.69	136.18	351.38
66.51	66.45	68.11	66.48	55.13	131.67	142.43	133.83	66.29	0.90	161.25	138.13	322.50
66.85	66.79	68.09	66.66	55.17	131.24	141.94	133.41	66.24	0.90	159.94	137.68	319.88
67.28	67.06	68.08	66.83	55.31	130.76	139.96	132.19	66.13	0.90	145.69	136.08	291.38
67.77	67.51	68.22	67.14	55.63	130.17	138.79	131.34	66.11	0.90	139.69	135.07	279.38
67.79	67.67	67.86	67.28	55.42	128.83	138.69	130.84	65.73	0.90	147.19	134.77	294.38
68.10	67.96	67.69	67.48	55.40	129.20	139.51	130.69	66.09	0.90	165.38	135.10	330.75
68.36	68.07	68.00	67.61	55.67	130.49	139.93	131.49	66.06	0.90	158.25	135.71	316.50
68.48	68.40	68.30	67.87	55.60	131.17	141.04	132.46	66.02	0.90	160.88	136.75	321.75
68.27	68.61	68.19	67.89	55.48	131.42	141.58	133.12	66.11	0.90	158.63	137.35	317.25

Note: Shaded Test Data was the experimental data

Experimental Data for 24-4 Panel, MWT = 71°C

A$_{panel}$ (ft^2)   24.00

T$_{rightwall}$ (F)	T$_{leftwall}$ (F)	T$_{frontwall}$ (F)	T$_{floor}$ (F)	T$_{cold}$ (F)	T$_{panel}$ (F)	T$_{water\,in}$ (F)	T$_{water\,out}$ (F)	T$_{air}$ (F)	Flow Rate (GPM)	Heat Flux (BTU/hrft^2)	MWT (F)	Heat Flux (BTU/hrft)
65.05	67.51	65.66	66.94	61.61	98.08	168.51	101.05	66.69	0.90	1264.88	134.78	2529.75
65.50	68.17	66.38	67.38	59.99	154.32	186.91	159.96	67.14	0.90	505.31	173.44	1010.63
66.20	68.95	66.86	67.92	58.80	162.55	184.68	167.14	67.78	0.90	328.88	175.91	657.75
65.78	68.90	66.73	68.23	57.40	155.88	172.09	163.08	68.02	0.90	168.94	167.59	337.88
65.99	69.06	66.74	68.28	56.13	150.59	169.36	156.79	68.07	0.90	235.69	163.08	471.38
66.18	69.15	66.89	68.34	55.28	151.88	162.66	161.71	67.75	0.90	17.81	162.19	35.62
66.32	69.22	66.95	68.33	54.71	150.35	160.54	155.66	67.84	0.90	91.50	158.10	183.00
66.63	69.33	67.07	68.36	54.66	149.86	158.50	155.91	67.96	0.90	48.56	157.21	97.13
66.77	69.34	67.04	68.38	54.47	147.69	160.84	153.21	67.80	0.90	143.06	157.03	286.13
66.63	66.97	64.60	68.05	53.42	146.90	167.36	152.46	67.44	0.90	279.38	159.91	558.75
66.65	65.94	64.08	68.32	53.68	147.72	168.19	153.70	67.93	0.90	271.69	160.95	543.38
66.56	65.80	64.16	68.27	53.59	147.76	168.39	153.75	67.82	0.90	274.50	161.07	549.00
67.35	67.96	65.72	68.20	53.43	147.58	168.42	153.97	67.66	0.90	270.94	161.20	541.88
68.29	70.12	67.81	68.59	53.83	147.54	167.05	153.91	67.69	0.90	246.38	160.48	492.75
68.57	70.72	68.63	69.13	54.12	147.81	164.79	153.55	68.40	0.90	210.75	159.17	421.50
68.57	70.75	68.48	69.69	54.00	148.01	164.95	154.27	67.82	0.90	200.25	159.61	400.50
68.62	70.78	68.41	69.96	53.86	148.23	165.49	155.14	67.71	0.90	194.06	160.32	388.13
68.79	70.87	68.55	70.19	54.19	148.83	165.69	155.50	68.34	0.90	191.06	160.60	382.13
68.95	70.87	68.56	70.14	54.34	149.01	165.30	155.21	68.67	0.90	189.19	160.26	378.38
68.87	70.93	68.52	70.17	54.28	148.47	164.82	154.69	68.92	0.90	189.94	159.76	379.88
67.41	69.31	68.40	70.40	53.38	147.64	164.64	154.47	68.99	0.90	190.69	159.56	381.38
67.28	69.20	68.33	70.38	53.38	147.63	164.62	154.45	69.01	0.90	190.69	159.54	381.38

Note: Shaded Test Data was the experimental data

Experimental Data for 24-4 Panel, MWT = 82°C

A_{panel} (ft^2)   24.00

$T_{rightwall}$ (F)	$T_{leftwall}$ (F)	$T_{frontwall}$ (F)	T_{floor} (F)	T_{cold} (F)	T_{panel} (F)	$T_{water\,in}$ (F)	$T_{water\,out}$ (F)	T_{air} (F)	Flow Rate (GPM)	Heat Flux (BTU/hrft^2)	MWT (F)	Heat Flux (BTU/hrft)
63.96	64.27	63.71	66.63	55.85	109.14	198.05	129.47	61.21	0.90	1285.88	163.76	2571.75
68.62	69.68	68.36	68.97	55.38	173.55	201.83	183.18	61.61	0.90	349.69	192.51	699.38
70.10	71.11	70.09	69.72	55.61	178.93	200.93	185.25	62.04	0.90	294.00	193.09	588.00
71.00	71.67	71.11	70.45	56.12	181.07	201.81	186.31	63.12	0.90	290.63	194.06	581.25
71.50	71.65	71.85	70.99	57.15	182.75	203.74	188.58	64.81	0.90	284.25	196.16	568.50
71.16	71.17	71.48	70.38	56.97	183.95	204.28	189.27	65.50	0.90	281.44	196.78	562.88
71.15	71.14	71.48	70.15	57.03	184.12	204.22	189.34	65.59	0.90	279.00	196.78	558.00
66.32	66.82	66.15	66.55	55.02	186.16	207.91	192.45	65.61	0.90	289.88	200.18	579.75
66.68	67.18	66.62	66.86	55.46	179.51	197.76	184.28	65.88	0.90	252.75	191.02	505.50
67.37	68.02	67.22	67.48	55.53	173.40	189.34	177.91	66.31	0.90	214.31	183.63	428.63
67.43	68.17	67.33	67.48	55.50	170.16	189.09	174.34	66.49	0.90	276.56	181.72	553.13
66.18	67.01	66.27	66.41	55.29	170.20	188.56	174.99	66.47	0.90	254.44	181.78	508.88
65.89	66.41	65.96	66.16	55.30	170.53	188.71	174.79	65.97	0.90	261.00	181.75	522.00
65.90	66.47	65.82	66.18	55.17	170.73	187.36	174.28	65.91	0.90	245.25	180.82	490.50
66.18	66.57	66.14	66.25	55.56	169.43	186.21	172.99	65.70	0.90	247.88	179.60	495.75
66.83	67.05	66.69	66.60	56.08	170.96	188.06	174.67	65.43	0.90	251.06	181.37	502.13
66.95	67.19	67.00	66.85	56.39	170.67	187.95	173.95	65.66	0.90	262.50	180.95	525.00
67.41	67.57	67.45	67.19	56.34	170.73	188.04	174.36	65.57	0.90	256.50	181.20	513.00
67.50	67.86	67.79	67.54	56.26	170.19	187.66	174.13	65.61	0.90	253.69	180.90	507.38
67.71	68.29	67.89	67.60	56.22	170.04	188.10	174.33	66.18	0.90	258.19	181.22	516.37
66.45	67.17	66.74	66.57	55.89	169.97	187.86	174.27	66.09	0.90	254.81	181.07	509.63
65.54	66.48	65.75	66.37	55.17	169.06	187.81	173.95	66.07	0.90	259.88	180.88	519.75
65.40	66.40	65.43	66.28	54.95	169.09	187.97	174.16	66.11	0.90	258.94	181.07	517.88
66.04	66.55	66.00	66.40	55.43	169.98	187.95	173.86	65.77	0.90	264.19	180.91	528.37
66.01	66.78	66.24	66.78	55.51	169.77	187.81	174.22	65.70	0.90	254.81	181.02	509.63
66.46	67.02	66.58	66.93	55.81	169.80	187.65	173.75	65.73	0.90	260.63	180.70	521.25

$T_{rightwall}$ (F)	$T_{leftwall}$ (F)	$T_{frontwall}$ (F)	T_{floor} (F)	T_{cold} (F)	T_{panel} (F)	$T_{water\ in}$ (F)	$T_{water\ out}$ (F)	T_{air} (F)	Flow Rate (GPM)	Heat Flux (BTU/hrft^2)	MWT (F)	Heat Flux (BTU/hrft)
66.70	67.27	66.75	67.02	55.80	169.84	187.48	173.62	65.52	0.90	259.88	180.55	519.75
66.35	67.59	66.27	67.20	55.16	169.40	188.89	174.83	65.62	0.90	263.62	181.86	527.25
66.89	68.01	66.78	67.60	55.33	170.12	189.36	175.12	65.82	0.90	267.00	182.24	534.00
67.31	68.48	67.24	68.04	55.67	169.81	187.90	175.05	66.40	0.90	240.94	181.48	481.88
66.18	67.64	66.32	66.96	55.48	169.23	187.59	174.78	66.96	0.90	240.19	181.19	480.38
65.07	66.55	65.12	66.43	54.80	167.87	186.93	173.95	67.06	0.90	243.38	180.44	486.75
65.03	66.38	65.11	66.49	55.13	167.94	188.92	173.89	66.83	0.90	281.81	181.41	563.63
65.53	66.57	65.54	66.78	55.14	169.42	189.39	175.28	66.96	0.90	264.56	182.34	529.12
66.43	66.61	66.31	66.75	55.62	169.69	187.38	174.52	66.02	0.90	241.13	180.95	482.25
66.56	66.85	66.29	66.85	55.31	168.48	186.71	173.88	66.18	0.90	240.56	180.30	481.13
67.08	67.24	66.80	67.16	55.56	168.78	189.01	174.47	66.31	0.90	272.63	181.74	545.25
67.12	67.48	66.73	67.23	55.32	169.72	189.81	175.46	66.61	0.90	269.06	182.64	538.13
67.67	67.72	67.16	67.42	55.59	169.23	187.02	173.88	66.42	0.90	246.38	180.45	492.75
68.01	67.99	67.43	67.58	55.81	168.55	186.85	173.21	66.38	0.90	255.75	180.03	511.50
68.04	68.28	67.69	68.04	55.62	169.49	188.78	175.03	66.72	0.90	257.81	181.91	515.63
68.05	68.34	67.67	67.95	55.53	169.93	187.91	174.87	66.61	0.90	244.50	181.39	489.00
68.33	68.50	67.88	68.03	55.51	168.90	187.25	174.09	66.49	0.90	246.75	180.67	493.50
67.91	67.73	67.57	66.64	54.83	167.75	188.17	173.01	66.36	0.90	284.25	180.59	568.50
65.94	66.20	67.38	65.92	54.23	168.50	189.07	174.94	66.90	0.90	264.94	182.01	529.88
65.68	65.92	67.27	66.06	53.85	168.51	187.77	175.53	67.17	0.90	229.50	181.65	459.00
65.72	65.88	67.12	66.16	53.78	167.71	187.84	174.72	67.48	0.90	246.00	181.28	492.00
65.92	66.18	66.77	66.19	53.68	166.70	186.89	173.82	67.60	0.90	245.06	180.36	490.13
66.13	66.43	66.88	66.64	53.93	166.25	187.45	173.70	67.69	0.90	257.81	180.58	515.63
66.43	66.80	67.10	67.05	54.06	166.70	187.50	174.29	68.05	0.90	247.69	180.90	495.38
66.74	67.23	67.07	67.29	54.33	167.49	189.46	175.08	68.32	0.90	269.63	182.27	539.25
67.07	67.59	67.02	67.35	54.42	168.35	189.82	176.13	68.00	0.90	256.69	182.98	513.38
67.14	67.90	67.07	67.62	54.20	166.72	187.27	174.49	68.07	0.90	239.63	180.88	479.25
67.28	68.12	66.96	67.62	54.11	165.86	187.20	173.61	68.04	0.90	254.81	180.41	509.62
67.40	68.22	67.32	68.04	54.27	167.32	188.73	174.97	68.16	0.90	258.00	181.85	516.00

T$_{rightwall}$ (F)	T$_{leftwall}$ (F)	T$_{frontwall}$ (F)	T$_{floor}$ (F)	T$_{cold}$ (F)	T$_{panel}$ (F)	T$_{water\ in}$ (F)	T$_{water\ out}$ (F)	T$_{air}$ (F)	Flow Rate (GPM)	Heat Flux (BTU/hrft^2)	MWT (F)	Heat Flux (BTU/hrft)
67.65	67.88	67.43	67.05	54.28	168.29	188.80	175.75	68.18	0.90	244.69	182.28	489.38
67.80	66.09	67.21	65.71	53.77	167.13	188.01	174.34	68.00	0.90	256.31	181.18	512.63
67.73	65.44	67.30	65.58	53.66	167.01	186.80	173.89	68.04	0.90	242.06	180.35	484.13
67.86	65.56	67.50	65.79	53.95	166.84	188.65	173.66	67.82	0.90	281.06	181.16	562.13
67.89	65.89	67.39	65.86	54.03	168.24	189.48	175.32	68.00	0.90	265.50	182.40	531.00
67.93	66.13	67.33	65.94	54.19	168.10	187.29	174.69	67.96	0.90	236.25	180.99	472.50
67.93	66.33	67.42	66.20	54.37	167.17	186.30	173.39	68.04	0.90	242.06	179.85	484.13
68.66	67.43	67.97	66.93	54.83	167.64	188.42	173.93	68.65	0.90	271.69	181.18	543.37
68.16	68.17	68.27	67.47	54.72	169.12	190.06	175.89	68.95	0.90	265.69	182.98	531.38
67.18	68.50	68.09	67.95	54.55	167.84	187.54	174.52	69.26	0.90	244.13	181.03	488.25
67.39	68.83	68.00	68.34	54.38	166.80	187.16	173.53	69.44	0.90	255.56	180.35	511.13
67.38	68.82	68.02	68.38	54.48	166.83	187.27	173.59	69.49	0.90	256.50	180.43	513.00

Note: Shaded Test Data was the experimental data and used for the steady state plot

146

Experimental Data for 24-4 Panel, MWT = 95°C

A_{panel} (ft^2)   24.00

$T_{rightwall}$ (F)	$T_{leftwall}$ (F)	$T_{frontwall}$ (F)	T_{floor} (F)	T_{cold} (F)	T_{panel} (F)	$T_{water\ in}$ (F)	$T_{water\ out}$ (F)	T_{air} (F)	Flow Rate (GPM)	Heat Flux (BTU/hrft^2)	MWT (F)	Heat Flux (BTU/hrft)
68.23	67.53	67.21	66.12	56.51	160.08	196.86	173.98	58.77	0.90	429.00	185.42	858.00
69.60	69.21	69.12	67.39	56.30	172.14	195.57	180.52	59.85	0.90	282.19	188.05	564.37
70.27	70.17	69.74	68.04	55.83	174.26	196.48	182.10	61.12	0.90	269.63	189.29	539.25
70.36	70.46	69.83	68.28	55.29	175.16	197.55	183.29	61.88	0.90	267.38	190.42	534.75
70.22	70.59	69.87	68.57	54.99	175.97	198.66	184.23	62.83	0.90	270.56	191.45	541.13
70.11	70.75	69.68	68.74	54.79	176.95	199.67	185.11	64.08	0.90	273.00	192.39	546.00
70.11	70.96	69.84	69.22	55.01	177.93	201.31	186.51	65.07	0.90	277.50	193.91	555.00
70.03	70.87	70.02	69.52	55.25	178.93	202.57	187.39	65.91	0.90	284.63	194.98	569.25
70.22	71.02	70.21	69.79	55.42	180.26	203.63	188.20	66.81	0.90	289.31	195.92	578.63
70.25	71.05	70.07	69.78	55.17	181.09	204.57	188.82	67.03	0.90	295.31	196.70	590.63
69.41	70.47	69.33	68.80	54.82	181.98	205.61	189.81	67.41	0.90	296.25	197.71	592.50
67.73	68.96	67.59	67.39	54.32	182.82	206.60	190.60	67.55	0.90	300.00	198.60	600.00
66.33	67.39	66.16	66.30	54.05	184.06	207.37	191.44	67.73	0.90	298.69	199.41	597.38
65.28	66.80	65.17	65.80	54.32	185.06	209.23	192.83	67.93	0.90	307.50	201.03	615.00
64.82	66.97	64.91	65.79	54.44	186.21	210.42	193.78	67.86	0.90	312.00	202.10	624.00
65.23	67.31	65.09	65.71	54.49	187.02	211.05	194.52	67.62	0.90	309.94	202.79	619.88
65.75	67.59	65.56	65.83	54.62	187.77	212.11	195.31	67.28	0.90	315.00	203.71	630.00
66.40	67.97	65.92	65.79	54.85	188.74	212.88	195.89	67.15	0.90	318.56	204.39	637.13
66.77	68.17	66.16	65.85	54.77	189.32	213.76	196.72	66.90	0.90	319.50	205.24	639.00
67.22	68.59	66.53	66.00	54.92	190.35	214.93	197.78	67.15	0.90	321.56	206.36	643.13
67.54	67.95	66.76	66.00	54.95	190.67	214.85	197.73	67.08	0.90	321.00	206.29	642.00
67.84	67.18	67.09	66.15	55.14	185.90	211.51	194.62	66.90	0.90	316.69	203.07	633.37
67.96	67.54	67.21	66.46	54.74	187.56	211.26	194.59	66.97	0.90	312.56	202.93	625.13
68.13	68.19	67.23	66.75	54.63	188.34	212.95	195.93	67.69	0.90	319.13	204.44	638.25
68.16	68.22	67.40	66.70	54.65	189.45	213.55	196.34	67.55	0.90	322.69	204.95	645.38
68.35	68.41	67.52	66.77	54.72	189.58	213.40	196.41	67.62	0.90	318.56	204.91	637.13

Note: Shaded Test Data was the experimental data

Experimental Data for 24-8 Panel, MWT = 49°C

A_{panel} (ft²)   24.00

$T_{rightwall}$ (F)	$T_{leftwall}$ (F)	$T_{frontwall}$ (F)	T_{floor} (F)	T_{cold} (F)	T_{panel} (F)	$T_{water\ in}$ (F)	$T_{water\ out}$ (F)	T_{air} (F)	Flow Rate (GPM)	Heat Flux (BTU/hrft²)	MWT (F)	Heat Flux (BTU/hrft)
73.47	73.53	73.61	72.52	65.79	76.84	131.04	73.40	71.96	0.90	1080.75	102.22	2161.50
71.58	71.72	72.00	71.59	61.11	120.66	152.55	121.75	72.07	0.90	577.50	137.15	1155.00
71.29	71.37	71.33	71.58	59.32	113.85	137.52	127.54	72.27	0.90	187.13	132.53	374.25
70.90	71.23	71.05	71.35	57.84	108.70	132.40	129.24	72.18	0.90	59.25	130.82	118.50
69.75	70.58	70.03	70.33	57.29	116.42	129.76	126.23	72.18	0.90	66.19	128.00	132.38
68.41	69.00	68.72	69.30	56.79	120.96	126.50	121.66	72.25	0.90	90.75	124.08	181.50
67.42	67.89	67.91	69.01	56.39	118.80	123.71	118.99	71.80	0.90	88.50	121.35	177.00
67.03	67.46	67.61	69.19	55.92	116.82	122.95	116.65	71.13	0.90	118.13	119.80	236.25
66.88	67.42	67.78	69.76	55.77	116.46	123.12	116.42	70.92	0.90	125.63	119.77	251.25
67.10	67.63	68.15	69.91	56.09	117.15	124.56	117.28	70.72	0.90	136.50	120.92	273.00
67.37	68.07	68.19	69.79	56.15	117.18	125.42	117.90	70.45	0.90	141.00	121.66	282.00
67.78	68.52	68.22	69.76	56.06	117.64	125.91	118.29	69.66	0.90	142.88	122.10	285.75
68.66	69.42	68.76	70.09	56.66	118.75	126.54	119.41	69.12	0.90	133.69	122.98	267.38
67.73	68.63	68.24	69.13	56.53	119.02	126.32	119.32	68.74	0.90	131.25	122.82	262.50
65.86	66.24	66.57	67.99	56.17	119.40	125.26	118.31	67.91	0.90	130.31	121.79	260.63
65.80	66.01	66.13	68.91	56.30	119.31	125.44	118.04	67.50	0.90	138.75	121.74	277.50
66.54	66.46	66.81	69.41	56.89	119.68	125.67	118.35	66.99	0.90	137.25	122.01	274.50
66.49	66.80	66.59	69.46	56.58	118.97	125.22	118.27	66.76	0.90	130.31	121.75	260.63
66.83	67.23	66.79	69.52	56.63	118.60	125.19	117.84	66.33	0.90	137.81	121.52	275.63
67.00	67.43	66.83	69.52	56.59	118.59	125.28	117.97	66.38	0.90	137.06	121.63	274.13

Note: Shaded Test Data was the experimental data

Experimental Data for 24-8 Panel, MWT = 60°C

A_{panel} (ft^2)   24.00

$T_{rightwall}$ (F)	$T_{leftwall}$ (F)	$T_{frontwall}$ (F)	T_{floor} (F)	T_{cold} (F)	T_{panel} (F)	$T_{water in}$ (F)	$T_{water out}$ (F)	T_{air} (F)	Flow Rate (GPM)	Heat Flux (BTU/hrft^2)	MWT (F)	Heat Flux (BTU/hrft)
67.13	68.26	66.74	68.73	57.25	153.29	190.44	159.53	66.51	0.90	579.56	174.99	1159.13
67.15	68.76	67.78	68.79	57.02	152.22	155.26	157.87	67.62	0.90	-48.94	156.57	-97.88
66.30	67.92	68.65	68.46	56.75	144.14	155.39	148.33	67.89	0.90	132.38	151.86	264.75
66.04	67.45	68.73	68.41	56.51	139.02	147.36	142.66	68.11	0.90	88.13	145.01	176.25
66.41	67.88	67.64	68.79	56.11	134.56	141.84	137.59	68.09	0.90	79.69	139.72	159.38
66.83	68.32	67.54	69.00	56.06	130.12	138.36	132.69	68.18	0.90	106.31	135.53	212.63
67.34	68.77	67.82	69.18	56.24	127.57	137.32	129.69	68.09	0.90	143.06	133.51	286.13
67.87	69.16	68.41	69.47	56.59	128.37	140.31	129.65	68.07	0.90	199.88	134.98	399.75
68.26	69.75	68.85	70.04	56.70	130.48	144.25	133.14	68.13	0.90	208.31	138.70	416.63
67.78	69.99	67.90	69.22	56.38	132.38	146.48	135.64	68.70	0.90	203.25	141.06	406.50
66.15	68.13	66.66	68.49	56.04	133.64	146.37	136.83	68.52	0.90	178.88	141.60	357.75
66.23	67.95	67.21	68.60	55.51	133.05	145.81	136.47	68.31	0.90	175.13	141.14	350.25
67.16	68.59	68.32	69.24	56.30	133.58	145.33	136.29	68.34	0.90	169.50	140.81	339.00
66.80	68.29	68.93	68.71	56.60	133.62	145.09	136.04	68.27	0.90	169.69	140.57	339.38
65.99	67.29	66.87	68.25	56.27	133.24	144.55	135.54	68.20	0.90	168.94	140.05	337.88
67.10	67.75	68.04	68.66	56.88	133.92	144.16	135.10	67.80	0.90	169.88	139.63	339.75
68.24	68.36	69.31	69.00	57.39	134.31	143.55	134.13	66.38	0.90	176.63	138.84	353.25

Note: Shaded Test Data was the experimental data

Experimental Data for 24-8 Panel, MWT = 70°C

A_{panel} (ft^2)   24.00

$T_{rightwall}$ (F)	$T_{leftwall}$ (F)	$T_{frontwall}$ (F)	T_{floor} (F)	T_{cold} (F)	T_{panel} (F)	$T_{water in}$ (F)	$T_{water out}$ (F)	T_{air} (F)	Flow Rate (GPM)	Heat Flux (BTU/hrft^2)	MWT (F)	Heat Flux (BTU/hrft)
66.49	67.09	67.15	67.89	56.48	155.65	164.59	154.71	67.30	0.90	185.25	159.65	370.50
66.92	67.72	67.67	68.26	56.53	153.59	161.01	153.00	67.24	0.90	150.19	157.01	300.38
67.35	68.20	68.21	68.68	56.71	152.22	164.77	150.98	67.10	0.90	258.56	157.88	517.13
67.72	68.80	68.48	69.10	56.50	152.50	164.10	152.22	67.01	0.90	222.75	158.16	445.50
68.15	69.52	68.62	69.25	56.60	153.00	165.27	153.25	67.68	0.90	225.38	159.26	450.75
66.51	68.02	66.86	68.01	56.27	153.93	166.62	153.86	67.98	0.90	239.25	160.24	478.50
65.66	67.12	66.84	67.75	55.79	153.80	165.87	154.00	68.16	0.90	222.56	159.94	445.13
66.04	67.50	67.50	68.10	55.89	153.70	164.82	154.17	68.23	0.90	199.69	159.50	399.38
66.77	68.11	68.34	68.62	56.08	153.06	163.78	152.85	68.32	0.90	204.94	158.32	409.88
66.76	68.25	68.72	68.43	56.07	152.84	163.11	152.11	68.77	0.90	206.25	157.61	412.50
65.40	66.94	66.68	67.50	55.67	152.99	164.95	152.83	68.27	0.90	227.25	158.89	454.50
65.50	66.97	66.38	67.66	55.68	153.64	165.70	153.30	68.47	0.90	232.50	159.50	465.00
65.75	67.13	66.67	67.84	55.42	153.73	166.14	153.59	68.07	0.90	235.31	159.87	470.62
66.21	67.72	67.30	68.36	55.52	153.90	165.42	154.47	68.22	0.90	205.31	159.95	410.63
66.81	68.52	67.76	68.93	55.42	153.14	165.06	153.68	68.40	0.90	213.38	159.37	426.75
67.58	69.49	68.71	69.37	55.59	152.55	164.19	153.07	68.86	0.90	208.50	158.63	417.00
65.61	68.15	67.29	68.08	55.19	151.92	163.67	152.42	69.04	0.90	210.94	158.05	421.88
66.11	68.01	66.83	68.43	55.24	151.92	164.05	152.80	68.65	0.90	210.94	158.43	421.88
66.82	68.70	67.48	69.09	55.10	152.26	165.22	154.03	68.63	0.90	209.81	159.63	419.63
67.65	69.67	68.32	69.75	55.43	152.74	166.32	154.97	68.83	0.90	212.81	160.65	425.63
68.46	70.48	69.14	70.22	55.58	153.31	165.61	154.62	69.17	0.90	206.06	160.12	412.13
66.71	68.86	66.86	68.72	54.94	152.76	165.00	153.86	69.60	0.90	208.88	159.43	417.75
64.63	66.78	67.01	67.57	53.88	151.69	164.35	152.94	69.24	0.90	213.94	158.65	427.88
65.75	66.64	67.52	67.51	53.92	150.93	164.28	152.74	68.83	0.90	216.38	158.51	432.75
67.47	67.36	68.37	68.05	54.81	151.25	164.23	152.71	68.99	0.90	216.00	158.47	432.00
67.45	67.35	68.36	68.05	54.82	151.26	164.23	152.69	69.04	0.90	216.38	158.46	432.75

Note: Shaded Test Data was the experimental data

Experimental Data for 24-8 Panel, MWT = 82°C

A_{panel} (ft^2)   24.00

$T_{rightwall}$ (F)	$T_{leftwall}$ (F)	$T_{frontwall}$ (F)	T_{floor} (F)	T_{cold} (F)	T_{panel} (F)	$T_{water in}$ (F)	$T_{water out}$ (F)	T_{air} (F)	Flow Rate (GPM)	Heat Flux (BTU/hrft^2)	MWT (F)	Heat Flux (BTU/hrft)
65.74	66.31	65.42	67.32	55.97	173.42	190.71	174.54	68.99	0.90	303.19	182.63	606.38
66.70	66.94	66.21	67.64	56.08	174.93	192.49	175.93	69.24	0.90	310.50	184.21	621.00
67.56	67.51	66.99	68.10	56.30	175.96	193.82	177.26	69.13	0.90	310.50	185.54	621.00
68.42	67.86	67.66	67.92	56.23	177.04	194.86	178.03	68.88	0.90	315.56	186.45	631.13
69.02	67.28	68.42	67.66	56.33	178.10	196.32	179.31	68.79	0.90	318.94	187.82	637.88
67.69	67.41	68.69	68.04	56.34	175.58	196.43	175.50	68.67	0.90	392.44	185.97	784.88
67.43	67.52	67.89	68.56	56.28	178.68	198.73	180.10	68.85	0.90	349.31	189.42	698.63
67.94	66.82	66.83	69.27	56.35	180.63	200.10	182.21	69.01	0.90	335.44	191.16	670.87
68.42	66.45	67.10	69.73	56.66	179.84	193.98	182.21	68.86	0.90	220.69	188.10	441.37
68.56	66.67	67.69	70.13	56.51	176.65	188.31	177.82	68.99	0.90	196.69	183.07	393.38
67.23	67.03	68.22	70.38	56.62	172.55	187.39	172.56	68.88	0.90	278.06	179.98	556.12
67.42	67.50	68.70	70.62	56.76	172.21	187.52	172.18	69.13	0.90	287.63	179.85	575.25
68.05	68.02	68.41	70.75	56.81	172.24	188.67	172.04	69.19	0.90	311.81	180.36	623.63
68.69	68.55	68.09	71.02	56.79	172.52	185.68	172.96	69.37	0.90	238.50	179.32	477.00
68.57	68.32	67.60	71.22	56.95	171.17	186.19	170.74	69.57	0.90	289.69	178.47	579.38
66.96	67.49	67.50	71.26	56.64	171.68	188.80	170.38	69.80	0.90	345.38	179.59	690.75
67.12	66.72	68.00	71.29	56.48	173.02	186.12	173.19	69.89	0.90	242.44	179.66	484.88
67.60	66.69	68.47	70.21	56.20	172.01	187.18	171.63	70.03	0.90	291.56	179.41	583.13
68.10	67.39	68.67	69.54	56.07	171.44	186.12	171.64	70.05	0.90	271.50	178.88	543.00
68.69	68.14	68.04	69.52	56.30	171.40	188.28	171.09	70.07	0.90	322.31	179.69	644.63
68.77	68.97	67.85	69.67	56.60	172.42	188.44	172.53	70.14	0.90	298.31	180.49	596.63
67.78	69.04	68.45	69.37	56.69	172.16	187.12	172.08	70.23	0.90	282.00	179.60	564.00
66.96	67.73	67.03	69.57	56.23	171.84	185.94	171.63	70.21	0.90	268.31	178.79	536.63
67.74	67.72	66.94	69.96	56.14	171.14	185.94	170.64	70.11	0.90	286.88	178.29	573.75
68.85	68.34	67.78	70.42	56.19	172.33	188.20	172.26	69.84	0.90	298.88	180.23	597.75
68.33	68.29	68.44	70.72	56.33	172.89	186.30	173.19	69.98	0.90	245.81	179.75	491.63
66.58	67.12	68.87	70.51	56.23	171.63	185.70	171.03	69.76	0.90	275.06	178.37	550.13

$T_{rightwall}$ (F)	$T_{leftwall}$ (F)	$T_{frontwall}$ (F)	T_{floor} (F)	T_{cold} (F)	T_{panel} (F)	$T_{water\ in}$ (F)	$T_{water\ out}$ (F)	T_{air} (F)	Flow Rate (GPM)	Heat Flux (BTU/hrft^2)	MWT (F)	Heat Flux (BTU/hrft)
67.06	67.41	67.57	69.10	56.28	171.15	187.68	170.47	69.66	0.90	322.69	179.08	645.38
67.78	67.84	67.27	68.89	56.35	172.32	187.81	171.97	69.57	0.90	297.00	179.89	594.00
68.61	68.50	67.59	68.96	56.38	172.64	187.65	172.51	69.48	0.90	283.88	180.08	567.75
68.76	68.79	68.08	69.42	56.51	171.92	186.58	171.63	69.64	0.90	280.31	179.11	560.63
67.46	68.37	68.63	69.94	56.57	171.84	185.61	171.27	69.67	0.90	268.88	178.44	537.75
67.46	67.95	68.49	68.70	56.43	171.34	187.72	170.31	69.44	0.90	326.44	179.02	652.88
67.77	68.06	67.90	68.69	56.44	171.95	187.93	171.41	69.48	0.90	309.75	179.67	619.50

Note: Shaded Test Data was the experimental data

Experimental Data for 24-8 Panel, MWT = 95°C

A_{panel} (ft^2)   24.00

$T_{rightwall}$ (F)	$T_{leftwall}$ (F)	$T_{frontwall}$ (F)	T_{floor} (F)	T_{cold} (F)	T_{panel} (F)	$T_{water\ in}$ (F)	$T_{water\ out}$ (F)	T_{air} (F)	Flow Rate (GPM)	Heat Flux (BTU/hrft^2)	MWT (F)	Heat Flux (BTU/hrft)
70.22	71.23	71.42	75.11	61.53	154.66	200.14	155.62	74.25	0.90	834.75	177.88	1669.50
69.16	70.26	69.93	74.77	60.73	175.47	196.36	175.87	74.43	0.90	384.19	186.12	768.38
69.18	70.15	69.39	72.46	60.63	179.34	197.02	179.85	73.51	0.90	321.94	188.44	643.88
68.43	69.72	68.61	72.30	60.45	180.66	199.06	181.51	73.33	0.90	329.06	190.29	658.13
67.50	68.87	67.42	70.95	59.65	181.25	200.80	182.89	72.32	0.90	335.81	191.85	671.63
68.54	69.84	68.22	71.36	59.88	182.50	202.35	184.35	72.19	0.90	337.50	193.35	675.00
68.85	70.14	68.38	70.84	60.31	184.11	204.13	185.72	71.82	0.90	345.19	194.93	690.38
68.54	69.91	68.13	70.67	60.31	184.97	205.36	187.21	71.76	0.90	340.31	196.29	680.63
68.22	69.19	68.02	70.27	60.35	186.08	206.13	187.47	71.11	0.90	349.88	196.80	699.75
68.27	69.41	67.66	70.33	59.83	186.46	207.81	188.83	70.59	0.90	355.88	198.32	711.75
69.13	70.35	68.50	71.48	60.27	188.28	209.82	190.58	71.10	0.90	360.75	200.20	721.50
68.96	70.30	68.72	72.53	60.89	189.89	211.62	192.40	71.67	0.90	360.38	202.01	720.75
68.30	69.44	68.08	70.78	60.51	190.59	212.90	193.24	70.75	0.90	368.63	203.07	737.25
67.83	68.99	67.59	70.33	60.34	191.88	214.75	194.77	71.04	0.90	374.63	204.76	749.25

Note: Shaded Test Data was the experimental data

Appendix D

Uncertainty Analysis for Experimental Data and RSC Model

In any experiment there is a certain amount of error associated with obtaining data to compare to theoretical models. The following portion will discuss the uncertainty associated with the data obtained running the experiment.

D.1   Uncertainty in Measured Surface Temperatures

Omega T-Type thermocouples were used to measure the surface temperatures. From the Omega handbook (Omega, 2005), for brown thermocouple grade, the error with each measurement is +/-0.5°C (OMEGA, 2005).   Doing an uncertainty analysis on the wall temperatures based on an average of 4 thermocouples, shown and derived in the MathCad worksheet below (Figure D.1), shows that they are accurate within +/-0.25°C. Since the radiant panel surface temperature is averaged over six thermocouples the uncertainty in temperature measurement can be shown to equal +/-0.2°C.

Uncertainty in Measured Panel and Wall temperatures

For the Walls and Floor

$$T_{wavg} := \frac{T_{q1} + T_{q2} + T_{q3} + T_{q4}}{4}$$

Using the Root Sum Squared Method (RSS)

$$\delta T_{wavg}{}^2 := \left(\delta T_{q1} \cdot \frac{dT_{wavg}}{dT_{q1}}\right)^2 + \left(\delta T_{q2} \cdot \frac{dT_{wavg}}{dT_{q2}}\right)^2 + \left(\delta T_{q3} \cdot \frac{dT_{wavg}}{dT_{q3}}\right)^2 + \left(\delta T_{q4} \cdot \frac{dT_{wavg}}{dT_{q4}}\right)^2$$

$\delta T_{q1} := 0.5$

$\delta T_{q2} := 0.5$

$+$

$\delta T_{q3} := 0.5$

$\delta T_{q4} := 0.5$

$$\frac{dT_{wavg}}{dT_{q1}} := \frac{1}{4} \qquad \frac{dT_{wavg}}{dT_{q2}} := \frac{1}{4} \qquad \frac{dT_{wavg}}{dT_{q3}} := \frac{1}{4} \qquad \frac{dT_{wavg}}{dT_{q4}} := \frac{1}{4}$$

$$\delta T_{wallavg} := \left[\frac{\left(\delta T_{q1}\right)^2}{16} + \frac{\left(\delta T_{q2}\right)^2}{16} + \frac{\left(\delta T_{q3}\right)^2}{16} + \frac{\left(\delta T_{q4}\right)^2}{16}\right]^{\frac{1}{2}}$$

$\delta T_{wallavg} = 0.25$

For the Radiant Panel

$\delta T_{q5} := 0.5$

$\delta T_{q6} := 0.5$

$$\delta T_{panel} := \left[\frac{\left(\delta T_{q1}\right)^2}{36} + \frac{\left(\delta T_{q2}\right)^2}{36} + \frac{\left(\delta T_{q3}\right)^2}{36} + \frac{\left(\delta T_{q4}\right)^2}{36} + \frac{\left(\delta T_{q5}\right)^2}{36} + \frac{\left(\delta T_{q5}\right)^2}{36}\right]^{\frac{1}{2}}$$

$\delta T_{panel} = 0.204$

Figure D.1: MathCad Worksheet to Determine Temperature Uncertainties

155

D.2 Uncertainty in Calculated Heat Output

The panel heat output is determined by measuring the mass flow rate of the water and the temperature difference between the radiant panel inlet and outlet water. From the attached MathCad worksheet (Figure D.2), it is shown that the heat output equation is:

$$q'_{panel} = \frac{51.62Q(T_{in} - T_{out})}{P_{width}}$$
(D.1)

Uncertainty in Panel Heat Output

Using the Equation used to calculate the heat output from the measured experimental data

$$q_{flux} := 500 \cdot Q \cdot \frac{(T_{in} - T_{out})}{Area}$$

where : Q is the volumetric flow rate in GPM

T_{in} is the inlet water temperature in °F

T_{out} is the outlet water temperature in °F

Area is the panel area in ft²

Converting this equation into SI units

1 ft = 0.3048 m
1 GPM = 0.0631 L/s
ΔT of 1 °F = ΔT of 0.556 °C

$$q_{flux} := 188.82 \cdot Q \cdot \frac{(T_{in} - T_{out})}{Area}$$

where : Q is the volumetric flow rate in L/s

T_{in} is the inlet water temperature in °C

T_{out} is the outlet water temperature in °C

Area is the panel area in m²

Since we want the heat output per unit length we divide the panel by 12ft or 3.66m

$$q_{panel} := 51.62 \cdot Q \cdot \frac{(T_{in} - T_{out})}{W_p}$$

Figure D.2: MathCad Worksheet to Derive the Equation for Panel Heat Output Uncertainty

The water inlet and outlet temperature was measured using T-Type thermocouples. A thermopile was installed for a more accurate measurement, however due to the resolution of the DA system, the thermopile was ineffective. The error associated with each temperature measurement is +/-0.5°C. The water flow rate was measured using a circuit balancing valve. The pressure difference across the venturi tube is converted into a flow rate, which is accurate within 2% of the measured reading. For a 0.057 L/s reading, the circuit balancing valve is accurate within 0.0011 L/s. The panel width is made from standard sized panels and minimal error is associated with it. Using the root sum of the squares method (RSS) the uncertainty of the heat output of the panel can be estimated. From Equation D.1, Equation D.2 can be derived estimating the uncertainty with the heat output from the panel. The derivation can be found in Figure D.3.

$$\frac{\delta q_{panel}{'}}{q_{panel}{'}} = \left[\left(\frac{\delta \Delta T}{\Delta T} \right)^2 + \left(\frac{\delta V}{V} \right)^2 \right]^{1/2} \tag{D.2}$$

The water flow rate was constant for each test at a value of 0.057L/s. The water temperature difference changed for each different panel temperature. Ultimately, the uncertainty for the heat output of the panel can be shown to be +/-50W/m (Table D.1).

Another source is the accuracy of the temperature measurement. The error could easily be reduced if the thermopile would work (+/-0.05°C) (Huang, 2005) or a thermistor (+/-0.1°C). If the thermopile had been used, it can be shown that the uncertainty of the heat output is between 2 to 2.5%. Using two thermistors to measure the inlet and outlet temperature, the uncertainty of the temperature difference can be shown to equal +/-0.14°C. The uncertainty of the heat output can be estimated to be between 2.5 to 5% (Table D.1).

Using the RSS method to determine the uncertainty for a 0.6096 m wide panel

$$q_{panel} := 84.678 \cdot Q \cdot \left(T_{in} - T_{out}\right)$$

$$\delta q_{panel} := \left[\left(\delta Q \cdot \frac{dq_{panel}}{dQ}\right)^2 + \left(\delta(\Delta T) \cdot \frac{dq_{panel}}{d\Delta T}\right)^2\right]^{\frac{1}{2}}$$

$$\delta Q := 0.0011$$

$$\delta(\Delta T) := \left[\left(\delta T_{in} \cdot \frac{d(\Delta T)}{dT_{in}}\right)^2 + \left(\delta T_{out} \cdot \frac{d(\Delta T)}{dT_{out}}\right)^2\right]^{\frac{1}{2}}$$

$$\delta T_{in} := 0.5$$

$$\delta T_{out} := 0.5$$

$$\delta \Delta T := \left[\left(\delta T_{in}\right)^2 + \left(\delta T_{out}\right)^2\right]^{\frac{1}{2}}$$

$$\delta \Delta T = 0.707$$

$$\delta q_{panel} := \left[\left[\delta Q \cdot 84.678 \cdot (\Delta T)\right]^2 + \left(\delta \Delta T \cdot 84.678 \cdot Q\right)^2\right]^{\frac{1}{2}}$$

Isolating for ΔT and Q in the 1st equation, subbing into the last equation and isloating for q_{panel}

$$\delta q_{panel} := q_{panel} \left[\left(\frac{\delta Q}{Q}\right)^2 + \left(\frac{\delta \Delta T}{\Delta T}\right)^2\right]^{\frac{1}{2}}$$

Knowing the inlet and outlet water temperature difference and flow rate the % uncertainty can be calculated with the above equation - see the attached excel spreadhseet for values

Figure D.3: MathCad Worksheet to Determine Heat Output Uncertainty

Table D.1: Panel Heat Output Uncertainty due to Temperature Difference Method

Summary of Results from the 24-4 Test

Based on an average steady state test run of 30 minutes - so 8 readings

Fluid Inlet Temp (^{o}C)	Panel Heat Output (W/m)	Regular Thermocouple			Thermopile			Thermistor		
		% Error	+ Error	- Error	% Error	+ Error	- Error	% Error	+ Error	- Error
51.78	207.8884267	23.72083	49.31285635	49.31286	2.584122	5.37209	5.3721	4.966	10.324	10.32374
61.35	298.4715319	16.37261	48.8675928	48.86759	2.294695	6.849011	6.849	3.7102	11.074	11.07391
73.91	374.1811396	13.1273	49.1198832	49.11988	2.192435	8.203677	8.2037	3.1977	11.965	11.96507
86.66	490.7424858	10.84181	53.20534571	53.20535	2.131715	10.46123	10.461	2.8634	14.052	14.05199
100.4	613.2888872	7.904272	48.476019	48.47602	2.068883	12.68823	12.688	2.4825	15.225	15.22468

Summary of the 24-8 Results

Based on an average steady state test run of 30 minutes - so 8 readings

Inlet Fluid Temp (^{o}C)	Heat Output (W/m)	Regular Thermocouple			Thermopile			Thermistor		
		% Error	+ Error	- Error	% Error	+ Error	- Error	% Error	+ Error	- Error
51.96	261.6752184	23.72083	62.07152876	62.07153	2.584122	6.762007	6.762	4.966	12.995	12.99479
62.77	332.0331246	16.37261	54.36250295	54.3625	2.294695	7.619147	7.6191	3.7102	12.319	12.31911
73.71	407.6840682	13.1273	53.51791338	53.51791	2.192435	8.938207	8.9382	3.1977	13.036	13.03638
86.11	553.6117509	10.84181	60.02150913	60.02151	2.131715	11.80142	11.801	2.8634	15.852	15.8522
99.66	700.0820049	7.904272	55.3363827	55.33638	2.068883	14.48388	14.484	2.4825	17.379	17.37929

D.3 Uncertainty in Bond Conductance due to heat paste thickness

Using the RSS method as described the above, an attempt was made to measure the uncertainty associated with the bond conductance due to the measurement uncertainty in the heat paste thickness and width. The effect of bond conductance on panel temperature can be seen in Equation 4.18 (Equation D.3).

$$T_{panel} = T_f - q'_{panel}\left(\frac{1}{h_w \pi D_i} + \frac{1}{C_b}\right) \tag{D.3}$$

The uncertainty in the panel temperature can be quantified if the uncertainty in the bond conductance is known based on the measured values. The bond conductance equation is shown below:

$$C_b = \frac{k_b b}{t_b} \tag{D.4}$$

Assuming all other variables in Equation D.3 have no uncertainty, the panel temperature uncertainty due to bond thickness measurement error can be quantified. The following MathCad worksheets summarize the calculations (Figures D.4 to D.6).

Uncertainty in Predicted Panel Temperature due to Bond Conductance, 2/4

To determine the uncertainty in the bond conductance, we need to know the uncertainty in the heat paste thickness

$\delta t_{bi} := 0.0005$ $\qquad$ $b_i := 0.005$

$\delta b_i := 0.0005$ $\qquad$ $t_i := 0.003$

$\qquad\qquad\qquad\qquad$ $k_b := 1.5$

$V_i := b_i \cdot t_i$

$V_i = 1.5 \times 10^{-5}$

Assuming that the final bond width is equal to surface area of the tube in contact with the panel:

$V_f := V_i$

$t_{bf} := \dfrac{V_f}{0.0167}$

$t_{bf} = 8.982 \times 10^{-4}$

Uncertainty related with the final bond thickness

Step 1: Calculate the uncertainty in the heat paste volume

$$\delta V := \left[\left(\delta t_{bi} \cdot \frac{dV}{dt_{bi}} \right)^2 + \left(\delta b_i \cdot \frac{dV}{db_i} \right)^2 \right]^{\frac{1}{2}}$$

$$\delta V := \left[\left(\delta t_{bi} \cdot b_i \right)^2 + \left(\delta b_i \cdot t_i \right)^2 \right]^{\frac{1}{2}}$$

$$\delta V = 2.915 \times 10^{-6}$$

Figure D.4: MathCad Worksheet to Determine Panel Temperature Uncertainty Associated with Bond Conductance

Step 2: Uncertainty in the final heat paste thickness

    We can assume that the final bond thickness is equivalent to the area in contact

$$b_f := 0.0167$$

$$\delta t_{bf} := \left[\left(\delta V_f \frac{dt_{bf}}{dV_f} \right)^2 \right]^{\frac{1}{2}}$$

$$\delta t_{bf} := \frac{\delta V}{0.0167}$$

$$\delta t_{bf} = 1.746 \times 10^{-4}$$

Now the Uncertainty in the bond conductance can be calculated

$$C_b := \frac{k_b \cdot b_f}{t_{bf}}$$

$$\delta C_b := \left[\left(\delta t_{bf} \cdot \frac{dC_b}{dt_{bf}} \right)^2 \right]^{\frac{1}{2}}$$

$$\delta C_b := \delta t_{bf} \cdot \frac{k_b \cdot b_f}{t_{bf}^2}$$

$$\delta C_b = 5.421$$

To calculte the uncertainty in the predicted panel temperature consider Equation 5.1
Assuming that everything is known except the bond conductance the equation to determine
the panel temperature can be written as:

$$T_{panel} := D - \frac{q_{panel}}{C_b}$$

Figure D.5: MathCad Worksheet to Determine Panel Temperature Uncertainty Associated with Bond Conductance

162

Performaing an uncertainty analysis on the above equation:

$$\delta T_b := \left[\left(\delta C_b \cdot \frac{dT_b}{dC_b} \right)^2 \right]^{\frac{1}{2}}$$

$$\delta T_b := \delta C_b \cdot \frac{q_{panel}}{C_b^2}$$

$$\delta T_b(q_{panel}) := \delta C_b \cdot \frac{q_{panel}}{C_b^2}$$

For the 24-4 Panel Experiment

$$C_b = 27.889$$

$$\delta T_b(216.65) = 1.51$$

$$\delta T_b(291.39) = 2.031$$

$$\delta T_b(378.25) = 2.636$$

$$\delta T_b(478.46) = 3.335$$

$$\delta T_b(586.56) = 4.088$$

Figure D.6: MathCad Worksheet to Determine Panel Temperature Uncertainty Associated with Bond Conductance

Appendix E

Solution to the Radiosity Equations

E.1   View Factor Calculations for Radiant Panel Test Chamber

To solve the set of radiosity equations, the view factors for a 2 ft wide radiant panel was calculated first. Using the same method as described in Appendix B, the view factor calculations are summarized on the following MathCad worksheets (Figures E.1 to E.3).

View Factors Calculations for Radiant Heating Panel

Radiant Panel Width

$length := 24$ length is in Inches

Radiant Panel Location (Coordinates)

x is the width of the radiant panel

y is the length of the radiant panel

z is the height of the radiant panel

$x_{i1} := 0$ $y_{i1} := 3.9624 - length \cdot 0.0254$ $z_i := 3.048$

$x_{i2} := 3.9624$ $y_{i2} := 3.9624$

View Factor from radiant panel to the floor

Front Wall Coordinates

$x_{j1} := 0$ $y_{j1} := 0$ $z_{j1} := 0$

$x_{j2} := 3.9624$ $y_{j2} := 3.9624$

$$F_{topbottom} := \frac{1}{\left[(x_{i2} - x_{i1}) \cdot (y_{i2} - y_{i1})\right]} \cdot \int_{x_{i1}}^{x_{i2}} \int_{y_{i1}}^{y_{i2}} \int_{x_{j1}}^{x_{j2}} \int_{y_{j1}}^{y_{j2}} \frac{z_i^2}{\pi \cdot \left[(x_i - x_j)^2 + (y_i - y_j)^2 + z_i^2\right]^2} \, dy_j \, dx_j \, dy_i \, dx_i$$

$F_{topbottom} = 0.238$

Figure E.1:   MathCad Worksheet to Calculate the View Factors for the Radiant Panel Test Chamber

View Factor from the radiant panel to the left/right wall

Left Wall Coordinates

$$x_j := 0 \qquad\qquad y_{j1} := 0 \qquad\qquad z_{j1} := 0$$

$$y_{j2} := 3.9624 \qquad\qquad z_{j2} := 3.048$$

$$F_{topside} := \frac{1}{\left[(x_{i2} - x_{i1})\cdot(y_{i2} - y_{i1})\right]} \cdot \int_{z_{j1}}^{z_{j2}} \int_{y_{j1}}^{y_{j2}} \int_{x_{i1}}^{x_{i2}} \int_{y_{i1}}^{y_{i2}} \frac{(3.048 - z_j)\cdot(x_i - 0)}{\pi\cdot\left[(x_j - x_i)^2 + (y_j - y_i)^2 + (z_j - z_i)^2\right]^2}\, dy_i\, dx_i\, dy_j\, dz_j$$

$$F_{topside} = 0.153$$

View Factor from the radiant panel to the exterior (cold wall)

Exterior Wall Coordinates

$$x_{j1} := 0 \qquad\qquad y_j := 3.9624 \qquad\qquad z_{j1} := 0$$

$$x_{j2} := 3.9624 \qquad\qquad z_{j2} := 3.048$$

$$F_{topback} := \frac{1}{(x_{i2} - x_{i1})\cdot(y_{i2} - y_{i1})} \cdot \int_{y_{i1}}^{y_{i2}} \int_{x_{i1}}^{x_{i2}} \int_{x_{j1}}^{x_{j2}} \int_{z_{j1}}^{z_{j2}} \frac{(3.048 - z_j)\cdot(3.9624 - y_i)}{\pi\cdot\left[(x_j - x_i)^2 + (y_j - y_i)^2 + (z_j - z_i)^2\right]^2}\, dz_j\, dx_j\, dx_i\, dy_i$$

$$F_{topback} = 0.401$$

Figure E.2: MathCad Worksheet to Calculate the View Factors for the Radiant Panel Test Chamber

View Factor from the radiant panel to the front wall

Front Wall Coordinates

$$x_{j1} := 0 \qquad\qquad y_j := 0 \qquad\qquad z_{j1} := 0$$

$$x_{j2} := 3.9624 \qquad\qquad\qquad\qquad z_{j2} := 3.048$$

$$F_{topfront} := \frac{1}{\left[(x_{i2} - x_{i1}) \cdot (y_{i2} - y_{i1})\right]} \cdot \int_{z_{j1}}^{z_{j2}} \int_{x_{j1}}^{x_{j2}} \int_{y_{i1}}^{y_{i2}} \int_{x_{i1}}^{x_{i2}} \frac{(3.048 - z_j) \cdot (y_i - 0)}{\pi \cdot \left[(x_j - x_i)^2 + (y_j - y_i)^2 + (z_j - z_i)^2\right]^2} \, dx_i \, dy_i \, dx_j \, dz_j$$

$$F_{topfront} = 0.057$$

Figure E.3:   MathCad Worksheet to Calculate the View Factors for the Radiant Panel Test Chamber

Using reciprocity and tabulated parallel and perpendicular view factor equations, the remaining view factors can be calculated as shown in the next few MathCad worksheets (Figure E.4 to E.7) and excel (Table E.1).

View Factors For Parallel Plates

For the Back Wall to the Front Wall

$$X := \frac{10}{13}$$

$$Y := \frac{13}{13}$$

$$F_{ij} := \frac{2}{\pi \cdot X \cdot Y} \cdot \left[\ln\left[\frac{\sqrt{(1+X^2) \cdot (1+Y^2)}}{\sqrt{1+X^2+Y^2}} \right] + X \cdot \sqrt{1+Y^2} \cdot \operatorname{atan}\left(\frac{X}{\sqrt{1+Y^2}} \right) + Y \cdot \sqrt{1+X^2} \cdot \operatorname{atan}\left(\frac{Y}{\sqrt{1+X^2}} \right) - X \cdot \operatorname{atan}(X) - Y \cdot \operatorname{atan}(Y) \right]$$

$$F_{ij} = 0.166$$

Figure E.4: MathCad Worksheet to Calculate the View Factors for the Radiant Panel Test Chamber

View Factors For Perpendicular Plates

For the Back Wall to the Floor

$$H := \frac{13}{13}$$

$$W := \frac{10}{13}$$

$$F_{ij} := \frac{1}{\pi \cdot W} \cdot \left[W \cdot \text{atan}\left(\frac{1}{W}\right) + H \cdot \text{atan}\left(\frac{1}{H}\right) - \sqrt{H^2 + W^2} \cdot \text{atan}\left(\frac{1}{\sqrt{H^2 + W^2}}\right) + \frac{1}{4} \cdot \ln\left[\frac{\left[(1 + W^2) \cdot (1 + H^2)\right]}{(1 + W^2 + H^2)} \cdot \left[\left[\frac{\left[W^2 \cdot (1 + W^2 + H^2)\right]^{W^2}}{\left[(1 + W^2) \cdot (W^2 + H^2)\right]^{W^2}} \right] \cdot \frac{\left[H^2 \cdot (1 + H^2 + W^2)\right]^{H^2}}{\left[(1 + H^2) \cdot (H^2 + W^2)\right]^{H^2}} \right] \right] \right]$$

$$F_{ij} = 0.236$$

Figure E.5: MathCad Worksheet to Calculate the View Factors for the Radiant Panel Test Chamber

For the Back Wall to the Left/Right Wall

$$H := \frac{13}{10}$$

$$W := \frac{13}{10}$$

$$F_{ij} := \frac{1}{\pi \cdot W} \cdot \left[W \cdot atan\left(\frac{1}{W}\right) + H \cdot atan\left(\frac{1}{H}\right) - \sqrt{H^2 + W^2} \cdot atan\left(\frac{1}{\sqrt{H^2 + W^2}}\right) + \frac{1}{4} \cdot \ln\left[\frac{\left[(1 + W^2) \cdot (1 - H^2)\right]}{(1 + W^2 + H^2)} \cdot \left[\left[\frac{\left[W^2 \cdot (1 + W^2 + H^2)\right]^{W^2}}{\left[(1 + W^2) \cdot (W^2 + H^2)\right]^{W^2}}\right] \cdot \frac{\left[H^2 \cdot (1 + H^2 + W^2)\right]^{H^2}}{\left[(1 + H^2) \cdot (H^2 + W^2)\right]^{H^2}}\right]\right]\right]$$

$$F_{ij} = 0.181$$

Figure E.6: MathCad Worksheet to Calculate the View Factors for the Radiant Panel Test Chamber

For the Floor to the Left/Right Wall

$$H := \frac{10}{13}$$

$$W := \frac{13}{13}$$

$$VF_{ij} := \frac{1}{\pi \cdot W} \cdot \left[W \cdot atan\left(\frac{1}{W}\right) + H \cdot atan\left(\frac{1}{H}\right) - \sqrt{H^2 + W^2} \cdot atan\left(\frac{1}{\sqrt{H^2 + W^2}}\right) + \frac{1}{4} \cdot \ln\left[\frac{\left[\left(1 + W^2\right) \cdot \left(1 + H^2\right)\right]}{\left(1 + W^2 + H^2\right)} \cdot \left[\left[\frac{\left[W^2 \cdot \left(1 + W^2 + H^2\right)\right]^{W^2}}{\left[\left(1 + W^2\right) \cdot \left(W^2 + H^2\right)\right]^{W^2}} \right] \cdot \frac{\left[H^2 \cdot \left(1 + H^2 + W^2\right)\right]^{H^2}}{\left[\left(1 + H^2\right) \cdot \left(H^2 + W^2\right)\right]^{H^2}} \right] \right] \right]$$

$$VF_{ij} = 0.181$$

Figure E.7: MathCad Worksheet to Calculate the View Factors for the Radiant Panel Test Chamber

171

Table E.1: Excel Worksheet Calculating View Factors using Reciprocity Equations

Surface 1	Panel	A_1 (ft^2)	26
Surface 2	Back Wall	A_2 (ft^2)	130
Surface 3	Front Wall	A_3 (ft^2)	130
Surface 4	Floor	A_4 (ft^2)	169
Surface 5	Left Wall	A_5 (ft^2)	130
Surface 6	Right Wall	A_6 (ft^2)	130
Surface 7	Ceiling	A_7 (ft^2)	143

F_{11}	0
F_{12}	0.401
F_{13}	0.057
F_{14}	0.238
F_{15}	0.153
F_{16}	0.153
F_{17}	0

F_{21}	0.0802	
F_{22}	0	
F_{23}	0.166	
F_{24}	0.236	
F_{25}	0.181	
F_{26}	0.181	0.8442
F_{27}	0.1558	

F_{31}	0.0114	
F_{32}	0.166	
F_{33}	0	
F_{34}	0.236	
F_{35}	0.181	
F_{36}	0.181	0.7754
F_{37}	0.2246	

F_{41}	0.036615	
F_{42}	0.181538	
F_{43}	0.181538	
F_{44}	0	
F_{45}	0.181538	
F_{46}	0.181538	0.762768
F_{47}	0.237232	

F_{51}	0.0306	
F_{52}	0.181	
F_{53}	0.181	
F_{54}	0.2359994	
F_{55}	0	
F_{56}	0.166	0.794599
F_{57}	0.2054006	

F_{61}	0.0306	
F_{62}	0.181	
F_{63}	0.181	
F_{64}	0.235999	
F_{65}	0.166	
F_{66}	0	
F_{67}	0.205401	

F_{71}	0
F_{72}	0.14163636
F_{73}	0.20418182
F_{74}	0.28036473
F_{75}	0.2054006
F_{76}	0.18672782
F_{77}	0

1.01831133

E.2 Radiosity Equations (Exact Solution)

With knowledge of the view factors, the radiosity equations could be solved as shown in attached MathCad worksheets (Figure E.8 and Figure E.9).

Radiosity Calculations

Matrix for the enclosure view factors

$$F := \begin{pmatrix} 0 & 0.0802 & 0.0114 & 0.036615 & 0.0306 & 0.0306 & 0 \\ 0.401 & 0 & 0.166 & 0.181538 & 0.181 & 0.181 & 0.142 \\ 0.057 & 0.166 & 0 & 0.181538 & 0.181 & 0.181 & 0.204 \\ 0.238 & 0.236 & 0.236 & 0 & 0.236 & 0.236 & 0.28 \\ 0.153 & 0.181 & 0.181 & 0.181538 & 0 & 0.166 & 0.205 \\ 0.153 & 0.181 & 0.181 & 0.181538 & 0.166 & 0 & 0.187 \\ 0 & 0.1558 & 0.2246 & 0.237232 & 0.205 & 0.205 & 0 \end{pmatrix}$$

$$V := F^{T}$$

Equation is of form Ax = B

A = View Factor Equation

x = Radiosities

B = Blackbody Radiation

Getting the View Factor Matrix

$$A := 0.1 \begin{pmatrix} 10 - V_{0,0} & -V_{0,1} & -V_{0,2} & -V_{0,3} & -V_{0,4} & -V_{0,5} & -V_{0,6} \\ -V_{1,0} & 10 - V_{1,1} & -V_{1,2} & -V_{1,3} & -V_{1,4} & -V_{1,5} & -V_{1,6} \\ -V_{2,0} & -V_{2,1} & 10 - V_{2,2} & -V_{2,3} & -V_{2,4} & -V_{2,5} & -V_{2,6} \\ -V_{3,0} & -V_{3,1} & -V_{3,2} & 10 - V_{3,3} & -V_{3,4} & -V_{3,5} & -V_{3,6} \\ -V_{4,0} & -V_{4,1} & -V_{4,2} & -V_{4,3} & 10 - V_{4,4} & -V_{4,5} & -V_{4,6} \\ -V_{5,0} & -V_{5,1} & -V_{5,2} & -V_{5,3} & -V_{5,4} & 10 - V_{5,5} & -V_{5,6} \\ -V_{6,0} & -V_{6,1} & -V_{6,2} & -V_{6,3} & -V_{6,4} & -V_{6,5} & 10 - V_{6,6} \end{pmatrix}$$

Inverting the View Factor Matrix to Solve for the Radiosities

$$C := A^{-1}$$

Figure E.8: MathCad Worksheet for Radiosity Calculations (Exact)

$$C = \begin{pmatrix} 1.001 & 0.041 & 7.517 \times 10^{-3} & 0.026 & 0.017 & 0.017 & 2.122 \times 10^{-3} \\ 8.272 \times 10^{-3} & 1.002 & 0.018 & 0.026 & 0.02 & 0.02 & 0.017 \\ 1.503 \times 10^{-3} & 0.018 & 1.002 & 0.026 & 0.02 & 0.02 & 0.024 \\ 3.974 \times 10^{-3} & 0.02 & 0.02 & 1.003 & 0.02 & 0.02 & 0.025 \\ 3.397 \times 10^{-3} & 0.02 & 0.02 & 0.026 & 1.002 & 0.018 & 0.022 \\ 3.397 \times 10^{-3} & 0.02 & 0.02 & 0.026 & 0.018 & 1.002 & 0.022 \\ 3.926 \times 10^{-4} & 0.016 & 0.022 & 0.03 & 0.022 & 0.02 & 1.002 \end{pmatrix}$$

x = B × C where B = $\sigma\varepsilon T^4$ and C is the inverted view factor matrix

$$J(a) := 0.9 \cdot 5.67 \cdot 10^{-8} C \cdot \begin{pmatrix} a^4 \\ 283^4 \\ 293^4 \\ 293^4 \\ 293^4 \\ 293^4 \\ 293^4 \end{pmatrix}$$

Solving for the panel heat flux at various panel temperatures

$$q_{panel}(a) := \sum_{j=0}^{6} \left[V_{0,j} \cdot \left(J(a)_0 - J(a)_j \right) \right]$$

$q_{panel}(318) = 163.553$ $\qquad$ $q_{panel}(343) = 347.513$

$q_{panel}(323) = 197.06$ $\qquad$ $q_{panel}(348) = 389.487$

$q_{panel}(328) = 232.159$ $\qquad$ $q_{panel}(353) = 433.31$

$q_{panel}(333) = 268.9$ $\qquad$ $q_{panel}(358) = 479.036$

$q_{panel}(338) = 307.334$ $\qquad$ $q_{panel}(363) = 526.717$

Figure E.9: MathCad Worksheet for Radiosity Calculations (Exact)

E.3 Radiosity Equations (Three Surface Solution)

For the assumed three-surface enclosure the view factors can be calculated using reciprocity equations and published view factor equations for perpendicular plates (shown above). The attached MathCad worksheet (Figure E.10 and Figure E.11) solves the radiosity equations for the known three-surface enclosure view factors.

For the three Surface Enclosure

Equation is of form:

$$Cy = D$$

C is the View Factor matrix

y is the radiosity matrix

D is the Temperature Matrix

Emissivity and View Factors

$$\varepsilon := 0.9$$

$$F_{12} := 0.401 \qquad\qquad F_{21} := 0.08 \qquad\qquad F_{31} := 0.102$$

$$F_{13} := 1 - F_{12} \qquad\qquad F_{23} := 1 - F_{21} \qquad\qquad F_{32} := 0.784$$

$$F_{33} := 1 - F_{31} - F_{32}$$

View Factor Matrix

$$C := \begin{bmatrix} 1 & -F_{12}\cdot(1-\varepsilon) & -F_{13}\cdot(1-\varepsilon) \\ -F_{21}\cdot(1-\varepsilon) & 1 & -F_{23}\cdot(1-\varepsilon) \\ -F_{31}\cdot(1-\varepsilon) & -F_{32}\cdot(1-\varepsilon) & 1-F_{33}\cdot(1-\varepsilon) \end{bmatrix}$$

Inverting the Matrix

$$C^{-1} = \begin{pmatrix} 1.001 & 0.045 & 0.065 \\ 9.024 \times 10^{-3} & 1.008 & 0.094 \\ 0.011 & 0.08 & 1.02 \end{pmatrix} \qquad H := C^{-1}$$

Figure E.10: MathCad Worksheet for Radiosity Calculations (Three Surface)

175

Solving for the Radiosity

$$y(a) := H \cdot \left[s \cdot 5.67 \cdot 10^{-8} \cdot \begin{bmatrix} (a)^4 \\ (283)^4 \\ (293)^4 \end{bmatrix} \right]$$

- -

Calculating the Panel Heat Flux at various temperatures

$$q_{panel}(a) := F_{12} \cdot (y(a)_0 - y(a)_1) + F_{13} \cdot (y(a)_0 - y(a)_2)$$

$q_{panel}(318) = 164.253$

$q_{panel}(323) = 197.546$

$q_{panel}(328) = 232.421$

$q_{panel}(333) = 268.928$

$q_{panel}(338) = 307.117$

$q_{panel}(343) = 347.039$

$q_{panel}(348) = 388.745$

$q_{panel}(353) = 432.289$

$q_{panel}(358) = 477.722$

$q_{panel}(363) = 525.1$

Figure E.11: MathCad Worksheet for Radiosity Calculations (Three Surface)

176

The following table (Table E.2) summarizes the total radiative heat exchange for the exact solution, the MRT method and the three-surface enclosure method.

Table E.2: Comparison of Radiative heat Exchange Methods

T_{panel} (K)	T_{cold} (K)	T_{front} (K)	T_{floor} (K)	T_{left} (K)	T_{right} (K)	$T_{ceiling}$ (K)	Exact q_{rad} (W/m^2)	MRT Method	%error	3 - Surface	% error
318	283	293	293	293	293	293	163.55	152.27	6.90	164.25	-0.43
323	283	293	293	293	293	293	197.06	185.19	6.02	197.55	-0.25
328	283	293	293	293	293	293	232.16	219.68	5.38	232.42	-0.11
333	283	293	293	293	293	293	268.90	255.78	4.88	268.93	-0.01
338	283	293	293	293	293	293	307.33	293.55	4.49	307.12	0.07
343	283	293	293	293	293	293	347.51	333.03	4.17	347.04	0.14
348	283	293	293	293	293	293	389.49	374.27	3.91	388.75	0.19
353	283	293	293	293	293	293	433.31	417.33	3.69	432.29	0.24
358	283	293	293	293	293	293	479.04	462.26	3.50	477.77	0.26
363	283	293	293	293	293	293	526.72	509.12	3.34	525.10	0.31

Appendix F

Grid Refinement, Model Validation and Numerical Results

F.1 Grid Refinement

The following excel worksheets summarize the grid refinement procedure.

Cavity: 3.9624m x 3.048m
Panel Size: 0.88315
Coarse Grid: 0.064m
Panel Boundary: 0.025cm start x 2expansion
Cold Wall Bound. 0.025cm start x 2expansion
Wall Boundary 0.05cm start x 2 expansion
x-dir fill cell: 0.05915m
y-dir fill cell: 0.040975m
Gridrefinement: 2 times

Cell No	Heat Flux (W/m^2)	Width	Heat (W)
4492	11.821	0.064	0.757
4493	13.459	0.064	0.861
4494	11.709	0.064	0.749
4495	11.302	0.064	0.723
4496	11.123	0.064	0.712
4497	11.048	0.064	0.707
4498	11.051	0.064	0.707
4499	11.125	0.064	0.712
4500	11.278	0.064	0.722
4501	11.555	0.064	0.740
4502	12.264	0.064	0.785
4503	15.155	0.064	0.970
4511	28.280	0.059	1.673
4568	62.968	0.032	2.015
4569	131.987	0.016	2.112
4570	258.441	0.008	2.068
		0.883	19.263

Cavity: 3.9624m x 3.048m
Panel Size: 0.883025
Coarse Grid: 0.064m
Panel Boundary: 0.0125cm start x 2expansion
Cold Wall Bound. 0.0125cm start x 2expansion
Wall Boundary 0.05cm start x 2 expansion
x-dir fill cell: 0.059025m
y-dir fill cell: 0.040625m
Gridrefinement: 2 times

Cell No	Heat Flux (W/m^2)	Width	Heat (W)
4611	11.843	0.064	0.758
4612	13.469	0.064	0.862
4613	11.714	0.064	0.750
4614	11.303	0.064	0.723
4615	11.121	0.064	0.712
4616	11.039	0.064	0.707
4617	11.034	0.064	0.706
4618	11.115	0.064	0.711
4619	11.276	0.064	0.722
4620	11.553	0.064	0.739
4621	12.263	0.064	0.785
4622	15.155	0.064	0.970
4631	28.443	0.059	1.679
4704	63.768	0.032	2.041
4705	135.258	0.016	2.164
4706	271.003	0.008	2.168
		0.883	19.474

Cavity: 3.9624m x 3.048m
Panel Size: 0.8829625
Coarse Grid: 0.064m
Panel Boundary: 0.00625cm start x 2expansion
Cold Wall Bound. 0.00625cm start x 2expansion
Wall Boundary 0.05cm start x 2 expansion
x-dir fill cell: 0.058965m
y-dir fill cell: 0.0405625m
Gridrefinement: 2 times

Cell No	Heat Flux (W/m^2)	Width	Heat (W)
4730	11.859	0.064	0.759
4731	13.463	0.064	0.862
4732	11.685	0.064	0.748
4733	11.286	0.064	0.722
4734	11.105	0.064	0.711
4735	11.028	0.064	0.706
4736	11.028	0.064	0.706
4737	11.105	0.064	0.711
4738	11.260	0.064	0.721
4739	11.537	0.064	0.785
4740	12.265	0.064	0.973
4741	15.208	0.064	0.973
4751	28.530	0.059	1.682
4842	64.048	0.032	2.050
4843	136.461	0.016	2.183
4844	276.635	0.008	2.213
		0.883	19.824

Cavity: 3.9624m x 3.048m
Panel Size: 0.88293125
Coarse Grid: 0.064m
Panel Boundary: 0.003125cm start x 2expansion
Cold Wall Bound. 0.003125cm start x 2expansion
Wall Boundary 0.05cm start x 2 expansion
x-dir fill cell: 0.058965m
y-dir fill cell: 0.0405625m
Gridrefinement: 2 times

Cell No	Heat Flux (W/m^2)	Width	Heat (W)
4849	11.840	0.064	0.758
4850	13.450	0.064	0.861
4851	11.672	0.064	0.747
4852	11.273	0.064	0.721
4853	11.092	0.064	0.710
4854	11.002	0.064	0.704
4855	11.002	0.064	0.704
4856	11.092	0.064	0.710
4857	11.260	0.064	0.721
4858	11.543	0.064	0.739
4859	12.252	0.064	0.784
4860	15.189	0.064	0.972
4871	28.549	0.059	1.682
4982	64.203	0.032	2.054
4983	137.140	0.016	2.194
4984	279.498	0.008	2.236
		0.883	19.591

Cavity:	3.9624m x 3.048m			Cavity:	3.9624m x 3.048m		
Panel Size:	0.88315			Panel Size:	0.883025		
Coarse Grid:	0.032m			Coarse Grid:	0.032m		
Panel Boundary:	0.025cm start x 2expansion			Panel Boundary:	0.0125cm start x 2expansion		
Cold Wall Bound.	0.025cm start x 2expansion			Cold Wall Bound.	0.05cm start x 2 expansion		
Wall Boundary	0.05cm start x 2 expansion			Wall Boundary	0.05cm start x 2 expansion		
x-dir fill cell:	0.029575			x-dir fill cell:	0.0295125		
y-dir fill cell:	0.0204875			y-dir fill cell:	0.0203125		
Gridrefinement:	2 times			Gridrefinement:	2 times		

Cell No	Heat Flux (W/m^2)	Width	Heat (W)	Cell No	Heat Flux (W/m^2)	Width	Heat (W)
14342	5.890	0.032	0.188	14566	5.933	0.032	0.190
14343	15.443	0.032	0.494	14567	15.539	0.032	0.497
14344	16.475	0.032	0.527	14568	16.511	0.032	0.528
14345	13.233	0.032	0.423	14569	13.215	0.032	0.423
14346	12.369	0.032	0.396	14570	12.355	0.032	0.395
14347	11.959	0.032	0.383	14571	11.946	0.032	0.382
14348	11.716	0.032	0.375	14572	11.703	0.032	0.374
14349	11.555	0.032	0.370	14573	11.543	0.032	0.369
14350	11.446	0.032	0.366	14574	11.435	0.032	0.366
14351	11.370	0.032	0.364	14575	11.363	0.032	0.364
14352	11.319	0.032	0.362	14576	11.313	0.032	0.362
14353	11.291	0.032	0.361	14577	11.284	0.032	0.361
14354	11.284	0.032	0.361	14578	11.276	0.032	0.361
14355	11.298	0.032	0.362	14579	11.289	0.032	0.361
14356	11.331	0.032	0.363	14580	11.324	0.032	0.362
14357	11.383	0.032	0.364	14581	11.377	0.032	0.364
14358	11.454	0.032	0.367	14582	11.447	0.032	0.366
14359	11.549	0.032	0.370	14583	11.540	0.032	0.369
14360	11.675	0.032	0.374	14584	11.669	0.032	0.373
14361	11.848	0.032	0.379	14585	11.846	0.032	0.379
14362	12.115	0.032	0.388	14586	12.113	0.032	0.388
14363	12.586	0.032	0.403	14587	12.585	0.032	0.403
14364	13.522	0.032	0.433	14588	13.532	0.032	0.433
14365	15.554	0.032	0.498	14589	15.587	0.032	0.499
14380	19.877	0.030	0.588	14606	19.953	0.030	0.589
14381	29.832	0.030	0.882	14607	30.008	0.030	0.886
14438	61.588	0.032	1.971	14680	62.311	0.032	1.994
14439	131.572	0.016	2.105	14681	134.605	0.016	2.154
14440	258.260	0.008	2.066	14682	270.499	0.008	2.164
		0.883	19.115			0.883	19.317

Cavity: 3.9624m x 3.048m
Panel Size: 0.8829625
Coarse Grid: 0.032m
Panel Boundary: 0.00625cm start x 2expansion
Cold Wall Bound. 0.00625cm start x 2expansion
Wall Boundary   0.05cm start x 2 expansion
x-dir fill cell: 0.02948125
y-dir fill cell: 0.02028125
Gridrefinement: 2 times

Cell No	Heat Flux (W/m^2)	Width	Heat (W)
14790	5.955	0.032	0.191
14791	15.576	0.032	0.498
14792	16.510	0.032	0.528
14793	13.189	0.032	0.422
14794	12.332	0.032	0.395
14795	11.920	0.032	0.381
14796	11.682	0.032	0.374
14797	11.527	0.032	0.369
14798	11.418	0.032	0.365
14799	11.344	0.032	0.361
14800	11.289	0.032	0.360
14801	11.263	0.032	0.360
14802	11.266	0.032	0.361
14803	11.276	0.032	0.361
14804	11.305	0.032	0.362
14805	11.366	0.032	0.364
14806	11.434	0.032	0.366
14807	11.524	0.032	0.369
14808	11.653	0.032	0.373
14809	11.830	0.032	0.379
14810	12.097	0.032	0.387
14811	12.577	0.032	0.402
14812	13.534	0.032	0.433
14813	15.588	0.032	0.499
14832	19.969	0.029	0.589
14833	30.069	0.029	0.886
14924	62.637	0.032	2.004
14925	136.048	0.016	2.177
14926	276.454	0.008	2.212
		0.883	19.398

Cavity: 3.9624m x 3.048m
Panel Size: 0.88293125
Coarse Grid: 0.032
Panel Boundary: 0.003125cm start x 2expansion
Cold Wall Bound. 0.003125cm start x 2expansion
Wall Boundary   0.05cm start x 2 expansion
x-dir fill cell: 0.0294825
y-dir fill cell: 0.02028125
Gridrefinement: 2 times

Cell No	Heat Flux (W/m^2)	Width	Heat (W)
15014	5.926	0.032	0.190
15015	15.537	0.032	0.497
15015	16.465	0.032	0.527
15017	13.141	0.032	0.421
15018	12.303	0.032	0.394
15019	11.904	0.032	0.381
15020	11.646	0.032	0.373
15021	11.492	0.032	0.368
15022	11.389	0.032	0.364
15023	11.311	0.032	0.362
15024	11.260	0.032	0.360
15025	11.234	0.032	0.359
15026	11.234	0.032	0.359
15027	11.260	0.032	0.360
15028	11.298	0.032	0.362
15029	11.337	0.032	0.363
15030	11.402	0.032	0.365
15031	11.505	0.032	0.368
15032	11.633	0.032	0.372
15033	11.814	0.032	0.378
15034	12.084	0.032	0.387
15035	12.548	0.032	0.402
15036	13.489	0.032	0.432
15037	15.563	0.032	0.498
15058	19.956	0.029	0.588
15059	30.069	0.029	0.886
15170	62.766	0.032	2.009
15171	136.715	0.016	2.187
15172	279.318	0.008	2.235
		0.883	19.419

F.2   2D and 3D Model Validation

The data shown below was obtained from STAR-CD simulating the ASHVE test chamber. From the data obtained, the Nusselt, Grashof and Prandtl numbers were calculated and compared to the ASHVE test facility to validate the 2D test chamber model.

The same data below was used to approximate the actual 3D case. As explained in Chapter 4, the panel width was calculated when the Nusselt number change was below 1%. The areas highlighted are where the boundary was measured. The overall Nusselt number was calculated by taking the area weighted average.

Included in this Appendix are the numerical model results for a ceiling temperature at 318K. The University of Waterloo, Solar Lab can be contacted if the other panel temperature numerical model results are requested.

The following Excel Worksheet summarizes model validation for a panel temperature of 318K. Table F.1 summarizes the results from every panel temperature simulated.

Panel Temp = 318K

T_{air} (K)	297.81
T_{panel} (K)	318
T_{avg} (K)	307.90

Properties of Air @ T_{avg}

ρ (kg/m^3)	1.1351	h (W/m^{2}K)	0.2539
β (1/K)	0.0032		
k (W/mK)	0.0269	Nu	46.3706
μ (Ns/m^2)	1.88E-05	Gr	2.767E+11
C_p (J/kgK)	1007.3161	Pr	0.7056
L (m)	4.9102		

Air Temp measured at 5ft from bottom surface - cell # 13926

Cell #	q" (W/m^2)	Width (m)	q (W)
21080	197.4264	0.0080	1.5794
21081	96.2879	0.0160	1.5406
21090	46.8428	0.0219	1.0241

22931	24.5809	0.0320	0.7866
22932	13.5659	0.0320	0.4341
22933	8.9408	0.0320	0.2861
22934	6.7700	0.0320	0.2166
22935	5.6943	0.0320	0.1822
22936	5.1403	0.0320	0.1645
22937	4.8247	0.0320	0.1544
22938	4.6250	0.0320	0.1480
22939	4.4962	0.0320	0.1439
22940	4.4124	0.0320	0.1412
22941	4.3416	0.0320	0.1389
22942	4.2707	0.0320	0.1367
22943	4.2192	0.0320	0.1350
22944	4.1741	0.0320	0.1336
22945	4.1355	0.0320	0.1323
22946	4.1033	0.0320	0.1313
22947	4.0646	0.0320	0.1301
22948	4.0324	0.0320	0.1290
22949	4.0066	0.0320	0.1282
22950	3.9809	0.0320	0.1274
22951	3.9615	0.0320	0.1268
22952	3.9422	0.0320	0.1262
22953	3.9164	0.0320	0.1253
22954	3.8971	0.0320	0.1247
22955	3.8842	0.0320	0.1243
22956	3.8714	0.0320	0.1239
22957	3.8520	0.0320	0.1233
22958	3.8327	0.0320	0.1226
22959	3.8198	0.0320	0.1222
22960	3.8005	0.0320	0.1216
22961	3.7941	0.0320	0.1214
22962	3.7812	0.0320	0.1210
22963	3.7683	0.0320	0.1206
22964	3.7747	0.0320	0.1208
22965	3.7619	0.0320	0.1204
22966	3.7425	0.0320	0.1198
22967	3.7361	0.0320	0.1196
22968	3.7361	0.0320	0.1196
22969	3.7232	0.0320	0.1191
22970	3.7103	0.0320	0.1187
22971	3.7103	0.0320	0.1187
22972	3.6974	0.0320	0.1183
22973	3.6781	0.0320	0.1177
22974	3.6781	0.0320	0.1177
22975	3.6846	0.0320	0.1179
22976	3.6717	0.0320	0.1175
22977	3.6588	0.0320	0.1171
22978	3.6588	0.0320	0.1171
22979	3.6588	0.0320	0.1171
22980	3.6459	0.0320	0.1167

22981	3.6330	0.0320	0.1163
22982	3.6330	0.0320	0.1163
22983	3.6266	0.0320	0.1161
22984	3.6201	0.0320	0.1158
22985	3.6266	0.0320	0.1161
22986	3.6266	0.0320	0.1161
22987	3.6137	0.0320	0.1156
22988	3.6008	0.0320	0.1152
22989	3.5944	0.0320	0.1150
22990	3.5944	0.0320	0.1150
22991	3.5879	0.0320	0.1148
22992	3.5815	0.0320	0.1146
22993	3.5750	0.0320	0.1144
22994	3.5686	0.0320	0.1142
22995	3.5750	0.0320	0.1144
22996	3.5750	0.0320	0.1144
22997	3.5686	0.0320	0.1142
22998	3.5622	0.0320	0.1140
22999	3.5557	0.0320	0.1138
23000	3.5557	0.0320	0.1138
23001	3.5557	0.0320	0.1138
23002	3.5493	0.0320	0.1136
23003	3.5428	0.0320	0.1134
23004	3.5428	0.0320	0.1134
23005	3.5428	0.0320	0.1134
23006	3.5428	0.0320	0.1134
23007	3.5428	0.0320	0.1134
23008	3.5364	0.0320	0.1132
23009	3.5300	0.0320	0.1130
23010	3.5300	0.0320	0.1130
23011	3.5300	0.0320	0.1130
23012	3.5300	0.0320	0.1130
23013	3.5235	0.0320	0.1128
23014	3.5171	0.0320	0.1125
23015	3.5171	0.0320	0.1125
23016	3.5171	0.0320	0.1125
23017	3.5171	0.0320	0.1125
23018	3.5171	0.0320	0.1125
23019	3.5171	0.0320	0.1125
23020	3.5106	0.0320	0.1123
23021	3.5042	0.0320	0.1121
23022	3.5042	0.0320	0.1121
23023	3.5042	0.0320	0.1121
23024	3.5042	0.0320	0.1121
23025	3.5106	0.0320	0.1123
23026	3.5106	0.0320	0.1123
23027	3.5042	0.0320	0.1121
23028	3.5042	0.0320	0.1121
23029	3.4977	0.0320	0.1119
23030	3.4913	0.0320	0.1117

23031	3.4913	0.0320	0.1117
23032	3.4913	0.0320	0.1117
23033	3.4977	0.0320	0.1119
23034	3.4977	0.0320	0.1119
23035	3.4913	0.0320	0.1117
23036	3.4913	0.0320	0.1117
23037	3.4913	0.0320	0.1117
23038	3.4913	0.0320	0.1117
23039	3.4913	0.0320	0.1117
23040	3.4977	0.0320	0.1119
23041	3.5042	0.0320	0.1121
23042	3.5042	0.0320	0.1121
23043	3.4977	0.0320	0.1119
23044	3.4913	0.0320	0.1117
23045	3.4913	0.0320	0.1117
23046	3.4913	0.0320	0.1117
23047	3.4977	0.0320	0.1119
23048	3.4977	0.0320	0.1119
23049	3.4913	0.0320	0.1117
23050	3.4913	0.0320	0.1117
23051	3.4913	0.0320	0.1117
23052	3.4913	0.0320	0.1117
23053	3.4913	0.0320	0.1117
23054	3.4977	0.0320	0.1119
23055	3.4977	0.0320	0.1119
23056	3.4977	0.0320	0.1119
23057	3.4977	0.0320	0.1119
23058	3.4977	0.0320	0.1119
23059	3.4977	0.0320	0.1119
23060	3.4913	0.0320	0.1117
23061	3.4977	0.0320	0.1119
23062	3.4977	0.0320	0.1119
23063	3.4977	0.0320	0.1119
23064	3.5042	0.0320	0.1121
23065	3.5042	0.0320	0.1121
23066	3.5042	0.0320	0.1121
23067	3.5106	0.0320	0.1123
23068	3.5171	0.0320	0.1125
23069	3.5106	0.0320	0.1123
23070	3.5106	0.0320	0.1123
23071	3.5106	0.0320	0.1123
23072	3.5106	0.0320	0.1123
23073	3.5171	0.0320	0.1125
23074	3.5235	0.0320	0.1128
23075	3.5300	0.0320	0.1130
23076	3.5235	0.0320	0.1128
23077	3.5235	0.0320	0.1128
23078	3.5235	0.0320	0.1128
23079	3.5235	0.0320	0.1128
23080	3.5300	0.0320	0.1130

23081	3.5300	0.0320	0.1130
23082	3.5300	0.0320	0.1130
23083	3.5300	0.0320	0.1130
23084	3.5364	0.0320	0.1132
23085	3.5428	0.0320	0.1134
23086	3.5428	0.0320	0.1134
23087	3.5428	0.0320	0.1134
23088	3.5493	0.0320	0.1136
23089	3.5557	0.0320	0.1138
23090	3.5622	0.0320	0.1140
23091	3.5622	0.0320	0.1140
23092	3.5557	0.0320	0.1138
23093	3.5622	0.0320	0.1140
23094	3.5686	0.0320	0.1142
23095	3.5750	0.0320	0.1144
23096	3.5750	0.0320	0.1144
23097	3.5815	0.0320	0.1146
23098	3.5879	0.0320	0.1148
23099	3.5815	0.0320	0.1146
23100	3.5879	0.0320	0.1148
23101	3.5944	0.0320	0.1150
23102	3.6008	0.0320	0.1152
23103	3.6073	0.0320	0.1154
23104	3.6073	0.0320	0.1154
23105	3.6137	0.0320	0.1156
23106	3.6201	0.0320	0.1158
23107	3.6201	0.0320	0.1158
23108	3.6201	0.0320	0.1158
23109	3.6266	0.0320	0.1161
23110	3.6395	0.0320	0.1165
23111	3.6459	0.0320	0.1167
23112	3.6459	0.0320	0.1167
23113	3.6523	0.0320	0.1169
23114	3.6588	0.0320	0.1171
23115	3.6717	0.0320	0.1175
23116	3.6781	0.0320	0.1177
23117	3.6781	0.0320	0.1177
23118	3.6846	0.0320	0.1179
23119	3.6910	0.0320	0.1181
23120	3.7039	0.0320	0.1185
23121	3.7103	0.0320	0.1187
23122	3.7168	0.0320	0.1189
23123	3.7296	0.0320	0.1193
23124	3.7425	0.0320	0.1198
23125	3.7490	0.0320	0.1200
23126	3.7554	0.0320	0.1202
23127	3.7683	0.0320	0.1206
23128	3.7747	0.0320	0.1208
23129	3.7876	0.0320	0.1212
23130	3.8069	0.0320	0.1218

23131	3.8069	0.0320	0.1218
23132	3.8134	0.0320	0.1220
23133	3.8392	0.0320	0.1229
23134	3.8649	0.0320	0.1237
23135	3.8778	0.0320	0.1241
23136	3.8842	0.0320	0.1243
23137	3.9036	0.0320	0.1249
23138	3.9229	0.0320	0.1255
23139	3.9422	0.0320	0.1262
23140	3.9615	0.0320	0.1268
23141	3.9809	0.0320	0.1274
23142	4.0131	0.0320	0.1284
23143	4.0388	0.0320	0.1292
23144	4.0646	0.0320	0.1301
23145	4.0968	0.0320	0.1311
23146	4.1290	0.0320	0.1321
23147	4.1741	0.0320	0.1336
23148	4.2192	0.0320	0.1350
23149	4.2707	0.0320	0.1367
23150	4.3351	0.0320	0.1387
23151	4.4124	0.0320	0.1412
23152	4.5026	0.0320	0.1441
23153	4.6250	0.0320	0.1480
23154	4.8183	0.0320	0.1542
23155	5.1339	0.0320	0.1643
23156	5.6943	0.0320	0.1822
23157	6.7765	0.0320	0.2168
23158	8.9537	0.0320	0.2865
23159	13.5723	0.0320	0.4343
23160	24.5873	0.0320	0.7868
23169	46.8557	0.0219	1.0244
23242	96.3073	0.0160	1.5409
23243	197.4585	0.0080	1.5797
		7.4517	5.1269

Table F.1: Model Validation Results

Star CD Simulation

(2D Approx)

Panel Temp (K)	Nu	GrPr	log(Nu)	log(GrPr)
308	45.988	1.242E+11	1.663	11.094
318	46.368	1.952E+11	1.666	11.291
328	48.864	2.400E+11	1.689	11.380
338	48.645	2.876E+11	1.687	11.459
348	48.407	3.266E+11	1.685	11.514

(3D Approx)

Panel Temp (K)	Nu	GrPr	log(Nu)	log(GrPr)
308	63.784	1.242E+11	1.805	11.094
318	62.944	1.952E+11	1.799	11.291
328	65.449	2.400E+11	1.816	11.380
338	64.575	2.876E+11	1.810	11.459
348	63.832	3.266E+11	1.805	11.514

ASHVE Data

log(Nu)	log(GrPr)	Nu	GrPr
1.795	11.26	62.3734835	1.82E+11
1.66	11.275	45.708819	1.884E+11
1.71	11.365	51.2861384	2.317E+11
1.78	11.41	60.2559586	2.57E+11
1.81	11.415	64.5654229	2.6E+11
1.69	11.44	48.9778819	2.754E+11
1.77	11.52	58.8843655	3.311E+11
1.82	11.53	66.0693448	3.388E+11

F.3 Numerical Model Results

The numerical model results for the 0.25m panel size have been included. Results for the other panel sizes simulated can be obtained from the University of Waterloo, Solar Lab.

Panel Size = 0.25m, Temperature range from 318K to 363K

Panel Size:	0.2429625
T_{panel} (K)	318

Cell No	Heat Flux (W/m^2)	Width	Heat (W)
14810	10.799	0.032	0.346
14811	28.510	0.032	0.912
14812	31.032	0.032	0.993
14813	26.758	0.032	0.856
14832	28.980	0.029	0.854
14833	37.342	0.029	1.101
14924	67.630	0.032	2.164
14925	138.805	0.016	2.221
14926	277.884	0.008	2.223
		0.243	48.034

T_{air} (K)	290.51501

Panel Size:	0.2429625
T_{panel} (K)	323

Cell No	Heat Flux (W/m^2)	Width	Heat (W)
14810	12.719	0.032	0.407
14811	33.634	0.032	1.076
14812	36.668	0.032	1.173
14813	31.570	0.032	1.010
14832	33.931	0.029	1.000
14833	43.248	0.029	1.275
14924	77.665	0.032	2.485
14925	159.057	0.016	2.545
14926	318.401	0.008	2.547
		0.243	55.645

T_{air} (K)	290.55

Panel Size:	0.2429625
T_{panel} (K)	328

Cell No	Heat Flux (W/m^2)	Width	Heat (W)
14810	14.651	0.032	0.469
14811	38.794	0.032	1.241
14812	42.366	0.032	1.356
14813	36.440	0.032	1.166
14832	38.920	0.029	1.147
14833	49.181	0.029	1.450
14924	87.721	0.032	2.807
14925	179.377	0.016	2.870
14926	359.109	0.008	2.873
		0.243	63.299

T_{air} (K)	290.5801

Panel Size:	0.2429625
T_{panel} (K)	333

Cell No	Heat Flux (W/m^2)	Width	Heat (W)
14810	16.606	0.032	0.531
14811	43.980	0.032	1.407
14812	48.115	0.032	1.540
14813	41.387	0.032	1.324
14832	43.970	0.029	1.296
14833	55.159	0.029	1.626
14924	97.840	0.032	3.131
14925	199.803	0.016	3.197
14926	400.016	0.008	3.200
		0.243	71.011

T_{air} (K)	290.60623

Panel Size:	0.2429625
T_{panel} (K)	338

Cell No	Heat Flux (W/m^2)	Width	Heat (W)
14810	18.571	0.032	0.594
14811	49.181	0.032	1.574
14812	53.870	0.032	1.724
14813	46.334	0.032	1.483
14832	49.039	0.029	1.446
14833	61.156	0.029	1.803
14924	107.960	0.032	3.455
14925	220.275	0.016	3.524
14926	441.084	0.008	3.529
		0.243	78.741

T_{air} (K)	290.62942

Panel Size:	0.2429625
T_{panel} (K)	343

Cell No	Heat Flux (W/m^2)	Width	Heat (W)
14810	20.542	0.032	0.657
14811	54.441	0.032	1.742
14812	59.707	0.032	1.911
14813	51.358	0.032	1.643
14832	54.160	0.029	1.597
14833	67.179	0.029	1.981
14924	118.118	0.032	3.780
14925	240.833	0.016	3.853
14926	482.355	0.008	3.859
		0.243	86.526

T_{air} (K)	290.6503

Panel Size:	0.2429625
T_{panel} (K)	348

Cell No	Heat Flux (W/m^2)	Width	Heat (W)
14810	22.532	0.032	0.721
14811	59.739	0.032	1.912
14812	65.601	0.032	2.099
14813	56.441	0.032	1.806
14832	59.346	0.029	1.750
14833	73.259	0.029	2.160
14924	128.338	0.032	4.107
14925	261.491	0.016	4.184
14926	523.815	0.008	4.191
		0.243	94.371

T_{air} (K)	290.6712

Panel Size:	0.2429625
T_{panel} (K)	353

Cell No	Heat Flux (W/m^2)	Width	Heat (W)
14810	24.533	0.032	0.785
14811	65.092	0.032	2.083
14812	71.562	0.032	2.290
14813	61.587	0.032	1.971
14832	64.583	0.029	1.904
14833	79.392	0.029	2.341
14924	138.618	0.032	4.436
14925	282.242	0.016	4.516
14926	565.473	0.008	4.524
		0.243	102.274

T_{air} (K)	290.6936

Panel Size:	0.2429625
T_{panel} (K)	358

Cell No	Heat Flux (W/m^2)	Width	Heat (W)
14810	26.549	0.032	0.850
14811	70.499	0.032	2.256
14812	77.595	0.032	2.483
14813	66.812	0.032	2.138
14832	69.903	0.029	2.061
14833	85.589	0.029	2.523
14924	148.938	0.032	4.766
14925	303.080	0.016	4.849
14926	607.320	0.008	4.859
		0.243	110.241

T_{air} (K)	290.71652

Panel Size:	0.2429625
T_{panel} (K)	363

Cell No	Heat Flux (W/m^2)	Width	Heat (W)
14810	28.581	0.032	0.915
14811	75.952	0.032	2.430
14812	83.688	0.032	2.678
14813	72.068	0.032	2.306
14832	75.243	0.029	2.218
14833	91.824	0.029	2.707
14924	159.315	0.032	5.098
14925	324.002	0.016	5.184
14926	649.332	0.008	5.195
		0.243	118.254

T_{air} (K)	290.7379

Appendix G

Methodology to Determine the Convective Heat Transfer Coefficient

G.1 Deriving the Correlation to Predict the Convective heat Flux versus Panel Temperature, Air Temperature and Panel Size

As shown in Figure G.1, the convective heat flux versus temperature difference follows a fairly linear equation.
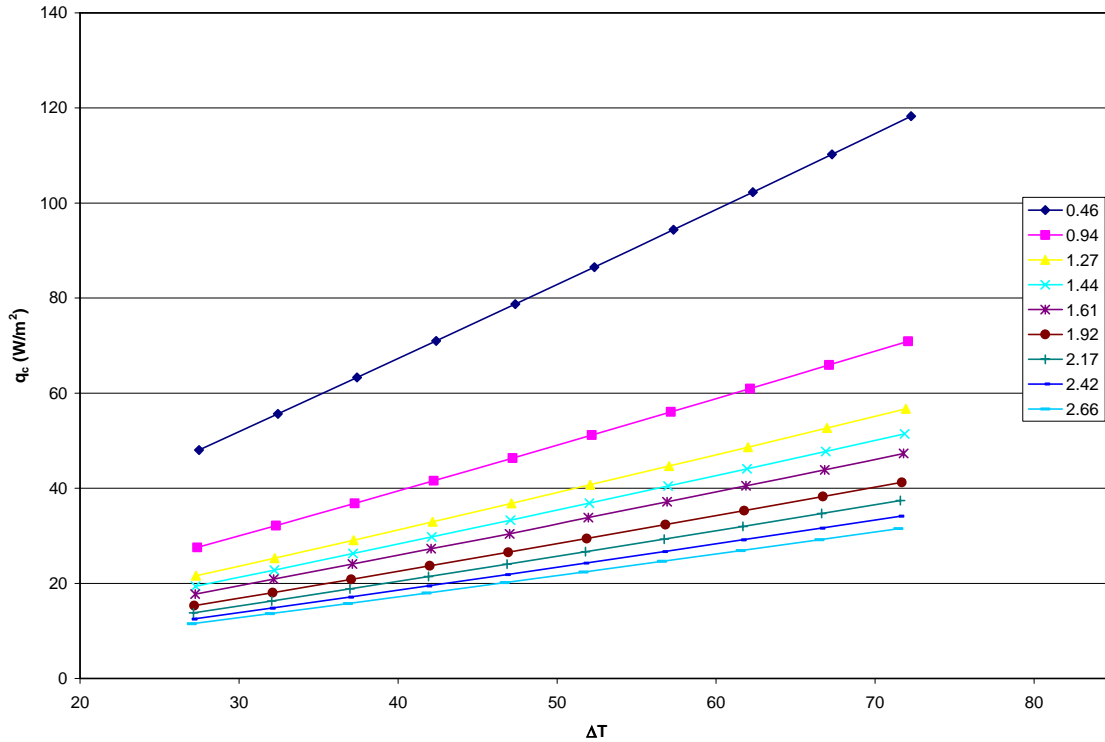
Figure G.1: Convective Heat Flux versus Panel minus Air Temperature for Various Panel Sizes

A correlation for each panel size could be written of the form:

$$q_c = A(T_p - T_a) + B \tag{G.1}$$

For the smallest panel size, a linear fit gives the following equation, with an r-squared value of 0.9999:

$$q_c = 1.5674(T_p - T_a) + 4.6821 \tag{G.2}$$

For the largest panel size, the linear fit gives the following equation with an r-squared value of 0.9999:

$$q_c = 0.4509(T_p - T_a) - 0.8476 \tag{G.3}$$

The A, B and r-squared values were obtained from applying a linear fit to each curve in Figure G.1 in excel.

From these equations it can be seen that the A and B coefficients vary significantly with panel size. With two coefficients dependant on panel size, the correlated equation can be very large and complex to use. To simplify, the heat flux plots in Figure I.1 could be correlated using an equation of the form:

$$q_c = A(T_p - T_a)^B \tag{G.4}$$

Applying the power fit to each panel size, there is a minor change in coefficient "B". Coefficient "A" and "B" would be correlated with the characteristic length for each panel to ensure an accurate fit is obtained. Table I.1 below summarizes the coefficients for the power fit for each panel size. The r-squared value varies from 0.9997 to 1 for each equation, showing that the fit accurately predicts the simulated heat flux values. Although coefficient B does not vary greatly over the panel sizes, since it is an exponent to the temperature difference, it will also be correlated to the effective panel diameter.

Table G.1: Coefficients for power law fit to each panel size simulated

Characteristic Length (m)	A	B
0.4579	2.1603	0.9334
0.9364	1.0709	0.9787
1.2683	0.7876	0.999
1.4441	0.6887	1.0078
1.6109	0.6155	1.0148
1.9200	0.5153	1.0249
2.1667	0.4559	1.0311
2.4248	0.407	1.0362
2.6609	0.3706	1.0399

Equation G.4 predicts the convective heat flux, knowing the panel to air temperature difference. However, for each panel size a different correlation is required. To include the effects of panel size in the heat flux correlation, coefficient A was plotted against the effective panel diameter (Figure G.2). From power fit trend line has been added to the plot, to show coefficient A can be approximated with an equation of the form:

$$A = FD_e^{\ G} \tag{G.5}$$
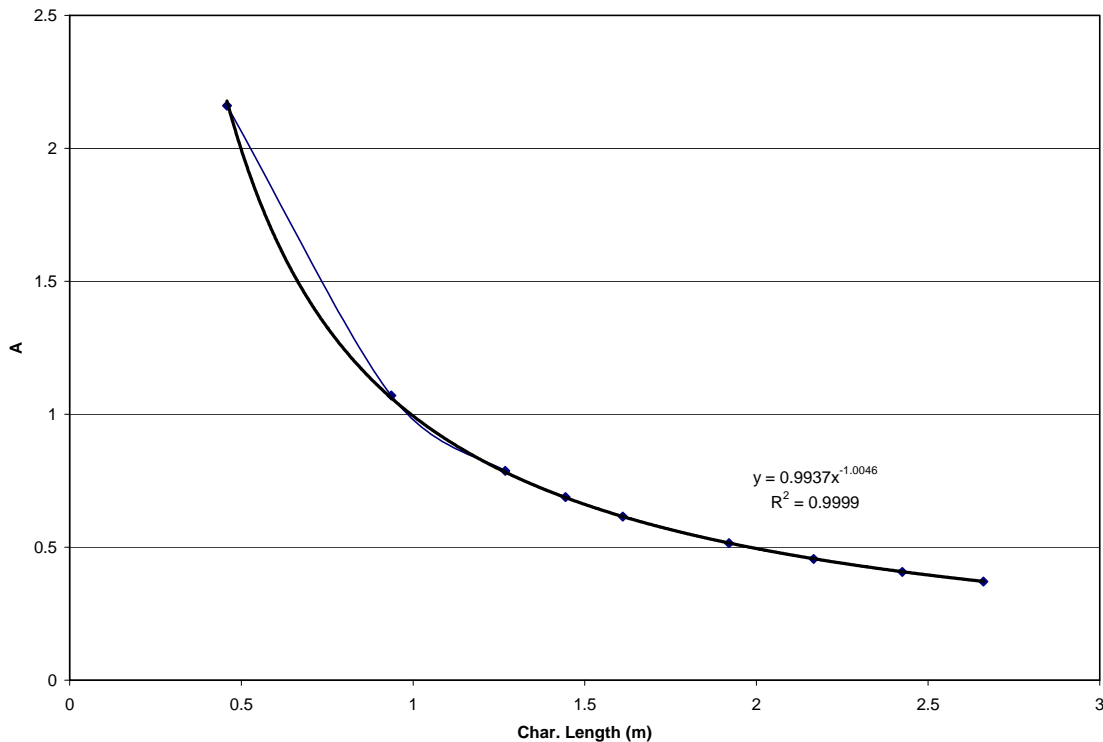
Figure G.2: Coefficient A versus Characteristic Length

Coefficient B was similarly plotted versus the panel characteristic length and is shown in Figure G.3. From a logarithmic fit to the curve, coefficient B can be correlated of the form:

$$B = H \ln(D_e) + K \tag{G.6}$$

194

y = 0.0615Ln(x) + 0.9832
R^2 = 0.9966
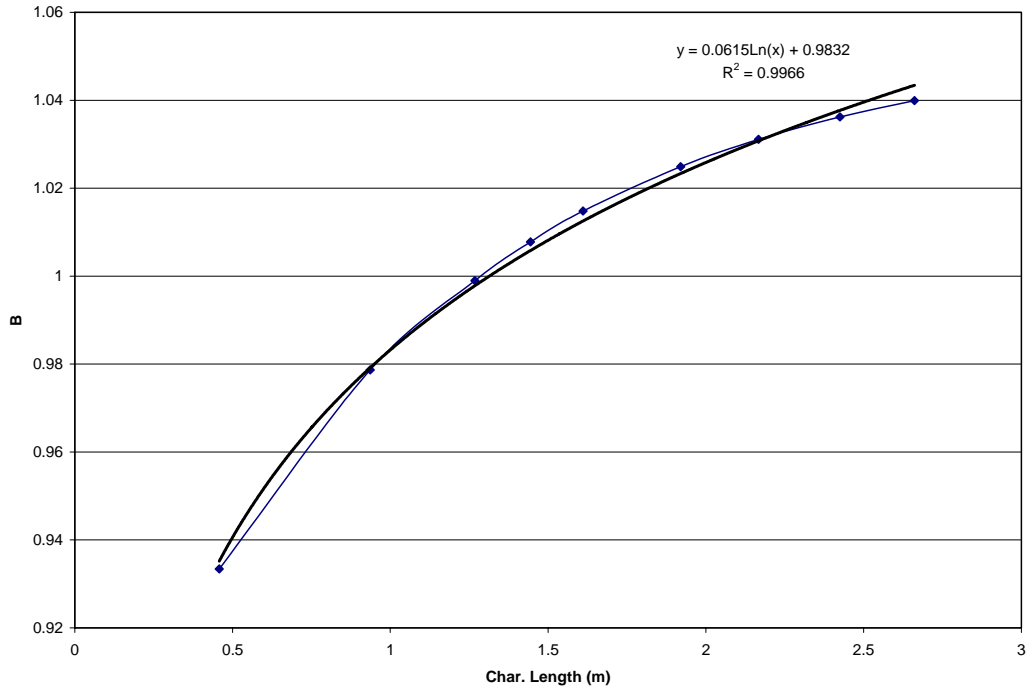
Figure G.3: Coefficient B versus Panel Characteristic Length

Combining the Equations G.4, G.5 and G.6, the convective heat flux can be approximated with the following equation:

$$q_c = \frac{0.9937}{D_e^{1.0046}}(T_p - T_a)^{0.0615\ln(D_e)+0.9832} \tag{G.7}$$

The correlation coefficient, r, is derived in excel below. The r-value was found to equal 0.9997. The r-value was found as follows:

- The numerical model convective heat fluxes was averaged, q_{cbar}

- $(q_{corr} - q_c)^2$ was done for each correlated value

- $(q_c - q_{cbar})^2$ was done for each value

- $r^2 = 1 - \dfrac{\sum (q_{corr} - q_c)^2}{\sum (q_c - q_{cbar})^2}$

q_c (W/m^2)	Corr. q_c (W/m^2)	$(q_{corr} - q_c)^2$	$(q_c - q_{cbar})^2$
48.0343448	47.49408413	0.29188163	114.025585
27.5344097	26.75727848	0.60393292	96.4649819
21.58106	20.97992157	0.36136737	248.850894
19.3982283	18.90534012	0.24293878	322.484024
17.7186353	17.31884243	0.15983432	385.628784
15.2840369	15.0449067	0.05718325	487.174579
13.7715147	13.65524774	0.01351802	556.231176
12.4679728	12.47646354	7.2093E-05	619.417309
11.4643155	11.58090772	0.01359374	670.382872
55.645184	55.67254824	0.0007488	334.491745
32.1618075	31.60025245	0.31534406	26.9803475
25.3114105	24.8558679	0.20751909	145.073786
22.8048258	22.42842477	0.14167776	211.738663
20.8642779	20.5697556	0.08674339	271.979157
18.044505	17.90178272	0.02036965	372.936484
16.2838043	16.26877287	0.00022594	444.040319
14.7654064	14.88187297	0.01356447	510.338016
13.5920565	13.82707112	0.05523186	564.728265
63.2991491	63.76821881	0.22002639	673.043431
36.8382168	36.42741794	0.16875572	0.26817036
29.0958423	28.73048641	0.13348493	68.2313369
26.2552171	25.95471754	0.09029999	123.228902
24.0519872	23.82706237	0.05059116	176.99858
20.8407772	20.76912914	0.00513345	272.754846
18.8290705	18.89493683	0.00433838	343.249656
17.0914663	17.30154145	0.04413159	410.654105
15.7438274	16.0885752	0.11885107	467.088967
71.0114066	71.79303613	0.6109448	1132.68178
41.5691786	41.24096713	0.10772274	17.7502964
32.9322096	32.60395809	0.10774903	19.570528
29.7524857	29.48378437	0.07220042	57.8144712
27.2809515	27.08990315	0.03649949	101.507982
23.6705121	23.64555263	0.00062297	187.294454
21.4074076	21.5320697	0.01554065	254.359786
19.4449196	19.73359756	0.08333494	320.809253
17.9245505	18.36341775	0.19260445	377.583892
78.7408514	79.7559929	1.03051223	1712.70026
46.3510059	46.04256115	0.09513818	80.9088992
36.8063976	36.47642044	0.10888495	0.30213806
33.283743	33.01529514	0.07206423	16.5838354
30.4163693	30.35762358	0.00345106	48.1594247
26.5287303	26.52999092	1.589E-06	117.231252
24.0122242	24.17889702	0.02777983	178.058181
21.8254461	22.1766117	0.12331728	241.200233
20.1312888	20.65006804	0.26913191	296.693036
86.5264597	87.6641007	1.29422712	2417.72737
51.1837016	50.83350212	0.12263971	191.203438
40.7206672	40.34798151	0.13889459	11.3205241
36.8540735	36.54899025	0.09307576	0.25199903

33.8397279	33.62970864	0.04410809	12.3646512
29.4225516	29.42160687	8.9246E-07	62.9406909
26.642505	26.8344135	0.03682888	114.780443
24.2328154	24.62945524	0.15732318	172.219773
22.3649537	22.9473168	0.33914676	224.733523
94.3707132	95.52297619	1.32771001	3250.66971
56.058807	55.61483806	0.19710845	349.792428
44.670012	44.2187284	0.20365687	53.4937691
40.4535676	40.08466014	0.13609268	9.59450037
37.1643415	36.9057423	0.06687355	0.03675924
32.3367425	32.31972344	0.00028965	25.1936339
29.2986896	29.4978055	0.03964713	64.9213543
26.6630323	27.09121403	0.1833396	114.341024
24.6136783	25.25418392	0.41024745	162.368508
102.27402	103.3372174	1.13038851	4214.34043
60.9762858	60.38743062	0.34675046	557.914666
48.6519179	48.08873289	0.31717736	127.596214
44.0829405	43.62213208	0.21234439	45.2508068
40.5133683	40.18538141	0.10757538	9.96854181
35.2770316	35.22378163	0.00283555	4.32239465
31.9829759	32.16840069	0.03438237	28.8701247
29.1182223	29.5611322	0.19616918	67.8621101
26.888144	27.56985856	0.46473476	109.577444
110.241258	111.1106558	0.75585232	5312.25087
65.9296746	65.15200063	0.60477687	816.450968
52.6670041	51.95805511	0.50260865	234.424748
47.7406751	47.16126123	0.33572047	107.840055
43.8954314	43.46833807	0.18240875	42.7632676
38.2420266	38.13331194	0.01181888	0.78492175
34.6855095	34.84563406	0.02563989	7.13188561
31.5879681	32.03857414	0.20304578	33.270982
29.1791144	29.89365851	0.51057329	66.8625784
118.254403	118.8465324	0.35061675	6544.54059
70.916762	69.90915997	1.01526179	1126.32015
56.710873	55.82674617	0.78168018	374.608456
51.4292078	50.70192437	0.52894123	198.05325
47.301616	46.7543672	0.29948123	98.9139146
41.2349453	41.04791439	0.03498057	15.0456855
37.4126359	37.52902397	0.01354619	0.00319987
34.0813323	34.52299769	0.19506831	10.7238972
31.4907539	32.22500166	0.5391198	34.4019156

37.3560685
0.99949712
0.99974853

G.2 Deriving the Correlation to Predict the Convective heat Flux versus Panel Temperature, Air Temperature and Panel Size

To develop an equation used to predict the natural convective heat flux with respect to the radiant panel to ceiling ratio, a similar derivation to Equation G.7 can be done. Assuming the power fit curve similar to the previous derivation, coefficients A and B were determined from Figure G.1 for various aspect ratios simulated. The coefficients are summarized in Table G.2 below.

Table G.2: Coefficients for power law fit to each aspect ratio simulated

Aspect Ratio	A	B
0.0613	2.1603	0.9334
0.1340	1.0709	0.9787
0.1905	0.7876	0.999
0.2228	0.6887	1.0078
0.2551	0.6155	1.0148
0.3197	0.5153	1.0249
0.3763	0.4559	1.0311
0.4409	0.407	1.0362
0.5055	0.3706	1.0399

Coefficients A and B are then plotted (Figure G.4 and G.5) versus the aspect ratios and correlated to give the following equations:

$$A = \frac{0.201}{AR^{0.8375}}$$

(G.8)

$$B = 0.0511\ln(AR) + 1.0808$$

(G.9)
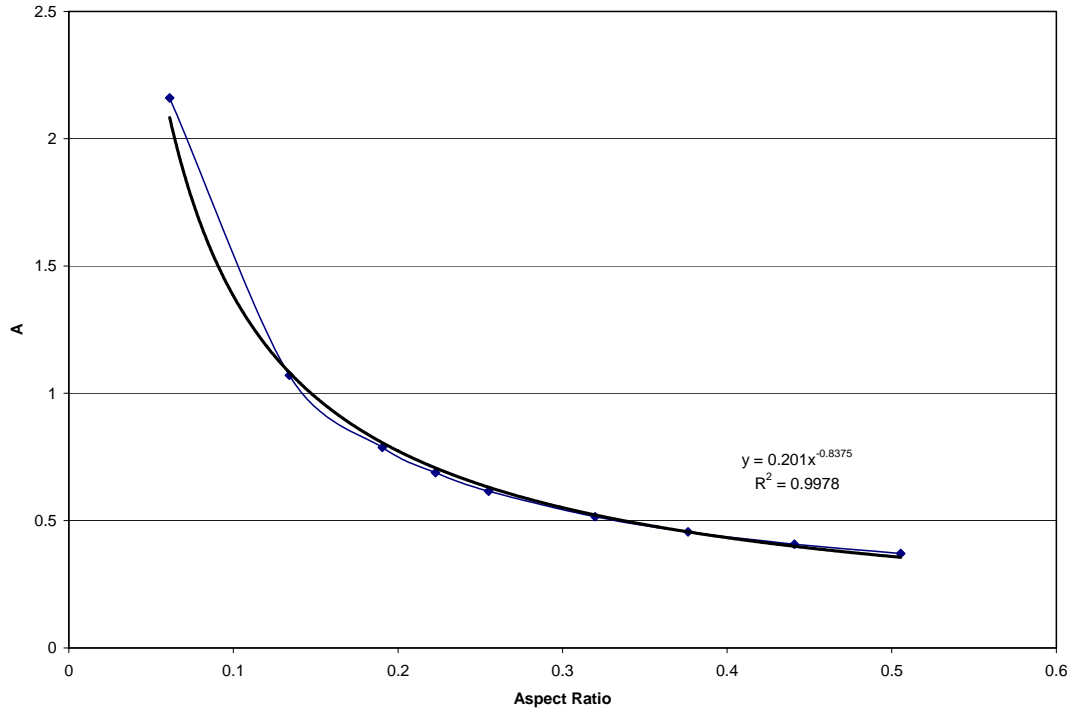
Figure G.4: Coefficient A versus AR

In Figure G.4, the fitted curve equation is:

$$y = 0.201x^{-0.8375}$$
$$R^2 = 0.9978$$
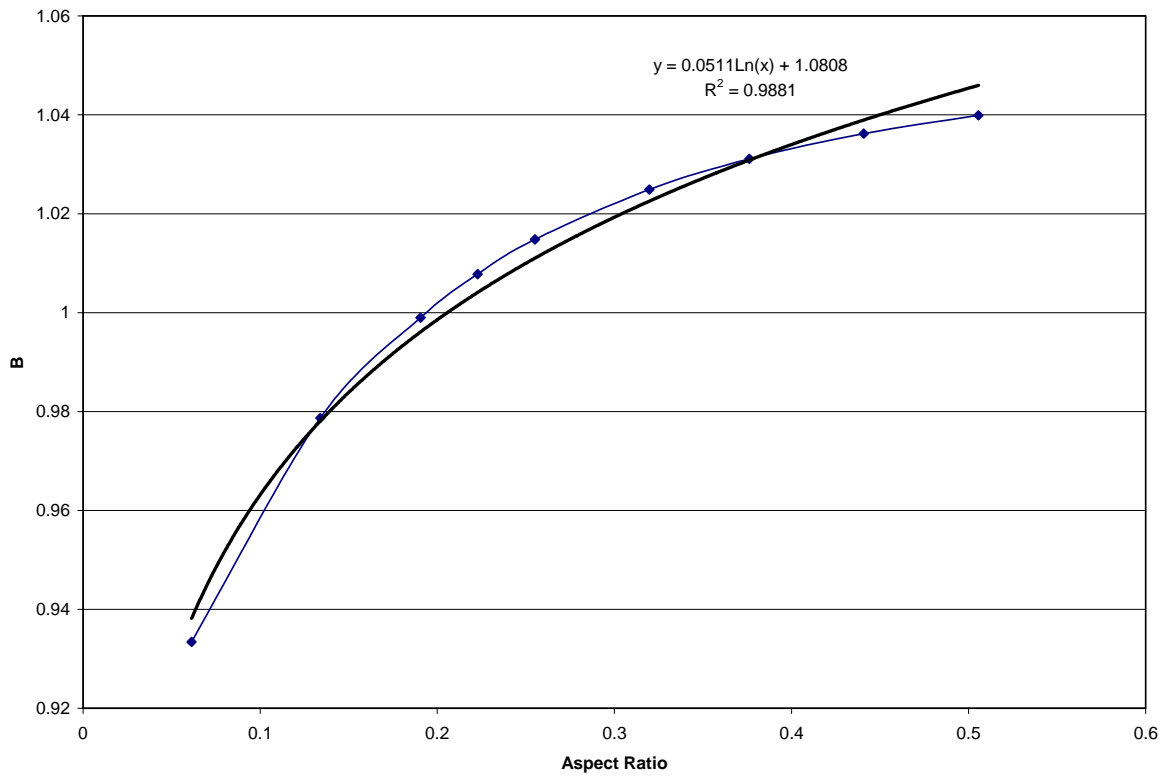
Figure G.5: Coefficient B versus Aspect Ratio

In Figure G.5, the fitted curve equation is:

$$y = 0.0511\ln(x) + 1.0808$$
$$R^2 = 0.9881$$

Combining Equations G.4, G.8 and G.9, the convective heat flux can be approximated using the following correlation:

$$q_c = \frac{0.201}{AR^{0.8375}} (T_{panel} - T_{air})^{0.0511\ln(AR)+1.0808}$$

(G.10)

The correlation coefficient for Equation G.10 is equal to the one found for Equation G.7, since similar coefficients were used for the correlation derivation.

Appendix H

Effects of Panel Insulation on Panel Performance

The Excel sheet below summarizes the effects of insulation thickness on the overall heat transfer coefficient

Insulation Detail	Panel Temp (°C)	Enclosure Wall Temp (°C)	Enclosure Cold Wall Temp (°C)	Enclosure Air Temp (°C)	h_r (W/m²K)	h_c (W/m²K)	h_{bl} (W/m²K)	U_L (W/m²K)
k=0.04W/mK	90	20	10	20	7.473	0.888	1.575	9.936
t=0.0254m	85	20	10	20	7.325	0.889	1.575	9.789
	75	20	10	20	7.052	0.891	1.575	9.518
	65	20	10	20	6.820	0.893	1.575	9.288
	55	20	10	20	6.652	0.896	1.575	9.123
	45	20	10	20	6.608	0.900	1.575	9.083
k=0.04W/mK	90	20	10	20	7.473	0.888	3.150	11.511
t=0.0127m	85	20	10	20	7.325	0.889	3.150	11.363
	75	20	10	20	7.052	0.891	3.150	11.093
	65	20	10	20	6.820	0.893	3.150	10.863
	55	20	10	20	6.652	0.896	3.150	10.698
	45	20	10	20	6.608	0.900	3.150	10.658
k=0.04W/mK	90	20	10	20	7.473	0.888	6.299	14.660
t=0.00635m	85	20	10	20	7.325	0.889	6.299	14.513
	75	20	10	20	7.052	0.891	6.299	14.242
	65	20	10	20	6.820	0.893	6.299	14.013
	55	20	10	20	6.652	0.896	6.299	13.847
	45	20	10	20	6.608	0.900	6.299	13.808
k=0.04W/mK	90	20	10	20	7.473	0.888	12.598	20.959
t=0.003175m	85	20	10	20	7.325	0.889	12.598	20.812
	75	20	10	20	7.052	0.891	12.598	20.541
	65	20	10	20	6.820	0.893	12.598	20.312
	55	20	10	20	6.652	0.896	12.598	20.147
	45	20	10	20	6.608	0.900	12.598	20.107
k=0.04W/mK	90	20	10	20	7.473	0.888	0.000	8.361
t=infinite	85	20	10	20	7.325	0.889	0.000	8.214
	75	20	10	20	7.052	0.891	0.000	7.943
	65	20	10	20	6.820	0.893	0.000	7.713
	55	20	10	20	6.652	0.896	0.000	7.548
	45	20	10	20	6.608	0.900	0.000	7.508

Appendix I

Reverse Solar Collector Model Panel Temperature and Panel Heat Output Results

I.1 Reverse Solar Collector Model Results

The Reverse Solar Collector Model was run for at the experimental inlet fluid temperatures for the 24-4 panel and 24-8 panel. The results are shown below. The complete results are summarized in Table I.1.

RSC Model for 24-4 Panel

Radiant Panel Variables:

Enclosure Dimensions:

Length (m)	3.9624
Width (m)	3.9624
Height (m)	3.048
Emmisivity	0.885

View Factors

Panel to Floor	0.238
Panel to Side Walls	0.306
Panel to Front Wall	0.057
Panel to Back Wall	0.401

Radiant Panel Dimensions

Length (m)	3.9624	(13 ft)
Width (m)	0.6096	(2.0 ft)
Thickness (m)	0.002	
Char Length (m)	1.05664	

Radiant Panel Details

# of Tubes	4	
Flow Rate (USGal/min, kg/s)	0.9	0.056782
Tube Spacing (in, m)	6	0.1524
Outer Tube Diameter (in, m)	0.625	0.015875
Innner Tube Diameter (in, m)	0.585	0.014859
k_{panel} (W/mK)	221	

Panel Insulation

k (W/mK)	0.08	
Thickness (m)	0.0127	1/2in

Bond Conductance

k (W/mK)	1.5
Thickness (m)	0.0009
Width (m)	0.0167

Fluid Inlet Temp ($^{\circ}$C)	Panel Temp ($^{\circ}$C) (Estimate)	Enclosure Wall Temp ($^{\circ}$C)	Enclosure Cold Wall Temp ($^{\circ}$C)	Enclosure Air Temp ($^{\circ}$C)	h_r (W/m^{2}K)	h_c (W/m^{2}K)	U_L (W/m^{2}K)	C_b (W/mK)	F	Re_D	Nu_D	k_{water} (W/mK)	h_{fi} (W/m^{2}K)	F'	Outlet Fluid Temp ($^{\circ}$C)	F_R	q_{panel} (W/m)	Panel Temp ($^{\circ}$C) (Calculated)
51.78	50	20	12	20.93	6.689833	0.898651	13.8877	27.833	0.9539	13822	68.297	0.67	3079.565	0.882	48.1637	0.829	216.562587	46.51045493
51.78	46.510455	20	12	20.93	6.695141	0.900193	13.89455	27.833	0.9539	13822	68.297	0.67	3079.565	0.8819	48.1622	0.829	216.6511	46.50829274
51.78	46.508293	20	12	20.93	6.695154	0.900194	13.89456	27.833	0.9539	13822	68.297	0.67	3079.565	0.8819	48.1622	0.829	216.651279	46.50828835
51.78	46.508288	20	12	20.93	6.695154	0.900194	13.89456	27.833	0.9539	13822	68.297	0.67	3079.565	0.8819	48.1622	0.829	216.65128	46.50828834
51.78	46.508288	20	12	20.93	6.695154	0.900194	13.89456	27.833	0.9539	13822	68.297	0.67	3079.565	0.8819	48.1622	0.829	216.65128	46.50828834
61.35	57	20	12	18.94	6.393897	0.895409	13.58852	27.833	0.9548	13822	68.297	0.67	3079.565	0.8842	56.4677	0.832	292.377936	54.236165
61.35	54.236165	20	12	18.94	6.337142	0.896315	13.53267	27.833	0.955	13822	68.297	0.67	3079.565	0.8846	56.4844	0.833	291.37778	54.2605932
61.35	54.260593	20	12	18.94	6.337622	0.896306	13.53314	27.833	0.955	13822	68.297	0.67	3079.565	0.8846	56.4843	0.833	291.386217	54.26038713
61.35	54.260387	20	12	18.94	6.337618	0.896306	13.53314	27.833	0.955	13822	68.297	0.67	3079.565	0.8846	56.4843	0.833	291.386146	54.26038886
61.35	54.260389	20	12	18.94	6.337618	0.896306	13.53314	27.833	0.955	13822	68.297	0.67	3079.565	0.8846	56.4843	0.833	291.386147	54.26038885
73.91	70	20	12	20.27	6.892219	0.892203	14.08363	27.833	0.9533	13822	68.297	0.67	3079.565	0.8805	67.5489	0.827	380.936662	64.64037238
73.91	64.640372	20	12	20.27	6.769648	0.893568	13.96243	27.833	0.9537	13822	68.297	0.67	3079.565	0.8814	67.5942	0.828	378.222605	64.7066752
73.91	64.706675	20	12	20.27	6.771071	0.893551	13.96383	27.833	0.9537	13822	68.297	0.67	3079.565	0.8814	67.5937	0.828	378.254117	64.70590539
73.91	64.705905	20	12	20.27	6.771054	0.893551	13.96382	27.833	0.9537	13822	68.297	0.67	3079.565	0.8814	67.5937	0.828	378.253751	64.70591434
73.91	64.705914	20	12	20.27	6.771054	0.893551	13.96382	27.833	0.9537	13822	68.297	0.67	3079.565	0.8814	67.5937	0.828	378.253755	64.70591424
86.66	80	20	12	19.3	7.039643	0.889821	14.22868	27.833	0.9528	13822	68.297	0.67	3079.565	0.8794	78.604	0.826	482.437496	74.92007913
86.66	74.920079	20	12	19.3	6.893945	0.890864	14.08402	27.833	0.9533	13822	68.297	0.67	3079.565	0.8805	78.6717	0.827	478.383246	75.01912792
86.66	75.019128	20	12	19.3	6.896714	0.890843	14.08677	27.833	0.9533	13822	68.297	0.67	3079.565	0.8805	78.6704	0.827	478.460394	75.01724317
86.66	75.017243	20	12	19.3	6.896661	0.890844	14.08672	27.833	0.9533	13822	68.297	0.67	3079.565	0.8805	78.6704	0.827	478.458926	75.01727906
86.66	75.017279	20	12	19.3	6.896662	0.890844	14.08672	27.833	0.9533	13822	68.297	0.67	3079.565	0.8805	78.6704	0.827	478.458954	75.01727837
100.4	90	19.26	12.61	19.57	7.38867	0.888048	14.57593	27.833	0.9517	13822	68.297	0.67	3079.565	0.8768	90.5392	0.822	590.518953	86.02881296
100.4	86.028813	19.26	12.61	19.57	7.266181	0.88874	14.45413	27.833	0.9521	13822	68.297	0.67	3079.565	0.8777	90.607	0.823	586.458718	86.12802344
100.4	86.128023	19.26	12.61	19.57	7.269194	0.888722	14.45713	27.833	0.9521	13822	68.297	0.67	3079.565	0.8777	90.6053	0.823	586.558698	86.12558053
100.4	86.125581	19.26	12.61	19.57	7.26912	0.888722	14.45705	27.833	0.9521	13822	68.297	0.67	3079.565	0.8777	90.6054	0.823	586.556235	86.12564071
100.4	86.125641	19.26	12.61	19.57	7.269122	0.888722	14.45706	27.833	0.9521	13822	68.297	0.67	3079.565	0.8777	90.6054	0.823	586.556296	86.12563922

24-8 RSC Model

Radiant Panel Variables:

Enclosure Dimensions:

Length (m)	3.9624
Width (m)	3.9624
Height (m)	3.048
Emmisivity	0.885

View Factors

Panel to Floor	0.238
Panel to Side Walls	0.306
Panel to Front Wall	0.057
Panel to Back Wall	0.401

Radiant Panel Dimensions

Length (m)	3.9624	(13 ft)
Width (m)	0.6096	(2.0 ft)
Thickness (m)	0.002	
Char Length (m)	1.05664	

Radiant Panel Details

# of Tubes	8	
Flow Rate (USGal/min, kg/s)	0.9	0.056782
Tube Spacing (in, m)	3	0.0762
Outer Tube Diameter (in, m)	0.625	0.015875
Innner Tube Diameter (in, m)	0.585	0.014859
k_{panel} (W/mK)	221	

Panel Insulation

k (W/mK)	0.08	
Thickness (m)	0.0127	1/2in

Bond Conductance

k (W/mK)	1.5
Thickness (m)	0.0013
Width (m)	0.0167

Inlet Fluid Temp (°C)	Panel Temp (°C) (Estimate)	Enclosure Wall Temp (°C)	Enclosure Cold Wall Temp (°C)	Enclosure Air Temp (°C)	h_r (W/m²K)	h_c (W/m²K)	U_L (W/m²K)	C_b (W/mK)	F	Re_D	Nu_D	k_{water} (W/mK)	h_{fi} (W/m²K)	F'	Outlet Fluid Temp (°C)	F_R	q_{panel} (W/m)	Panel Temp (°C) (Calculated)
51.96	50	20	12	20.13	6.51066108	0.89832346	13.7081971	19.269231	0.9907	13822	68.297	0.67	3079.565	0.9355	48.06447	0.8771	233.286	48.04662274
51.96	48.046623	20	12	20.13	6.49751029	0.89913867	13.6958616	19.269231	0.9907	13822	68.297	0.67	3079.565	0.9356	48.06754	0.8772	233.102	48.04974227
51.96	48.049742	20	12	20.13	6.49752598	0.89913732	13.6958759	19.269231	0.9907	13822	68.297	0.67	3079.565	0.9356	48.06754	0.8772	233.102	48.04973864
51.96	48.049739	20	12	20.13	6.49752596	0.89913733	13.6958759	19.269231	0.9907	13822	68.297	0.67	3079.565	0.9356	48.06754	0.8772	233.102	48.04973865
51.96	48.049739	20	12	20.13	6.49752596	0.89913733	13.6958759	19.269231	0.9907	13822	68.297	0.67	3079.565	0.9356	48.06754	0.8772	233.102	48.04973865
62.77	60	20	12	19.99	6.63020968	0.89480901	13.8242313	19.269231	0.9906	13822	68.297	0.67	3079.565	0.935	57.49558	0.8761	315.862	57.47096592
62.77	57.470966	20	12	19.99	6.58345046	0.89559297	13.778256	19.269231	0.9907	13822	68.297	0.67	3079.565	0.9352	57.51093	0.8765	314.942	57.48656632
62.77	57.486566	20	12	19.99	6.58372369	0.89558797	13.7785243	19.269231	0.9907	13822	68.297	0.67	3079.565	0.9352	57.51084	0.8765	314.947	57.48647527
62.77	57.486475	20	12	19.99	6.58372209	0.895588	13.7785227	19.269231	0.9907	13822	68.297	0.67	3079.565	0.9352	57.51084	0.8765	314.947	57.4864758
62.77	57.486476	20	12	19.99	6.5837221	0.895588	13.7785227	19.269231	0.9907	13822	68.297	0.67	3079.565	0.9352	57.51084	0.8765	314.947	57.48647579
73.71	70	20	12	20.52	6.9270421	0.89226318	14.1185179	19.269231	0.9904	13822	68.297	0.67	3079.565	0.9337	67.0303	0.8738	400.017	66.99770586
73.71	66.997706	20	12	20.52	6.85844084	0.89301256	14.050666	19.269231	0.9905	13822	68.297	0.67	3079.565	0.934	67.05833	0.8743	398.339	67.02619643
73.71	67.026196	20	12	20.52	6.85906972	0.89300522	14.0512875	19.269231	0.9905	13822	68.297	0.67	3079.565	0.934	67.05807	0.8743	398.354	67.0259353
73.71	67.025935	20	12	20.52	6.85906395	0.89300529	14.0512818	19.269231	0.9905	13822	68.297	0.67	3079.565	0.934	67.05807	0.8743	398.354	67.0259377
73.71	67.025938	20	12	20.52	6.85906401	0.89300529	14.0512819	19.269231	0.9905	13822	68.297	0.67	3079.565	0.934	67.05807	0.8743	398.354	67.02593768
86.11	85	20	12	21.01	7.38193795	0.88919112	14.5703417	19.269231	0.9901	13822	68.297	0.67	3079.565	0.9318	77.70728	0.8703	503.201	77.66353458
86.11	77.663535	20	12	21.01	7.18215049	0.89064451	14.3720076	19.269231	0.9903	13822	68.297	0.67	3079.565	0.9326	77.80684	0.8718	497.239	77.76480496
86.11	77.764805	20	12	21.01	7.18477541	0.89062318	14.3746112	19.269231	0.9903	13822	68.297	0.67	3079.565	0.9326	77.80553	0.8718	497.317	77.76347338
86.11	77.763473	20	12	21.01	7.18474087	0.89062346	14.3745769	19.269231	0.9903	13822	68.297	0.67	3079.565	0.9326	77.80555	0.8718	497.316	77.7634909
86.11	77.763491	20	12	21.01	7.18474132	0.89062346	14.3745774	19.269231	0.9903	13822	68.297	0.67	3079.565	0.9326	77.80555	0.8718	497.316	77.76349067
99.66	95	20	12	21.68	7.75145856	0.88756945	14.9382406	19.269231	0.9899	13822	68.297	0.67	3079.565	0.9302	89.37472	0.8674	615.939	89.31844784
99.66	89.318448	20	12	21.68	7.58209803	0.8885301	14.7698407	19.269231	0.99	13822	68.297	0.67	3079.565	0.9309	89.47528	0.8687	609.917	89.42079082
99.66	89.420791	20	12	21.68	7.58506351	0.88851208	14.7727882	19.269231	0.99	13822	68.297	0.67	3079.565	0.9309	89.47351	0.8687	610.023	89.41899706
99.66	89.418997	20	12	21.68	7.58501151	0.88851239	14.7727365	19.269231	0.99	13822	68.297	0.67	3079.565	0.9309	89.47355	0.8687	610.021	89.41902852
99.66	89.419029	20	12	21.68	7.58501242	0.88851239	14.7727374	19.269231	0.99	13822	68.297	0.67	3079.565	0.9309	89.47354	0.8687	610.021	89.41902796

Table I.1: Summary of the 24-4 and 24-8 RSC Model Results

24-4	Experimental			RSC Model			
Fluid Inlet Temperature (^{o}C)	Mean Plate Temperature (^{o}C)	Panel Heat Output (W/m)	Mean Plate Temperature (^{o}C)	Panel Heat Output (W/m)	Temperature Error	Heat Output Error	
51.78	46.98	207.89	46.51	216.65	1.004069085	-4.215171189	
61.35	55.18	298.47	54.26	291.39	1.666566056	2.373889823	
73.91	64.56	374.18	64.71	378.25	-0.226013377	-1.088407553	
86.66	75.92	490.74	75.02	478.46	1.189043239	2.503050477	
100.4	86.89	613.29	86.13	586.56	0.879687854	4.358890588	

24-8	Experiment			RSC Model			
Inlet Fluid Temp (^{o}C)	Mean Plate Temp (^{o}C)	Heat Output (W/m)	Mean Plate Temp (^{o}C)	Heat Output (W/m)	Temperature Error	Heat Output Error	
51.96	48.1	261.68	48.05	233.10	0.104493461	10.91932009	
62.77	56.46	332.03	57.49	314.95	-1.818058438	5.145780823	
73.71	66.75	407.68	67.03	398.35	-0.413389777	2.288524819	
86.11	77.75	553.61	77.76	497.32	-0.017351347	10.16877502	
99.66	87.46	700.08	89.42	610.02	-2.239913061	12.86432854	

I.2   Effect of Bond Thickness on Panel Performance

To determine the effect of bond conductance on the mean radiant panel temperature and heat output, the RSC model was run at various bond thicknesses. The results are summarized in Table I.2.

Table I.2: Effect of Bond Thickness on panel Temperature

Fluid Inlet Temperature (°C)	Bond Thickness (mm)										
	0.3mm	0.4mm	0.5mm	0.6mm	0.7mm	0.8mm	0.9mm	1.0mm	1.1mm	1.2mm	1.3mm
50.00	46.09	45.91	45.73	45.55	45.37	45.20	45.03	44.86	44.69	44.53	44.37
60.00	54.60	54.35	54.10	53.86	53.62	53.38	53.14	52.91	52.69	52.46	52.24
70.00	63.29	62.98	62.68	62.38	62.08	61.79	61.50	61.22	60.94	60.66	60.39
80.00	71.78	71.40	71.03	70.66	70.30	69.95	69.60	69.25	68.91	68.58	68.25
90.00	80.29	79.85	79.41	78.98	78.56	78.15	77.74	77.33	76.93	76.54	76.16

To see how the heat output is affected by the bond conductance, the two simulations run with a bond thickness of 0.8mm and 1.3mm is shown in Table I.3 at 90°C.

Table I.3: Effect of Bond Thickness on Panel Heat Output

Fluid Inlet Temperature (°C)	Panel Temp (°C) (Estimate)	Enclosure Wall Temp (°C)	Enclosure Cold Wall Temp (°C)	Enclosure Air Temp (°C)	U_L (W/m²K)	C_b (W/mK)	q_{panel} (W/m)
Bond Thickness (mm):	**0.8**						
90	90	19.26	12.61	19.57	14.58	31.31	518.31
90	77.90	19.26	12.61	19.57	14.22	31.31	507.73
90	78.15	19.26	12.61	19.57	14.22	31.31	507.94
90	78.15	19.26	12.61	19.57	14.22	31.31	507.93
90	78.15	19.26	12.61	19.57	14.22	31.31	507.93
Bond Thickness (mm):	**1.3**						
90	90	19.26	12.61	19.57	14.58	19.27	499.98
90	75.84	19.26	12.61	19.57	14.16	19.27	488.55
90	76.16	19.26	12.61	19.57	14.17	19.27	488.80
90	76.16	19.26	12.61	19.57	14.17	19.27	488.79
90	76.16	19.26	12.61	19.57	14.17	19.27	488.79